INVESTIGATION OF LONG-TERM STRENGTH PROPERTIES OF PARIS AND BEAUMONT CLAYS IN EARTH EMBANKMENTS

Mohamad Kasim Kayyal and
Stephen G. Wright

RESEARCH REPORT 1195-2F

PROJECT 3-8-89/1-1195

CENTER FOR TRANSPORTATION RESEARCH

BUREAU OF ENGINEERING RESEARCH

THE UNIVERSITY OF TEXAS AT AUSTIN

NOVEMBER 1991

1. Report No. FHWA/TX-92+1195-2F	2. Government Accession No.	3. L004052

4. Title and Subtitle	5. Report Date
INVESTIGATION OF LONG-TERM STRENGTH PROPERTIES OF PARIS AND BEAUMONT CLAYS IN EARTH EMBANKMENTS	November 1991
	6. Performing Organization Code

7. Author(s)	8. Performing Organization Report No.
Mohamad Kasim Kayyal and Stephen G. Wright	Research Report 1195-2F

9. Performing Organization Name and Address	10. Work Unit No. (TRAIS)
Center for Transportation Research The University of Texas at Austin Austin, Texas 78712-1075	
	11. Contract or Grant No. Research Study 3-8-89/1-1195

12. Sponsoring Agency Name and Address	13. Type of Report and Period Covered
Texas Department of Transportation Transportation Planning Division P. O. Box 5051 Austin, Texas 78763-5051	Final
	14. Sponsoring Agency Code

15. Supplementary Notes

Study conducted in cooperation with the U. S. Department of Transportation, Federal Highway Administration. Research Study Title: "Long-Term Strength Properties of Compacted Fills for Embankment Design"

16. Abstract

Shallow slope failures in compacted highly plastic clay embankments have been a common problem along Texas highways. Recent studies had shown that shallow slides might be the result of cyclic wetting and drying that takes place in the field. The purpose of this study was to examine the effect of wetting and drying on the long-term strength properties of compacted highly plastic clays. The impact of pore water pressures on the long-term stability of earth embankments was also investigated.

Consolidated-undrained triaxial compression tests with pore pressure measurements were performed on laboratory prepared soil specimens of clay from two embankments that experienced shallow slope failures. Triaxial test results indicated that a reduction in the effective-stress shear strength parameters occurred after compacted specimens were subjected to cyclic wetting and drying in the laboratory. Triaxial tests also showed that the long-term strength properties of compacted highly plastic clay embankments may be measured in the laboratory by conducting strength tests on laboratory prepared, normally consolidated specimens. Results obtained from X-ray diffraction analyses confirmed that normally consolidated specimens and specimens subjected to wetting and drying had a similar clay structure.

Slope stability computations, performed for the two embankments under consideration, revealed that the reduction in strength due to wetting and drying partially explained the observed failures. Stability analyses also confirmed that significant positive pore water pressures may have existed at failure. Pore water pressure conditions at failure were back-calculated for an additional 34 shallow slope failures in Texas. The results of the stability analyses were used to establish recommendations for predicting pore water pressure conditions at failure for design of future embankments.

17. Key Words	18. Distribution Statement
slope failures, highly plastic clay embankments, slides, wetting, drying, pore water pressures, soil specimens, compacted, compression, stability, consolidated, triaxial tests, strength	No restrictions. This document is available to the public through the National Technical Information Service, Springfield, Virginia 22161.

19. Security Classif. (of this report)	20. Security Classif. (of this page)	21. No. of Pages	22. Price
Unclassified	Unclassified	134	

Form DOT F 1700.7 (8-72)   Reproduction of completed page authorized

INVESTIGATION OF LONG-TERM STRENGTH PROPERTIES OF PARIS AND BEAUMONT CLAYS IN EARTH EMBANKMENTS

by

Mohamad Kasim Kayyal
and
Stephen G. Wright

Research Report 1195-2F

Long-Term Strength Properties of Compacted Fills for Embankment Design

conducted for

Texas Department of Transportation

in cooperation with the

**U.S. Department of Transportation
Federal Highway Administration**

by the

CENTER FOR TRANSPORTATION RESEARCH
Bureau of Engineering Research
THE UNIVERSITY OF TEXAS AT AUSTIN

November 1991

NOT INTENDED FOR CONSTRUCTION,

PERMIT, OR BIDDING PURPOSES

Stephen G. Wright, P.E. (Texas No. 49007)
Research Supervisor

PREFACE

The Texas Department of Transportation (formerly the Texas State Department of Highways and Public Transportation) has experienced significant problems with slope stability failures of embankments constructed of highly plastic clays. The failures generally occur a number of years (at least ten) after construction. Previous research conducted by the Center for Transportation Research showed that there was a significant discrepancy between the long-term shear strength properties of the clays based on the results of laboratory tests and the shear strength properties that were apparently developed in the field. Project 1195 was undertaken to understand better the reason for these discrepancies and to develop suitable procedures for determining the long-term strength properties of highly plastic clays suitable for design of embankments.

Particular attention has been paid to the long-term effects of wetting and drying and the associated cracking that occurs in highly plastic clays in the field. Laboratory procedures were developed and used to simulate the effects of cracking produced by drying in the field. A theoretical model was also developed to study the effects of drying and to determine the important parameters that might influence the effects of cracking. Results from the theoretical studies are presented in a companion report. The current report presents the results of laboratory studies on the shear strength properties, and provides comparisons of the results from the laboratory tests with observed field behavior of embankments that have failed.

LIST OF REPORTS

Report No. 1195-1, "Numerical Modeling of the Response of Cylindrical Specimens of Clay to Drying," by Douglas O. Bell and Stephen G. Wright, presents the results of the literature review and theoretical studies, including the development of a simple numerical model that was used to study the effects of drying rate on the development of tensile stresses and, thus, cracking in specimens that were dried.

Report No. 1195-2F, "Investigation of Long-Term Strength Properties of Paris and Beaumont Clays in Earth Embankments," by Mohamad K. Kayyal and Stephen G. Wright, presents the results of laboratory studies on the shear strength properties, and comparisons of results from laboratory tests with observed field behavior, of embankments which have failed.

ABSTRACT

Shallow slope failures in compacted highly plastic clay embankments have been a common problem along Texas highways. Recent studies had shown that shallow slides might be the result of cyclic wetting and drying that takes place in the field. The purpose of this study was to examine the effect of wetting and drying on the long-term strength properties of compacted highly plastic clays. The impact of pore water pressures on the long-term stability of earth embankments was also investigated.

Consolidated-undrained triaxial compression tests with pore pressure measurements were performed on laboratory prepared soil specimens of clay from two embankments that experienced shallow slope failures. Triaxial test results indicated that a reduction in the effective-stress shear strength parameters occurred after compacted specimens were subjected to cyclic wetting and drying in the laboratory. Triaxial tests also showed that the long-term strength properties of compacted highly plastic clay embankments may be measured in the laboratory by conducting strength tests on laboratory prepared, normally consolidated specimens. Results obtained from X-ray diffraction analyses confirmed that normally consolidated specimens and specimens subjected to wetting and drying had a similar clay structure.

Slope stability computations, performed for the two embankments under consideration, revealed that the reduction in strength due to wetting and drying partially explained the observed failures. Stability analyses also confirmed that significant positive pore water pressures may have existed at failure. Pore water pressure conditions at failure were back-calculated for an additional 34 shallow slope failures in Texas. The results of the stability analyses were used to establish recommendations for predicting pore water pressure conditions at failure for design of future embankments.

SUMMARY

Procedures were developed in which specimens were subjected to repeated cycles of wetting and drying in order to produce cracking and simulate what may occur in the field. After specimens were subjected to a number of cycles (typically 20) of wetting and drying, they were tested employing consolidated-undrained triaxial compression tests with pore water pressure measurements. Results of these tests were used to determine the shear strength properties of the soil in terms of effective stresses. The shear strength measured for the soil after wetting and drying was found to be significantly lower than the shear strength of specimens that were not subjected to repeated wetting and drying, but rather just saturated and sheared to failure.

Results from the laboratory tests were used to "back-analyze" a number of actual slope failures. The effects of wetting and drying on the shear strength properties were found to produce significantly lower factors of safety. However, in order to explain the observed slope failure in the field, it was also found necessary to assume pore water pressures that were much higher than had previously been expected. The results of these studies indicate that the combined effect of a deterioration in strength owing to repeated wetting and drying and high pore water pressures is the cause of the embankment failures observed in highly plastic clays in Texas.

IMPLEMENTATION STATEMENT

Future designs both for new embankments and for repair of existing embankments in highly plastic clays (liquid limit greater than 50) should be based on a reduced strength that reflects the effects of repeated wetting and drying. In addition, designs should be based on the assumption of relatively high pore water pressures (a shallow water table) near the face of the embankment.

Further work is recommended to develop simpler procedures for measuring the reduced long-term shear strength caused by repeated wetting and drying. The procedures employed in this study are time-consuming, typically requiring a total test duration of one month for a single specimen. Such long testing times seem impractical and dictate simpler procedures for practical designs.

Field measurements of pore water pressure would also be useful to confirm what has been inferred from "back-analysis." However, it should be cautioned that such measurements of pore water pressures may be difficult and time-consuming to make: the critical period of interest may occur only very briefly, at intervals of several years or more.

ACKNOWLEDGEMENTS

TABLE OF CONTENTS

CHAPTER 1. INTRODUCTION

BACKGROUND

Clay embankments along Texas highways have been prone to shallow slope failures that occur a number of years after construction. Typical embankments that have failed are constructed of highly plastic clays, with heights ranging from 10 to 30 feet, and side slopes flatter than 2:1 (horizontal: vertical). Such embankments have typically failed during a period of 10 to 30 years after construction. Failures are characterized by a shallow slip surface which rarely exceeds 5 to 7 feet in depth.

In 1982, research was initiated at The University of Texas at Austin to investigate the cause of these shallow slope failures. Stauffer and Wright (1984) back-calculated the effective-stress shear strength parameters from a number of embankment slides, assuming zero pore water pressures at failure. Gourlay and Wright (1984) measured the effective-stress shear strength parameters for laboratory compacted soil specimens from an embankment slide in Houston, Texas. Results obtained from the two studies indicated that a significant discrepancy existed between the laboratory measured and the back-calculated strength parameters; a significant cohesion intercept was measured in the laboratory, while negligible cohesion value was back-calculated for the field. Green and Wright (1986) measured effective-stress shear strength parameters for undisturbed soil specimens taken from the same Houston embankment investigated by Gourlay and Wright (1984). Laboratory test results by Green and Wright (1986) again confirmed the existence of a significant cohesion intercept for the shear strength envelope. Further studies by Rogers and Wright (1986) and by Kayyal (1986) identified cyclic wetting and drying in the field as a process that might explain the discrepancy between the laboratory measured and the back-calculated shear strength parameters.

RESEARCH OBJECTIVES

The objectives of the current study were to investigate the source of the discrepancy between the laboratory measured and the back-calculated effective-stress shear strength parameters for a number of embankment slides in Texas. The research was divided into two parts. In the first part, the effect of cyclic wetting and drying on the behavior of compacted highly plastic clays was investigated. In the second part, the impact of the pore water pressure conditions in embankments at failure was examined.

ORGANIZATION

The laboratory investigation of the effects of wetting and drying on soil properties are presented in Chapters 2 through 6. The location, history, and material properties for two embankment slopes that experienced slides and were selected for study are presented in Chapter 2. The apparatus and laboratory procedures developed for subjecting compacted specimens to cyclic wetting and drying are described in Chapter 3. The effect of cyclic wetting and drying on the effective-stress shear strength envelopes of compacted clay specimens is presented in Chapter 4. A comparison between the consolidation and shear strength properties of specimens subjected to wetting and drying and those of normally consolidated specimens is presented in Chapter 5. The effect of wetting and drying on clay particle orientations is examined in Chapter 6.

The impact of pore water pressure conditions on the long-term stability of embankments in examined in Chapters 7 and 8. In Chapter 7, the effect of reduced shear strength caused by wetting and drying on long-term stability is examined, and pore water pressures are back-calculated for the primary embankments under consideration. In Chapter 8, pore water pressure conditions are back-calculated for a number of additional embankments to establish recommendations for design. In Chapter 9, a summary, conclusions, and recommendations for future work are presented.

CHAPTER 2. PHYSICAL PROPERTIES AND MINERALOGICAL COMPOSITION OF EMBANKMENT SOILS

INTRODUCTION

Two embankments were selected for detailed study. The embankments are briefly described in this chapter. A quantity of soil was obtained from each embankment for testing. The index properties, mineralogical composition, and elemental constituents determined for the soils are also included in this chapter.

DESCRIPTION OF SITES

The two embankments selected for study are located in District 1 (Paris) and in District 12 (Houston) of the Texas State Department of Highways and Public Transportation (SDHPT). Both embankments were constructed of highly plastic clays, and both have experienced sliding in the past.

The Paris Embankment

The Paris embankment is part of Loop 286 near the crossing of the Missouri Pacific (T&P) railroad. The embankment was constructed in 1966. A map with the location of the embankment is shown in Figure 2.1. The embankment is approximately 20 feet high, with a 3:1 side slope (horizontal:vertical) in the vicinity of the slide. In 1984, the west side of the embankment failed. The soil that slid was subsequently lime stabilized and was compacted in place with Tensar reinforcement. In 1987, the west side of the slope failed again. The depth of the slide and the length of slide (in the direction parallel to the highway) were estimated by SDHPT personnel to be approximately 5 feet and 75 feet, respectively. The sliding soil was reworked and compacted in place. In 1990, both the east and west sides of the Paris embankment appeared to be on the

verge of failure. This condition was manifested by the formation of cracks parallel to the length of the slope and by evidence of rolls and dips near the toe of the slope.

Soil samples were obtained from the east side of the embankment at a depth of approximately 3 feet below the surface. The east side was chosen because lime had been added previously to the soil on the west side. Initially, a block sample was obtained from the west side of the embankment at a depth of 3 feet (prior to knowing that the soil was mixed with lime). When the block sample was brought to the laboratory, it crumbled into small fragments, showing the presence of fissures and cracks in the soil.

The Houston Embankment

The Houston embankment is located on Loop 610 and Scott Street (see map, Fig 2.2). The embankment was built in 1966. The embankment was constructed of common roadway excavation and fill material which consisted mainly of a clay referred to locally as "Beaumont Clay." The height of the embankment is approximately 19 feet, with side slopes varying from 2.4:1 to 2.6:1 in the vicinity of the slide. In 1983, the northeast side of the embankment failed. The depth of slide was estimated by Stauffer and Wright (1984) to be approximately 4 feet. The soil was reworked and compacted in place; no additives (e.g., lime) were used in the repair. Concrete rip-rap was also cast on the surface of the slope. In 1989, the northeast side of the embankment failed again following a period of heavy rain. The failure caused the concrete rip-rap to fracture laterally along the length of the slope. The depth of the slide was estimated to be 6 feet, and the length of the slide (in the direction parallel to the highway) was approximately 70 feet.
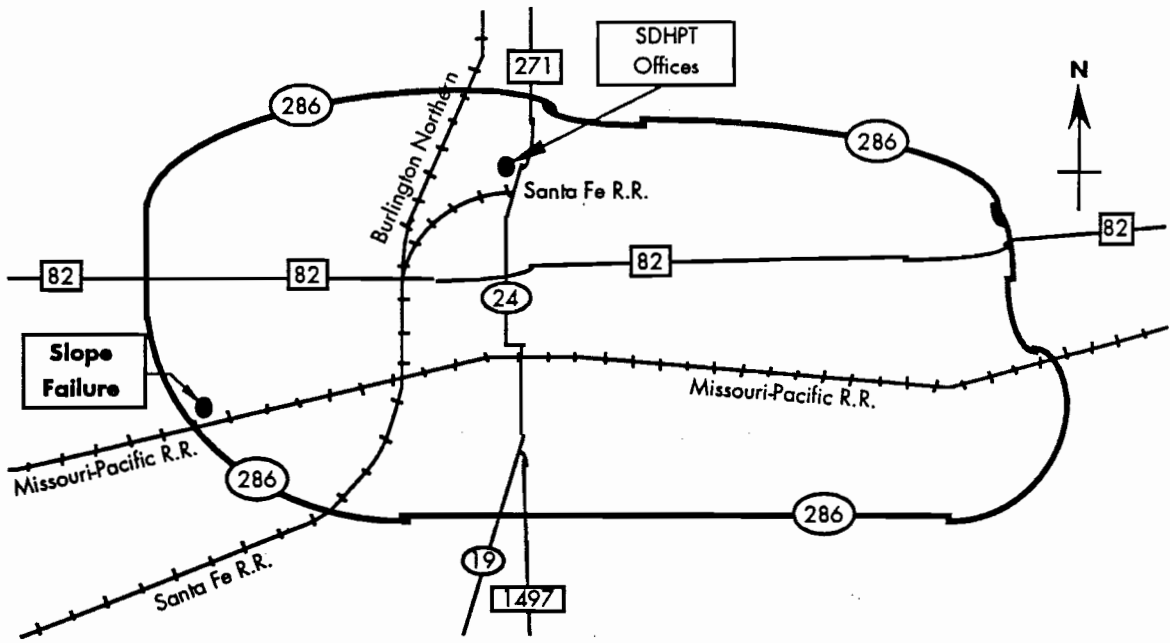
Figure 2.1   Location of the Paris Embankment Slope Failure
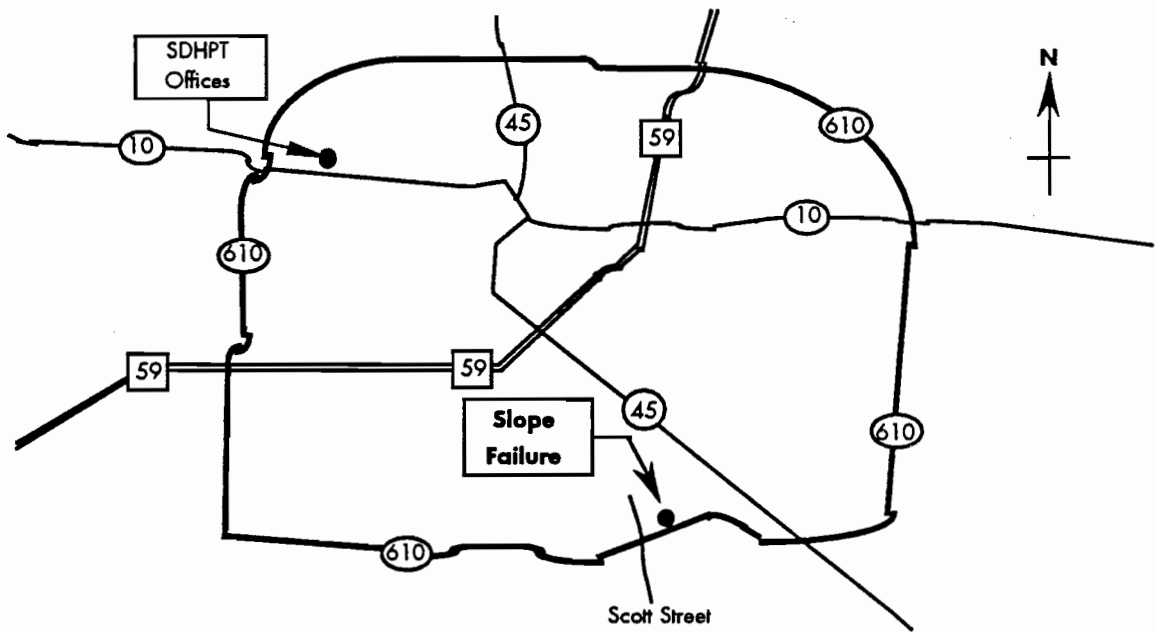
Figure 2.2   Location of the Houston Embankment Slope Failure

Soil samples were obtained from the Houston embankment soon after it failed in 1989. The soil was excavated from the exposed sliding surface before remedial work was started. The soil that slid was recompacted in place, and concrete rip-rap was recast on the surface of the slope.

PHYSICAL PROPERTIES OF THE EMBANKMENT SOILS

Index properties and compaction moisture density relationships were determined for both the Paris and the Houston embankment soils and are presented in this section.

Index Properties

Atterberg Limits, specific gravity, and grain size distributions were determined for both the Paris and Beaumont clays. The activities were also computed. Index properties were determined according to ASTM (American Society for Testing and Materials) specifications (ASTM, 1989); the relevant ASTM Standards are D4318 for the Liquid and Plastic Limits, D427 for the Shrinkage Limit, D854 for specific gravity, and D422 for particle size analyses. Index properties are summarized in Table 2.1.

Atterberg Limits

Atterberg Limits were determined for an air-dry fraction of soil passing the No. 40 sieve. Both soils possess Liquid Limits exceeding 70 and Plasticity Indices over 50 (Table 2.1), and both classify as highly plastic (CH) according to the Unified Soil Classification system.

Table 2.1   Index properties for the Paris and Beaumont clays

Index Parameters	Paris Clay	Beaumont Clay
Test site	Paris, Texas	Houston, Texas
Soil color	Yellow	Red
Liquid limit (LL)	80	73
Plastic limit (PL)	22	21
Shrinkage limit (SL)	11	10
Plasticity index (PI)	58	52
Specific gravity (G_S)	2.72	2.70
Activity	1.0	1.1
Unified soil classification symbol	CH	CH

Specific Gravity

Specific gravity measurements were performed for an air-dry fraction of soil passing the No. 10 sieve. Three measurements were obtained for each of the two soils. The specific gravities varied from 2.71 to 2.74 for the Paris clay and from 2.68 to 2.71 for the Beaumont clay. The average of these measurements for each soil is reported in Table 2.1.

Grain Size Analyses

Sieve analyses were conducted on portions of soil retained on the No. 10 sieve; hydrometer tests were performed on portions passing the No. 10 sieve. At the end of a hydrometer test, the proportion of soil retained on a No. 200 sieve was determined.

Grain size distributions for the Paris and the Beaumont clays are presented in Figure 2.3. Less than 8 percent of the Paris soil consists of sand sizes (coarser than the No. 200 sieve; opening 0.075 mm), whereas approximately 12 percent of the Beaumont soil consists of sand sizes. The grain size distribution curves also indicate that 59 percent of the Paris soil is clay sized (finer than 0.002 mm) and that 46 percent of the Beaumont soil is clay sized.

Activities

Activities, defined as the ratio of the Plasticity Index of the soil to the percentage by weight of soil finer than 0.002 mm, were determined for the Paris and the Beaumont clays. Results in Table 2.1, indicate that the activities of both soils exceed 1.0.

Moisture Density Relationships

A series of Standard Proctor compaction tests was performed using ASTM D698 procedures (ASTM, 1989), which called for using the air-dry fraction of soil passing the No. 10 sieve. The moisture density curves are shown in Figure 2.4 for the Paris clay and in Figure 2.5 for the Beaumont clay. The data obtained by Gourlay and Wright (1984) for the Beaumont clay are also shown in Figure 2.5. The maximum dry density is approximately 93 pcf for the Paris clay and 101 pcf for the Beaumont clay. The optimum moisture content is approximately 27 percent for the Paris clay and 23 percent for the Beaumont clay.

4
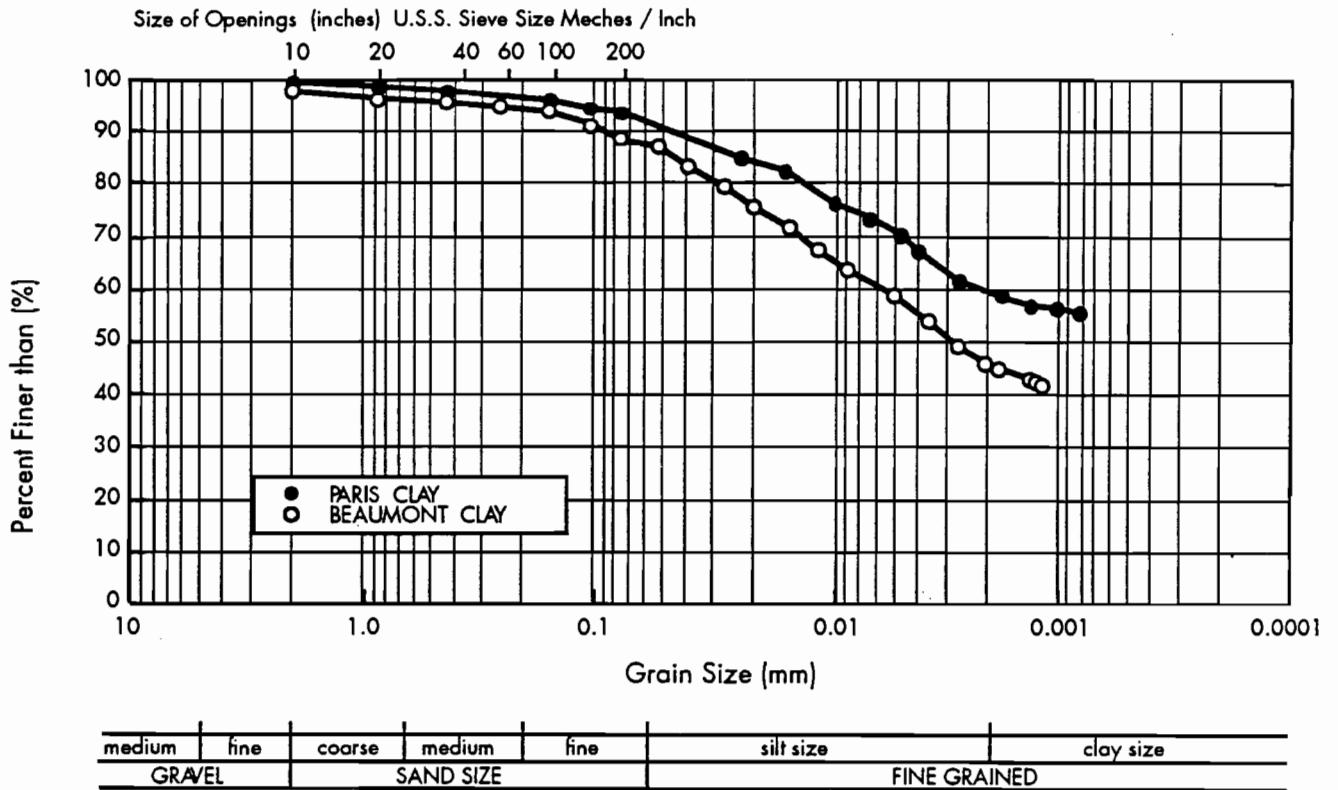
Figure 2.3   Grain size distribution curves for the Paris and Beaumont clays
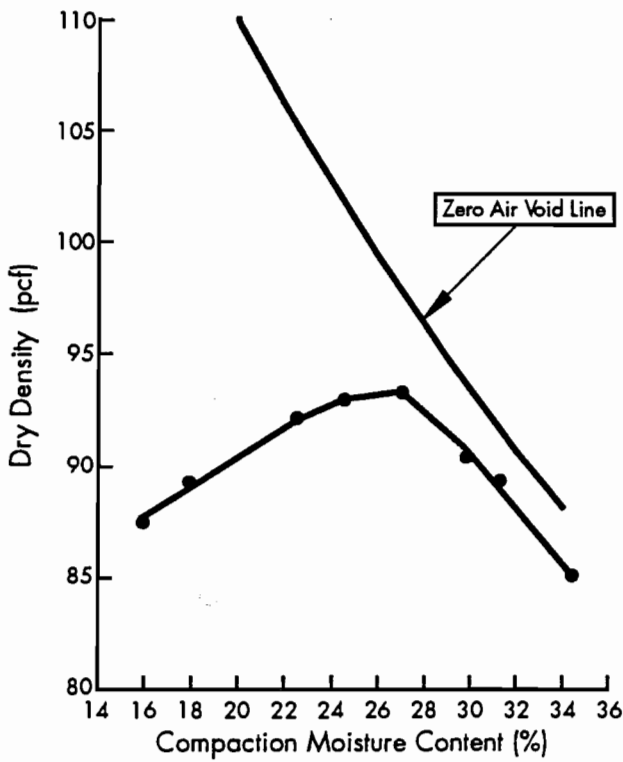
Figure 2.4   Standard proctor density curve for the Paris clay
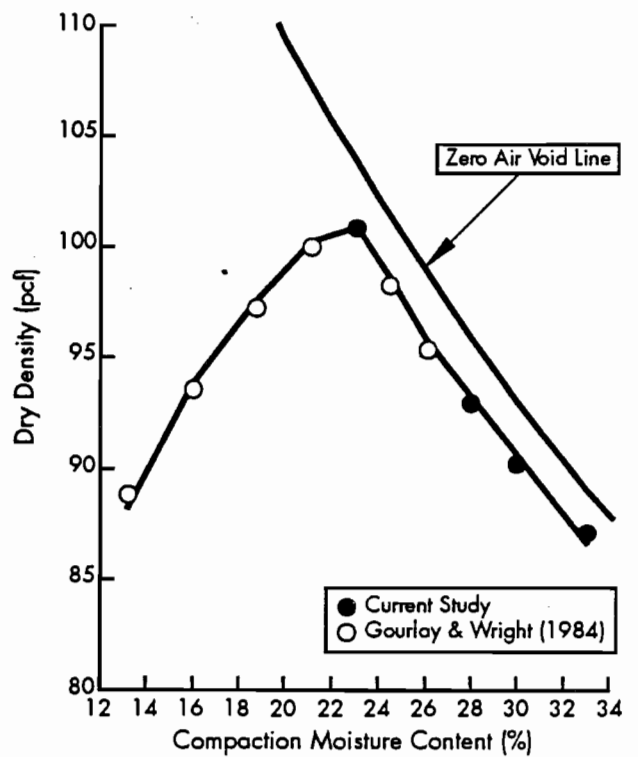
Figure 2.5   Standard proctor density curve for the Beaumont clay

MINERALOGICAL COMPOSITION OF THE EMBANKMENT SOILS

X-ray diffraction methods were used to identify the clay minerals in the Paris and Beaumont clays. The X-ray diffraction studies are presented in this section.

Principle of X-Ray Diffraction

The basic principle underlying the identification of clay minerals by X-ray is that each crystalline substance has its own characteristic atomic structure which diffracts X-rays in a characteristic pattern. When an X-ray beam strikes a crystal, at each atomic plane, a minute portion of the beam is scattered by individual atoms that then oscillate as dipoles and radiate in all directions. Radiation in certain directions will be in phase and can be interpreted in a *simplistic* fashion as a wave resulting from a reflection of the incident beam. This condition is expressed by Bragg's Law:

$$n \lambda = 2 d \sin\theta$$

where d is the spacing of the atomic planes, λ is the wave length of the X-rays, θ is the angle of diffraction, and n is the order of diffraction which may assume a value of any whole number.

Evaluation of X-Ray Powder Diagrams

The basic data from an X-ray powder diagram consists of two quantities: the spacings between the planes of atoms in the crystal (d), and the intensities of the X-ray reflections from the corresponding planes. These two quantities are known for many crystalline materials, and have been published by the Joint Committee for Powder Diffraction Standards (JCPDS, 1989). Identification of minerals is accomplished by matching the experimentally determined spacing and intensity values with the published values. More than one crystalline component is generally present in a sample, and difficulty is often experienced in assigning sets of powder lines to particular components. It is for this reason that auxiliary pre-treatments and other analytical methods are frequently used in clay-mineral identification.

Experimental Procedures

X-Ray diffraction is particularly well suited for the identification of clay mineral groups because clay groups have similar silica sheet structures, but they differ in interlayer spacing. For that reason, the *(00l)* spacings determined from X-ray diffraction diagrams are characteristic for clay mineral groups. To identify the clay mineral groups in the Paris and Beaumont clays, oriented clay particles were sedimented onto glass slides by air drying from dilute suspensions. In oriented X-ray powder diffraction, the intensities of the *(00l)* diagnostic lines are accentuated, while the non-diagnostic *(hkl)* lines are almost eliminated from the pattern. The glass slide with the sedimented clay could be inserted directly into a Philips type X-ray diffractometer. X-ray diffraction scanning was conducted for 2θ angles ranging from 2 degrees to 60 degrees. The angular velocity of the detector was set at 2 degrees per minute, while the effective step size of the run was fixed at 0.05 degrees. The oriented powder X-ray diagrams are shown in Figure 2.6 for the Paris clay and in Figure 2.7 for the Beaumont clay. The mineralogical composition for both clays are identified on the diffraction diagrams along with the corresponding spacings (d).

Additional X-ray diffraction analyses were performed on ethylene-glycol-treated samples. The purpose of these analyses was to confirm the presence of montmorillonite in the Paris and the Beaumont clays. In this procedure, a glass slide with a sedimented clay suspension is subjected to ethylene glycol vapor at room temperature for a period of 24 hours. Ethylene glycol is a low-volatility liquid miscible with water. The resulting X-ray powder diagrams indicated that the observed (001) first-order basal reflections had shifted from 14.5 Å to 17.7 Å for both clays. This shift in the spacing (d) it typical of montmorillonites that have been treated with ethylene glycol, and it confirms that the Paris and Beaumont clays are expansive in nature (Dixon and Weed, 1989).
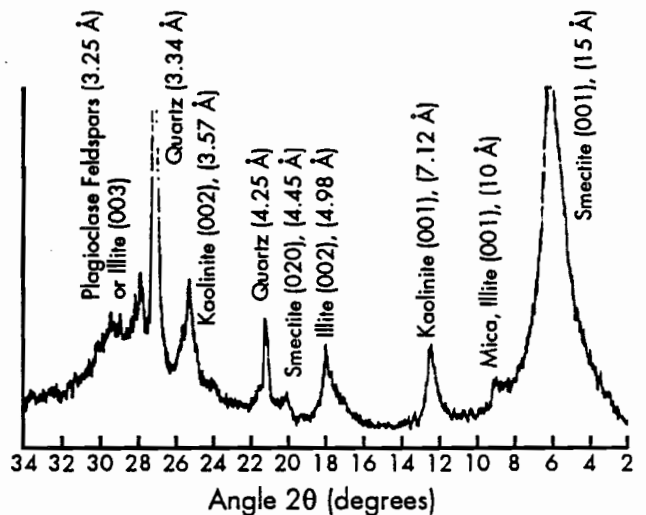
Figure 2.6 **X-ray diffraction pattern for the Paris clay with the mineral constituents and their corresponding d spacings in angstroms (Å)**
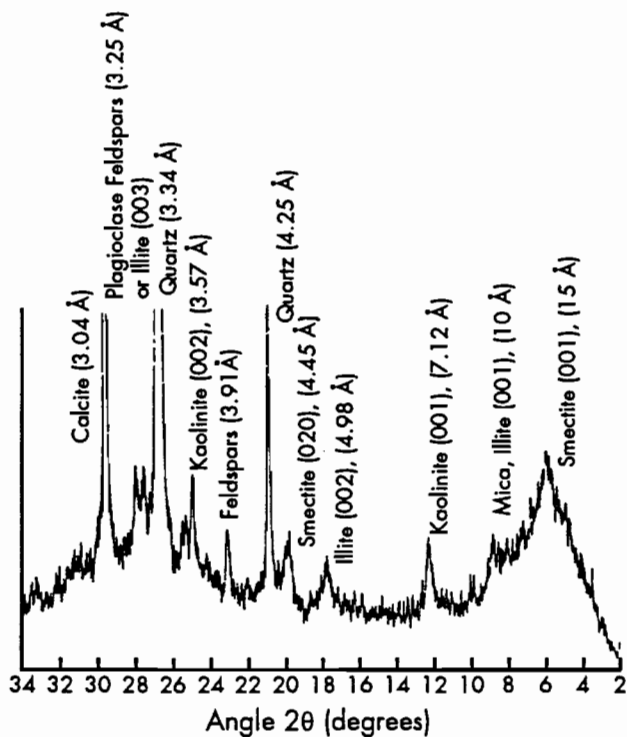
Figure 2.7   X-ray diffraction pattern for the Beaumont clay with the mineral constituents and the corresponding *d* spacings in angstroms (Å)

The mineral constituents that were identified in the Paris and Beaumont clays consist of calcium montmorillonite, mica, illite, kaolinite, quartz, and plagioclase feldspars. Calcium carbonate was identified only in the Beaumont clay and could not be found in the Paris clay.

The presence of calcium carbonate was confirmed by treating samples from the Paris and Beaumont clays with hydrochloric acid (HCl). Samples of Paris clay did not react when treated with the acid, while samples of Beaumont clay fizzed upon contact.

ELEMENTAL CONSTITUENTS OF THE EMBANKMENT SOILS

The elemental constituents of the minerals in the Paris and Beaumont clays were identified by means of qualitative X-ray microanalysis. The purpose of these analyses was to identify elements in the clay minerals that were present in various crystallographic sites because of isomorphous substitution of elements. The principle of this method, and the experimental procedures and test results, are presented in the following section.

Qualitative X-Ray Microanalysis

Qualitative X-ray microanalysis is often used for identification of elements present in various materials. X-ray microanalysis is performed using a scanning electron microscope (SEM). Elements are typically identified by means of an energy dispersive spectrometer detector (EDS). Because of the limitations of this detector, elements recognized are restricted to those with atomic numbers higher than sodium (Na). As a result, oxygen, an element lower than sodium on the atomic scale, cannot be identified in this test.

Principle

Qualitative X-ray microanalysis is based on the principle that when an atom of an element is bombarded with an electron beam, the atom produces intense X-rays *characteristic* of this element. The X-rays are emitted following the ejection of an electron from an inner shell by the electron beam, and the substitution of an electron from the outer shell for the ejected electron. The inter-shell electron transitions in the bombarded atom are accompanied by the release of excess energy that lies in the X-ray range of the electromagnetic spectrum.

Experimental Procedures

Qualitative X-ray microanalysis was performed in a scanning electron microscope (SEM). The microscope was linked to a computer-based multichannel analyzer that recognizes the specific energy of the characteristic X-ray peaks for each element. An energy dispersive X-ray spectrometer (EDS) was employed to observe the relative peak heights for the family of X-ray lines emitted from the clay specimens.

The soil specimens used for the analyses consisted of air-dried flakes of random shapes with dimensions not exceeding 0.2 inches. The flakes were obtained by sedimenting a thick soil suspension on a glass slide. The soil water evaporated, and a thin solid clay crust dried on the glass slide. The crust was broken into flakes of random shapes, and the flakes were placed on a 0.75-inch diameter solid graphite cylinder. The graphite was fixed to a holder and inserted in the SEM for analysis. The soil flakes were located on a visual screen, and measurements of X-ray peak intensities from the individual flakes were obtained with the EDS detector, which determined the spectrum input counts of the emitted X-rays per second. The specific energy

(reported in Kev) for each of the characteristic X-ray lines was determined using the emitted wave length.

Typical plots of the measured characteristic X-rays are shown in Figure 2.8 for the Paris clay and in Figure 2.9 for the Beaumont clay. The elements corresponding to the X-ray peaks are identified on these plots. All the elements present in the Paris clay were also found in the Beaumont clay, except Chlorine (Cl), whose peak could not be identified from the characteristic X-ray lines of the Paris clay. The elemental constituents include magnesium (Mg), aluminum (Al), silicon (Si), chlorine (Cl), potassium (K), calcium (Ca), titanium (Ti), and iron (Fe). Larger amounts of calcium were measured in the Beaumont clay than in the Paris clay. This discrepancy is due to the presence of calcium carbonate in the Beaumont clay. Calcium carbonate was not found in the Paris clay.

EVALUATION OF THE CHANGE IN THE MATERIAL PROPERTIES OF THE PARIS CLAY

A study was conducted to evaluate the change in properties of the Paris clay from the time of construction to the time of failure. Soil samples were obtained for the study from the original borrow site, which was used to construct the Paris embankment in 1966. Laboratory tests were conducted to evaluate the physical, chemical, mineralogical, elemental, and soil strength properties.

Test results are presented in Appendix A. Results indicate that the material properties were similar for Paris clay samples obtained from a depth of 3 feet below the top of the embankment and those obtained from a depth of 10 feet below the ground surface of the borrow pit.
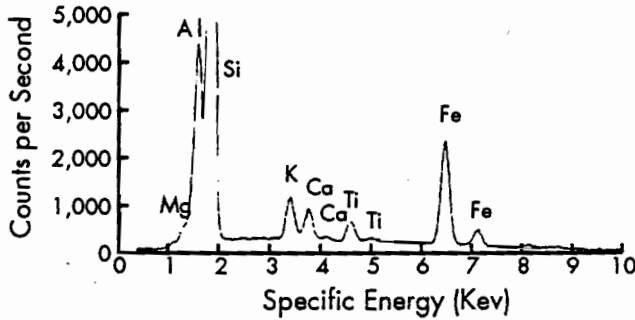
Figure 2.8   Elemental constituents for the Paris clay based on X-ray microanalyses results
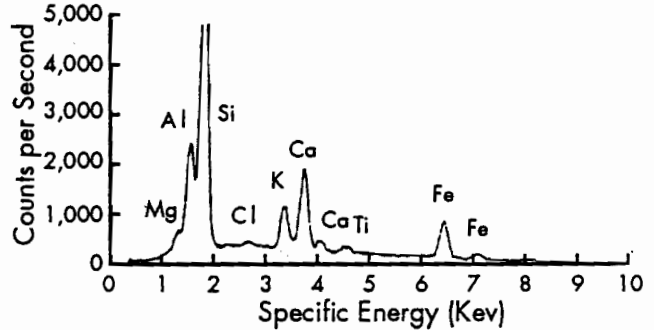
Figure 2.9   Elemental constituents for the Beaumont clay based on the X-ray microanalyses results

CHAPTER 3. THE WETTING AND DRYING PROCESS

INTRODUCTION

The potential impact of wetting and drying on the development of shallow slope failures in embankment fills was identified in an earlier study by Rogers and Wright (1986) and by Kayyal (1986). In the current study, the effects of cyclic wetting and drying on the long-term strength and structure of compacted Paris and Beaumont clay specimens were investigated further. Prior to examining the effects of wetting and drying, it was necessary to devise an appropriate laboratory procedure for reproducing the effects of wetting and drying in the field.

In this chapter, the laboratory process for wetting and drying is presented. The apparatus and procedures for wetting and drying are both described. The wetting and drying apparatus consists of a soil specimen holder, a water bath, and an oven. The procedure for preparing compacted soil specimens is also presented. Establishment of the number of cycles of wetting and drying, and the duration for each cycle, are also discussed.

THE WETTING AND DRYING APPARATUS

Research on the development of the wetting and drying apparatus was initiated in an earlier study by Kayyal (1986). A holder was developed for subjecting laboratory 1.5-inch-diameter soil specimens to repeated cycles of wetting and drying. In the current study, further modifications were made to improve the design of the specimen holder.

The Specimen Holder

The specimen holder is sketched in Figure 3.1. The holder consists of a loosely wrapped 2-inch-diameter cylindrical stainless steel wire mesh screen with 0.075-millimeter openings (sieve No. 200). The wire mesh is 6 inches long, and is constrained to its cylindrical shape at the top, middle, and bottom by acrylic plastic rings. The base that supports the soil specimen in the holder is composed of a No. 40 stainless steel wire screen overlaid by a filter paper, and covered by a No. 200 wire screen. The base is secured between two rings and three threaded stainless steel rods. One of the three rods extends to the top acrylic ring, and serves to support the top ring as well as providing a handling arm for moving the specimen holder between the oven and water.

The specimen holder with its cylindrical screen permits free exposure of the soil surface to wetting and drying while retaining a specimen with a shape suitable for subsequent triaxial testing. With its 2-inch inside diameter, the screen allows the 1.5-inch-diameter specimen to swell to a radial strain of approximately 33 percent.

The holder is also designed to reduce possible disturbance to the soil when it is subsequently set up for triaxial testing. For that purpose, the cylindrical screen can be freely unwrapped from around the soil specimen, which facilitates the set-up of the specimen for shear testing.

The Wetting Equipment

The equipment used for wetting soil specimens consists of 1,000-milliliter containers filled with distilled water, each of which is large enough to enclose a specimen holder. Distilled water was used because of a study conducted by Liljestrand et al (1986), who showed that the chemical properties of rain water in the areas known for their slope stability problems in Texas are similar to the chemical properties of distilled water. The use of distilled water was also justified by the fact that salty water would result in significant concentration of salts in the soil. This process occurs because salts would enter the soil specimen with the water during wetting, but could not diffuse back into the surrounding solution when the specimen is separated from the water solution for drying. As a result, salts accumulate in the soil with further cycles of wetting and drying. A water container and specimen holder are shown in Figure 3.2.
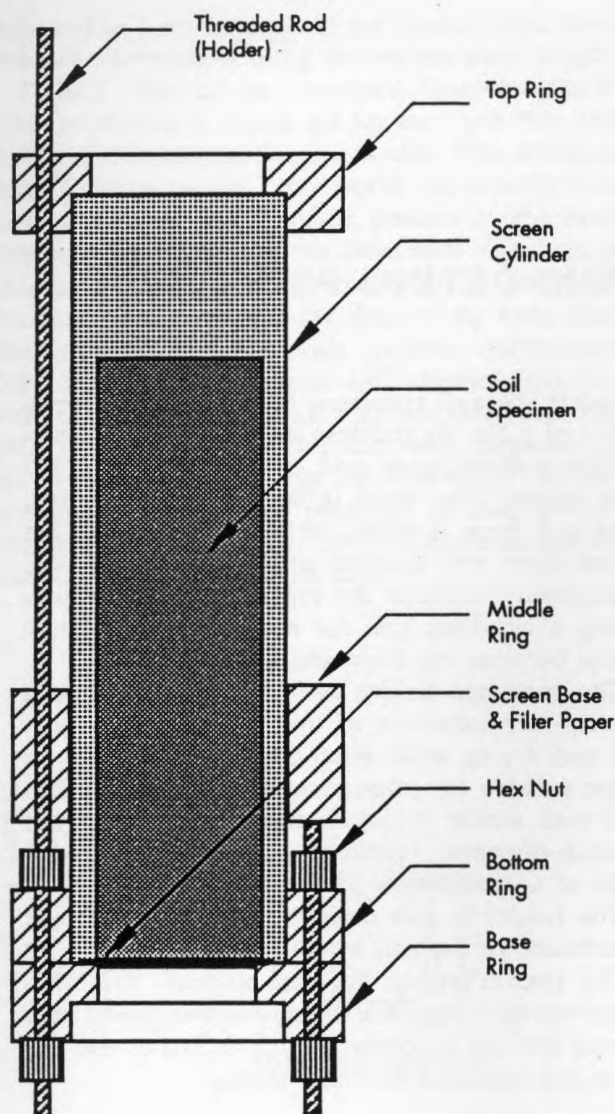
Figure 3.1 A cross section in the wetting and drying holder

Labels (top to bottom):
- Threaded Rod (Holder)
- Top Ring
- Screen Cylinder
- Soil Specimen
- Middle Ring
- Screen Base & Filter Paper
- Hex Nut
- Bottom Ring
- Base Ring

The Drying Equipment

The drying equipment consists of a 1.4-ft³ forced air convection oven set at a temperature of 60°C. Based on previous research conducted by Kayyal (1986), air circulation by forced air convection was found to be necessary for the development of fissures and cracks in specimens by reducing the relative humidity in the oven atmosphere. The formation of cracks in the laboratory prepared specimens was intended to reproduce the cracking observed in embankment fills prior to failure.

The temperature of 60°C was based on the recommendations stated in various material testing manuals which provide guidelines concerning

maximum drying temperatures that will not alter soil index properties. AASHTO T 87-72 and AASHTO T 146-49 of the American Association of State Highway and Transportation Officials (AASHTO, 1975), Tex-101-E of the Texas State Department of Highways and Public Transportation (SDHPT, 1978), and ASTM D 2217-66 specify drying at a maximum temperature of 60°C. BS 1377:1975 of the British Standards Institute recommends a maximum temperature of 50°C.
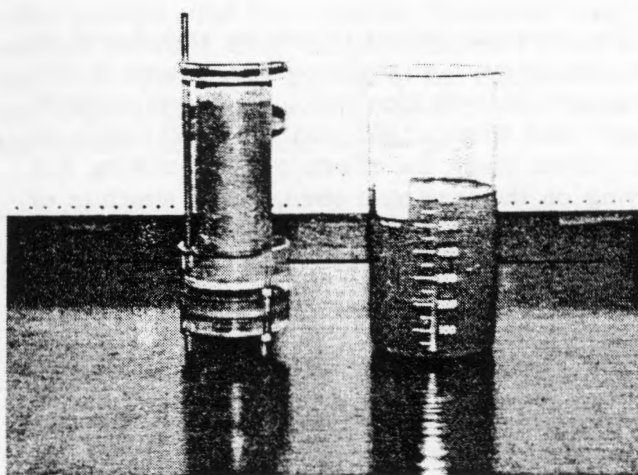
Figure 3.2 The distilled water container and the specimen holder

Liquid and Plastic Limits for the Paris and Beaumont clays dried at room temperature and at a temperature of 60°C are tabulated in Table 3.1. The results indicate that the liquid and plastic limits do not change, as a result of drying at 60°C, by more than 6 percent and 1 percent, respectively. After this confirmation that soil index properties (Atterberg Limits) were not altered by drying to a temperature of 60°C, it was decided to utilize an ambient oven temperature of 60°C for drying all soil specimens.

Table 3.1 Atterberg limits for the Paris and Beaumont clays at room temperature and at 60°C

Atterberg Limits	Paris Clay	Beaumont Clay
At room temperature		
Liquid Limit (LL)	80	73
Plastic Limit (PL)	22	21
At 60°C temperature		
Liquid Limit (LL)	76	70
Plastic Limit (PL)	23	20

PROCEDURE FOR PREPARING COMPACTED SPECIMENS

Soil specimens were compacted to a dry density within 95 to 100 percent of the Standard Proctor maximum dry density (88 to 93 pcf for the Paris clay and 97 to 102 pcf for the Beaumont clay), and to a moisture content within 2 percent of the optimum moisture content of 26 percent for the Paris clay and 22 percent for the Beaumont clay (optimum moisture contents for the Standard Proctor moisture density curves). Soil processing and preparation procedures, and the method for soil compaction, are presented below.

Soil Processing Procedure

All specimens were prepared from air-dried soil with an initial moisture content of approximately 5 percent. Large lumps of soil were broken apart, crushed and pulverized. The processed soil was then placed in a mechanical shaker and sieved to remove particles coarser than the No. 40 sieve.

Soil coarser than the No. 40 sieve was not used. However, 96 percent of the Paris and Beaumont soils were finer than the No. 40 sieve.

Procedure for Soil Preparation Prior to Compaction

Approximately 200 to 300 grams of processed soil (200 grams for 3-inch-high specimens, and 300 grams for 5-inch-high specimens) were mixed to a moisture content of approximately 29 percent for the Paris clay and 25 percent for the Beaumont clay. These values correspond to a moisture content approximately 3 percent higher than the optimum moisture content at Standard Proctor maximum dry density. Distilled water was sprayed in a fine mist onto the soil during the mixing process. The soil was then sealed in double plastic bags and stored at room temperature to allow the moisture content to equilibrate in the clay. After a 24-hour hydration period, the soil was forced in small quantities (between 30 and 40 grams) through the screen framework shown in Figure 3.3 using a rubber pestle to force the soil through the screen. The framework consists of an aluminum frame which supports a stainless steel screen of No. 40 (0.0165-inch) sieve size. The screen framework has been described by Rogers and Wright (1986). The purpose of forcing the soil through the screen was to eliminate large lumps of clay prior to compaction. The soil processed (through the screen) was then stored in covered containers to prevent moisture from evaporating, while the rest of the soil was processed through the screen. Approximately 2 to 3 percent of the soil's initial moisture content was typically lost after forcing the soil through the screen.
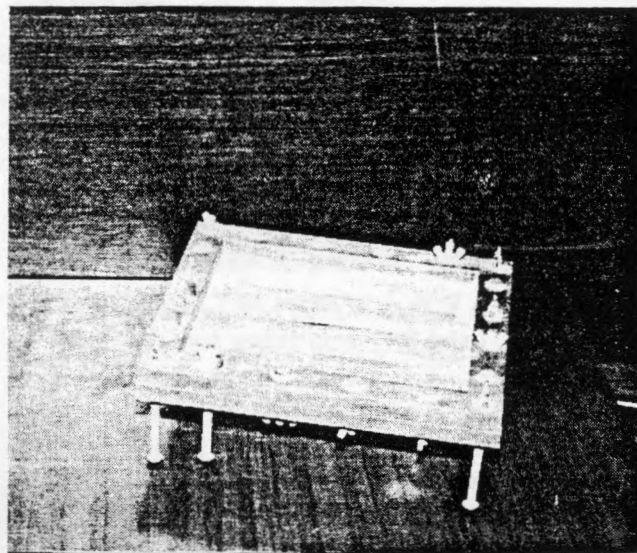
Figure 3.3   The screen framework used for processing soil prior to compaction

Soil Compaction Method

Soil specimens were compacted in 1.5-inch-diameter molds designed to produce either 3- or 5-inch-high specimens. The 3-inch-high specimens were set up directly for triaxial testing, whereas the 5-inch-high specimens were subjected to cyclic wetting and drying prior to triaxial testing. The 5-inch height was used to accommodate the loss in specimen height as a result of radial swelling in the specimen holder during wetting and drying. At the end of the wetting and drying process, the specimen height was at least 3 inches.

The compaction mold, shown in Figure 3.4 (for the 3-inch specimens), has also been described by Rogers and Wright (1986). The mold consists of four aluminum quadrants which can be disassembled at the end of compaction to remove the compacted specimen. Two sets of aluminum parts, one set 3 inches long and the other set 5 inches long, were manufactured to compact the 3-inch-and 5-inch-high specimens.
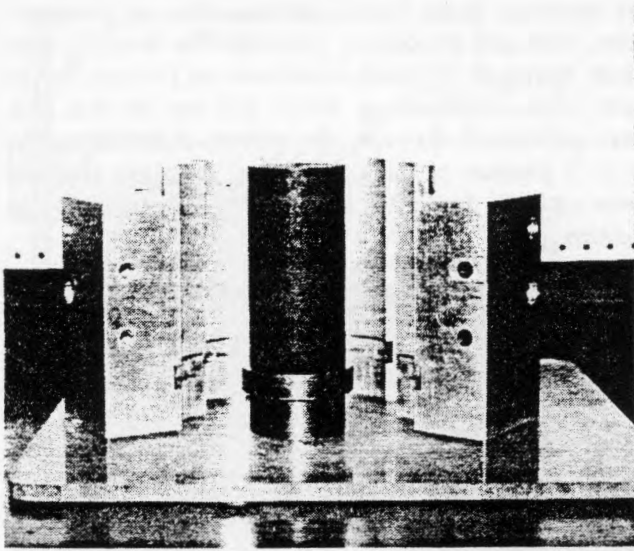
Figure 3.4   A disassembled compaction mold used for compacting soil specimens

Soil specimens were compacted in ten lifts for the 3-inch-high specimens, and in sixteen lifts for the 5-inch-high specimens. Approximately 15.4 grams of moist soil were typically compacted for each lift for the Paris clay, while 16.1 grams were used for each lift of the Beaumont clay. The surface of each compacted lift was scarified prior to compaction of the next lift.

An impact compaction hammer was utilized to compact each lift. The hammer consisted of a 2.15-pound weight which was dropped on a 1.48-inch-diameter acrylic, cylindrical anvil. Trial and error was used to determine the necessary height from which the weight should be dropped and the number of drops needed to produce the required dry density. It was found that each lift should be compacted with three blows of the hammer, dropped from a height of 8 inches for the Paris clay and from a height of 6 inches for the Beaumont clay. It was not necessary to change the weight of the compacted soil per lift nor to change the applied compaction energy when varying the heights of the compacted specimens.

Once compaction was completed, the specimen was trimmed flush with the top of the mold. The mold was disassembled, and the specimen was weighed to determine its total unit weight. Soil trimmings were used to measure the as-compacted moisture content prior to setting the specimen in the specimen holder. The dry unit weight of the compacted specimen was calculated using the measured total unit weight and moisture content.

THE WETTING AND DRYING PROCEDURES

Specimens subjected to wetting and drying were set up by first assembling the wire screen base of the specimen holder. A soil specimen was then positioned on the screen base, and the cylindrical screen was loosely wrapped around the specimen. The middle and top rings were subsequently placed around the screen. A minimum distance of 0.2 inches was typically maintained between the specimen and the screen to allow for swelling of the soil.

Wetting was accomplished by immersing the specimen holder and specimen in the container filled with distilled water. Drying was performed by placing the holder in the oven. During wetting, each specimen was immersed in its own container separate from other specimens. Sufficient water was added to the containers to substitute for any water absorbed by the soil. This ensured that specimens were entirely submerged during wetting. During drying, no more than three specimens were simultaneously dried in the 1.4-ft³ oven. Relative humidity measurements indicated that, for such drying conditions, the relative humidity in the oven did not exceed approximately 5 percent.

The first cycle of wetting and drying consisted of wetting, drying, and rewetting. Each additional cycle consisted of one additional drying period and one additional wetting period. After completion of the wetting and drying process, the specimen holder was removed from the water, and the screen was unwrapped after removing the top and middle rings. A typical specimen after wetting and drying is shown in Figure 3.5.
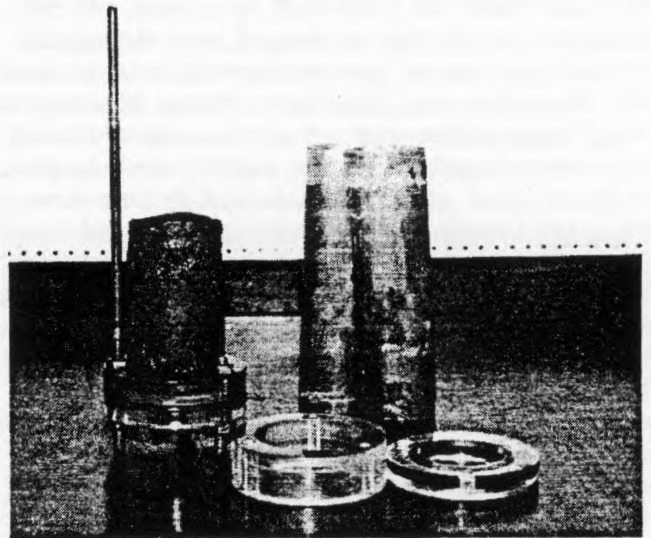
Figure 3.5   Soil specimen after removing the cylindrical screen at the end of wetting and drying

Duration of the Wetting Cycle

The duration of the wetting cycle was controlled by the time necessary for the specimen to

reach an equilibrium moisture content that would not change appreciably with time if the soil was allowed to remain submerged longer. To determine the necessary time for wetting, fourteen specimens of both Paris clay and Beaumont clay were compacted. The specimens were 1.5 inches in diameter and 3 inches high (the 3-inch-high mold was used). The specimens were submerged in water for approximately 2 days until no further change in their weight was observed. The specimens were then dried in an oven at a temperature of 60°C until soil moisture evaporation had ceased. The fourteen specimens were then soaked in water for various periods varying from 0.1 to 2880 minutes (48 hours). At the end of the wetting period, each specimen was removed from water, and the screen was unwrapped from around the specimen. The moisture content of the entire specimen was then measured.

Plots of moisture content versus wetting time are shown in Figure 3.6 for the Paris clay and in Figure 3.7 for the Beaumont clay. The measured moisture contents indicate that a large increase in soil moisture occurred during the first 10 minutes of wetting. Subsequent increase in moisture occurred at a much slower rate, and eventually stabilized after approximately 1,000 minutes for the Paris clay and 800 minutes for the Beaumont clay. Based on these results, it was concluded that a 24-hour wetting period was suitable. At the end of this period, no significant increase in the amount of moisture absorbed by the soil should be expected. At such time, the moisture content for the Paris clay (LL=80) was approximately 70 percent, and the moisture content for the Beaumont clay (LL=73) was approximately 50 percent.
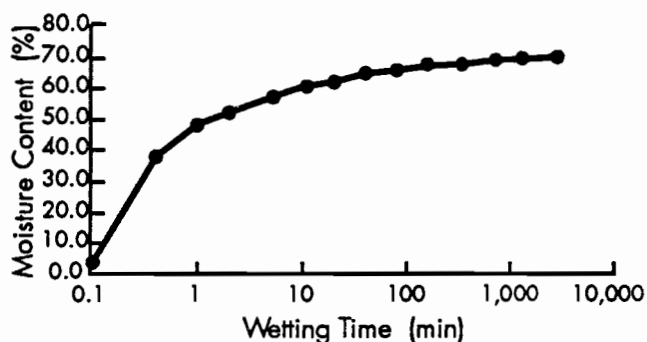
Figure 3.7 Measured moisture contents for Beaumont clay specimens which were wetted in distilled water to various wetting times

Duration of the Drying Cycle

The duration of the drying cycle was also selected based on the time necessary for a typical specimen to reach an equilibrium moisture content. Fourteen additional specimens each of Paris clay and Beaumont clay were prepared. The specimens were 1.5 inches in diameter and 3 inches high. The specimens were first subjected to one cycle of wetting and drying (wetting, drying, and rewetting). Wetting was conducted for 24 hours, drying was maintained until soil moisture evaporation had ceased (approximately 2 days), and rewetting was done for an additional 24 hours. The specimens were subsequently placed in an air convection oven set at a temperature of 60°C and containing no more than 3 specimens at one time. Specimens were dried for various periods ranging from zero to 72 hours. At the end of each drying period, the specimen was removed from the oven, and the screen was unwrapped from around the specimen. The moisture content of the entire specimen was then measured.

Plots of the moisture content versus drying time are presented in Figure 3.8 for the Paris clay and in Figure 3.9 for the Beaumont clay. The measured moisture contents indicate that the moisture decreases rapidly at first, and then occurs at a much slower rate. After approximately 1,000 minutes, very little change occurs. After 24 hours of drying, moisture contents varied from 3 to 4 percent for both clays. Based on these results, it was decided that specimens would be dried for 24 hours.

Figure 3.6 Measured moisture contents for Paris clay specimens which were wetted in distilled water to various wetting times
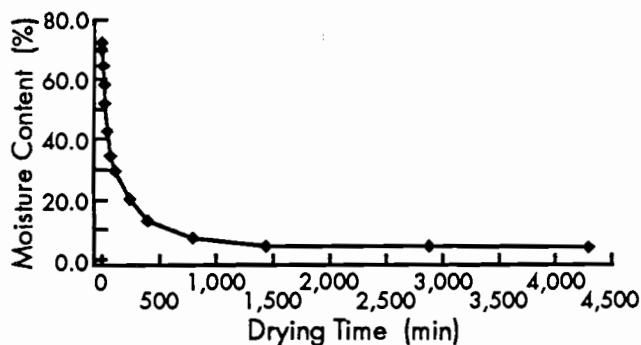
Figure 3.8   Measured moisture contents at various drying times for Paris clay specimens dried at a temperature of 60°C
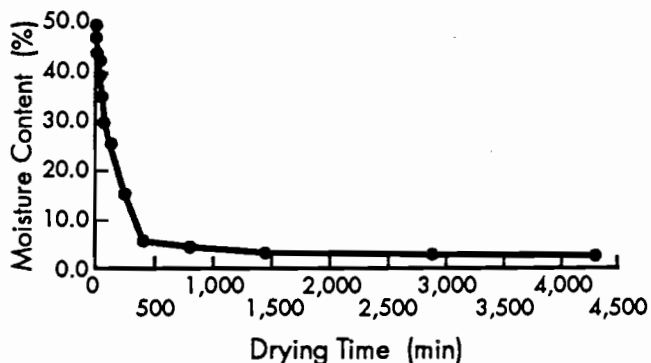
Figure 3.9   Measured moisture contents at various drying times for Beaumont clay specimens dried at a temperature of 60°C

Number of Cycles

The final variable that needed to be addressed for establishing the wetting and drying procedure was the number of cycles wetting and drying. According to Osipov et al (1987), cyclic wetting and drying results in a state of equilibrium moisture in soils which does not depend on the initial soil density, moisture, or scheme of cyclic wetting and drying adopted. The equilibrium moisture is a function of the soil composition and of changes in soil-water chemistry occurring during wetting. To investigate the effect of the number of cycles of wetting and drying, a number of specimens were prepared at different densities, moisture contents, and degrees of saturation. Specimens were prepared both by compaction and by consolidation from a slurry (procedures for consolidation of specimens from a slurry are included in Chapter Five). The specimens were subjected to from 1 to 35 cycles of wetting and drying. At the end of the last wetting cycle, the moisture content and degree of saturation were determined by measuring the specimen weight, and volume.

The measured moisture contents and degrees of saturation are plotted versus the number of wetting and drying cycles for the Paris clay specimens in Figures 3.10 and 3.11 and for the Beaumont clay specimens in Figures 3.12 and 3.13, respectively. For each specimen, there are two points shown: one (at zero cycles) representing initial conditions, and the other (at a cycle greater than zero) representing the condition after wetting and drying. It can be seen that the final equilibrium moisture content and degree of saturation after wetting and drying were largely independent of the initial moisture content and degree of saturation. In addition, for specimens which were subjected to approximately three cycles of wetting and drying or more, the final moisture content and degree of saturation were also independent of the number of wetting and drying cycles. The equilibrium moisture contents were approximately 70 percent for the Paris clay (Figure 3.10) and 50 percent for the Beaumont clay (Figure 3.12). The respective liquidity indices for these moisture contents are 0.83 and 0.56. It can be seen that the final degree of saturation for the Paris clay specimens reached 100 percent after approximately three cycles of wetting and drying (Figure 3.11). In contrast, the final degree of saturation for the Beaumont clay specimens did not exceed 85 to 90 percent regardless of the number of cycles of wetting and drying. This was possibly due to air bubbles getting trapped within the soil, although some specimens were initially fully saturated. Based on these results, it appears that the wetting and drying process caused the soil specimens to achieve a state of moisture equilibrium, regardless of the initial moisture content, after approximately three cycles of wetting and drying.

Prior to selecting the number of wetting and drying cycles to be employed in the subsequent laboratory tests, consideration was given to the issue of generating a fragmented clay structure in the laboratory to reproduce the cracking network typically observed in the field. Visual observations recorded during the wetting and drying experiments indicated that the orientation pattern and position of cracks would vary for each specimen and would vary from one cycle to another. A gradual breakdown in soil aggregates was observed as the number of cycles increased. The breakdown was observed to progress for approximately ten to fifteen cycles of wetting and drying. Based on these visual observations, twenty cycles of wetting and drying were selected for the subsequent testing. Twenty cycles were chosen because it was observed that no further breakdown in soil aggregates would occur after these cycles, and because cracks had propagated in all orientations as viewed from the top of the specimens.
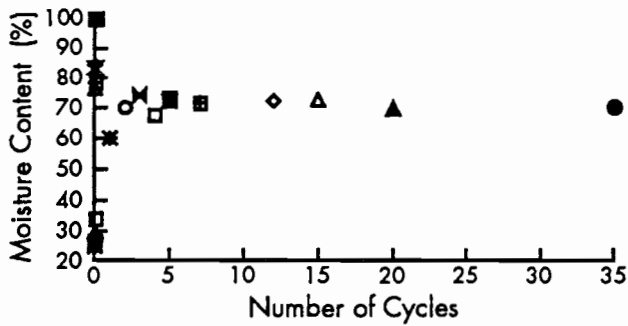
Figure 3.10 Equilibrium moisture contents for Paris clay specimens at a variable number of wetting and drying cycles *(moisture contents at zero cycles are the initial moisture contents prior to wetting and drying)*
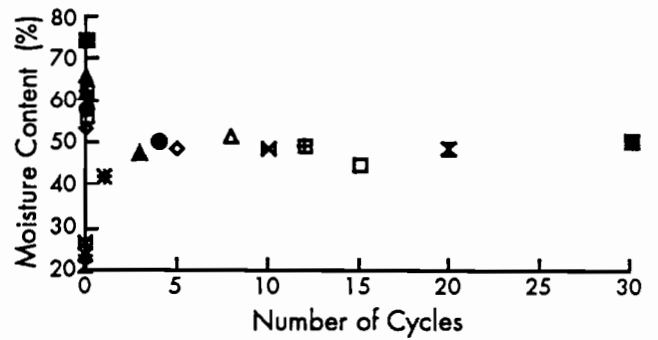
Figure 3.12 Equilibrium moisture contents for Beaumont specimens at a variable number of wetting and drying cycles *(moisture contents at zero cycles are the initial moisture contents prior to wetting and drying)*
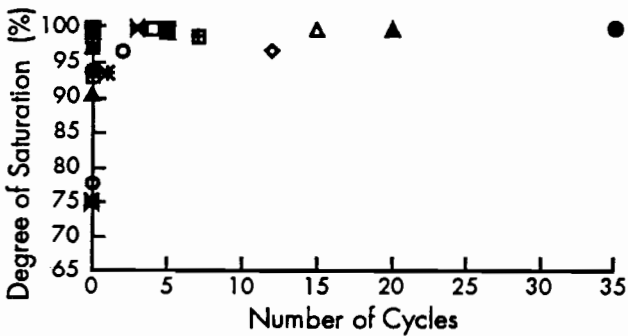
Figure 3.11 Degrees of saturation for Paris clay specimens at a variable number of wetting and drying cycles *(degrees of saturation at zero cycles are the initial degrees of saturation prior to wetting and drying)*
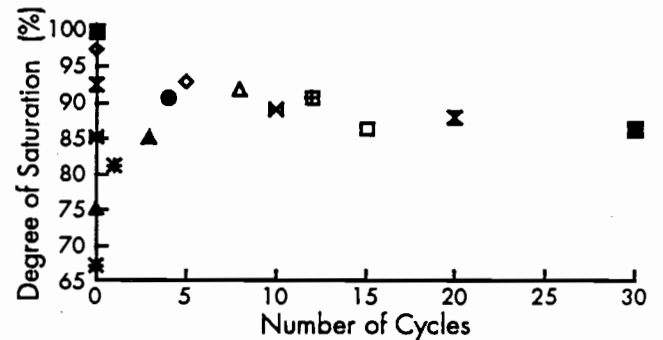
Figure 3.13 Degrees of saturation for Beaumont specimens subjected to a variable number of wetting and drying cycles *(degrees of saturation at zero cycles are the initial degrees of saturation prior to wetting and drying)*

15

CHAPTER 4. EFFECTS OF WETTING AND DRYING ON LONG-TERM STRENGTH OF COMPACTED CLAY SPECIMENS

INTRODUCTION

A series of consolidated-undrained triaxial compression tests with pore water pressure measurements was performed on specimens which were subjected to cyclic wetting and drying following the procedures described in Chapter 3. Tests were performed on specimens of both Paris and Beaumont clays. The purpose of these tests was to determine the effects of wetting and drying on the shear strength properties. To provide a basis for determining the effects, additional tests were performed on specimens tested in their as-compacted condition, without wetting and drying.

The strength tests were performed to determine long-term strength properties corresponding to drained strengths and characterized by effective stress failure envelopes. Consolidated-undrained ($\overline{CU}$) tests with pore pressure measurements were chosen for determining the effective-stress shear strength properties because the tests required somewhat less time to perform than consolidated-drained (CD) tests. Past experience has shown that the two test procedures ($\overline{CU}$ and CD) provide essentially identical effective-stress shear strength envelopes; one consolidated-drained test was performed in this study to confirm this.

PREPARATION OF SPECIMENS FOR TESTING IN AS-COMPACTED CONDITION

Triaxial specimens tested in the as-compacted condition were prepared following the procedures described in Chapter 3. The moisture content, total weight, and volume of compacted specimens were measured prior to set-up in the triaxial cell. The dry unit weight was calculated using the measured total unit weight and moisture content.

SAMPLING OF SPECIMENS SUBJECTED TO WETTING AND DRYING

Wetting and drying was conducted following the procedures described in Chapter 3. Five-inch-high compacted specimens were subjected to wetting and drying in the special specimen holders. At the end of twenty cycles of wetting and drying, the specimens were approximately 3.5 inches high and 2 inches in diameter (see Figure 3.5). After the wetting and drying, the specimens were trimmed to a diameter of 1.5 inches and a height of 3 inches for triaxial testing.

To trim the specimen, a 5-inch-long stainless steel tube, with a sharp cutting edge was used. The tube is 1.5 inches in inside diameter, with a 0.1-inch wall thickness. The area ratio of the sampling tube was 28 percent. This high area ratio was not believed to be significant because the specimen was not laterally constrained during sampling (the cylindrical screen in the specimen holder was removed prior to sampling). The tube was pushed slowly into the soil specimen until it reached the bottom of the specimen. Soil on the exterior of the sampling tube was removed, and the end of the soil inside the tube was trimmed flush with the bottom of the tube. A filter paper was placed on the trimmed surface, and the specimen was positioned on top of a 1.49-inch-diameter acrylic plastic rod as shown in Figure 4.1. The tube was slid down the acrylic rod to the level where the soil remaining inside the tube was approximately 3 inches high. Typically, approximately 0.3 to 0.5 inches of soil had been extruded from the top of the sampling tube at this stage. The tube was fixed at that level for trimming the extruded soil. The tube was fixed in place with a peg that fit into holes drilled transversely into the acrylic rod on which the specimen rested. The extruded soil was removed from the top of the specimen by trimming flush with the top of the sampling tube. A filter paper was placed on top of the specimen. The peg was removed, and the tube was slid down further until the specimen was completely extruded, as shown in Figure 4.2. The sampling tube was pushed in the same direction relative to the soil during the sampling *and* extrusion of the specimen. The extruded specimen was subsequently transferred to the triaxial cell by

means of a thin plastic wrap. The plastic wrap was sprinkled with talcum powder to prevent soil from adhering to it.

Figure 4.1 The sampling tube placed on top of the acrylic rod to extrude the soil specimen *(shown supported on the lateral bar after trimming the top soil surface)*

Figure 4.2 A specimen subjected to wetting and drying after being extruded from the sampling tube and prior to set-up in a triaxial cell

Effect of the Sampling Procedure on the Effective Stress Envelope

To investigate the effect of the sampling procedure on the measured effective-stress shear strength envelopes, a series of consolidated-undrained triaxial compression tests with pore water pressure measurements was performed on specimens of Beaumont clay which were consolidated from a slurry. The use of specimens consolidated from a slurry was justified based on subsequent observations which showed that specimens subjected to wetting and drying had similar strength properties to those of specimens consolidated from a slurry. One specimen was consolidated in a 3-inch-diameter tube, and three specimens were consolidated in 1.5-inch-diameter tubes. A 1.5-inch-diameter specimen was obtained from the sample consolidated in the 3-inch-diameter tube using the sampling procedure described earlier. The specimens consolidated in the 1.5-inch-diameter tubes did not need to be sampled prior to set-up in the triaxial cells (this procedure is described in Chapter 5). The effective stress paths for the specimens, and the measured failure envelope based on stress path tangency, are shown in Figure 4.3. The moisture contents of the trimmed and untrimmed specimens consolidated to a consolidation pressure of 4 psi and the strains and $\overline{A}$ coefficients at peak principal stress ratio are tabulated in Table 4.1. It can be seen that the stress path of the specimen which was sampled from the 3-inch sample reaches the same effective stress failure envelope as the specimens which were not sampled. In addition, the difference in the moisture contents and strains at failure is less than 2 percent. The difference in the $\overline{A}$ coefficients is approximately 7 percent, suggesting that the sampling procedure had a small effect on the undrained behavior of the soil. However, the sampling procedure does not appear to influence the effective-stress shear strength properties of the soil.
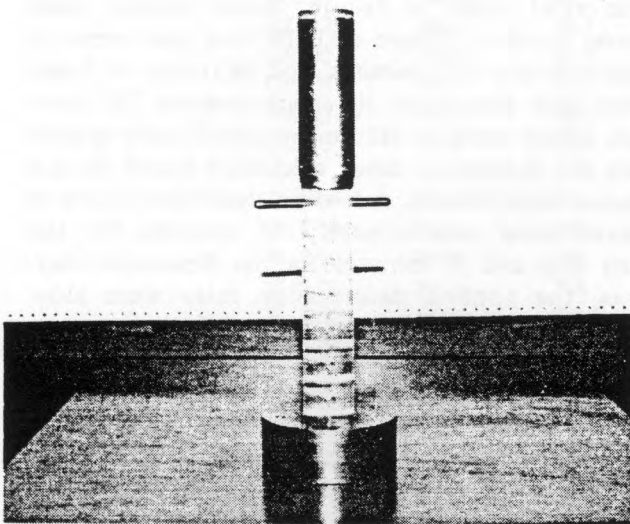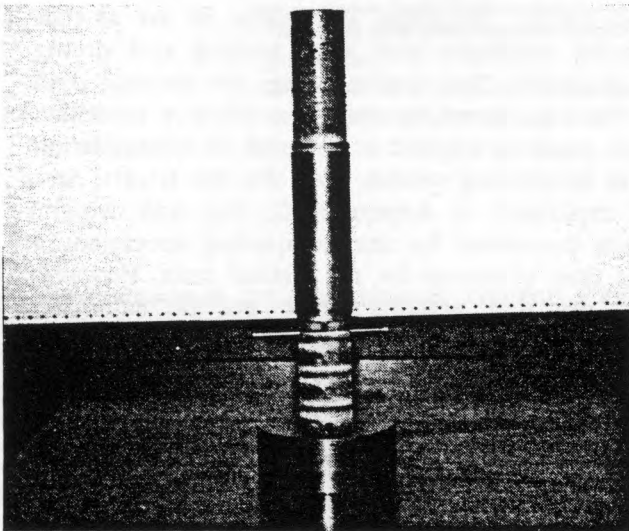
SUMMARY OF TRIAXIAL TEST PROCEDURES

Procedures for back-pressure saturation, isotropic consolidation, and shear are summarized below. A detailed description of these procedures is included in Appendix B.

Figure 4.3 **Effective stress path curves for 1.5-inch diameter Beaumont clay specimens and for a 3.0-inch diameter specimen sampled with the 1.5-inch diameter sampling tube**

Table 4.1 **Comparison of triaxial data for trimmed and untrimmed specimens**

Test Number	Moisture Content (%)	Strain (%)	$\bar{A}$ - Coefficient
3-inch-diameter specimen (trimmed)			
S51.04	43.2	5.9	0.86
1.5-inch-diameter specimen (untrimmed)			
S53.04	42.5	6.0	0.80

Specimens were back-pressure saturated prior to isotropic consolidation to the final effective consolidation pressure. For tests with a final effective consolidation pressure of 5 psi or less, the effective consolidation pressure used during back-pressure saturation was typically 1 psi lower than the final effective consolidation pressure. For tests with a final effective consolidation pressure higher than 5 psi, the effective consolidation pressure used during back-pressure saturation was 5 psi.

Specimens were consolidated to effective stresses ranging from 1 to 35 psi. The relatively low pressures were chosen to represent the low

overburden pressures typically acting along the shallow slide surfaces which were of interest.

The deformation rates used to shear the Paris and Beaumont clay specimens were 0.0009 and 0.0047 inches per hour, respectively. For a 1 percent axial strain at failure, these loading rates would result in failure of Paris clay specimens in approximately 900 minutes, and in failure of Beaumont clay specimens in approximately 300 minutes. These times to failure are significantly greater than the theoretical times calculated based on the triaxial consolidation data. The theoretical times to failure were approximately 45 minutes for the Paris clay and 30 minutes for the Beaumont clay. Thus, the applied deformation rates were slow enough to ensure the equalization of the pore water pressures along the height of the specimens. Furthermore, since effective stress path tangency was of interest for the current study, the deformation rates were believed to be even more adequate because effective stress path tangency occurred later than peak principal stress difference.

TRIAXIAL CONSOLIDATION RESULTS

Moisture contents and dry unit weights of Paris and Beaumont clay specimens, at the time of set-up and at the end of consolidation are tabulated in Table 4.2. The prefix letters "C" and "W" in the test names designate specimens in an as-compacted condition and after wetting and drying, respectively. The numbers after the decimal point in the test names represent the effective consolidation pressure applied at the end of consolidation. The numbering system used for the triaxial tests is explained in Appendix C. Dry unit weights were computed for the compacted specimens at the time of set-up for the triaxial tests. However, the dry unit weights could not be calculated for the specimens which were subjected to wetting and drying because representative moisture content measurements could not be obtained. Dry unit weights at the end of consolidation (and during shear) were calculated for all specimens based on the measured moisture contents at the end of testing, and assuming 100 percent saturation after undrained shear.

Table 4.2 Triaxial specimen properties at set-up and at end of consolidation for the Paris and Beaumont clays

Test Number	Soil Type	At Set-Up		At End of Consolidation	
		ω_c (%)	γ_d (pcf)	ω_c (%)	γ_d (pcf)
C20.35	Paris	26.5	89.8	34.7	87.4
C22.12	Paris	26.7	88.8	38.7	82.7
C23.23	Paris	25.3	87.4	36.6	85.0
C25.015	Paris	27.3	89.7	45.0	76.3
C26.01	Paris	28.4	88.7	45.8	75.5
C27.05	Paris	26.4	89.6	41.7	79.6
W40.08	Paris	NA	NA	44.4	76.9
W41.12	Paris	NA	NA	40.9	80.4
W42.20	Paris	NA	NA	36.8	84.8
W43.04	Paris	NA	NA	51.6	70.6
W44.30	Paris	NA	NA	35.6	86.3
W45.02	Paris	NA	NA	56.5	66.9
C70.08	Beaumont	22.3	101.0	26.5	100.4
C71.25	Beaumont	21.8	102.5	23.9	102.9
C72.02	Beaumont	21.6	102.1	27.6	97.5
C73.05	Beaumont	21.3	102.0	25.8	100.0
C74.16	Beaumont	22.7	100.8	24.2	102.6
C75.03	Beaumont	24.5	98.2	27.5	97.2
W60.07	Beaumont	NA	NA	29.4	94.7
W61.20	Beaumont	NA	NA	23.9	103.1
W62.03	Beaumont	NA	NA	32.5	90.4
W63.12	Beaumont	NA	NA	26.0	99.6
W64.30	Beaumont	NA	NA	22.1	106.2
W65.02	Beaumont	NA	NA	35.2	87.0

- Numbers after decimal points represent the applied effective consolidation pressures.
- Letters C and W in test names designate specimens in as-compacted condition, and after wetting and drying, respectively.

The variation in the final moisture contents with the effective consolidation pressures is shown in Figure 4.4 for the Paris clay and in Figure 4.5 for the Beaumont clay. It can be seen from these plots that, at low effective stresses (which are of interest for the current study) the moisture contents for the specimens tested in the as-compacted condition were lower than the moisture contents for the specimens which were subjected to wetting and drying. The differences between the two sets of moisture contents are evident for both the Paris and the Beaumont clays. The difference in moisture content decreases as the effective consolidation pressure acting on the soil increases.

TRIAXIAL SHEAR TEST RESULTS

Axial stress-strain curves, effective stress paths, and modified Mohr-Coulomb failure envelopes were plotted and examined for specimens tested in the as-compacted condition, and for specimens subjected to wetting and drying. Triaxial shear test data including axial strains (ε), effective consolidation pressures ($\overline{\sigma}_3$), principal stress differences ($\sigma_1 - \sigma_3$), principal stress ratios ($\overline{\sigma}_1 / \overline{\sigma}_3$), and $\overline{A}$ coefficients are tabulated in Appendix C.

Stress-Strain Curves

The variation in the principal stress difference ($\sigma_1 - \sigma_3$) with axial strain (ε) for the Paris clay is shown in Figure 4.6 for specimens which were tested in the as-compacted condition and in Figure 4.7 for specimens which were subjected to wetting and drying. The corresponding curves for the Beaumont clay specimens are shown in Figures 4.8 and 4.9, respectively.
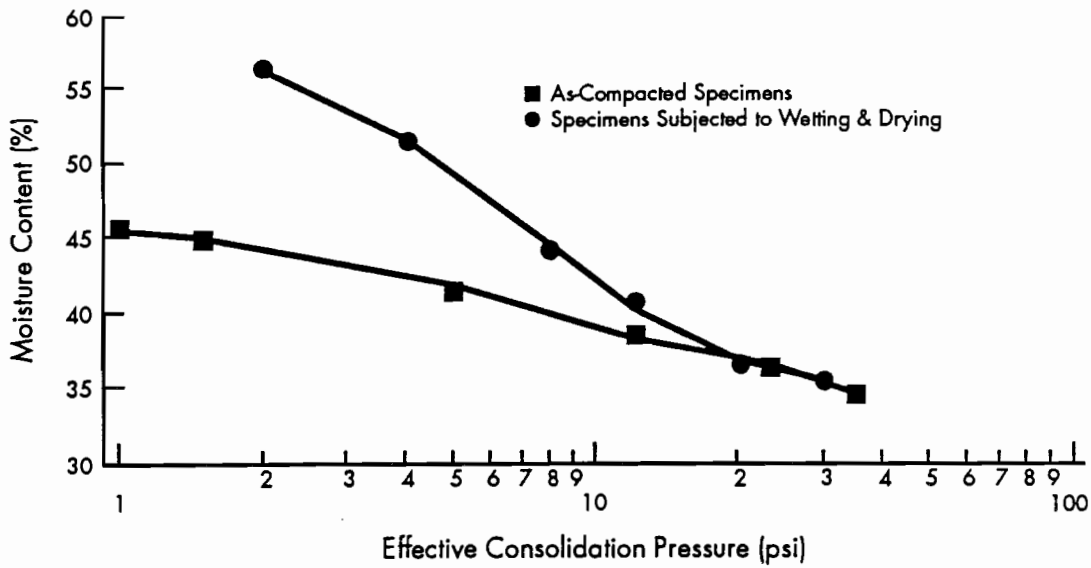
Figure 4.4 Final moisture contents versus the effective consolidation pressures for as-compacted Paris clay specimens and for specimens subjected to wetting and drying
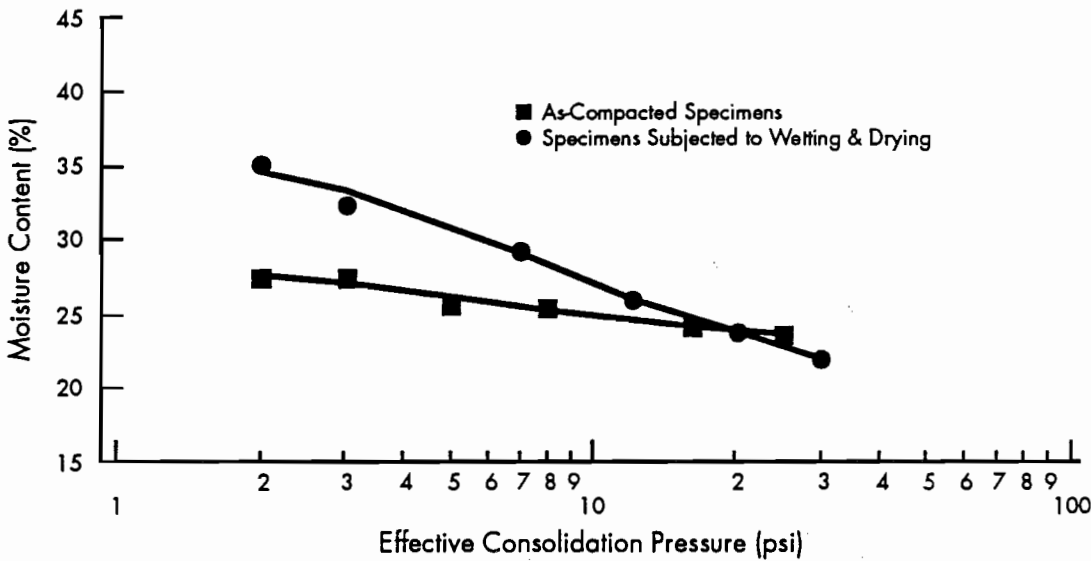
Figure 4.5 Final moisture contents versus the effective consolidation pressures for as-compacted Beaumont clay specimens and for specimens subjected to wetting and drying
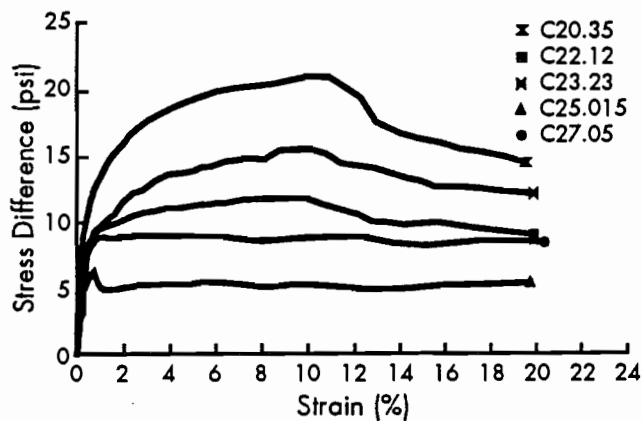
Figure 4.6 Stress strain curves for Paris clay specimens tested in an as-compacted condition
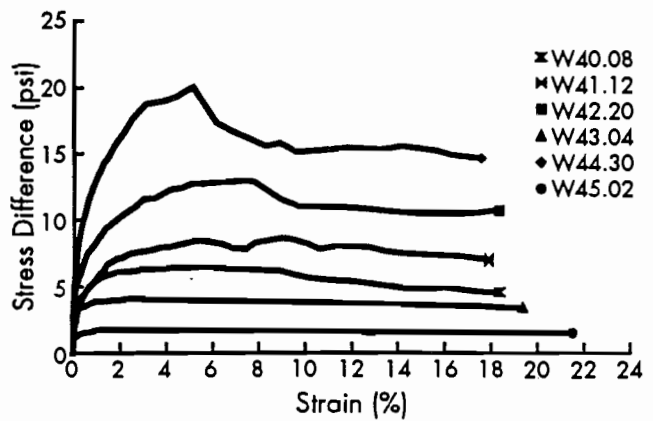
Figure 4.7 Stress strain curves for Paris clay specimens subjected to wetting and drying
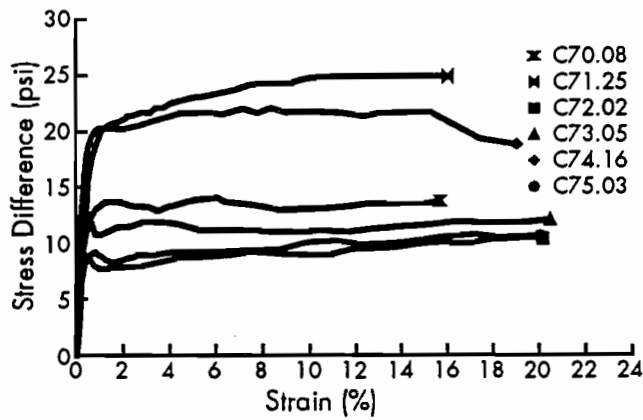
Figure 4.8 **Stress strain curves for Beaumont clay specimens tested in an as-compacted condition**
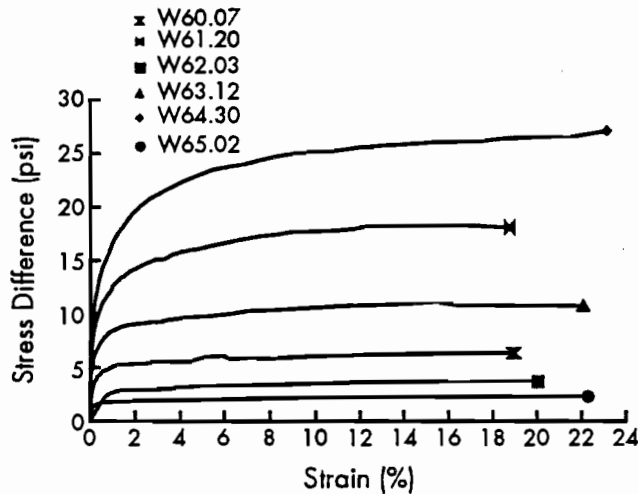
Figure 4.9 **Stress strain curves for Beaumont clay specimens subjected to wetting and drying**

The stress-strain curves for the Paris clay indicate that the principal stress difference decreases slightly at strains beyond the peak principal stress difference. The decrease in principal stress difference is relatively small for all specimens (10 to 25 percent of the peak stress difference). The decrease in principal stress difference is also similar for specimens tested in the as-compacted condition, as well as for specimens subjected to wetting and drying. The stress-strain curves for the Beaumont clay also indicate that the undrained stress-strain behavior for the as-compacted specimens is similar to that of the specimens which were subjected to wetting and drying. The decrease in principal stress difference at large strains for the Beaumont clay is relatively insignificant (less than 10 percent).

Effective Stress Paths and Failure Envelopes

Effective stress paths were plotted in terms of principal stress difference ($\sigma_1-\sigma_3$) versus the minor principal effective stress ($\overline{\sigma}_3$). The effective stress paths for the Paris clay are shown in Figure 4.10 for specimens tested in the as-compacted condition, and in Figure 4.11 for specimens which were wetted and dried. The corresponding plots for the Beaumont clay specimens are shown in Figures 4.12 and 4.13, respectively. Also shown on these plots are the modified Mohr-Coulomb failure envelopes drawn approximately tangent to the effective stress paths (stress path tangency).
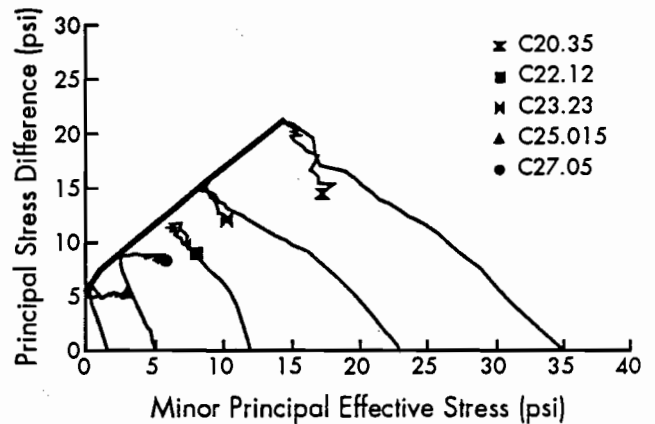
Figure 4.10 **Effective stress paths for Paris clay specimens tested in the as-compacted condition**
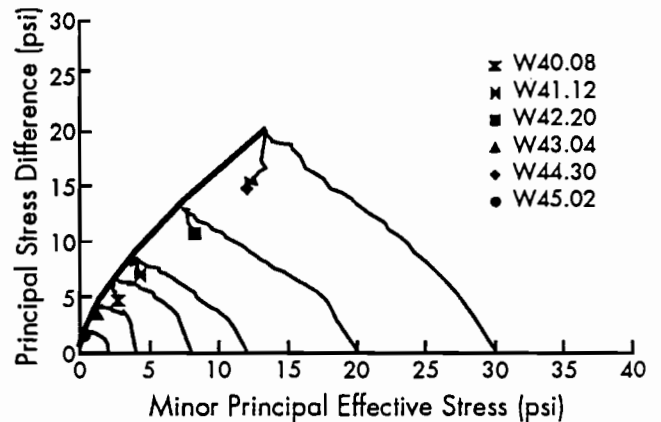
Figure 4.11 **Effective stress paths for Paris clay specimens subjected to wetting and drying**

21
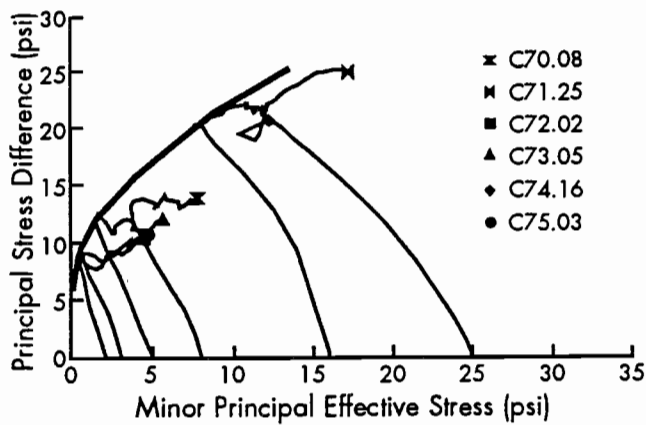
Figure 4.12 Effective stress paths for Beaumont clay specimens tested in the as-compacted condition

Legend:
- x C70.08
- H C71.25
- ■ C72.02
- ▲ C73.05
- ◆ C74.16
- ● C75.03
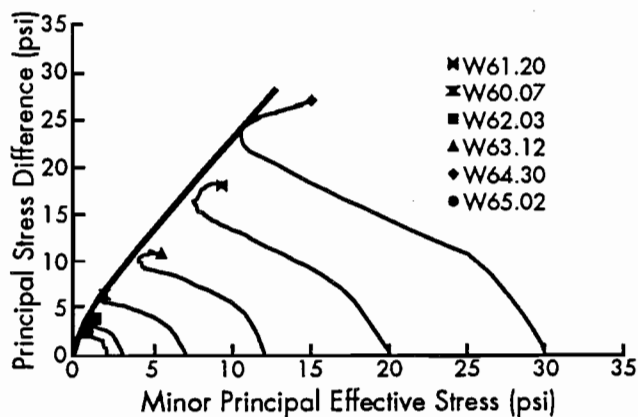
Figure 4.13 Effective stress paths for Beaumont clay specimens subjected to wetting and drying

Legend:
- H W61.20
- x W60.07
- ■ W62.03
- ▲ W63.12
- ◆ W64.30
- ● W65.02

In comparing the effective stress paths for specimens tested in the as-compacted condition with the stress paths for specimens subjected to wetting and drying, it is apparent that the specimens which were wetted and dried generated higher pore water pressures during shear. The increase in the magnitude of the generated pore pressures can be represented in terms of the $\overline{A}$ coefficients (Skempton, 1954). $\overline{A}$ is defined as the ratio of generated pore pressure during shear divided by the principal stress difference. Plots of $\overline{A}$ at the peak principal stress difference versus the effective consolidation pressures are shown in Figure 4.14 for the Paris clay and in Figure 4.15 for the Beaumont clay. The $\overline{A}$ coefficients for specimens which were wetted and dried show a slight variation with the applied consolidation pressures (in the range of 0.7 to 1.0). In contrast, the $\overline{A}$ coefficients for specimens tested in the as-compacted condition show a gradual increase with the consolidation pressure, from a value of

$\overline{A}$ of approximately 0.2 at low pressures to between 0.6 and 1.0 at higher pressures.

Modified Mohr-Coulomb failure envelopes based on stress path tangency were compared for specimens tested in the as-compacted condition and for specimens which were wetted and dried. This comparison is shown in Figure 4.16 for the Paris clay and in Figure 4.17 for the Beaumont clay. It can be seen from these plots that wetting and drying leads to lower strengths over a range of confining pressures as compared to the strengths of as-compacted specimens. This loss in strength was also observed in similar tests performed on Taylor Marl clay by Kayyal (1986). The loss in strength manifests itself by producing a distinct curvature in the Mohr-Coulomb failure envelopes at low effective stresses. The envelopes for the soils which were wetted and dried exhibit almost no *cohesion* intercept at zero effective stress. The envelope at higher pressures tends to merge with the envelopes for the soil in the as-compacted condition.
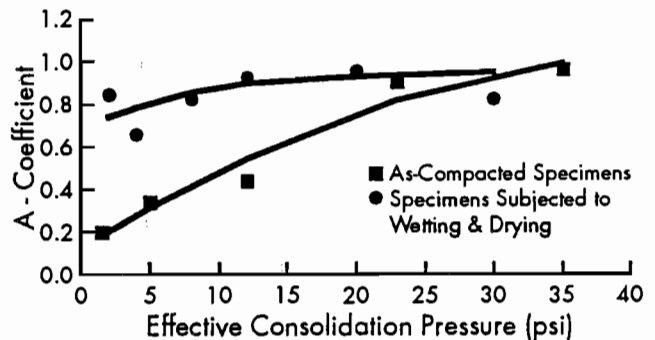
Figure 4.14 $\overline{A}$ coefficients at peak stress difference versus effective consolidation pressure for as-compacted Paris clay and for specimens subjected to wetting and drying

Legend:
- ■ As-Compacted Specimens
- ● Specimens Subjected to Wetting & Drying
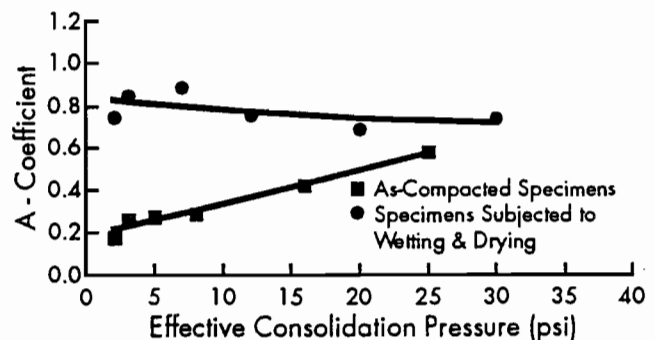
Figure 4.15 $\overline{A}$ coefficients at peak stress difference versus effective consolidation pressure for as-compacted Beaumont clay and for specimens subjected to wetting and drying

Legend:
- ■ As-Compacted Specimens
- ● Specimens Subjected to Wetting & Drying
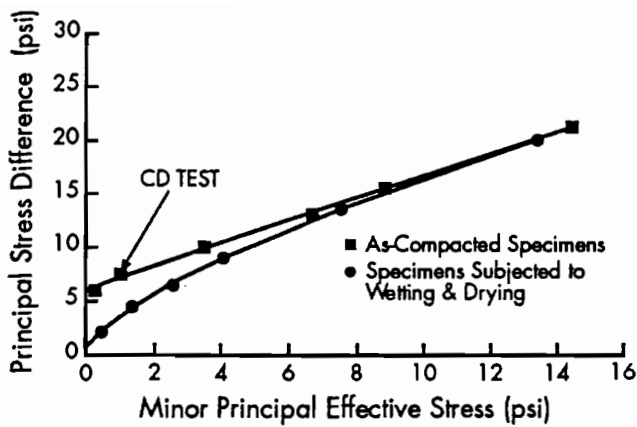
Figure 4.16 Modified Mohr-Coulomb failure envelopes for as-compacted Paris clay specimens and for specimens subjected to wetting and drying
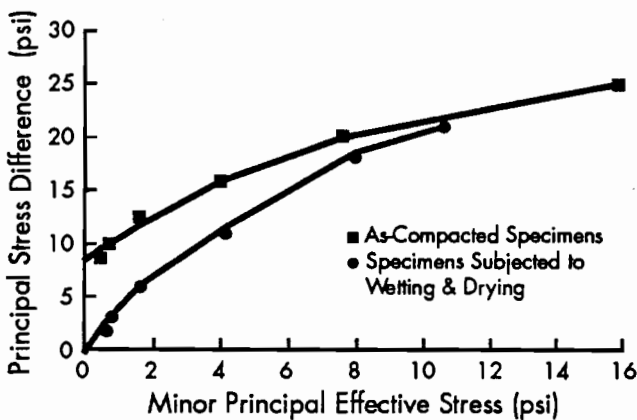
Figure 4.17 Modified Mohr-Coulomb failure envelopes for as-compacted Beaumont clay specimens and for specimens subjected to wetting and drying

Comparison of Effective Stress Envelopes for $\overline{CU}$ and CD Tests

A single consolidated-drained triaxial compression test (CD) was performed on a compacted specimen of Paris clay to determine whether the effective-stress shear strength envelopes obtained from $\overline{CU}$ and CD tests were similar. The CD test was performed following the same procedures described for performing $\overline{CU}$ tests. The specimen was back-pressure saturated prior to consolidation. The deformation rate used during shear was 0.0009 inches per hour. Similar CD tests were also performed on compacted Beaumont clay specimens by Gourlay and Wright (1986).

The effective stress path for the Paris clay specimen tested under drained conditions is shown in Figure 4.18 along with the effective stress paths from the $\overline{CU}$ tests. It can be seen from these plots

that the strength from the CD test agrees well with the strength envelope derived from the $\overline{CU}$ tests. This agreement confirms that the effective stress failure envelope for the Paris clay may be obtained from either $\overline{CU}$ or CD tests. Gourlay and Wright (1986) reached a similar conclusion for the Beaumont clay.
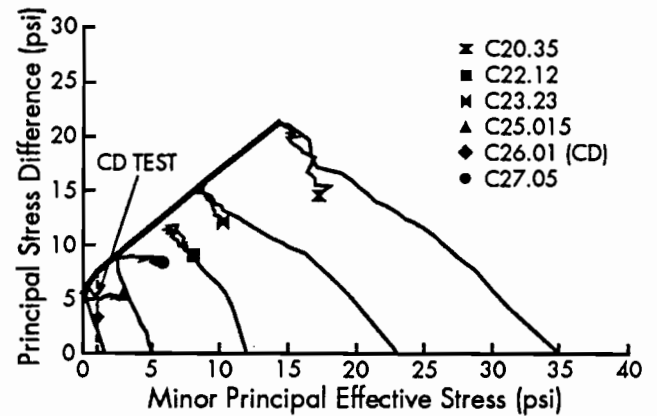
Figure 4.18 Effective stress paths for Paris clay specimens tested in the as-compacted condition using consolidated-drained and consolidated-undrained tests

COMPARISON BETWEEN PEAK STRENGTH AND LARGE STRAINS ENVELOPES

The effective stress paths for the Paris and Beaumont clays in the as-compacted condition indicate that a noticeable drop in strength occurs at strains beyond the peak strength. This drop in strength suggested that there might be some similarities between the strength at large strains for the as-compacted specimens and the peak strength for specimens which were wetted and dried.

Determination of failure envelopes at large strains involved some assumptions concerning the cross-sectional area of the specimens used to compute stresses. Area corrections used for the computation of stresses are discussed in Appendix D.

The failure envelope based on stresses at large strains for specimens tested in as-compacted condition is compared with the peak strength envelopes for the specimens which were subjected to wetting and drying. The "large strains" envelope consists of the measured strength values at axial strains in the range of approximately 17 to 23 percent. The comparison between the peak strength and large strains envelopes is shown in Figure 4.19 for the Paris clay and in Figure 4.20 for the Beaumont clay. It can be seen from the plots in Figures 4.19 and 4.20 that the peak strength envelope for specimens which were subjected to wetting and drying and the large strains envelope for the as-compacted specimens converge at low

effective stresses, indicating similar strength properties. However, at higher effective stresses, the peak strengths of specimens that were subjected to wetting and drying are higher than the strengths of as-compacted specimens at large strains.

Comparisons between the strength envelopes at large strains for specimens tested in the as-compacted condition, and those for specimens tested after wetting and drying, are shown in Figure 4.21 for the Paris clay and in Figure 4.22 for the Beaumont clay. The plotted envelopes are in reasonably close agreement.

Figure 4.19 Modified Mohr-Coulomb failure envelopes for as-compacted Paris clay at large strains and for specimens subjected to wetting and drying at peak strength

Figure 4.20 Modified Mohr-Coulomb failure envelopes for as-compacted Beaumont clay at large strains and for specimens subjected to wetting and drying at peak strength
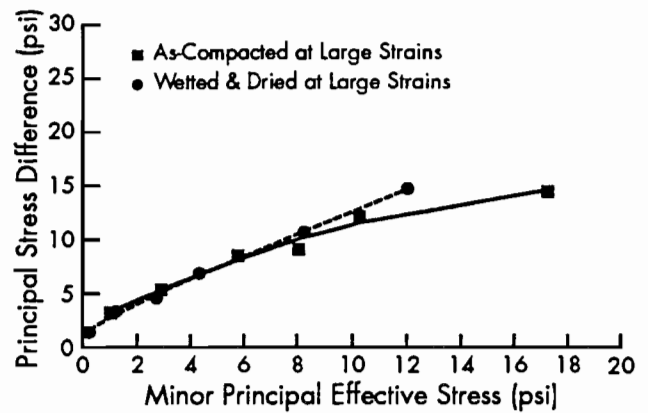
Figure 4.21 Modified Mohr-Coulomb failure envelopes at large strains for as-compacted Paris clay specimens and for specimens subjected to wetting and drying
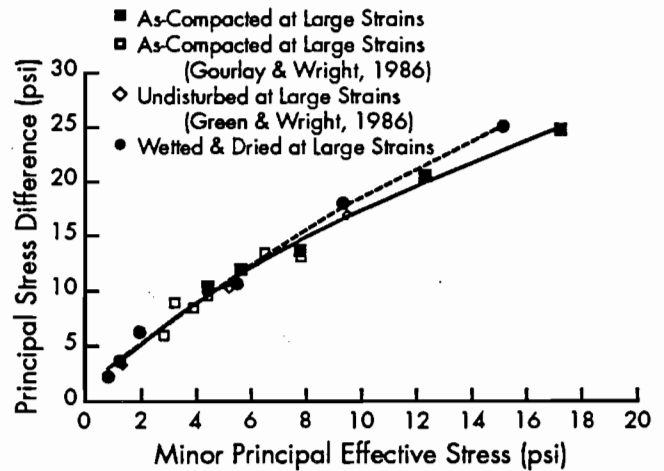
Figure 4.22 Modified Mohr-Coulomb failure envelopes at large strains for as-compacted Beaumont clay specimens and for specimens subjected to wetting and drying

SUMMARY AND CONCLUSIONS

A series of consolidated-undrained triaxial compression tests with pore pressure measurements was performed on specimens in their as-compacted condition and on specimens which were subjected to wetting and drying. The purpose of these tests was to determine the effect of wetting and drying on the long-term strength of compacted Paris and Beaumont clays.

Test results indicated that wetting and drying led to a drop in strength from that which was measured for specimens tested in the as-compacted condition. This loss in strength occurred over a range of stresses below approximately 8 psi; which is applicable to shallow slides in the field. Comparisons between the envelopes at large strains for specimens which were subjected to wetting and drying, and for specimens which were tested in the as-compacted condition, indicate that the envelopes were similar.

The effective-stress shear strength envelopes for the soils which were subjected to wetting and drying exhibited almost no *cohesion* intercept and showed a pronounced curvature downward. The envelopes for the soil subjected to wetting and drying gradually merged at higher pressures with the envelopes for the soil in the as-compacted condition.

The negligible cohesion intercept suggested that there might be similarities between the strength envelope of compacted specimens which were wetted and dried and the strength envelope of normally consolidated clays. Also, Skempton (1977) has shown that, with time, certain clay soils may reach a "fully softened strength" that is equivalent to the strength of remolded normally consolidated clays. Accordingly, it was decided to proceed with the current investigation to measure the strength properties of laboratory prepared normally consolidated specimens.

CHAPTER 5. EVALUATION OF THE CONSOLIDATION AND SHEAR STRENGTH PROPERTIES FOR NORMALLY CONSOLIDATED SPECIMENS

INTRODUCTION

A series of consolidated-undrained triaxial compression tests with pore water pressure measurements was performed on specimens which were normally consolidated from a slurry. The purpose of the tests was to measure the effective-stress shear strength properties for normally consolidated specimens and to compare their consolidation and shear strength properties with the properties of specimens which were subjected to wetting and drying.

SPECIMENS PREPARATION PROCEDURES

The soil used to prepare normally consolidated specimens was processed by sieving to a particle size passing the No. 40 sieve. The processed soil was mixed with water to form a slurry which was normally consolidated one-dimensionally to produce 1.5-inch-diameter, 3-inch-high specimens.

Soil Preparation Procedure

Specimens were prepared by mixing approximately 300 grams of air-dried soil with 400 grams of distilled water to form a slurry with a moisture content of approximately 150 percent. Water was placed in the bowl of a low speed mixer, and soil was then slowly added until a homogeneous slurry was formed. Once all the soil was mixed, the slurry was transferred to the consolidation apparatus.

Consolidation Apparatus

The consolidation apparatus was designed to produce approximately 3-inch-high specimens.

The apparatus is shown in Figure 5.1. It consists of three acrylic plastic tubes, 1.5 inches in inside diameter and 0.25 inches in wall thickness. The three tubes are 3.1 inches, 3.2 inches, and 12 inches long. When assembling the apparatus, the set of tubes was stacked on top of each other in the order shown in Figure 5.1; the 12-inch-long tube being on top. The tubes were then aligned along their inside wall by means of a 1.5-inch-diameter rod, and secured in place between a bottom base and a top ring connected with three threaded rods. A porous stone that fits into the bottom base provides for drainage of water during consolidation. Load is applied to the soil by means of a loading piston. The piston consists of a 1.5-inch-diameter solid acrylic cylinder. A porous stone fits on the bottom of the piston and allows drainage of water through two vertical holes. A Teflon ring is attached to the bottom of the piston to seal against possible leaks of soil slurry during consolidation. Load is transferred to the piston by means of a 15-inch-long acrylic rod with a 3-inch-diameter plate connected to the top of the rod.

Consolidation Procedure

Once the soil slurry is mixed, it is poured into the consolidation apparatus. The piston is advanced into the tube until contact is made with the soil slurry. A vertical consolidation pressure of 2 psi is then applied to the piston. The 2-psi pressure was chosen to produce adequate strengths in specimens for set-up in the triaxial cell. The period of consolidation of the soil specimens varied from ten days to two weeks.
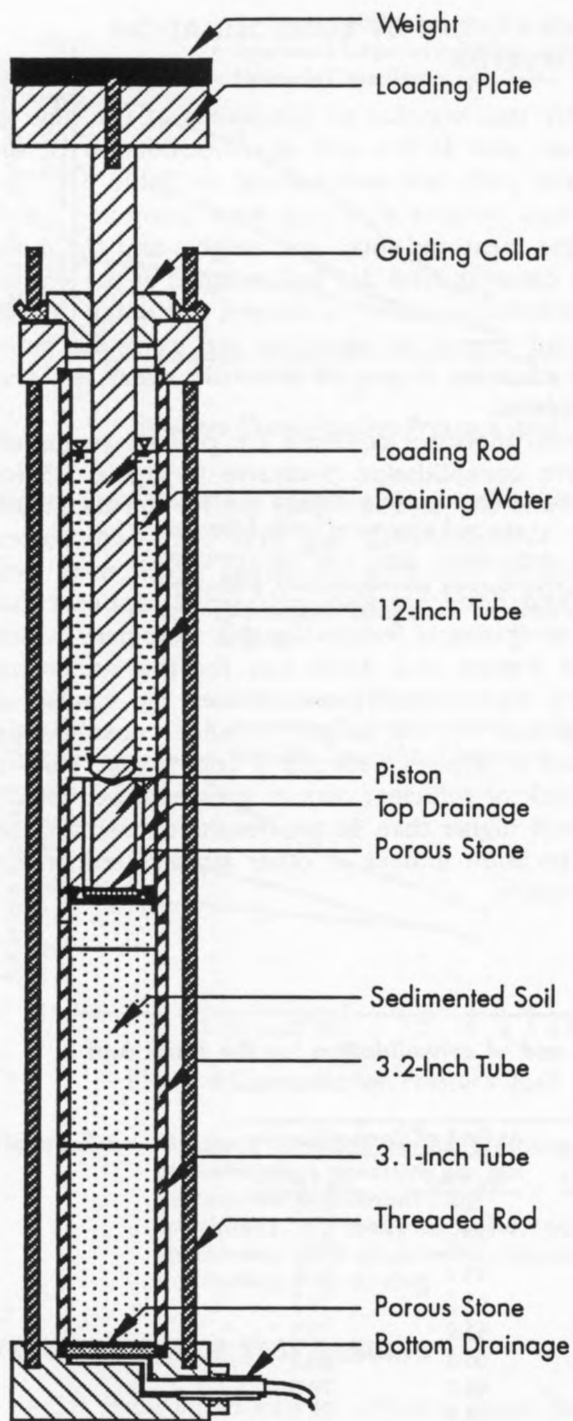
Figure 5.1 Consolidation apparatus with a consolidated specimen

Labels (top to bottom):
- Weight
- Loading Plate
- Guiding Collar
- Loading Rod
- Draining Water
- 12-Inch Tube
- Piston
- Top Drainage
- Porous Stone
- Sedimented Soil
- 3.2-Inch Tube
- 3.1-Inch Tube
- Threaded Rod
- Porous Stone
- Bottom Drainage

Preparation of Triaxial Specimens

At the end of the consolidation period, the vertical loads were removed and the free water was poured out from the consolidation apparatus. The top ring and the threaded rods were then disassembled, leaving the three tubes stacked vertically with the soil in them. Cautiously, each of the top two tubes was displaced laterally with respect to the tube below. This process resulted in three separate sections of consolidated soil. The soil in the top and bottom tubes was used to measure the moisture content of the soil. The soil in the middle tube was trimmed at both ends, and the trimmings were discarded. The middle tube containing the soil specimen was weighed, and a filter paper was placed on the bottom of the specimen. Since the weight of the tube was known, it was possible to compute the weight of the soil specimen prior to set-up in the triaxial cell. The specimen was extruded by means of a 1.49-inch-diameter solid acrylic rod, as shown in Figure 5.2, using the same procedure described for extruding the wetted and dried specimens from the sampling tube. The extruded specimen was transferred to the triaxial cell by means of a thin plastic wrap. The plastic was sprinkled with talcum powder to prevent soil from adhering to it.

Hydrometer analyses were performed for soil samples from the middle tube and from specimens which were wetted and dried. Results are shown in Figure 5.3 for the Paris clay and in Figure 5.4 for the Beaumont clay. It can be seen that the differences in the grain size distributions for each soil are negligible.
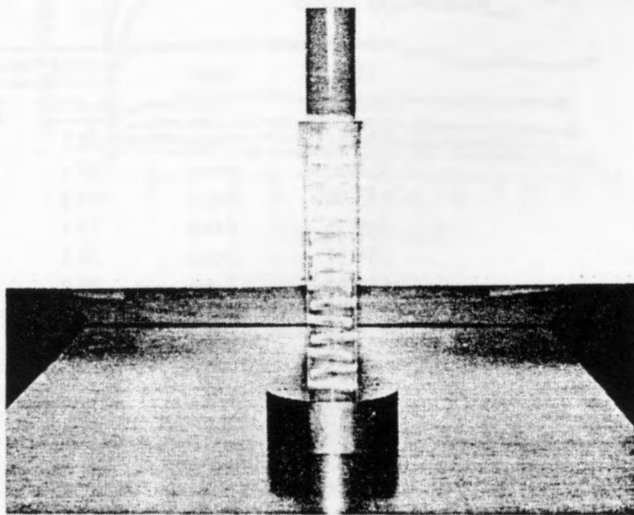
Figure 5.2 Extrusion of a specimen consolidated from a slurry with the 1.49-inch-diameter acrylic plastic rod
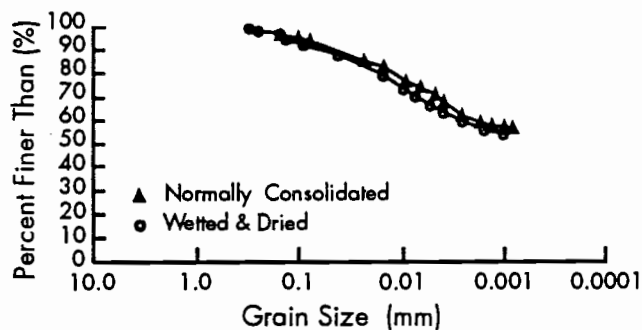
Figure 5.3 **Grain size distributions from a normally consolidated Paris clay specimen and from a compacted specimen which was wetted and dried**
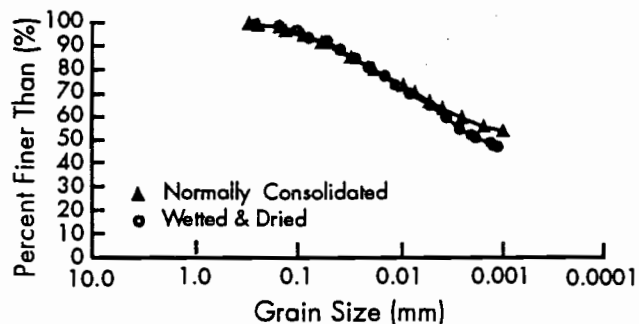
Figure 5.4 **Grain size distributions from a normally consolidated Beaumont clay specimen and from a compacted specimen which was wetted and dried**

COMPARISON OF CONSOLIDATION PROPERTIES

Dry unit weights of specimens at the time of set-up, and at the end of consolidation in the triaxial cells, are summarized in Table 5.1. The dry unit weights at set-up were computed based on the measured total unit weights and the moisture contents. The dry unit weights at the end of consolidation were calculated assuming a 100 percent degree of saturation and using the moisture contents measured after the shear test was completed.

Final moisture contents are plotted versus effective consolidation pressures in Figure 5.5 for the Paris clay and in Figure 5.6 for the Beaumont clay. Corresponding data from the as-compacted specimens and from specimens which were wetted and dried are also included. It appears that the compression indices for the specimens which were wetted and dried and for the specimens which were normally consolidated are similar, as suggested by the nearly parallel consolidation curves at stresses between 5 and 30 psi. Due to the lack of sufficient data at stresses lower than 5 psi and higher than 30 psi, results concerning the compression indices at other stresses remain inconclusive.

Table 5.1 **Triaxial specimen properties at set-up and at end of consolidation for the Paris and Beaumont clays**

Test Number	Soil Type	At Set-Up		At End of Consolidation	
		ω_c (%)	γ_d (pcf)	ω_c (%)	γ_d (pcf)
S31.35	Paris	88.1	50.6	39.7	81.6
S32.10	Paris	85.4	50.0	53.6	69.1
S33.04	Paris	92.2	48.7	64.9	61.4
S34.25	Paris	77.2	54.1	41.5	79.7
S35.17	Paris	79.1	53.9	45.9	75.5
S36.02	Paris	86.6	52.2	66.8	60.2
S51.04	Beaumont	57.9	66.2	43.2	78.3
S52.25	Beaumont	59.4	64.9	28.5	95.5
S53.04	Beaumont	68.6	62.4	42.5	79.0
S55.08	Beaumont	56.7	65.9	36.2	85.9
S56.02	Beaumont	62.3	62.2	53.1	69.7
S57.15	Beaumont	58.9	65.5	31.8	91.3
S58.34	Beaumont	61.0	63.2	26.2	99.4
S59.05	Beaumont	57.5	65.0	40.0	81.6

- Letter S in test names designates specimens consolidated from a slurry.
- Numbers after decimal points represent the applied effective consolidation pressures.
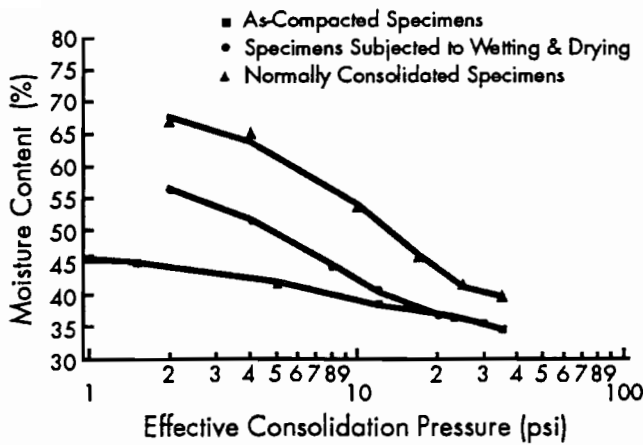
Figure 5.5 Moisture contents versus effective consolidation pressure for as-compacted Paris clay specimens, normally consolidated specimens, and specimens subjected to wetting and drying
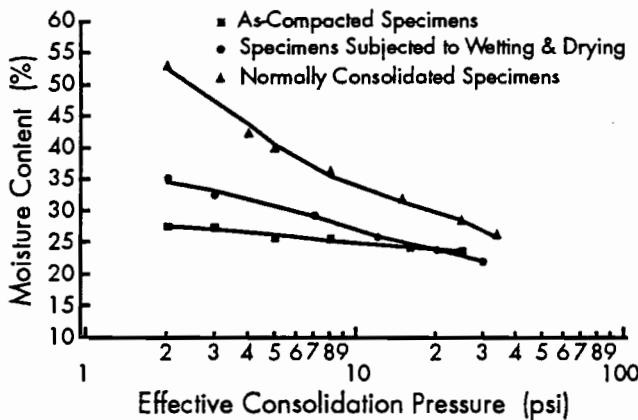
Figure 5.6 Moisture contents versus effective consolidation pressure for as-compacted Beaumont clay specimens, normally consolidated specimens, and specimens subjected to wetting and drying

TRIAXIAL SHEAR TEST RESULTS

Axial stress-strain curves, effective stress paths, and modified Mohr-Coulomb failure envelopes were plotted and examined for the specimens consolidated from a slurry. Triaxial shear test data including axial strains (ε), effective consolidation pressures ($\overline{\sigma}_3$), principal stress differences ($\sigma_1-\sigma_3$), principal stress ratios ($\overline{\sigma}_1/\overline{\sigma}_3$), and $\overline{A}$ coefficients are tabulated in Appendix C.

Stress-Strain Curves

Stress-strain curves for the Paris and Beaumont clays are presented in Figure 5.7 and in Figure 5.8,

respectively. The stress-strain curves show a decrease in strength after the peak strength similar to what was observed for the specimens subjected to wetting and drying (previously shown in Figures 4.7 and 4.9). The decrease in strength is approximately 10 to 25 percent of the peak principal stress difference for the Paris clay, and is less than 10 percent for the Beaumont clay.
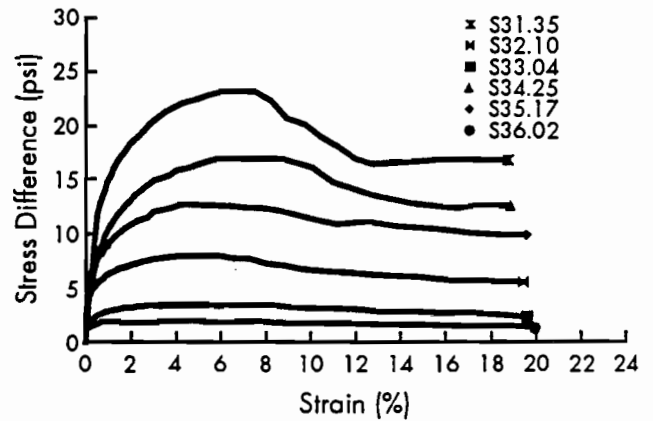
Figure 5.7 Stress strain curves for Paris clay specimens which were consolidated from a slurry
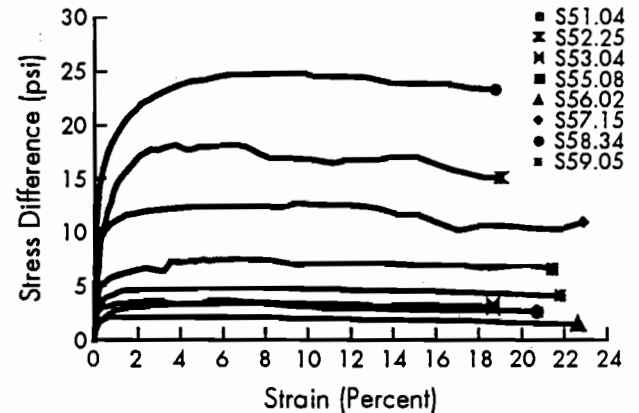
Figure 5.8 Stress strain curves for Beaumont clay specimens which were consolidated from a slurry

Effective Stress Paths and Failure Envelopes

The effective stress paths plotted in terms of the principal stress difference ($\sigma_1 - \sigma_3$) versus the minor principal effective stress ($\overline{\sigma}_3$) are shown in Figure 5.9 for the Paris clay and in Figure 5.10 for the Beaumont clay. Also shown on these plots are the modified Mohr-Coulomb failure envelopes based on stress path tangency.

It can be seen from the effective stress paths that positive pore water pressures were generated during shear. A comparison of the $\overline{A}$ coefficients at peak principal stress difference versus the effective consolidation pressures for both the normally consolidated and the compacted specimens after wetting and drying is shown in Figure 5.11 for the Paris clay and in Figure 5.12 for the Beaumont clay. It is apparent that the $\overline{A}$ is similar for the specimens which were wetted and dried and for the normally consolidated specimens.

The modified Mohr-Coulomb failure envelopes based on stress path tangency indicate that the failure envelope is non-linear. The failure envelopes for both soils show a distinct curvature at low stresses with a negligible cohesion intercept.

Figure 5.11 $\overline{A}$ **coefficients at peak principal stress difference versus effective consolidation pressure for normally consolidated and wetted and dried Paris clay specimens**
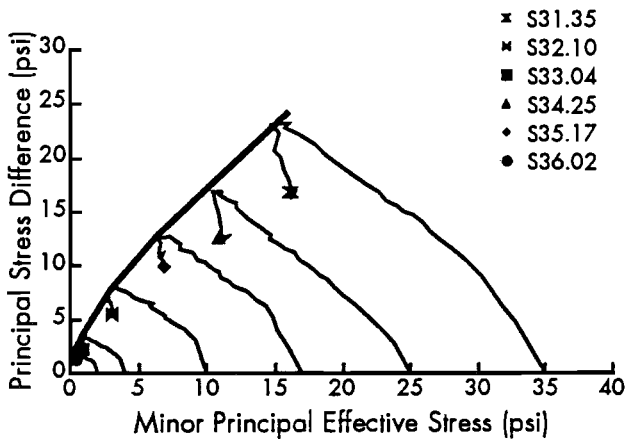
Figure 5.9 **Effective stress paths for Paris clay specimens which were consolidated from slurry**

x S31.35
x S32.10
■ S33.04
▲ S34.25
◆ S35.17
● S36.02
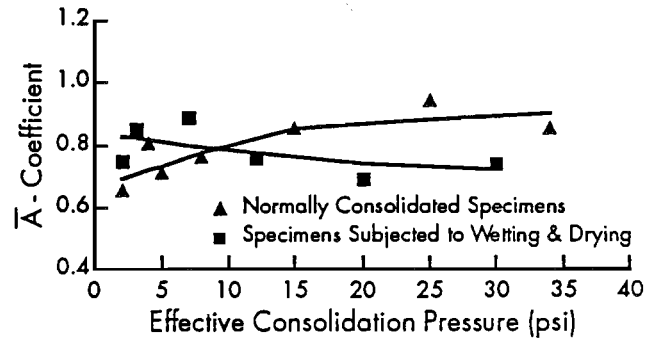
Figure 5.12 $\overline{A}$ **coefficients at peak principal stress difference versus effective consolidation pressure for normally consolidated and wetted and dried Beaumont clay specimens**

DISCUSSION OF RESULTS AND CONCLUSIONS

Comparisons of the modified Mohr-Coulomb failure envelopes for the normally consolidated specimens and for the specimens which were subjected to wetting and drying are presented in Figure 5.13 for the Paris clay and in Figure 5.14 for the Beaumont clay. It is apparent that, for both soils, the failure envelopes for the normally consolidated specimens and for the specimens subjected to wetting and drying are in very close agreement. Further comparisons between the strength envelopes at large strains for the specimens tested in the as-compacted condition, for the normally consolidated specimens, and for the specimens subjected to wetting and drying are shown in Figure 5.15 for the Paris clay and in Figure 5.16 for the Beaumont clay. It can be seen that, for both soils, the large strains envelopes for the as-compacted specimens are in close agreement with the large strains envelopes for the normally consolidated and the wetted and dried specimens.

Figure 5.10 **Effective stress paths for Beaumont clay specimens which were consolidated from slurry**

■ S51.04
x S52.25
x S53.04
■ S55.08
▲ S56.02
◆ S57.15
● S58.34
■ S59.05

Although the consolidation data, shown previously in Figures 5.5 and 5.6, indicated that the moisture contents are different for normally consolidated specimens and for compacted specimens which were subjected to wetting and drying, it is unclear why the differences exist between the moisture contents at the end of consolidation.

These differences might be related to the effect of hysteresis, or they might be the result of physico-chemical processes. In the current study, this was not explored further.

The similarities in the effective-stress shear strength properties for the normally consolidated specimens, and for the compacted specimens after wetting and drying, suggested that both materials may have a similar structure. Consequently, it was decided to examine the clay particle orientations for normally consolidated specimens, and for compacted specimens after wetting and drying, to see if the particle structures were similar.

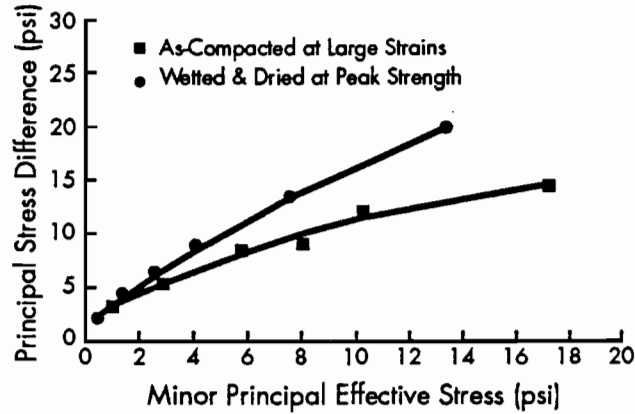**Figure 5.13 Modified Mohr-Coulomb failure envelopes for normally consolidated Paris clay and for specimens subjected to wetting and drying (based on stress path tangency)**
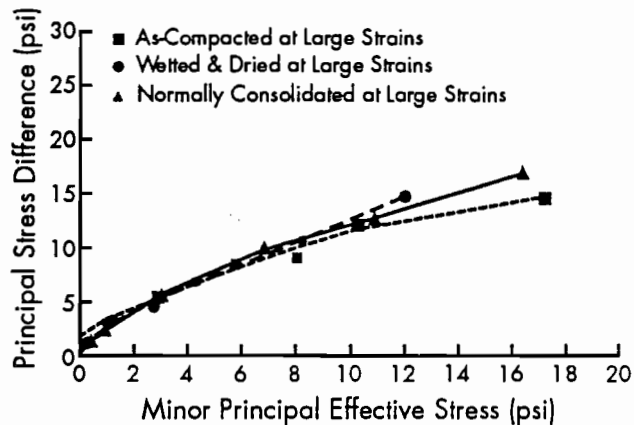
Figure 5.15 Modified Mohr-Coulomb failure envelopes at large strains for Paris clay specimens in as-compacted condition, normally consolidated, and wetted and dried

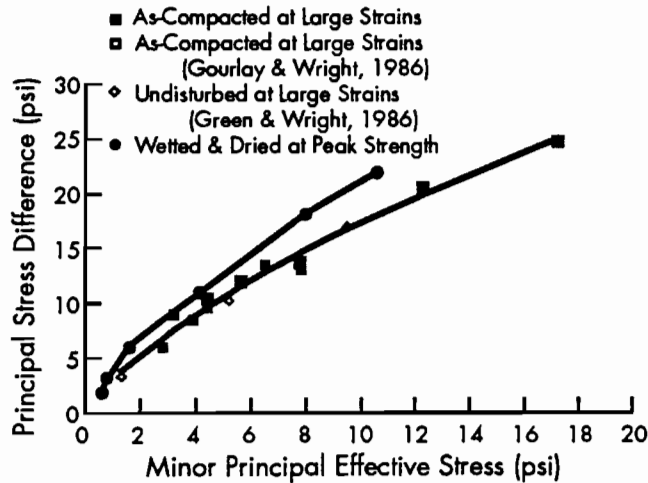**Figure 5.14 Modified Mohr-Coulomb failure envelopes for normally consolidated Beaumont clay and for specimens subjected to wetting and drying (based on stress path tangency)**
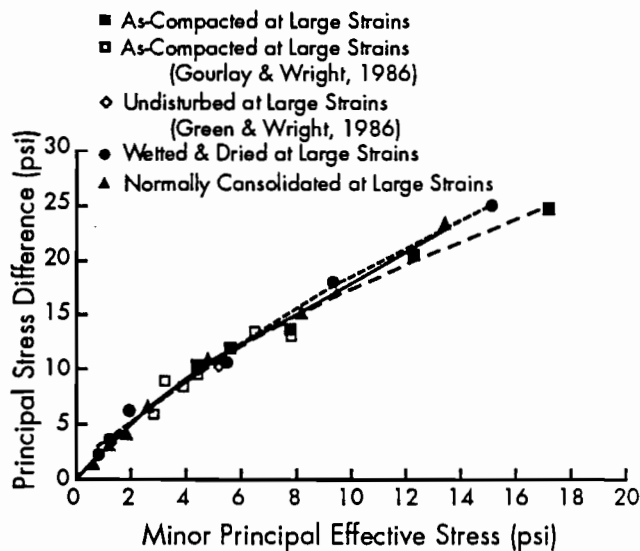
Figure 5.16 Modified Mohr-Coulomb failure envelopes at large strains for Beaumont clay specimens in as-compacted condition, normally consolidated, and wetted and dried

31

CHAPTER 6. EFFECTS OF WETTING AND DRYING ON CLAY PARTICLE ORIENTATIONS

INTRODUCTION

The triaxial shear test results presented in Chapter 4 showed that cyclic wetting and drying decreased the effective-stress shear strength properties at low confining pressures. This decrease in shear strength may be attributed to a reorientation of clay particles as a result of wetting and drying. The reorientation of clay particles might also explain triaxial test results, presented in Chapter 5, which showed a close agreement between the strength envelope for normally consolidated specimens and the envelope for specimens subjected to wetting and drying. Accordingly, the effect of cyclic wetting and drying on clay particle orientations of compacted Paris and Beaumont clays was investigated. This was accomplished by examining the *orientation ratios* which are based on intensities of X-ray reflections for certain clay minerals.

DESCRIPTION OF THE TESTING SCHEME

Four sets of laboratory experiments were designed to investigate the effects which wetting and drying have on clay particle orientations. In the first set of experiments, the change in the clay particle orientations with the number of cycles of wetting and drying was investigated. The results of these experiments were used to determine the number of cycles that a compacted specimen should be subjected to prior to measuring the orientation ratios. In the second set of experiments, compacted specimens were subjected to wetting and drying with the applied consolidation pressures being increased at the end of every wetting and drying period. The results of these experiments established the change in the clay particle orientations with wetting and drying at different consolidation pressures. The third set of experiments was designed to investigate the effects of the initial clay particle orientations at the end of compaction on the final clay particle orientations after wetting and drying. The fourth set of experiments was carried out to compare the clay particle orientations of compacted specimens which were subjected to wetting and drying with the orientations of clay particles for normally consolidated sedimented specimens.

PRINCIPLE OF THE ORIENTATION RATIOS METHOD

The method of orientation ratios is based on the fact that platy clay particles cause variations in the magnitude of diffracted X-ray intensities when their orientations change. With a high degree of basal plane orientation (orientation along the plane with largest area), the basal reflections are strongly developed, and the non-basal reflections are largely suppressed. A quantitative evaluation of clay particle orientations is obtained by measuring in an X-ray diffractometer the intensity of a suitable basal reflection *(00l)* to the intensity of a non-basal reflection *(hk0)* for a particular clay mineral (Brindly and Brown, 1980). Such a ratio is referred to as the "Orientation Index" (O.I.). For the purpose of this study, the O.I. was defined according to the orientation of the *montmorillonite* clay mineral as follows:

$$O.I. = \frac{\text{Intensity of the Basal Reflection (001)}}{\text{Intensity of the Non-Basal Reflection (020)}} \quad (1)$$

The (001) reflection for the montmorillonite clay corresponds to a d-spacing between 9.6 Å and 21.6 Å, while the (020) reflection occurs at a d-spacing of 4.5 Å. As the basal plane orientation increases, the O.I. rapidly increases reflecting a more orientated structure.

DESCRIPTION OF THE TESTING APPARATUS

To prepare specimens, the soil testing apparatus, shown in Figure 6.1, was designed and fabricated. In principle, the apparatus functions as a miniature consolidation cell. The apparatus was fabricated from stainless steel, and was designed specifically to fit into the Philips X-ray diffractometer, which was used for the X-ray diffraction analyses. The apparatus consists of six parts,

pictured in Figure 6.2 and illustrated by an exploded drawing in Figure 6.3: the loading piston, the porous stone, the collar, the specimen holder, a glass slide, and an L-shaped supporter. The holder was designed to prepare a soil specimen inside a square-shaped opening for testing in the X-ray diffractometer. This opening has a cross-sectional area of approximately 0.5 in², and it is 0.4 inch deep. The L-shaped supporter can be attached to the side of the holder to support a soil specimen from either the top or bottom surface of the holder. The L-shaped supporter is overlaid by a 1-millimeter-thick glass slide which fits between the soil and the supporter. The glass slide ensures that the soil surface, which is to be exposed to the X-rays, will remain flush with the surface of the holder. This is necessary to maintain accurate measurements of the X-ray diffraction angles. The glass slide also prevents disturbance of the clay particle orientations by eliminating the need for trimming the soil flush with the surface of the holder prior to testing. The collar fits on top of the holder during wetting and drying. The holder is intended to prevent the loss of soil due to swelling, and it acts as a guide for the loading piston. The loading piston is made of acrylic plastic and fits inside the square opening of the holder. The loading piston is used to apply loads to the soil specimen. A porous stone and a filter paper fit into the square opening of the holder and separate the loading piston from the soil specimen. The porous stone allows drainage during consolidation.
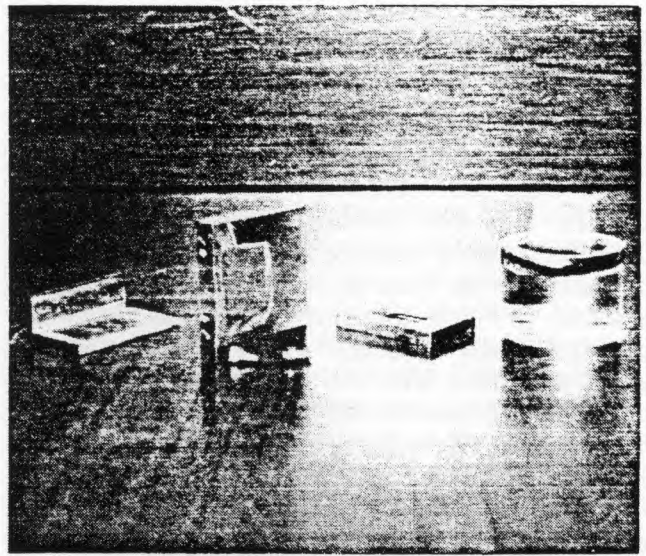
Figure 6.2 The testing apparatus after disassembling it into its parts (shown left to right): the supporter, the specimen holder, the collar, and the loading piston
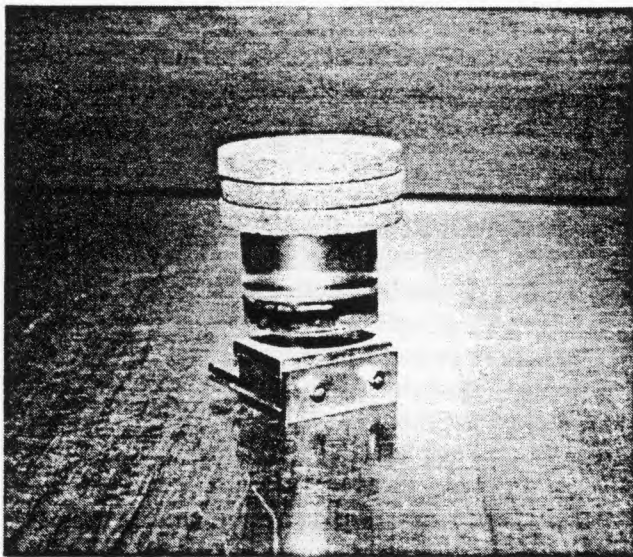
Figure 6.1 The testing apparatus assembled after preparing a soil specimen being consolidated with some loads applied on the loading piston
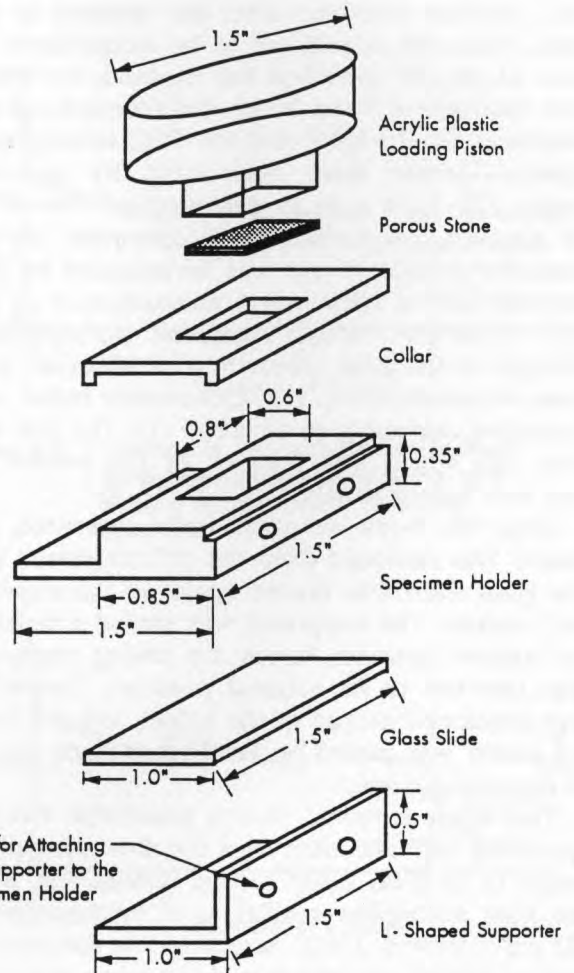
Figure 6.3 The six parts of the testing apparatus used for measuring the orientation index for soil specimens

33

PROCEDURE FOR MEASUREMENT OF THE ORIENTATION INDEX

The Orientation Index (O.I.) was determined as follows: the loading piston and the collar were removed from the specimen holder. The L-shaped supporter was then detached from the holder and turned around to support the soil specimen and the porous stone from the top side of the holder, as shown in Figure 6.4. This process was designed to obtain a soil specimen with a smooth surface which was flush with the bottom surface of the holder, and to prevent any physical disturbance to the specimen that might alter the clay particle orientations. Thin flat spacers were placed between the supporter and the porous stone to prevent the specimen from sliding. The holder was inverted, and the glass slide which served to protect the specimen during wetting and drying was lifted from the top of the specimen to expose a soil surface flush with the surface of the holder. Soil particles did not adhere to the glass slide when lifted from top of the soil, and any disturbance to the soil structure resulting from the removal of the glass slide was considered to be insignificant. As soon as the soil specimen was exposed, the holder was inserted into the X-ray diffractometer. X-ray intensities for the (001) and the (020) reflections of montmorillonite were determined by scanning angles (2θ) from 4 to 10 degrees, and from 18 to 22 degrees, respectively. Soil specimen heating from the emitted X-rays was investigated by performing several consecutive measurements of the (001) peak for a single specimen. No significant changes in the peak intensity were observed after three measurements. The Orientation Index was computed according to equation (1). The soil surface area which was scanned by the emitted X-rays was approximately 1 cm^2 (0.15 in^2).

Once the X-ray intensities were measured, the holder was removed from the diffractometer, and the glass slide was placed again on the exposed soil surface. The supporter was turned around to its original position; hence the testing apparatus was inverted to its original position. The collar was positioned on top of the holder, and the loading piston was placed on the porous stone on top of the soil specimen.

The depth to which X-rays penetrated the soil specimens was calculated from the diminution of intensity of an X-ray beam passing through soil, using the mass absorption coefficient of montmorillonite (32 cm^{-1}; Brown, 1961). Assuming that the penetration of X-rays is limited to a depth where the diminution of intensity is no more than 75 percent of the incident intensity, the depth of penetration is approximately 2 microns (10^{-6} m). Depending on the orientation of the montmorillonite clay particles, this depth could range between 200 and 2000 particles.
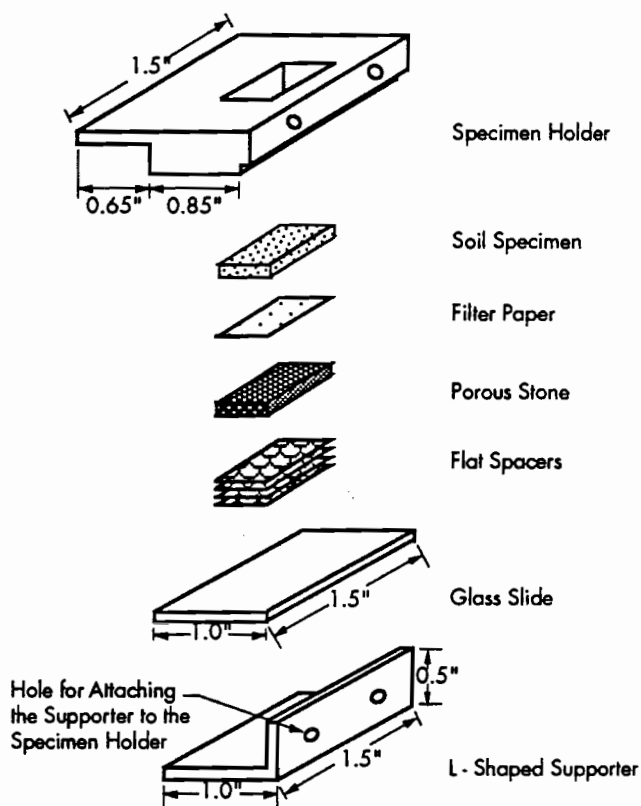
Figure 6.4 · Assembly of the testing apparatus for testing a soil specimen in the X-ray diffractometer

DESCRIPTION AND TEST RESULTS OF THE FIRST SET OF EXPERIMENTS

The first set of experiments was designed to measure the change in the clay particle orientations with the number of cycles of wetting and drying. The results of these experiments were used to determine the number of cycles which a compacted specimen was subjected to prior to measuring the clay particle orientations. Tests were performed on two compacted specimens from the Paris and Beaumont clays. The procedures for preparing compacted soil specimens and for subjecting these specimens to cyclic wetting and drying are explained below.

Procedure for Preparing Compacted Soil Specimens

Prior to preparing a soil specimen, the testing apparatus was assembled as shown in Figure 6.3; with the glass slide and the L-shaped supporter on the bottom of the holder. Specimens were prepared by loosely spreading very small amounts of soil

(less than 2 grams) onto the glass slide inside the holder. The soil was mixed at optimum moisture content, sieved through a No. 40 sieve, and compacted in place by static compaction with a dead load of 5 pounds applied on the loading piston for a period of 1 minute. Impact compaction was not used to avoid fracturing the glass slide. A saturated porous stone underlaid by a filter paper was placed between the soil and the loading piston during compaction. Once compaction was completed, the loading piston was removed, with the porous stone remaining on top of the compacted specimen. A soil specimen, approximately 1 to 2 millimeters thick, was obtained at the end of compaction.

Procedure for Subjecting Compacted Specimens to Wetting and Drying

Once a soil specimen was compacted, the initial Orientation Index (O.I.) was determined following the procedure described earlier in this chapter. The testing apparatus (containing the soil specimen) was then reassembled and placed in distilled water for approximately 24 hours. No loads were applied on the loading piston. At the end of the wetting period, the O.I. was again measured. The apparatus was reassembled, and placed in an oven at a temperature of 60°C. After a 24-hour drying period, the O.I. was measured once more. The first "cycle" of wetting and drying actually consisted of wetting, drying, and rewetting. Each additional cycle consisted of drying and wetting. The Orientation Indices were determined at the end of every wetting and drying period for four consecutive wetting and drying cycles.

Test Results

Plots of the Orientation Indices versus the number of wetting and drying cycles are shown in Figure 6.5 for the Paris clay specimen and in Figure 6.6 for the Beaumont clay specimen. It can be seen that the Orientation Indices decrease from the initial value, and then increase and decrease by approximately the same amount for every wetting and drying cycle. The O.I. did not appear to change after the first wetting and drying cycle. Therefore, it was decided to use a single cycle of wetting and drying for subsequent measurement of the Orientation Indices.

DESCRIPTION AND TEST RESULTS OF THE SECOND SET OF EXPERIMENTS

The second set of experiments was designed to measure the change in clay particle orientations for compacted specimens after wetting and drying

for different effective consolidation pressures. Testing procedures and results are presented below.

Testing Procedures

Tests were performed for two compacted specimens from the Paris and Beaumont clays. Specimens were compacted following the procedure explained in the previous section. The initial O.I. was determined prior to subjecting the specimen to wetting and drying. For the first cycle, no loads were applied on the loading piston; the O.I. was determined at the end of wetting and drying. For the second cycle, loads were placed on the loading piston such that the soil specimen was consolidated to an effective consolidation pressure of 1 psi. The O.I. was again determined at the end of wetting and drying. The loads were then systematically increased with a load increment ratio of two at the end of each additional wetting and drying cycle. Measurements of the Orientation Indices were conducted for consolidation pressures up to a maximum effective consolidation pressure of 16 psi.
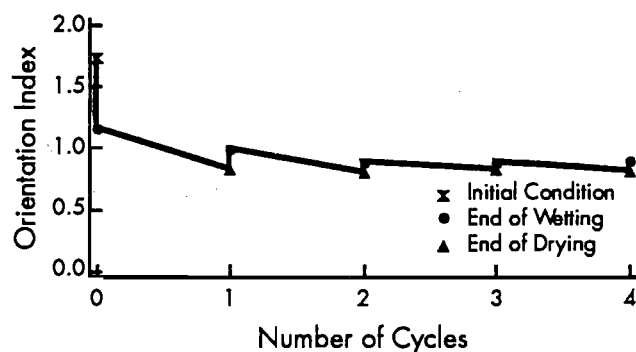
Figure 6.5 **Change in the orientation indices with the number of wetting and drying cycles for a Paris clay specimen**
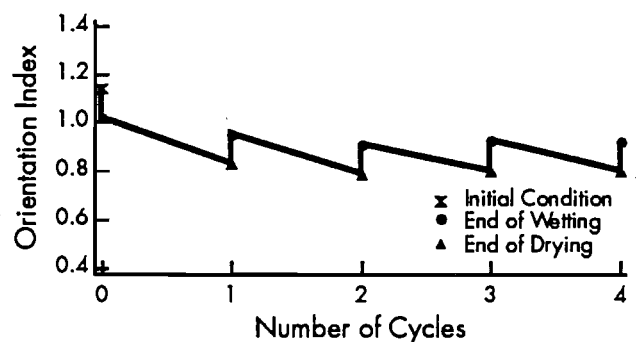
Figure 6.6 **Change in the orientation indices with the number of wetting and drying cycles for a Beaumont clay specimen**

Determination of the Orientation Indices for this set of experiments required the temporary removal (for approximately 15 minutes) of the loading piston and the applied loads from the soil specimen. It was practically impossible to measure the X-ray intensities in the diffractometer with the loads applied on the soil specimen. Experiments performed in the early stages of this research showed that unless a load increment of at least two was used after measuring the X-ray intensities, the effect of unloading on the clay particle orientations would influence the measured X-ray intensities for the subsequent loading increment. For example, if the consolidation pressure was increased from 6 to 8 psi, the O.I. measured at 8 psi would be lower than the value determined at 6 psi. Such a result would indicate that the clay particle orientations decrease with increasing consolidation pressure, which is improbable. For that reason, a load increment ratio of two was selected for this set of experiments, following the same guidelines adopted for one-dimensional consolidation tests.

Test Results

Plots of the Orientation Indices versus the effective consolidation pressures are shown in Figure 6.7 for the Paris clay specimen and in Figure 6.8 for the Beaumont clay specimen. It can be seen that, for every wetting cycle, the degree of orientation of the clay particles increases as a result of wetting, but, after drying, it decreases again, indicating the development of a less oriented structure. In addition, the degree of orientation of the clay particles increases with increasing consolidation pressures. A comparison of the Orientation Indices for the Paris and Beaumont clays shows that the Paris clay specimen has a more oriented structure in comparison with the Beaumont clay specimen.
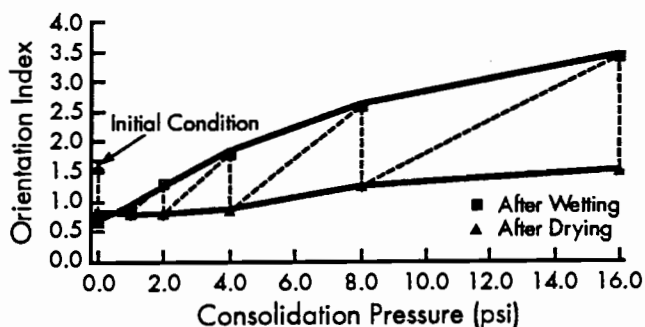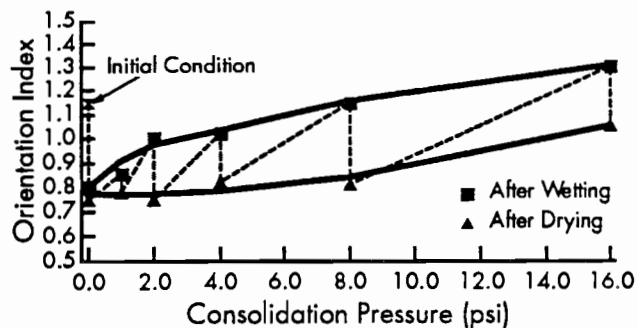
Figure 6.8 Orientation indices at the end of wetting and drying for a Beaumont clay specimen versus the applied effective consolidation pressures

Measurements of Exchangeable Water During Wetting and Drying

The change in the interlayer spacing (d), which is determined from the (001) basal reflections in X-ray diffraction analyses, can be used to determine the amount of water exchanged with the soil at the end of wetting and drying. According to Van Olphen (1963), when clays come into contact with water or with water vapor, one to four monomolecular layers of water, each 3 Å thick, penetrate between the unit layers. This process, which is referred to as the *interlayer swelling* or *crystalline swelling*, results in an increase in the basal spacing of the clay particles from 9.6 Å, for a completely dry clay, to a range of values between 12.6 Å and 21.6 Å, depending on the number of monomolecular layers of water that penetrate the unit layers. Interlayer swelling leads to, at most, a doubling of the volume of dry clay when four layers of water are adsorbed.

The amount of water exchanged by the Paris and Beaumont clays was determined based on the d-spacings of the (001) reflections for montmorillonite. The d-spacings were measured at the end of every wetting and drying cycle. This information is plotted versus the applied effective consolidation pressure in Figure 6.9 for the Paris clay and in Figure 6.10 for the Beaumont clay. Lines indicating the basal spacings for montmorillonites with zero, one, three, and four monomolecular layers of water are also plotted. It can be seen from these plots that, regardless of the applied effective consolidation pressure, between zero and one layers of water remained between the unit layers at the end of drying. In contrast, between three and four layers of water penetrated between the unit layers at the end of wetting.

Figure 6.7 Orientation indices at the end of wetting and drying for a Paris clay specimen versus the applied effective consolidation pressures
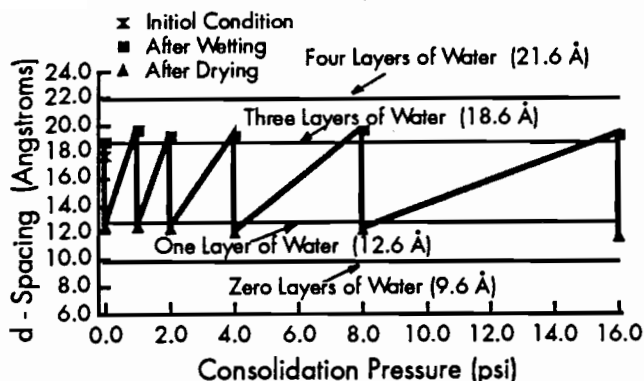
Figure 6.9 Change in the basal unit layer spacings at the end of wetting and drying for montmorillonite in a Paris clay specimen versus the applied consolidation pressure
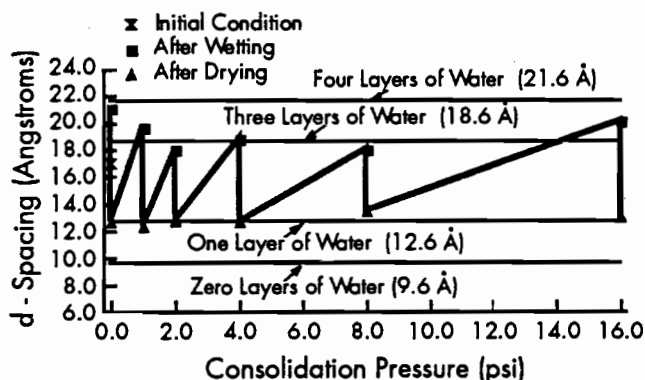
Figure 6.10 Change in the basal unit layer spacings at the end of wetting and drying for montmorillonite in a Beaumont clay specimen versus the applied consolidation pressure

DESCRIPTION AND TEST RESULTS OF THE THIRD SET OF EXPERIMENTS

The third set of experiments was designed to investigate the effects of the initial clay particle orientations of compacted specimens on the measured Orientation Indices after wetting and drying. The results obtained from this set of experiments are compared with the results obtained from the second set of experiments. Testing procedures and results are presented below.

Testing Procedures

Tests were performed on four compacted specimens from the Paris clay and on four compacted

specimens from the Beaumont clay. Specimens were compacted statically following the procedure explained earlier in this chapter. To obtain different initial Orientation Indices, the compaction moisture contents and the applied static loads were varied for the four specimens (to obtain different dry densities). The four specimens were consolidated to effective consolidation pressures of 0, 1, 2, and 4 psi, respectively. The consolidation pressure was applied on each specimen after the initial O.I. was determined. The consolidation pressure was not changed once wetting and drying was initiated. Hence, these experiments may be viewed as single-stage experiments in comparison with the multi-stage experiments described in the previous section. A *single* wetting and drying cycle was performed for each specimen. The Orientation Indices were measured for the four specimens at the end of each wetting and drying period.

Test Results

The initial Orientation Indices at the end of compaction and the final Orientation Indices at the end of wetting are shown in Figure 6.11 for the Paris clay and in Figure 6.12 for the Beaumont clay. Also shown on these plots are the Orientation Indices at the end of wetting (which were presented previously in Figures 6.7 and 6.8). Similar results at the end of drying are shown in Figure 6.13 for the Paris clay and in Figure 6.14 for the Beaumont clay. It can be seen from the plotted data that the final clay particle orientations at the end of wetting or drying were the same for the four specimens regardless of their initial clay particle orientations at the time of compaction. This is apparent from the equivalent Orientation Indices which were determined from the single and the multi-stage experiments. Therefore, clay particle orientations, at the end of wetting or drying, depend only on the applied effective consolidation pressure, and do not vary with the initial conditions at the time of compaction, prior to wetting and drying.

DESCRIPTION AND TEST RESULTS OF THE FOURTH SET OF EXPERIMENTS

The fourth set of experiments was conducted to compare the clay particle orientations of compacted specimens at the end of wetting with the clay particle orientations of normally consolidated sedimented specimens. The procedures for preparing normally consolidated specimens, the testing procedures, and test results are presented below.
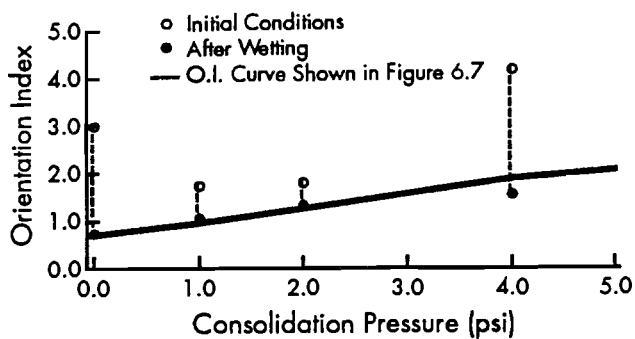
Figure 6.11 Orientation Indices at the end of wetting for four Paris clay specimens with different initial orientation indices consolidated to various consolidation pressures

Figure 6.12 Orientation Indices at the end of wetting for four Beaumont specimens with different initial orientation indices consolidated to various consolidation pressures
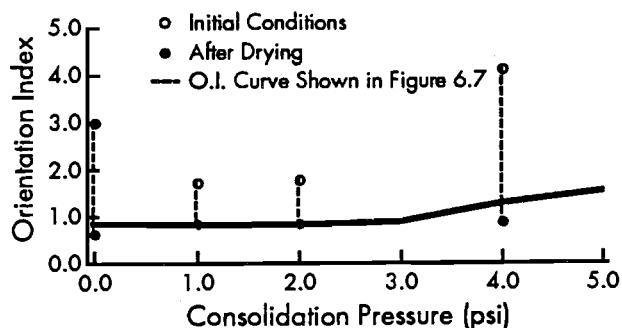
Figure 6.13 Orientation Indices at the end of drying for four Paris clay specimens with different initial orientation indices consolidated to various consolidation pressures

Figure 6.14 Orientation Indices at the end of drying for four Beaumont specimens with different initial orientation indices consolidated to various consolidation pressures

Preparation of Normally Consolidated Specimens

Specimens were prepared by sedimenting a soil slurry directly onto the glass slide in the holder. Soil was allowed to settle to the bottom of the holder, and excess water either was allowed to evaporate or was removed by means of a small filter paper which drained excess water out of the holder. Care was exercised to prevent the soil from drying in the holder. A porous stone covered with filter paper was subsequently placed on the soil surface.

Testing Procedures

Several specimens from the Paris and Beaumont clays were sedimented, and their initial Orientation Indices were determined at the end of sedimentation. Specimens were consolidated to a loading sequence that was identical to the one used for the second set of experiments. A load increment ratio of two was used, and pressures ranging from 0 to 16 psi were applied. A consolidation period of 24 hours was maintained for all loading increments. The specimen holder was immersed in distilled water during consolidation. At the end of each pressure increment, the O.I. was determined, and the weights on the loading piston were increased.

Test Results

The Orientation Indices of the normally consolidated specimens at the end of consolidation with the applied effective consolidation pressures are shown in Figure 6.15 for the Paris clay (three specimens) and in Figure 6.16 for the Beaumont clay (two specimens). Also shown on these figures are the Orientation Indices at the end of wetting (which were

presented previously in Figures 6.7 and 6.8). It can be seen from these plots that the clay particle orientations of the compacted specimens which were subjected to wetting and drying are in close agreement with the Orientation Indices determined for the normally consolidated sedimented specimens. The agreement in the clay particle orientations between the two types of materials is further evidence supporting the triaxial test results presented in Chapter 5. The triaxial test results showed a very close agreement between the strength envelopes for normally consolidated specimens and for compacted specimens which were subjected to wetting and drying.

CONCLUSIONS

Cyclic wetting and drying changes clay particle orientations with every wetting and drying cycle. A clay soil shows a more oriented soil structure after wetting in comparison with the structure that develops after drying.

The change of soil structure caused by wetting and drying does not depend on the initial clay particle orientations. The final clay particle orientations were found to vary only with the applied effective consolidation pressure and with the type of clay being tested.

The clay particle orientations of the compacted specimens which were subjected to wetting and drying were in close agreement with the clay particle orientations which were measured for the normally consolidated sedimented specimens. The similarities in soil structure between the two types of materials are in agreement with the results presented in the previous chapter, which also showed the similarities in the effective-stress shear strength envelopes for the two materials. The reduction in the effective-stress shear strengths owing to cyclic

wetting and drying at low confining pressures appears to be due to a change in the soil structure.
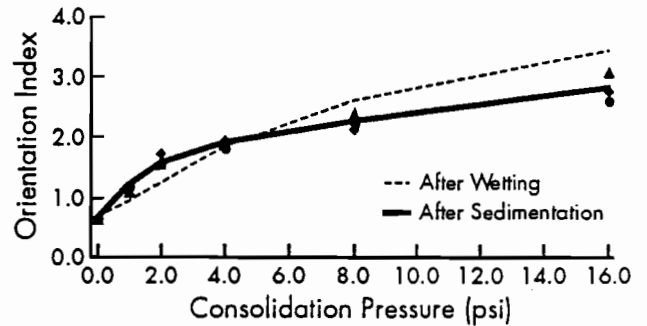
Figure 6.15 Measured Orientation Indices for normally consolidated and compacted Paris clay specimens after wetting and drying versus the effective consolidation pressure
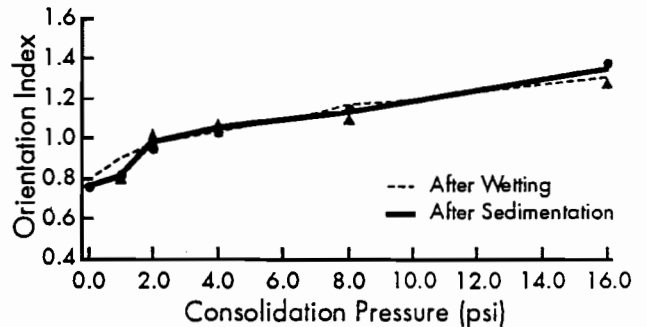
Figure 6.16 Measured Orientation Indices for normally consolidated and compacted Beaumont clay specimens after wetting and drying versus the effective consolidation pressure

CHAPTER 7. COMPARISON OF CALCULATED AND OBSERVED STABILITY CONDITIONS FOR THE PARIS AND HOUSTON EMBANKMENT SLOPES

INTRODUCTION

The effect of the reduction in effective-stress shear strength properties caused by wetting and drying was examined by comparing calculated and observed stability conditions for the Paris and Houston embankment slopes. These slopes were described previously in Chapter 2. All stability calculations were performed for the anticipated long-term conditions, using effective stresses. Stability calculations were first performed assuming zero pore water pressures in accordance with previous assumptions made by Stauffer and Wright (1984) and by Green and Wright (1986). Subsequent analyses were performed in which a variety of pore water pressures were assumed. The subsequent analyses were performed to find what pore water pressures would be required to produce factors of safety of unity.

STABILITY ANALYSES WITH ZERO PORE WATER PRESSURES

Stability analyses were performed using the computer program UTEXAS2 (Wright and Roecker, 1984). The location and geometry of the Paris and Houston embankments, for which calculations were performed, were described previously in Chapter 2. Pertinent quantities required to model the embankment slopes are presented in Table 7.1. The unit weights used in the computations were the long-term saturated unit weights. For soils in an as-compacted condition (prior to wetting and drying), the total unit weights of specimens before wetting and drying were used. For soils which were subjected to wetting and drying, the total unit weights after wetting and drying were used. These were estimated from the triaxial consolidation data for specimens consolidated to stresses ranging from 2 to 3 psi. Separate analyses revealed that a 5 percent change in the total unit weight, from a 100- to an 85-percent degree of saturation, affected the factor of safety by 1 to 3 percent.

Two sets of strength envelopes were used in the analyses: *as-compacted* (before wetting and drying) and *after wetting and drying*. The strength envelopes were based on effective stresses, and were determined in the laboratory for specimens which were fully saturated. Curved Mohr-Coulomb failure envelopes were used in the computations; they are presented in tabular form in Table 7.1.

An automatic search was conducted using the computer program to locate a critical circle (circle with the lowest factor of safety). Spencer's procedure was used to perform the stability computations. Separate analyses revealed that a 2-foot vertical crack filled with water reduced the factor of safety by only 1 to 3 percent. Accordingly, no vertical tension cracks were used in the remaining stability analyses.

Discussion of Results

The computed factors of safety and corresponding critical circles for zero pore water pressures are presented in Figure 7.1 for the Paris embankment and in Figure 7.2 for the Houston embankment. It can be seen that wetting and drying resulted in a reduction in the factor of safety, from 2.6 to 2.2 for the Paris embankment and from 3.1 to 2.2 for the Houston embankment. Even though the factors of safety decreased by 18 to 40 percent with wetting and drying, the computed factors of safety were still greater than unity, and thus were inconsistent with the observed failures in the field.

The effective-stress shear strength parameters required to obtain a factor of safety of unity for both the Paris and Houston embankment slopes were back-calculated using the charts and procedures developed by Stauffer and Wright (1984) and assuming zero pore water pressures. Effective-stress cohesion and friction angle values were back-calculated using the charts with the embankment height, slope angle, depth of slide, and total unit weight of soil. These parameters are summarized for the Paris and Houston embankments in Table 7.1. The total unit weight after wetting and drying was used. The back-calculated effective-stress cohesion and friction angle values were 5 psf and 16° for the Paris embankment, and 25 psf and 17° for the Houston

Table 7.1 Input parameters for stability analyses of the Paris and Houston embankments

Input Parameters	Paris Embankment	Houston Embankment
Total unit weight:		
As-compacted	112 pcf	120 pcf
After wetting & drying	107 pcf	114 pcf
Height	20 feet	19 feet
Side slope ratio	3 : 1	2.5 : 1
Depth of slide	5 feet	4 feet

As-compacted Mohr-Coulomb failure envelopes (psf)

Paris Clay		Beaumont Clay	
σ_n	τ	σ_n	τ
0	287	0	342
275	402	324	540
322	422	396	584
413	458	435	609
719	576	584	685
1,118	719	977	900
1,378	812	1,543	1,185
2,056	1,055	2,528	1,468

Mohr-Coulomb failure envelopes after wetting & drying (psf)

Paris Clay		Beaumont Clay	
σ_n	τ	σ_n	τ
0	24	0	0
22	42	117	112
111	111	157	138
261	207	330	286
460	325	747	545
688	453	1,354	918
1,182	650	1,861	1,237
1,923	948		

embankment. The back-calculated strength parameters are shown in Figure 7.3 for the Paris clay and in Figure 7.4 for the Beaumont clay. Also shown in Figures 7.3 and 7.4 are the laboratory measured Mohr-Coulomb failure envelopes for the compacted specimens prior to and after wetting and drying. Significant differences can be seen between the laboratory measured and the back-calculated failure envelopes. These differences coincide with the relatively high factors of safety presented previously in Figures 7.1 and 7.2.

STABILITY ANALYSES WITH POSITIVE PORE PRESSURES

Stability computations for the Paris and Houston embankments were repeated assuming various positive pore water pressure conditions to determine what pore pressures would be required to obtain factors of safety of unity. The strength envelopes for the *as-compacted* and the *wetted and dried* conditions were again used. The pore water pressures used in the stability computations were represented in terms of the pore pressure

coefficient, (r_u), defined by Bishop and Morgenstern (1960) as follows:

$$r_u = \frac{u}{\gamma z}$$

where "z" is the vertical depth below the surface, "u" is the pore water pressure at the depth "z," and "g" is the total unit weight of soil. A value for r_u of approximately 0.5 to 0.6 corresponds to very high pore water pressures with horizontal seepage near the face of the slope. Stability computations were performed for pore pressure coefficients ranging from zero to values high enough to produce factors of safety of unity.

Discussion of Results

The variations in the computed factors of safety with the assumed pore water pressure coefficients are shown in Figure 7.5 for the Paris embankment and in Figure 7.6 for the Houston embankment. The pore water pressure coefficients required to produce a factor of safety of unity using the as-compacted strength, and using the strength after wetting and drying, are tabulated in Table 7.2. It can be seen from the computed factors of safety that slope failures would not be predicted using the as-compacted strengths because the pore water pressures would have to be excessively high (r_u = 0.9 to 1.0). In contrast, calculations reveal that failure is probable based on the strengths of specimens that were subjected to wetting and drying, provided that the pore water pressures are relatively high (r_u = 0.5 to 0.6).

CONCLUSIONS

Stability calculations for the Paris and Houston embankment slopes confirmed that the reduction in strength caused by wetting and drying partially explains the observed shallow slope failures. Stability analyses also revealed that the back-calculated pore water pressures at failure were higher than anticipated at the outset of this study, and assumed previously by Stauffer and Wright (1984) and by Green and Wright (1986). Based on the stability analyses, significant positive pore water pressures must have existed in the Paris and Houston embankments to cause failure. In order to better understand the pore water pressure conditions that might exist at failure, further analyses were performed to evaluate the pore water pressures at failure for a number of shallow slides that occurred in compacted embankments constructed of the Paris and Beaumont clays. Results of these analyses are presented in the following chapter.

PARIS EMBANKMENT IN AS-COMPACTED CONDITION

Factor of Safety Calculated For a Pore Water Pressure Coefficient of Zero

FACTOR OF SAFETY = 2.60

3:1 Slope

20 feet

Critical Circle

PARIS EMBANKMENT AFTER WETTING & DRYING

Factor of Safety Calculated For a Pore Water Pressure Coefficient of Zero

FACTOR OF SAFETY = 2.23

3:1 Slope

20 feet

Critical Circle

HOUSTON EMBANKMENT IN AS-COMPACTED CONDITION

Factors of Safety Calculated For a Pore Water Pressure Coefficient of Zero

FACTOR OF SAFETY = 3.12

2.5:1 Slope

19 feet

Critical Circle

HOUSTON EMBANKMENT AFTER WETTING & DRYING

Factors of Safety Calculated For a Pore Water Pressure Coefficient of Zero

FACTOR OF SAFETY = 2.17

2.5:1 Slope

19 feet

Critical Circle

Figure 7.1 Factors of safety for the Paris embankment prior to and after wetting and drying
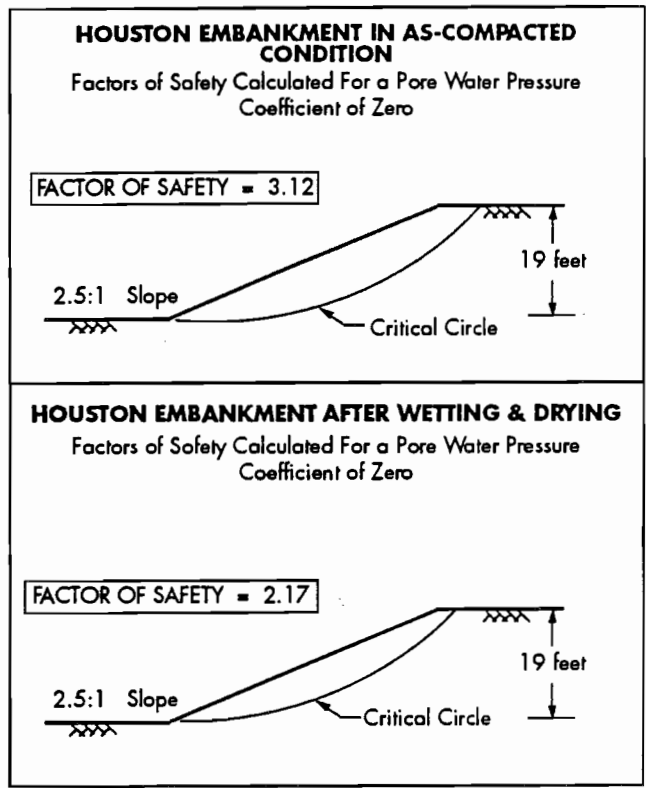
Figure 7.2 Factors of safety for the Houston embankment prior to and after wetting and drying

▲ As-Compacted
● After Wetting & Drying
— Back-Calculated
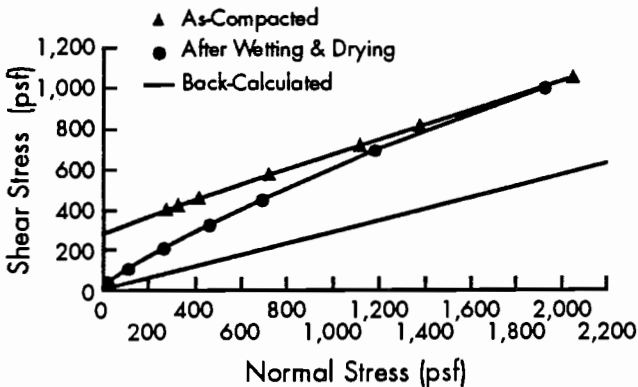
Figure 7.3 Mohr-Coulomb failure envelopes for the Paris clay specimens

▲ As-Compacted
● After Wetting & Drying
— Back-Calculated
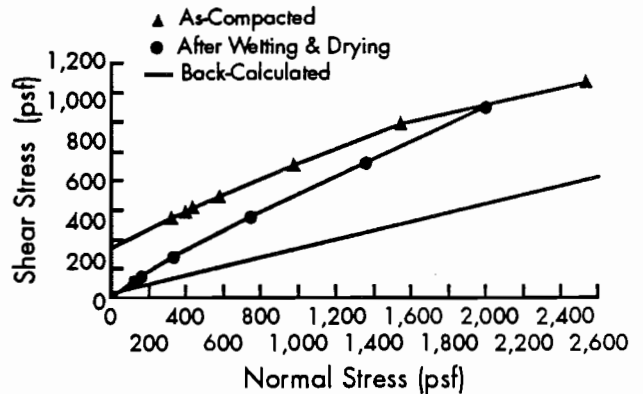
Figure 7.4 Mohr-Coulomb failure envelopes for the Beaumont clay specimens
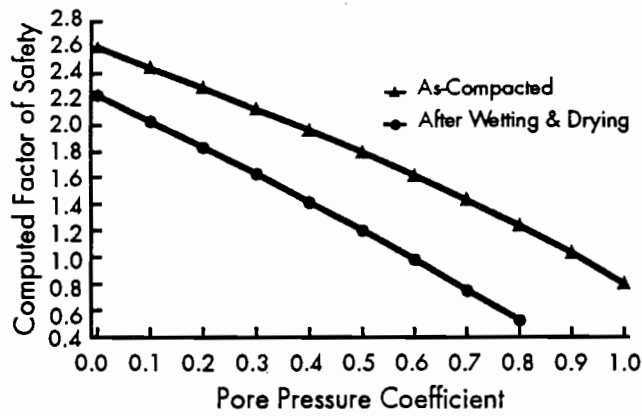
Figure 7.5 Computed factors of safety versus the pore water pressure coefficients for the Paris embankment slope
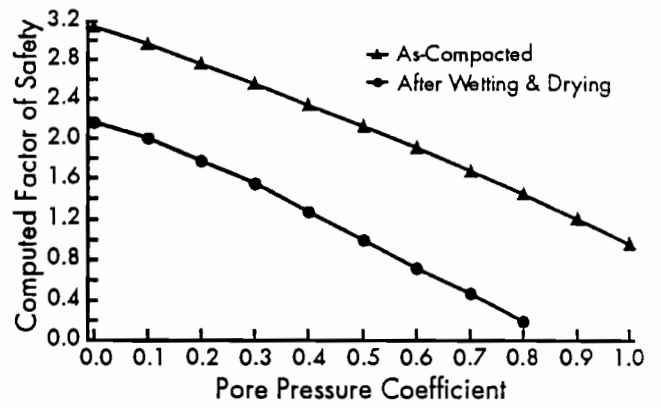
Figure 7.6 Computed factors of safety versus the pore water pressure coefficients for the Houston embankment slope

Table 7.2 Back-calculated pore water pressure coefficients for the Paris and Houston embankment slopes at failure

Embankment Clay Condition	Paris Embankment	Houston Embankment
Prior to wetting & drying	1.0	1.0
After wetting & drying	0.6	0.5

CHAPTER 8. EVALUATION OF PORE WATER PRESSURE CONDITIONS IN PARIS AND BEAUMONT CLAY FILL EMBANKMENTS

INTRODUCTION

In the previous chapter, it was shown that significant positive pore water pressures would need to exist in the Paris and Houston embankments for the observed slides to have occurred. To determine whether similar pore water pressures would need to exist in other embankments which had failed, pore pressure conditions at failure were calculated for a number of other embankments constructed of Paris and Beaumont clays. Results of these calculations were compared with data found in the literature, and were used to establish recommendations for design.

LITERATURE REVIEW

To obtain insight into the probable pore water pressures in compacted clay embankments, a literature survey was conducted. The literature survey focused on non-water-impounding clay fill embankments. Twelve case histories of shallow slides were found in the literature. For all the cases, the pore water pressures at failure were measured. The location of these embankments, the age of the slope when it failed, the slope geometry, the soil index and strength properties, and available information concerning pore water pressure conditions at the time of failure are summarized in Table 8.1. References from which the information was obtained are also listed.

The climatic conditions at failure for the embankments listed in Table 8.1 indicate that slides were typically preceded by a period of rainfall, or by ground thaw. An increase in frequency of shallow slides in clay fill embankments during periods of wet weather has been reported by Symons (1979), Vail and Beattie (1985), Lumb (1975), Vaughan and Walbancke (1973), Anderson et al, (1982), Greenwood et al (1985), and Vaughan et al (1978). According to these reports, surface water enters through shrinkage cracks

and soil permeability decreases with depth, leading to a somewhat *perched* water table in the embankment with a band of nearly saturated soil parallel to the face of the slope. Shrinkage cracking was reported in embankment fills by Byrd (1982), Day and Axten (1989), and Al-Shaikh-Ali (1979).

The development of a saturated zone of soil parallel to the face of the slope was investigated by Anderson and Kneale (1980), who conducted continuous monitoring of pore water pressures in a clay fill embankment associated with a 1-meter-(3-foot)-deep slip surface. The pore water pressure profiles were measured at four different dates, and are shown with the precipitation record in Figure 8.1. Anderson and Kneale note that, prior to failure, low intensity precipitation, aided by snow, resulted in pore water pressure increases culminating in the slip on March 3. It is apparent that a zone of positive pore water pressures developed in the vicinity of the toe of the slope; while remaining at some depth below the crest of the embankment.

The development of a zone of positive pore water pressures in non-water-impounding clay fill embankments was reported by a number of investigators. Chandler (1974) indicated that, for many embankment slopes in Britain, the depth of the water table for the zone of positive pore water pressures varies between 0.5 and 2 meters (1.6 to 6.5 feet), while Snedker (1979) noted that the depth of the water tables varies between 1 to 1.5 meters (3 to 5 feet). Day and Axten (1978), reported that Los Angeles County requires that embankments be designed for seepage with flow parallel to the slope at a depth of 4 feet. Odom (1990) reported that SDHPT (State Department of Highways and Public Transportation) personnel have found holes for guard-rail posts partially filled with water some time after the holes were drilled at the top of highway embankment slopes in southeast Texas, even though recent precipitation records indicated zero rainfall.

Table 8.1a   Piezometric and slope data for selected case records

Embankment Slope Location	Climatic Conditions at Failure	Slope Age (years)	Slope Height (ft)	Slope Ratio (H:V)	Soil Index Properties	Undrained & Drained Strength	Pore Pressure Conditions at Failure
Gretton Rail Embank. Britain (Refs 1,5)	Embankment Slip preceded by heavy rain	80	15	2.6:1	LL – 70 PL – 31 PI – 39	S_u – 800 psf c' – 0 psf ϕ' – 23° (Extrapolated)	Piezometers indicated the presence of two water tables: a perched WT at a depth of 5 feet & regular WT at a depth of 13 feet
Seaton Rail Embank. Britain (Ref 1)	Embankment Slip preceded by heavy rain	70	26	2.4:1	LL – 59 PL – 29 PI – 30	S_u – 800 psf c' – 0 psf ϕ' – 21° (Back-calc.)	Piezometric surface measured at a depth of 5 to 7 feet. Piezometric surface intersects toe of slope
Highway Embankment Britain (Ref 2)	NA	5	22	2:1	LL – 79 PL – 27 PI – 52	S_u – 2000 psf c' – 100 psf ϕ' – 18° (Back-calc.)	Piezometers indicated the presence of two water tables: a perched WT at a depth of 7 feet & regular WT at a depth of 18 feet
M25 Motorway Earth Highway Embankment Britain (Ref 3)	Embankment Slip preceded by heavy rain	NA	11m (36 ft)	NA	NA	NA	Slope was fissured and saturated after a rainfall. Drainage blanket was not draining freely, and acted as a reservoir of water

Ref 1: Chandler & Pachakis, 1973. Ref 2: Threadgold, 1979. Ref 3: Byrd, 1982

Table 8.1b   Piezometric and slope data for selected case records

Embankment Slope Location	Climatic Conditions at Failure	Slope Age (years)	Slope Height (ft)	Slope Ratio (H:V)	Soil Index Properties	Undrained & Drained Strength	Pore Pressure Conditions at Failure
M4 Motorway Earth Highway Embankment Britain (Ref 4)	Embankment Slip preceded by heavy rain	NA	32	2.5:1	LL – 73 PL – 29 PI – 44	NA	Maximum pore pressure occured at the end of precipitation. A wedge of zero pressures extended from toe of slope upwards approx. 3 ft deep
Weedon Road Embank. Britain (Ref 5)	Embankment Slip preceded by heavy rain	15	16	1.5:1	LL – 67 PL – 28 PI – 39	c' – 0 psf ϕ' – 24° (Back-calc.)	Piezometers indicated the presence of two water tables: a perched WT at a depth of 3 feet & regular WT at a depth of 16 feet
Evesham Road Embank. Britain (Ref 5)	Embankment Slip preceded by heavy rain	110	10	2:1	LL – 62 PL – 25 PI – 37	c' – 0 psf ϕ' – 18° (Extrapolated)	Piezometers indicated the presence of two water tables: a perched WT at a depth of 4 feet & regular WT at a depth of 26 feet
Gillingham Rail Embank. Britain (Ref 5)	Embankment Slip preceded by heavy rain	110	13	2.5:1	LL – 78 PL – 25 PI – 53	c' – 0 psf ϕ' – 18° (Extrapolated)	Piezometers indicated the presence of a perched water table which receded at the end of precipitation

Ref 4: Anderson & Kneale, 1980.   Ref 5: Chandler et al, 1973

Table 8.1c   Piezometric and slope data for selected case records

Embankment Slope Location	Climatic Conditions at Failure	Slope Age (years)	Slope Height (ft)	Slope Ratio (H:V)	Soil Index Properties	Undrained & Drained Strength	Pore Pressure Conditions at Failure
Belle Plaine (East Bound) Canada (Ref 6)	Embankment Slip preceded by rainfall or ground thaw	Failed after: 4, 8, 9	20	3:1	LL = 80 PL = 27 PI = 53	S_u = 850 psf c´ = 100 psf φ´ = 20° (Extrapolated)	Average piezometric surface at time of failure measured at a depth of 4 feet below top of the embankment
Belle Plaine (West Bound) Canada (Ref 6)	Embankment Slip preceded by rainfall or ground thaw	Failed after: 5,14,15	Initially: 23 After 9 years: 33	2:1	LL = 80 PL = 27 PI = 53	S_u = 850 psf c´ = 100 psf φ´ = 17.5° (Extrapolated)	Average piezometric surface at time of failure measured at a depth of 2.5 feet below the surface of the embankment
Highway Embankment Britain (Ref 7)	Embankment Slip preceded by a period of prolonged heavy rain	NA	40	2:1	LL = 58 PL = 22 PI = 36	S_u = 1,600 psf c´ = 0 φ´ = 27° (Back-calc.)	Seepage occurred from the median drain flowing down-slope which generated high pore pressures at the toe of the slope
Fort Benton Rail Embank. Montana, USA (Ref 8)	NA	NA	37	2.5:1	NA	NA	Piezometric surface located at a depth of 3 to 10 feet. Piezometric surface intersects toe of slope

Ref 6: Widger & Fredlund, 1978.   Ref 7: Ingold & Clayton, 1978.   Ref 8: Wilson & Mikkelsen, 1978.

EVALUATION OF PORE PRESSURE CONDITIONS AT FAILURE

To estimate pore water pressures for typical embankments in Texas, pore water pressures were back-calculated using data from 34 slope failures. Sixteen of the slope failures occurred in embankments constructed of Paris clay; 18 slope failures occurred in embankments constructed of Beaumont clay. A number of these slides (5 slides in Paris clay and 18 slides in Beaumont clay) were previously identified and examined by Stauffer and Wright (1984). The rest of the slides (11 slides in Paris clay) were reported by personnel from the Texas State Department of Highways and Public Transportation in District 1. A close examination of the material properties for the embankments investigated by Stauffer and Wright (1984), and for the embankments reported by SDHPT personnel, revealed that the embankment soils are similar to the soils tested in the current study. A summary of the slope failures, including their location, age, slope height, slope inclination, and height and depth of slide, is presented in Appendix E. The inclination of these slopes varies from 2:1 to 3.5:1 (horizontal:vertical). Slope heights range from 10 to 30 feet, and ages of the slopes at failure range from 12 to 25 years.

Slope stability computations were performed to back-calculate the pore water pressure conditions at the time of failure. The peak strength effective-stress failure envelopes determined for compacted Paris and Beaumont clays after wetting and drying were used in the computations. Additional stability computations were also performed using the strength envelopes at large strains. The peak strength and large strains envelopes for the Paris and Beaumont clays are presented in tabular form in Table 8.2.
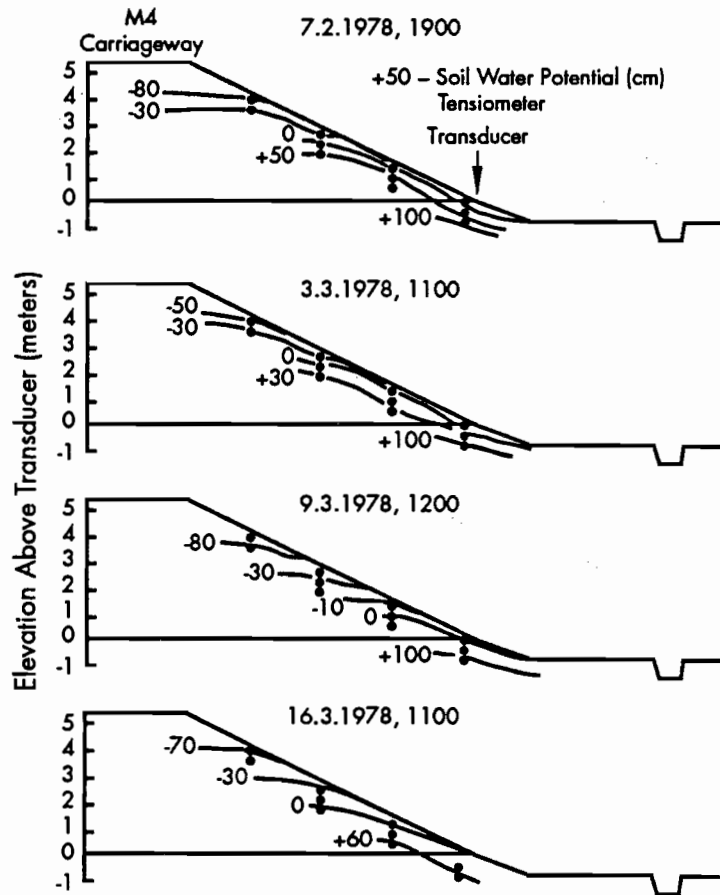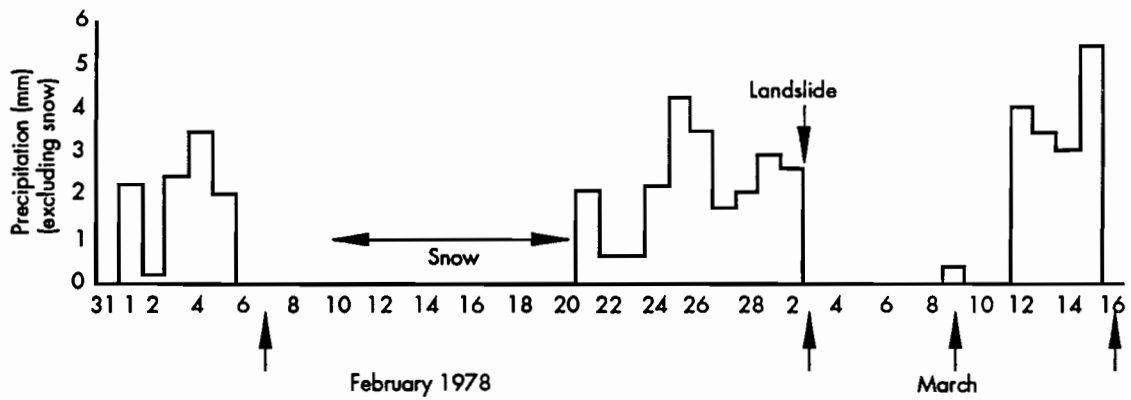
Figure 8.1 Pore water pressure profiles and precipitation record determined for a clay fill embankment in Britain (Anderson and Kneale, 1980)

Relationship Between the Pore Pressure Coefficient and Slope Ratio

Pore pressure coefficients, (r_u), were back-calculated for each slope failure using the peak strength envelope for specimens subjected to wetting and drying. The values of r_u are tabulated, for each slope, in Appendix E. The relationship between the pore pressure coefficients and slope ratio is shown in Figure 8.2. The plotted data indicate that pore water pressure conditions at failure are similar for embankments constructed of Paris or Beaumont clays. Furthermore, as the slope ratio increases (the slope becomes flatter), the pore water pressure required to cause failure increases. The pore pressure coefficients vary from approximately 0.45 for a 2:1 slope to 0.6 for a 3:1 slope. For slopes flatter than 3:1, the pore pressure coefficients appear to reach a limiting value of approximately 0.6 for both soils.

47

A close examination of the pore water pressure coefficients, back-calculated using the peak strength envelopes, reveals that their values are relatively high. The high pore water pressures could be explained by the fact that laboratory measured strengths are too high. For example, the strengths are based on peak values, and do not take into account the effect of shearing stresses during cyclic wetting and drying. The shearing stresses could lower the strengths and, hence, would result in lower back-calculated pore water pressure values. To examine possible effects of a reduced strength, and the effect shearing stresses and strains might have, additional stability computations were performed using the measured strength envelopes at large strains.

Table 8.2 Peak strength and large strains failure envelopes for the Paris and Beaumont clays

As-Compacted Condition				After Wetting & Drying			
Peak Strength (psf)							
Paris Clay		Beaumont Clay		Paris Clay		Beaumont Clay	
σ_n	τ	σ_n	τ	σ_n	τ	σ_n	τ
0	287	0	342	0	24	0	0
275	402	324	540	22	42	117	112
322	422	396	584	111	111	157	138
413	458	435	609	261	207	330	286
719	576	584	685	460	325	747	545
1,118	719	977	900	688	453	1,354	918
1,378	812	1,543	1,185	1,182	650	1,861	1,237
2,056	1,055	2,528	1,468	1,923	948		

Large Strains (psf)			
Beaumont Clay		Paris Clay	
σ_n	τ	σ_n	τ
0	0	0	0
99	73	176	130
241	154	348	252
461	255	662	442
720	380	806	518
1,106	530	1,012	605
2,010	803	2,130	1,070

Pore pressure coefficients (r_u), back-calculated using the strength envelopes at large strains, are tabulated for each slope in Appendix E. The variation of the pore pressure coefficients with slope ratio, calculated for the embankment slopes which failed, is shown in Figure 8.3. The data indicate that pore water pressure coefficients at failure are lower than the corresponding values back-calculated using the peak strength envelopes for slopes constructed from Paris and Beaumont clays. The pore pressure coefficients vary from 0.3 for a 2:1 slope to 0.5 for a 3:1 slope. The decrease in the back-calculated pore pressure coefficients, calculated using the envelope at large

strains as compared to the peak strength envelope, varies between approximately 30 percent for a 2:1 slope and 20 percent for a 3:1 slope.
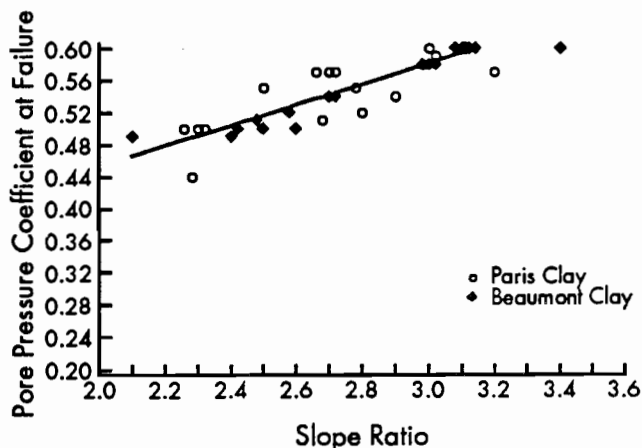
Figure 8.2 Pore water pressure coefficients versus slope ratio for Paris and Beaumont clay fill embankments back-calculated based on the peak strength failure envelope
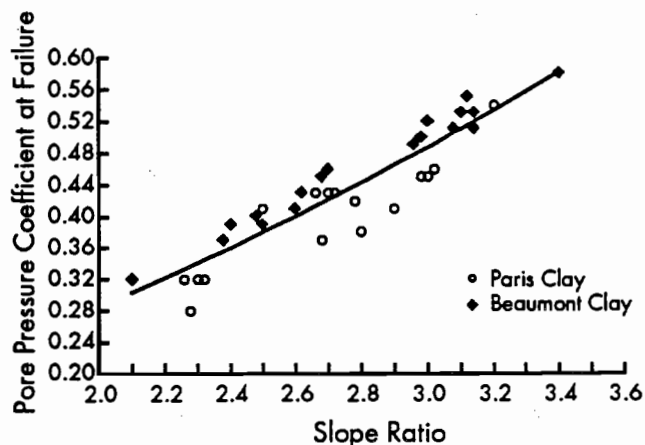
Figure 8.3 Pore water pressure coefficients versus slope ratio for Paris and Beaumont clay fill embankments back-calculated based on the large strains failure envelope

Relationship Between the Depth of Water Table and Slope Geometry

Additional stability computations were performed to establish the depths of a hypothetical piezometric surface required to cause failure. Several combinations of piezometric surfaces were used for this purpose.

Examination of the Piezometric Surfaces

The piezometric surfaces determined by Anderson and Kneale (1980), shown in Figure

48

8.1, indicate that a water table which is tangent to the slope surface near the toe of the slope developed at the time of failure. However, this does not sufficiently or precisely define a piezometric surface for analyses, especially at locations beyond the toe and top of the embankment. To investigate the effect of the assumed piezometric surface geometry, factors of safety were computed for four hypothetical slopes with varying piezometric conditions.

Two of the hypothetical slopes were inclined at 2:1, and the other two were inclined at 3:1. The assumed slope height was 20 feet. Two forms of piezometric surfaces were considered. In the first form, the water table is parallel to the ground surface behind the crest of the slope, as shown in Tables 8.3 and 8.4 (A and C). In the second form, the water table drops abruptly to the level of the toe of the embankment behind the crest of the slope (B and D). In the first form (A and C), the water table is also parallel to the ground surface beyond the toe of the slope. In the second form (B and D), the water table slopes downward at the same inclination as the face of the slope. The vertical distance from the crest of the slope to the top of the piezometric line was defined as the *depth of water table*.

The depth of the water table was selected to produce factors of safety *close* to unity. These depths were zero for the 3:1 slopes, and 3 and 2.5 feet for the 2:1 slopes, in the Paris and Beaumont clays, respectively. Stability analyses were performed using the failure envelopes for specimens subjected to wetting and drying. Two cases were considered regarding pore water pressures above the water table. In the first case, hydrostatic suction pressures were assumed above the water table. In the second case, zero pore water pressures were assumed above the water table.

The computed factors of safety are presented in Table 8.3 for the Paris slopes and in Table 8.4 for the Beaumont slopes. Also included in these tables are the percentage differences in the calculated factors of safety for the two forms of piezometric surfaces. It is evident that the orientation of the water table behind the crest, or beyond the toe of the slope, does not influence the computed factor of safety. The largest percentage differences for the two piezometric surfaces are 2.4 percent for a 2:1 slope in Paris clay, and 2.9 percent for a 2:1 slope in Beaumont clay. Furthermore, the assumption of zero or negative pore water pressures above the water table does not significantly affect the values of the computed factors of safety. Accordingly, a piezometric surface similar to the form represented by "C" was chosen for back-calculating the depth of water tables for the 34 slopes considered in this study.

Relationship Between the Water Table Position and Slope Ratio

The depth of water table was back-calculated for the 34 slopes considered in this study using the peak strength envelopes for the compacted Paris and Beaumont clays after wetting and drying. Negative pore water pressures were assumed above the water table. The depth of water table at failure, which was back-calculated for each slope, is tabulated in Appendix E. For plotting purposes, the position of the water table was expressed in terms of a height of water table (H_w), defined as the vertical distance from the toe of the embankment to the horizontal portion of the water table beneath the crest of the slope. Thus, *the water table height* is the slope height minus the depth of the water table. The water table height was divided by the slope height (H) to obtain a dimensionless quantity which was then plotted versus the slope ratio. The dimensionless ratio (H_w/H) is plotted versus slope ratio in Figure 8.4 for each of the slope failures. The results indicate that for slopes flatter than 3:1, the water table coincides with the slope surface (i.e. H_w/H is unity). For steeper slopes, the height of the water table gradually decreases as the slope becomes steeper. The height of the water table for embankments constructed of Beaumont clay is greater than the corresponding height for embankments constructed of Paris clay. For a 2:1 slope in Paris clay, it may be expected that the slope would fail when the water table height reaches approximately 80 percent of the slope height. The corresponding value for a slope in Beaumont clay is approximately 90 percent of the slope height. If a water table that coincides with the surface of a 2:1 slope was assumed, the calculated factor of safety would be lower by approximately 30 percent for the Paris clay slope (from 0.95 to 0.67) and by 40 percent for the Beaumont clay slope (from 1.06 to 0.60).

Table 8.3 Influence of assumed piezometric surface profiles on calculated factors of safety for Paris clay

Slope Geometry and Piezometric Surface Profile	Factors of Safety with Negative Pore Pressures	Factors of Safety with Zero Pore Water Pressures
A 3:1 SLOPE	1.017	1.017
B 3:1 SLOPE	1.012	1.012
Percentage Difference (A vs. B)	0.5	0.5
C 2:1 SLOPE	0.952	0.940
D 2:1 SLOPE	0.975	0.943
Percentage Difference (C vs. D)	2.4	0.3

Additional stability computations similar to these described above were performed using the strength envelopes at large strains. The depth of the water table was back-calculated for each slope and is tabulated in Appendix E. The dimensionless ratio (H_w/H) is plotted versus the slope ratio in Figure 8.5 for each of the slopes. As expected, the results show that a decrease in the ratio H_w/H occurs when the strength at large strains is used. The decrease in the ratio H_w/H varies for slopes in Beaumont clay between approximately 3 percent for a 3:1 slope and 7 percent for a 2:1 slope. The corresponding decrease in the ratio H_w/H for slopes in Paris clay varies from approximately 17 percent for a 3:1 slope to 35 percent for a 2:1 slope.

Relationship Between the Age of Slopes and Pore Pressure Coefficients

Pore water pressure coefficients back-calculated using the peak strength envelopes are plotted versus the age of the slope at failure in Figure 8.6. There appears to be no relationship between the age of the slope and the pore water pressure coefficients at failure.

Table 8.4   Influence of assumed piezometric surface profiles on calculated factors of safety for Beaumont clay

Slope Geometry and Piezometric Surface Profile	Factors of Safety with Negative Pore Pressures	Factors of Safety with Zero Pore Water Pressures
A 3:1 SLOPE	1.004	1.004
B 3:1 SLOPE	1.004	1.004
Percentage Difference (A vs. B)	0.5	0.5
C 2:1 SLOPE	1.056	1.046
D 2:1 SLOPE	1.087	1.049
Percentage Difference (C vs. D)	2.9	0.3

Comparison Between the Measured and Calculated Depths of Slide

The depths of slide reported for the case histories are compared in Figure 8.7, with the calculated depths of slide obtained from the critical circles in the stability computations. Stability computations were performed using the peak strength envelopes. It can be seen that good agreement was obtained between the computed and reported depths of slide. The critical circles determined from the stability analyses are representative of the shallow slide surfaces that develop in the field.

CONCLUSIONS AND RECOMMENDATIONS

Stability analyses indicate that relatively high pore water pressures may have existed in many of the embankments constructed of Paris and Beaumont clays which failed. Although there is relatively little data in the literature, significant positive pore water pressures have been measured in other clay embankments which failed, as reported in the literature. The literature suggests that relatively shallow water tables may develop very near the surface of the slope. Such shallow water tables agree closely with what has been back-calculated for the slope failures in Paris and Beaumont clays.
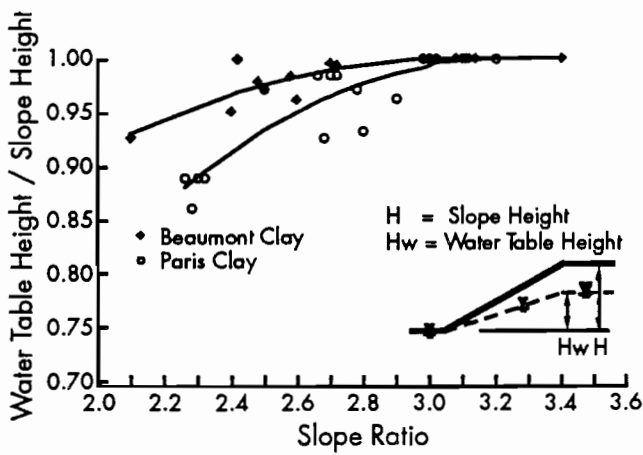
Figure 8.4 Height of water table over slope height versus slope ratio for Paris and Beaumont clay fill embankments back-calculated based on the peak strength failure envelope
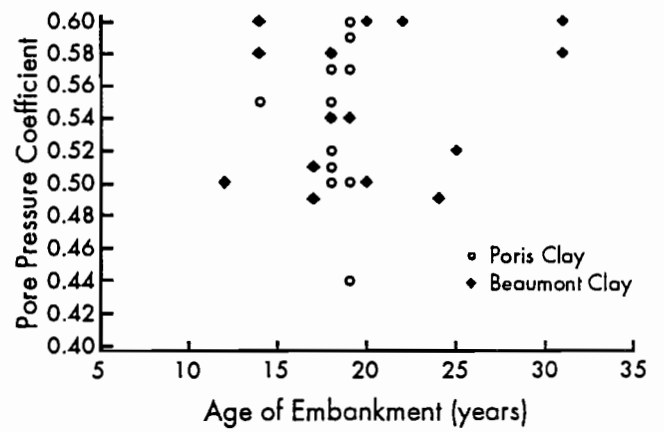
Figure 8.6 Age of Paris and Beaumont clay fill embankments from time of construction to failure versus pore water pressure coefficients
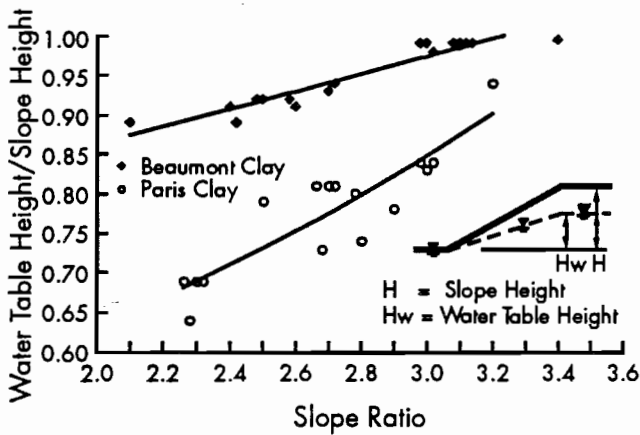
Figure 8.5 Height of water table over slope height versus slope ratio for Paris and Beaumont clay fill embankments back-calculated based on the large strains failure envelope
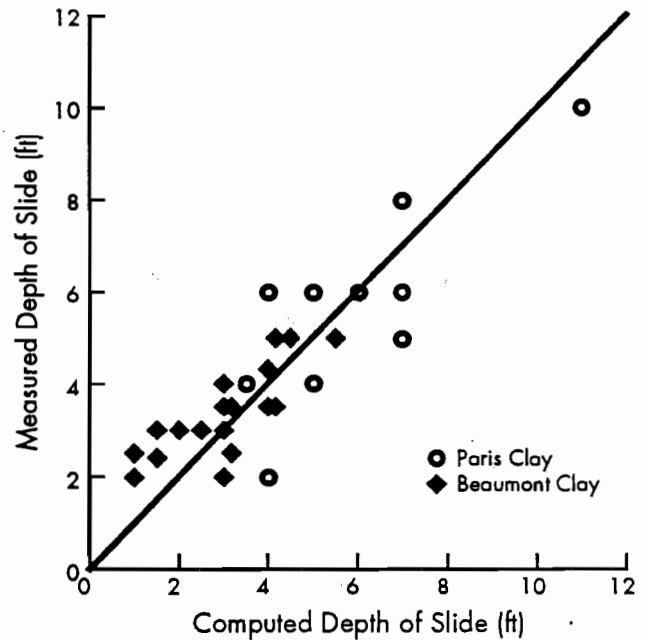
Figure 8.7 Measured depth of slide versus computed depth of slide for Paris and Beaumont clay fill embankments

52

The position of the water table beyond the toe of the slope, or behind the crest of the embankment, has little influence on the stability of the embankments considered. Furthermore, the development of negative suction pressures above the water table did not appear to influence the stability significantly.

Using peak strength envelopes, water table heights corresponding to 80 and 90 percent of the slope height were calculated for 2:1 slopes in Paris and Beaumont clays, respectively. The water table height coincides with the height of the slope for 3:1 slopes in both clays. Using the strength envelope at large strains, water table heights decreased by 3 to 7 percent for slopes in Beaumont clay and by 17 to 35 percent for slopes in Paris clay.

Back-calculated pore water pressures indicate that, for slopes flatter than 3:1, either a water table that coincides with the surface of the slope or pore water pressure coefficients ranging from approximately 0.5 to 0.6 should be used for design. This is based on pore water pressures that were back-calculated using the peak effective-stress shear strength envelope for specimens that were subjected to wetting and drying. Accordingly, the strengths used for design should be equivalent to the strengths of specimens subjected to wetting and drying. As shown earlier, these strengths may be obtained either from specimens which have been subjected to wetting and drying, or by measuring the "fully softened" strengths using specimens that are normally consolidated from a slurry.

For slopes steeper than 3:1, back-calculated pore water pressures were lower by as much as 30 to 40 percent than those calculated for 3:1 slopes and flatter. However, it is not known if higher pore water pressures would have developed had the slopes not failed first. Accordingly, the same pore water pressure conditions are recommended for design of slopes steeper than 3:1, as have been recommended for design of slopes 3:1 and flatter. That is, either a water table that coincides with the surface of the slope or pore water pressure coefficients ranging from approximately 0.5 to 0.6 are recommended for design.

CHAPTER 9.   CONCLUSIONS AND RECOMMENDATIONS

SUMMARY AND CONCLUSIONS

A series of consolidated-undrained triaxial compression tests with pore water pressure measurements was performed on compacted specimens subjected to repeated cycles of wetting and drying. The purpose of these tests was to determine the effect of wetting and drying on the long-term shear strength properties of compacted highly plastic clays used to construct embankments in Texas. Additional tests were performed on specimens tested in their as-compacted condition, without wetting and drying, to compare the strength properties before and after wetting and drying. A third series of tests was performed on normally consolidated specimens to determine if the fully softened strength might be applicable for the problem of shallow slides in embankments.

Wetting and drying was found to produce a drop in strength from that which was measured for specimens tested in the as-compacted condition. This loss in strength occurred in the effective-stress failure envelope over a range of stresses which is applicable to the problem of shallow slides in the field. Test results also revealed that normally consolidated specimens, and compacted specimens subjected to wetting and drying have comparable effective-stress shear strength envelopes. Other experiments were performed to determine the clay particle orientations for compacted specimens which were subjected to wetting and drying as well as those for normally consolidated specimens. These experiments indicated that the clay particle orientations were very similar for the two types of specimens. This agreement suggests that similar effective-stress shear strength envelopes correspond to similar soil structures. Hence, the long-term strength properties of compacted highly plastic clay embankments exposed to cyclic wetting and drying may be measured in the laboratory by performing tests on laboratory prepared specimens of the soil in a normally consolidated state.

Computations were performed to compare the calculated and observed stability conditions for two case histories. Stability analyses confirmed that the reduction in strength due to wetting and drying partially explains the observed shallow slope failures. Stability analyses also revealed that the back-calculated pore water pressures at failure were higher than anticipated at the outset of the current study, and assumed previously by Stauffer and Wright (1984) and by Green and Wright (1986). The stability analyses showed that significant positive pore water pressures would have to exist in the two embankments to cause failure.

Pore water pressures were back-calculated for 34 shallow slope failures in embankments constructed of Paris and Beaumont clays. These calculations indicated that relatively high pore water pressures may exist at failure. A survey of the literature for clay embankments, where pore water pressures were measured at failure, revealed that relatively shallow piezometric surfaces may develop very near the surface of the slope. Such shallow piezometric surfaces agree closely with what has been back-calculated for the slope failures in this study.

Back-calculated pore water pressures indicate that for slopes flatter than 3:1, either a water table that coincides with the surface of the slope or pore water pressure coefficients ranging from approximately 0.5 to 0.6 should be used for design. This is based on pore water pressures that were back-calculated using the peak effective-stress shear strength envelope for specimens that were subjected to wetting and drying. Accordingly, the strengths used for design should be equivalent to the strengths of specimens subjected to wetting and drying

For slopes steeper than 3:1, back-calculated pore water pressures were lower by as much as 30 to 40 percent than those calculated for 3:1 slopes and flatter. However, it is not known if higher pore water pressures would have developed had the slopes not failed first. Accordingly, the same pore water pressure conditions are recommended for design of slopes steeper than 3:1, as have been recommended for design of slopes 3:1 and flatter. That is, either a water table that coincides with the

surface of the slope or pore water pressure coefficients ranging from approximately 0.5 to 0.6 are recommended for design.

RECOMMENDATIONS FOR FUTURE RESEARCH

Determination of the pore water pressures that develop in embankment slopes constructed of Paris and Beaumont clays is necessary to confirm the pore pressure values back-calculated from the slope failures in the current study. In-situ pore water pressure measurements may also be used to back-calculate a failure envelope that takes into account the effect of the shearing stresses, due to cyclic wetting and drying, in the field.

Remedial measures also need to be explored for resolving the problem of delayed shallow slides in embankment slopes. Vaughan et al (1978), Lumb (1975), and Symons (1979) have considered the effect of vegetation on impeding the infiltration of a wetting front into the embankment soils. Parsons and Perry (1985) and Vail and Beattie (1985) have evaluated the effectiveness of placing gravel layers beneath the top soil to reduce the depth of seasonal fluctuations. Parsons and Perry (1985) investigated the effect of open ditches and the ability of slopes to shed water on the observed failure rates in fill embankments. Detailed investigation of some of these remedial measures and others should be conducted to explore their application to the shallow embankment slides in Texas.

APPENDIX A.   INVESTIGATION OF CHANGES IN MATERIAL PROPERTIES OF THE PARIS CLAY

INTRODUCTION

A laboratory investigation was conducted to compare the material properties of the soil in the Paris embankment with the soil from the original borrow area used to construct the embankment in 1966. Soil was obtained both from the embankment and from the borrow area. Laboratory tests were performed on these soils to measure the physical, mineralogical, chemical, and shear strength properties.

DESCRIPTION OF BORROW SITE

Design plans for the Paris embankment indicated that a borrow site located approximately one-half mile north of the actual embankment was used to obtain soil for construction. The location of the borrow site is shown in Figure A.1. The soil profile at the site consists of 6 feet of dark clay over 5 feet of light yellow clay underlain by light grey clay. Plans for the embankment specified that only the yellow clay be used for construction.

Two borings, 25 feet apart, were drilled at the site, and soil samples were obtained from depths varying from 7 to 10 feet. Samples obtained from the borrow site are referred to as the Paris *borrow clay* (Boring 1 or Boring 2); samples acquired from the existing embankment are designated as the Paris *embankment clay.*

PHYSICAL PROPERTIES

Tests conducted to measure the physical properties of the borrow and embankment clays consisted of index tests, grain size analyses, and Standard Proctor compaction tests. Consolidated-undrained triaxial compression tests with pore water pressure measurements were also performed to evaluate the consolidation properties and the as-compacted shear strength properties of the two soils.

Figure A.1   Location of borrow site used for the construction of the Paris embankment

Index Property Tests

Results of Atterberg limit and specific gravity determinations are tabulated in Table A.1. The results indicate that the clays from the two sources are similar; the liquid limits are within 10 percent of each other, and the difference in specific gravities is less than 1 percent.

Grain Size Analyses

Grain size distribution curves are shown in Figure A.2. It can be seen that the differences in the grain size distributions for the borrow and the embankment clays are insignificant.

Standard Proctor Compaction Tests

Standard Proctor compaction curves for the borrow and the Paris embankment clays are shown in Figure A.3. The difference in the

maximum dry density for the two clays is less than 5 percent.

Triaxial Compression Tests

A series of isotropically consolidated-undrained triaxial compression tests with pore water pressure measurements was performed on laboratory compacted specimens from the embankment and borrow clays (Boring 1). Soil specimen preparation methods are presented in Chapter Three. Triaxial testing procedures and triaxial test results are presented in Appendices B and C, respectively. Plots of the isotropic consolidation curves are shown in Figure A.4. It appears that the compression indices for the two types of materials may be similar, as suggested by the nearly parallel consolidation curves. The effective stress paths are plotted in Figure A.5. It can be seen that both clays produce essentially the same failure envelope.

Table A.1   Index properties for Paris clay samples from the embankment and borrow sites

Index Parameters	Embankment Clay	Borrow Clay (Boring 1)	Borrow Clay (Boring 2)
Liquid Limit (LL)	80	72	72
Plastic Limit (PL)	22	21	24
Plasticity Index (PI)	58	51	48
Specific Gravity (G_S)	2.71	2.72	2.73
Activity	0.97	0.84	0.84
Unified Soil Classification Symbol	CH	CH	CH
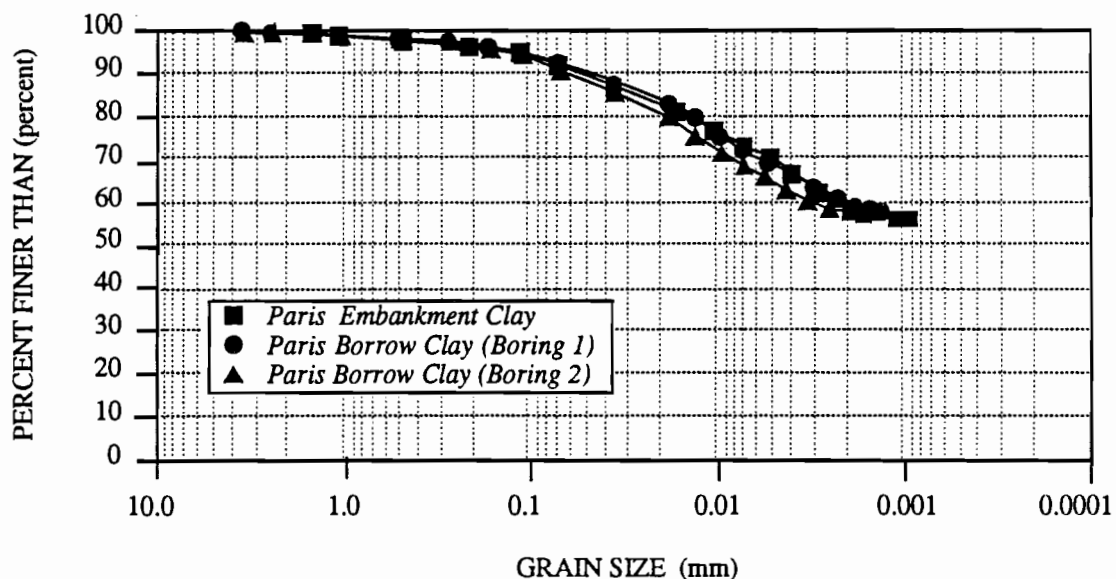
Figure A.2   Grain size distributions for Paris clay samples obtained from the embankment and borrow sites
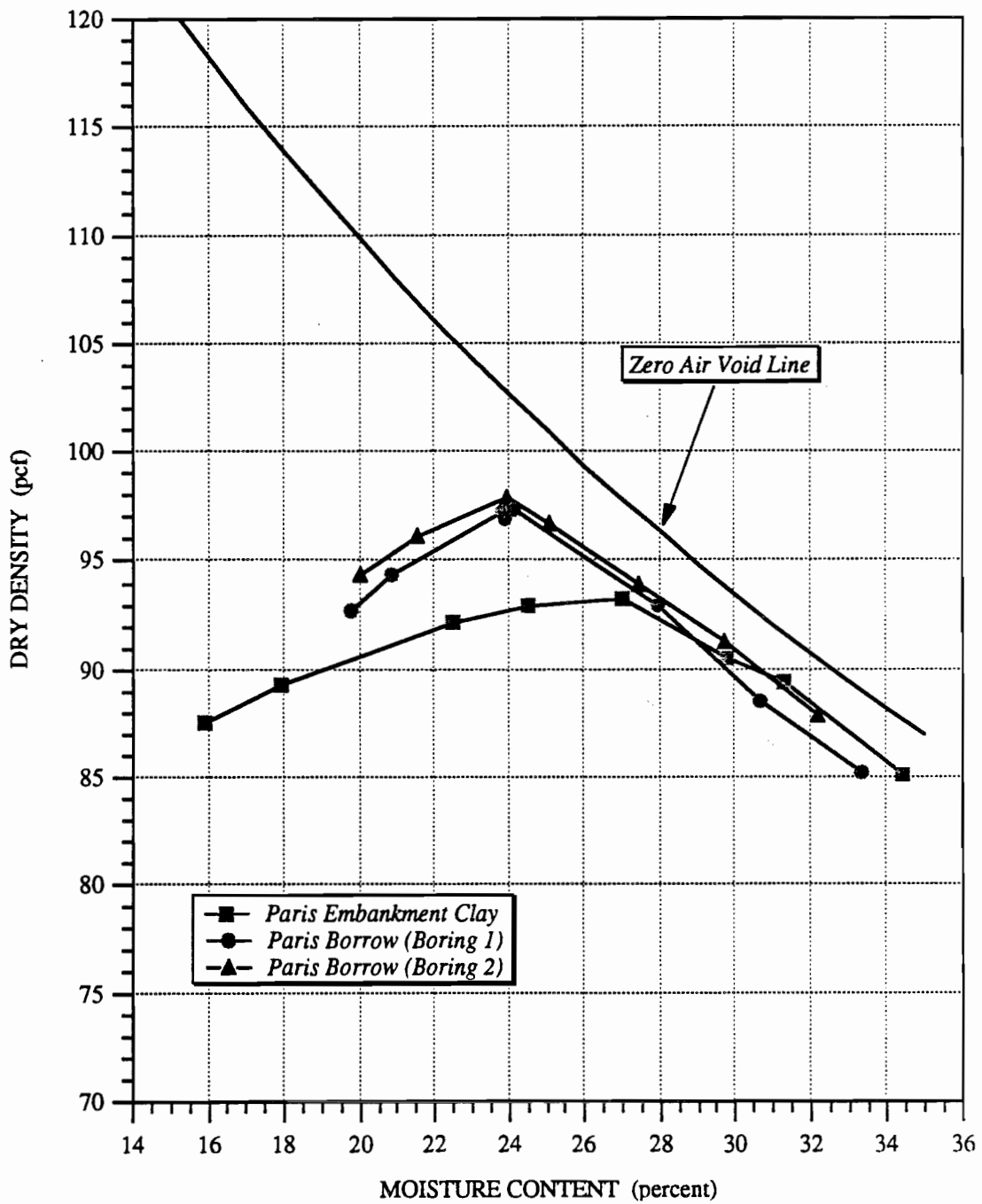
Figure A.3 **Standard Proctor moisture density curves for Paris clay samples obtained from the embankment and borrow sites**
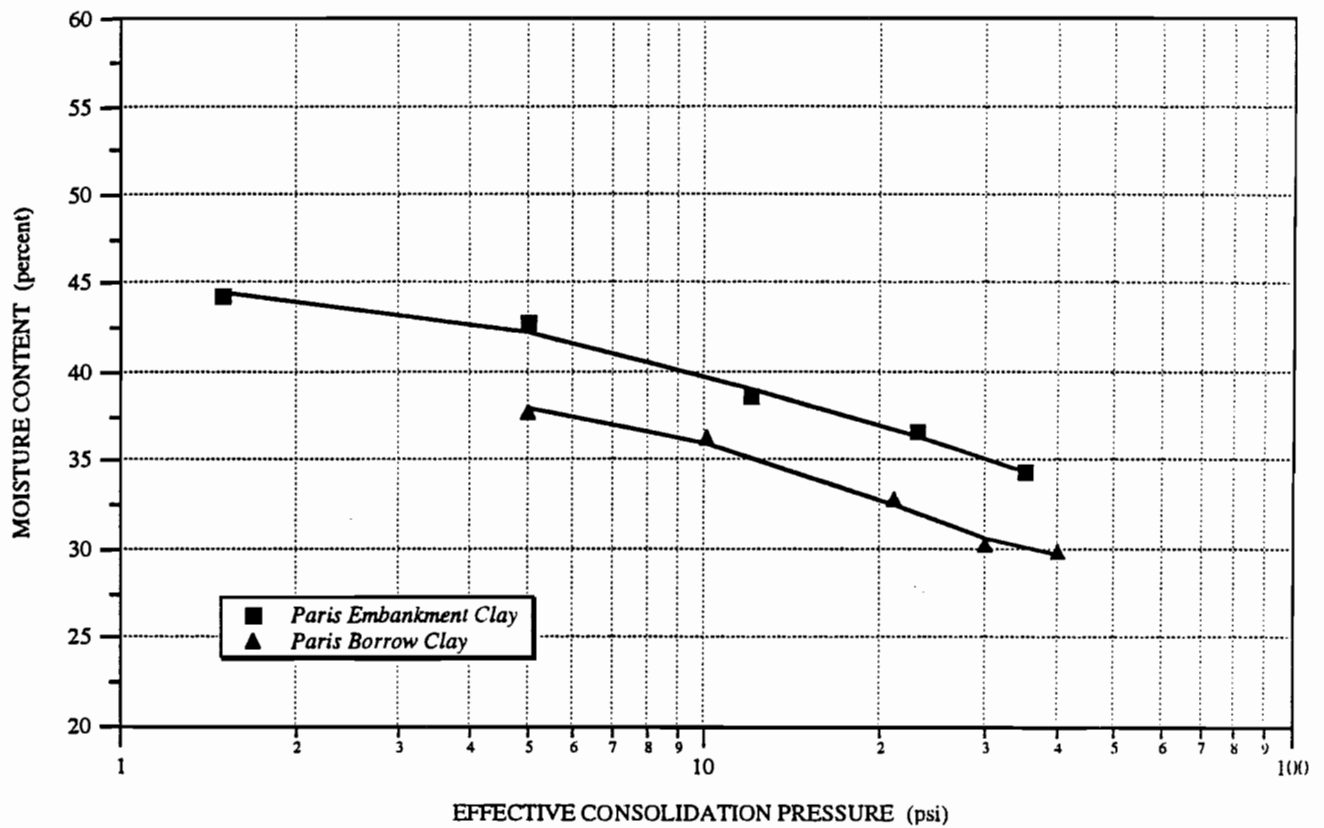
Figure A.4   Moisture contents at the end of shear versus effective consolidation pressures for compacted Paris clay specimens from the embankment and borrow sites
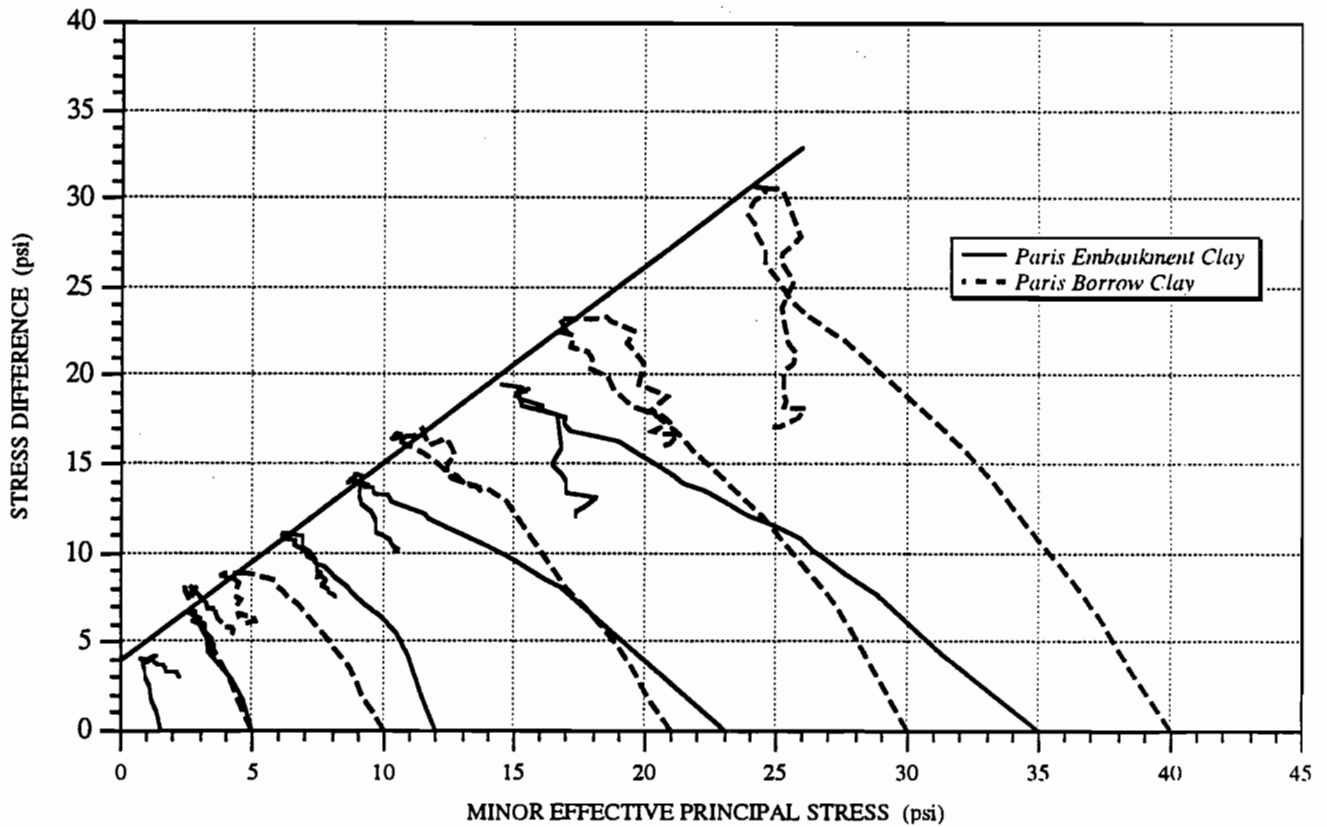
Figure A.5   Effective stress paths and modified Mohr-Coulomb failure envelope for compacted Paris clay specimens from the embankment and borrow sites

ELEMENTAL CONSTITUENTS AND MINERALOGICAL PROPERTIES

The mineralogical properties of the Paris borrow and embankment clays were determined by means of the X-ray diffraction method. Qualitative X-ray microanalyses were also performed to determine the elemental constituents of both clays. Results from these tests are presented in the following sections.

X-Ray Diffraction Tests

The mineral constituents which were identified in the embankment and borrow clays consist of calcium montmorillonite, mica, illite, kaolinite, quartz, and plagioclase feldspars. New minerals, such as calcium carbonate, were not identified in the embankment clay.

Qualitative X-Ray Microanalyses

X-ray peaks obtained from X-ray microanalyses are shown in Figure A.6 for the embankment clay and in Figure A.7 for the borrow clay. The elements corresponding to the X-ray peaks are listed on these plots. All the elements identified in the borrow clay were also found in the embankment clay, except chlorine (Cl), which could not be identified for the embankment clay. The presence of chlorine in the borrow clay may be attributed to local variations in the chemical composition of the ground water at the borrow site.

CHEMICAL PROPERTIES

Tests performed to determine the chemical properties consisted of soil pH measurements and measurements for concentrations of exchangeable cations by the Flame photometer Atomic Absorption method (FAA). Test results are presented in the following sections.
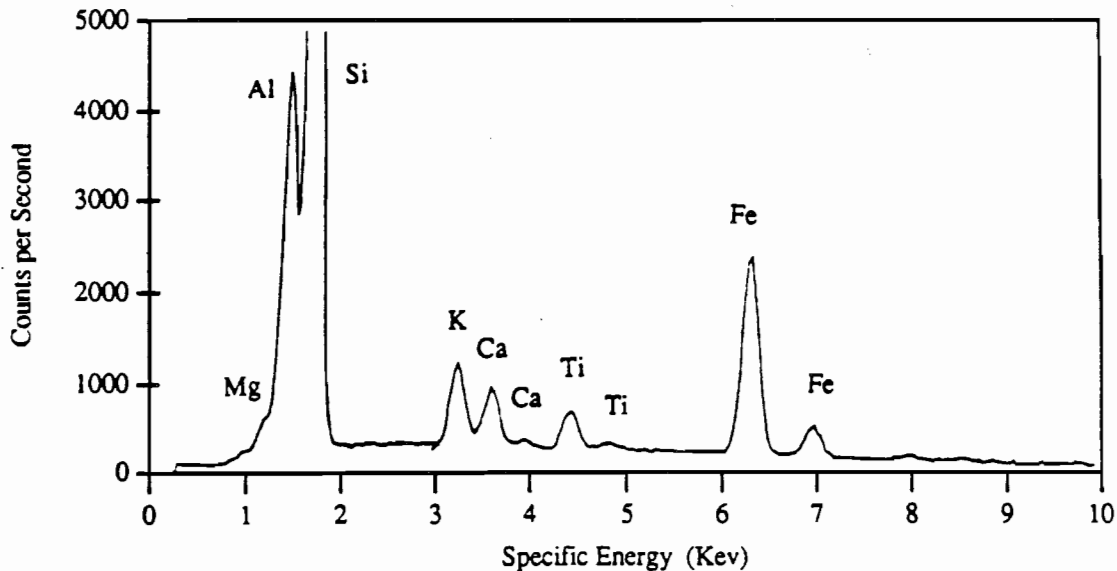
Figure A.6   Elemental Constituents for Paris Clay Specimens from the Embankment Site Using X-ray Microanalyses Techniques
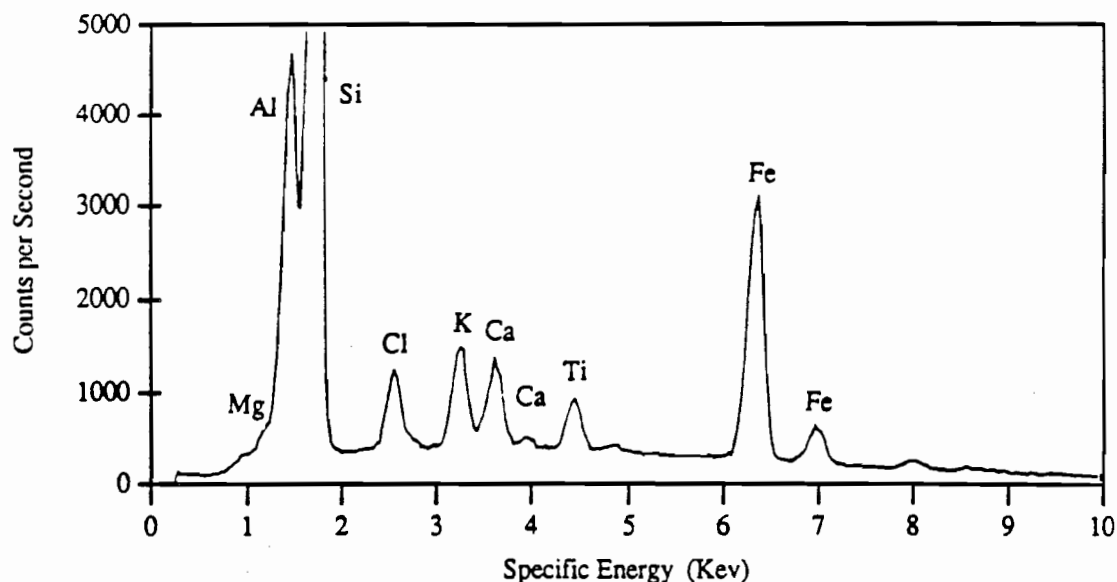
Figure A.7 Elemental constituents for Paris clay specimens from the borrow site using X-ray microanalyses techniques

Soil pH Tests

Soil pH was used to determine whether the soil was acidic, neutral, or basic. The pH of a solution is defined as the negative logarithm (base 10) of the hydrogen ion activity according to the following equation:

$$pH = -\log_{10}[H^+]$$

A pH of less than 4 indicates the presence of free acids; a pH of less than 5.5 suggests the likely occurrence of exchangeable aluminum; and a pH from 7.8 to 8.2 indicates the presence of calcium carbonate, $CaCO_3$ (Methods of Soil Analysis, 1982).

There are a number of factors that may influence the measured pH, including the nature and type of inorganic and organic constituents in the soil, the soil solution ratio, the salt or electrolyte content, and the CO_2 content. CO_2 dissolved directly from the atmosphere lowers the pH of the soil solution (Methods of Soil Analysis, 1982).

Experimental Procedures

Soil pH measurements were performed by measuring 5 grams of soil (oven-dry weight) and 20 ml of $0.1M$ NaCl solution. The soil and the NaCl solution were mixed for a period of 30 minutes prior to measuring the pH values. A commercial pH meter connected to a glass electrode paired with a Calomel (Hg-Hg_2Cl) reference electrode was used. The glass electrode was placed in the soil solution, and pH values were recorded once the readings had stabilized.

Soil samples used for testing consisted of air-dried soil at a 5 percent moisture content and wet soil at a 30 percent moisture content. The air-dried soil was in contact with the air (CO_2) in the laboratory atmosphere for approximately 3 months. The wet soil was stored in double plastic bags from the time it was obtained from the field until the time of testing. Soil pH measurements are tabulated in Table A.2. The difference in pH values between the borrow and embankment clays, and between the wet and dry soil, is insignificant.

Measurement of the Exchangeable Cations

The concentrations of four exchangeable cations—Ca^{2+}, Mg^{2+}, K^+, and Na^+—were determined for the Paris borrow and embankment clays. Exchangeable cations are those that can be exchanged by a cation of an added salt solution. Measurement of these cations was performed according to the guidelines provided by the manual on Methods of Soil Analysis (1982). The soil was combined with an excess of $1N$ NH_4OAc (ammonium acetate) solution such that maximum exchange occurs in a few minutes. The soil solution was mixed for 10 minutes, and then was placed in a centrifuge at 2,000 rpm for an additional 10 minutes. The supernatant liquid was extracted, and the concentrations of the exchangeable cations were determined based on the Flame photometer Atomic Absorption method. An Inductively Coupled Plasma Emission Spectrophotometer (ICP) was used to measure the cations concentrations. Cation concentrations for the embankment and the

borrow clays (Boring 2) are presented in Table A.3. These results indicate that the Paris clay is mainly a calcium clay. The difference in the concentrations of the calcium cations between the embankment and the borrow clay is insignificant (less than 7 percent). The cation concentrations for the other elements (K^+, Mg^{2+}, Na^+) are relatively small.

CONCLUSIONS

Physical properties, mineralogical composition, elemental constituents, and chemical properties were determined for samples of Paris clay taken from the embankment and original borrow sites. Test results indicated that the clays from the two sources are similar.

Table A.2   pH values for Paris clay samples from the embankment and borrow sites

Soil Type	Soil Dry	Soil Wet
Embankment Clay	7.2	7.3
Borrow Clay (Boring 1)	7.3	7.4
Borrow Clay (Boring 2)	7.3	7.3

Table A.3   Cation concentrations for Paris clay samples from the embankment and borrow sites

Cations	Concentrations [Mg/L]	
	Embankment Clay	Borrow Clay
Ca^{2+}	460	430
K^+	100	50
Mg^{2+}	45	20
Na^+	50	100

APPENDIX B. TRIAXIAL SHEAR TEST PROCEDURES

INTRODUCTION

The triaxial shear test procedures employed for consolidated-undrained triaxial compression tests with pore water pressure measurements are presented in this Appendix. Procedures for setting up specimens in the triaxial cells, back-pressure saturation and consolidation, and triaxial shear are described.

PROCEDURE FOR SETTING UP TRIAXIAL SPECIMENS

Prior to setting up a specimen in the triaxial cell, the lines leading to the base of the cell and specimen were saturated with deaired water. For compacted soil specimens, the specimens were placed directly on the porous stone in the triaxial cell. For normally consolidated specimens, and specimens subjected to wetting and drying, a porous stone was placed on the specimen prior to transferring it to the triaxial cell. The specimen, underlain by the porous stone, was then transferred to the base pedestal of the triaxial cell using a plastic wrap sprinkled with talcum powder. With this procedure, it was possible to adjust the position of the specimen on the base pedestal without disturbing the soil specimen A 1.5-inch-diameter disk of filter paper was placed between the porous stone and the specimen. The top cap was positioned on top of the specimen, and a vertical filter paper drain prepared from Whatman No. 1 chromatography paper was moistened and wrapped around the perimeter of the specimen. The filter paper was cut to remove alternating vertical strips such that approximately 50 percent of the perimeter of the specimen was covered. Two membranes were placed on the specimen using a suction membrane expander. The membranes were sealed against the top and bottom caps with rubber O-rings. The cell and top plate of the triaxial apparatus were then assembled and secured. The loading rod was coated with silicon oil, slowly pushed through the ball bushing assembly in the top plate of the cell, and seated in the top cap.

The triaxial cell was filled with deaired water, and the height of the specimen was measured. At this stage, the specimen was ready for back-pressure saturation.

BACK-PRESSURE SATURATION AND CONSOLIDATION

Specimens were back-pressure saturated prior to isotropic consolidation to the final effective consolidation pressure. For specimens consolidated to a final effective consolidation pressure of 5 psi or less, the effective consolidation pressure used during back-pressure saturation was typically 1 psi lower than the final effective consolidation pressure. For specimens consolidated to final effective consolidation pressures higher than 5 psi, the effective consolidation pressure during back-pressure saturation was 5 psi.

A soil specimen was brought to full saturation by incrementally increasing the applied back-pressure and cell pressure. The back-pressure was increased in 5-psi pressure increments. Skempton's B-coefficient (Skempton, 1954) was measured at the end of each increment to determine whether the soil specimen had achieved full saturation.

Once the measured B-value indicated full saturation, the specimen was isotropically consolidated to the effective consolidation pressure. Specimens were consolidated to pressures ranging from 1 psi to 35 psi. The pressure increments applied for consolidation did not exceed 10 psi. Prior to applying the final consolidation pressure, the triaxial cell was placed on the loading press to establish equilibrium. This was necessary because the triaxial cell was 15 inches higher in the loading press than the laboratory level. A 15-inch-high water column increases the applied pressure on the specimen by approximately 0.5 psi.

TRIAXIAL SHEAR PROCEDURE

Once a specimen was saturated and consolidated, it was sheared to failure at a constant rate of deformation with no drainage. The rate of

deformation was determined by estimating the times to failure for a number of specimens. Selection of the rate of shear is explained below.

Selection of Rate of Deformation

Constant rates of deformation of 0.0009 inches per hour and 0.0047 inches per hour were selected for the Paris and the Beaumont clays, respectively. These rates were applied to *all* specimens of the respective soils. The rates of deformation were determined based on estimates of the times required to failure for several tests. However, because of the uncertainties involved in computing an actual rate of deformation from theoretical calculations of times to failure, slower rates than the theoretically calculated values were chosen.

Times to failure values (t_f) were calculated based on the coefficient of consolidation (c) and the drainage path within the specimen (H). Bishop and Henkel (1962) suggested that for drainage from one end and through the radial boundary, the coefficient of consolidation (c) can be calculated with the following equation:

$$c = \frac{\pi H^2}{81 t_{100}}$$

where H is one-half the height of the specimen during consolidation, and t_{100} is determined from consolidation data using Bishop and Henkel's approach (1957), in which the volume change during consolidation is plotted versus the square root of consolidation time.

Times to failure (t_f) were determined based on the minimum time to failure which corresponds to a degree of pore pressure equalization of 95 percent in an undrained triaxial shear test with all-around drainage (Blight, 1963):

$$t_f = \frac{0.07 H^2}{c}$$

The calculated times to failure are presented in Table B.1 for a selected number of tests. The selected rates of deformation (0.0009 inches per hour for the Paris specimens, and 0.0047 inches per hour for the Beaumont specimens) are considerably slower than the rates based on the calculated times to failure (approximately twenty times slower for the Paris specimens, and ten times slower for the Beaumont specimens). Such slow rates were intended to ensure the equalization of the pore water pressures during shear along the height of the specimen. The equalization of pore pressures in the specimen was necessary since pore water pressures were being measured through the base of the specimen.

During shear, the axial deformation, axial load, and pore water pressure were measured at regular time intervals. These values were recorded by means of an automated data acquisition system. Specimens were sheared to maximum axial strains ranging from approximately 18 to 22 percent.

CONCLUSION OF TEST

At the conclusion of each triaxial test, all valves connected to the base pedestal of the triaxial cell were closed, pressure lines were disconnected, and the triaxial cell was dismantled. For approximately twenty specimens, either the dimensions of the shear plane and its inclination were determined (in the case of failure along a shear plane), or the diameter of the specimen at different heights was measured (in the case of a bulging failure). The membranes and the vertical filter paper drains were removed after measuring the applicable dimensions. The triaxial specimen was then removed from the base pedestal and placed in an oven to dry at a temperature of 110°C. The final moisture content of the specimen was determined after drying for approximately 48 hours.

Table B.1 Times to primary consolidation, times to failure and coefficients of consolidation for Paris and Beaumont clay specimens

Test No.	Soil Type	σ_c (psi)	t_{100} (min)	c (in^4/min)	t_f (min)
C26.01	Paris	1.0	25	3.5×10^{-3}	45
C20.35	Paris	35.0	400	2.2×10^{-4}	716
S36.02	Paris	2.0	30	2.9×10^{-3}	55
S31.35	Paris	35.0	350	2.5×10^{-4}	630
S45.02	Paris	2.0	25	3.5×10^{-3}	45
S44.30	Paris	30.0	370	2.4×10^{-4}	656
C72.02	Beaumont	2.0	15	5.8×10^{-3}	27
C71.25	Beaumont	25.0	150	5.8×10^{-4}	272
S53.04	Beaumont	4.0	25	3.5×10^{-3}	45
S58.34	Beaumont	34.0	190	4.6×10^{-4}	342
W65.02	Beaumont	2.0	20	4.4×10^{-3}	35
W64.30	Beaumont	30.0	160	5.4×10^{-4}	292

APPENDIX C. TRIAXIAL TEST RESULTS

Tabulated results for triaxial compression tests performed on the Paris and Beaumont clay specimens are presented in this Appendix. Results are summarized for compacted specimens tested in both the as-compacted condition and after wetting and drying, as well as for specimens which were consolidated from a slurry. Summary plots of these results were presented in Chapters 4 and 5. Test results for each test consist of axial strain, minor principal effective stress, principal stress difference, effective principal stress ratio, and $\overline{A}$ coefficients. The measured deformations, loads, and pore water pressures, the effective consolidation pressure, the area correction factor (Appendix D), and the height of the specimen at the end of consolidation are also tabulated for each test.

Triaxial tests were identified by names consisting of letters and numbers. Triaxial test names were divided into three groups based on the type of specimen at the time of set-up. Specimens tested in the as-compacted condition were designated by the letter "C," specimens consolidated from a slurry were designated by the letter "S," and specimens subjected to wetting and drying were designated by the letter "W." Specimens in a given group were numbered according to the sequence in which they were tested. A suffix was appended to the test names to designate the effective consolidation pressure (consolidation pressures are preceded with a decimal point in the test name). For example, test C20.35 designates a specimen of Paris clay which was tested in an as-compacted condition, and was isotropically consolidated to an effective consolidation pressure of 35 psi. The specimen numbering system is shown in Table C.1. Tabulated test data are presented in the following pages. The first line of each page gives the test name; there is one page per test. Tests results are arranged according to the sequence in which they were tested.

Table C.1   Specimen numbering system

Condition of Specimen at the Time of Set-Up	Test Number
As-Compacted Paris Clay *(Soil from Borrow Site)*	C10.XX to C19.XX
As-Compacted Paris Clay *(Embankment Soil)*	C20.XX to C29.XX
Consolidated from a Slurry *(Paris Clay)*	S30.XX to S39.XX
After Wetting & Drying *(Paris Clay)*	W40.XX to W49.XX
Consolidated from a Slurry *(Beaumont Clay)*	S50.XX to S59.XX
After Wetting & Drying *(Beaumont Clay)*	W60.XX to W69.XX
As-Compacted Beaumont Clay *(Embankment Soil)*	C70.XX to C79.XX

TEST NAME: C11.40
CONSOLIDATED-UNDRAINED TEST, COMPACTED PARIS BORROW CLAY

HEIGHT PRIOR TO SHEAR   3.04 in
DIAMETER PRIOR TO SHEAR   1.50 in

AREA CORRECTION FACTOR   1.00
EFFECTIVE CONSOLIDATION PRESSURE   40.00 psi

DEF. (in)	FORCE (lb)	P.PRES. (psi)	AXIAL STRAIN %	MINOR PRIN STRESS psi	DEVIATORIC STRESS psi	STRESS RATIO	A COEF
.00	.00	.00	.00	40.00	.00	1.00	.00
.00	6.56	1.63	.02	38.37	3.71	1.10	.44
.00	11.32	2.68	.05	37.32	6.40	1.17	.42
.00	14.86	3.66	.08	36.34	8.39	1.23	.44
.00	20.76	5.53	.14	34.47	11.71	1.34	.47
.01	24.70	6.67	.21	33.33	13.92	1.42	.48
.01	27.85	7.81	.27	32.19	15.68	1.49	.50
.01	30.46	8.79	.34	31.21	17.13	1.55	.51
.01	32.25	9.48	.39	30.52	18.13	1.59	.52
.02	36.05	11.08	.53	28.92	20.22	1.70	.55
.02	38.81	12.18	.67	27.82	21.73	1.78	.56
.02	41.21	13.29	.81	26.71	23.03	1.86	.58
.03	43.13	14.19	.94	25.81	24.06	1.93	.59
.04	45.69	14.84	1.16	25.16	25.41	2.01	.58
.04	47.83	15.36	1.38	24.64	26.52	2.08	.58
.05	49.60	15.39	1.59	24.61	27.42	2.11	.56
.06	51.52	15.77	1.93	24.23	28.34	2.17	.56
.07	53.02	15.86	2.28	24.14	29.06	2.20	.55
.08	54.27	16.06	2.62	23.94	29.64	2.24	.54
.09	55.31	15.95	2.98	24.05	30.10	2.25	.53
.10	56.21	15.86	3.32	24.14	30.47	2.26	.52
.13	58.15	15.34	4.11	24.66	31.26	2.27	.49
.14	59.26	15.55	4.77	24.45	31.63	2.29	.49
.16	59.90	15.74	5.39	24.26	31.75	2.31	.50
.18	60.29	14.76	6.02	25.24	31.74	2.26	.47
.22	56.54	14.07	7.30	25.93	29.31	2.13	.48
.25	55.48	14.78	8.13	25.22	28.48	2.13	.52
.27	55.42	14.78	8.98	25.22	28.17	2.12	.52
.31	54.37	14.37	10.03	25.64	27.29	2.06	.53
.34	52.46	14.76	11.09	25.25	25.98	2.03	.57
.36	50.11	14.62	11.97	25.39	24.53	1.97	.60
.40	49.21	14.26	13.16	25.75	23.74	1.92	.60
.43	48.56	14.42	14.01	25.59	23.17	1.91	.62
.44	48.58	14.64	14.64	25.37	22.99	1.91	.64
.49	46.63	14.77	16.09	25.24	21.65	1.86	.68
.51	46.41	14.70	16.74	25.32	21.36	1.84	.69
.53	46.28	14.80	17.37	25.22	21.12	1.84	.70
.55	47.01	13.96	17.99	26.06	21.29	1.82	.66
.57	46.34	14.23	18.62	25.79	20.80	1.81	.68
.60	45.93	15.19	19.61	24.83	20.34	1.82	.75

TEST NAME: C12.30
CONSOLIDATED-UNDRAINED TEST, COMPACTED PARIS BORROW CLAY

HEIGHT PRIOR TO SHEAR   3.05 in
DIAMETER PRIOR TO SHEAR   1.52 in

AREA CORRECTION FACTOR   1.00
EFFECTIVE CONSOLIDATION PRESSURE   30.00 psi

DEF. (in)	FORCE (lb)	P.PRES. (psi)	AXIAL STRAIN %	MINOR PRIN STRESS psi	DEVIATORIC STRESS psi	STRESS RATIO	A COEF
.00	.00	.00	.00	30.00	.00	1.00	.00
.00	5.26	1.05	.02	28.95	2.90	1.10	.36
.00	10.37	2.11	.05	27.89	5.71	1.20	.37
.00	13.88	2.95	.09	27.05	7.63	1.28	.39
.00	18.70	4.44	.15	25.56	10.27	1.40	.43
.01	21.91	5.45	.21	24.55	12.02	1.49	.45
.01	24.52	6.50	.29	23.50	13.44	1.57	.48
.01	26.42	7.25	.36	22.75	14.46	1.64	.50
.01	28.74	8.16	.48	21.84	15.70	1.72	.52
.02	30.78	8.79	.61	21.21	16.78	1.79	.52
.02	32.53	9.56	.74	20.44	17.70	1.87	.54
.03	33.74	10.41	.86	19.59	18.33	1.94	.57
.03	35.51	11.15	1.07	18.85	19.22	2.02	.58
.04	36.99	11.32	1.27	18.68	19.97	2.07	.57
.04	38.21	12.04	1.47	17.96	20.56	2.14	.59
.05	39.38	11.94	1.75	18.06	21.10	2.17	.57
.06	40.48	12.16	2.10	17.84	21.59	2.21	.56
.07	41.23	12.75	2.46	17.25	21.90	2.27	.58
.09	42.81	12.68	2.97	17.32	22.62	2.31	.56
.11	43.67	13.06	3.51	16.94	22.95	2.35	.57
.13	44.53	12.75	4.13	17.25	23.24	2.35	.55
.14	44.91	13.01	4.75	16.99	23.27	2.37	.56
.16	46.65	13.25	5.38	16.75	24.02	2.43	.55
.18	47.14	12.16	6.00	17.84	24.10	2.35	.50
.20	47.74	11.89	6.62	18.11	24.24	2.34	.49
.23	48.93	11.51	7.51	18.49	24.60	2.33	.47
.25	49.14	11.26	8.36	18.74	24.46	2.30	.46
.28	48.77	10.41	9.18	19.59	24.04	2.23	.43
.31	48.33	10.67	10.03	19.34	23.57	2.22	.45
.33	46.64	10.08	10.85	19.93	22.51	2.13	.45
.36	44.81	10.21	11.70	19.80	21.39	2.08	.48
.38	44.85	9.81	12.59	20.19	21.17	2.05	.46
.40	44.47	9.18	13.15	20.83	20.84	2.00	.44
.43	43.18	9.90	13.93	20.11	20.03	2.00	.49
.47	44.00	9.28	15.34	20.73	20.05	1.97	.46
.49	44.08	9.10	16.16	20.91	19.87	1.95	.46
.52	43.79	9.77	16.98	20.25	19.53	1.96	.50
.54	44.02	9.37	17.57	20.65	19.48	1.94	.48
.56	44.51	8.84	18.20	21.18	19.54	1.92	.45
.59	43.71	9.63	19.41	20.39	18.87	1.93	.51

TEST NAME: C13.10
CONSOLIDATED-UNDRAINED TEST, COMPACTED PARIS BORROW CLAY

HEIGHT PRIOR TO SHEAR   3.07 in
DIAMETER PRIOR TO SHEAR   1.56 in

AREA CORRECTION FACTOR   1.00
EFFECTIVE CONSOLIDATION PRESSURE   10.00 psi

DEF. (in)	FORCE (lb)	P.PRES. (psi)	AXIAL STRAIN %	MINOR PRIN STRESS psi	DEVIATORIC STRESS psi	STRESS RATIO	A COEF
.00	.00	.00	.00	10.00	.00	1.00	.00
.00	3.88	.77	.02	9.23	2.02	1.22	.38
.00	6.59	1.27	.05	8.73	3.44	1.39	.37
.00	8.17	1.66	.08	8.34	4.26	1.51	.39
.00	9.61	2.03	.12	7.97	5.01	1.63	.41
.01	11.82	2.68	.18	7.32	6.15	1.84	.44
.01	13.51	3.18	.25	6.82	7.02	2.03	.45
.01	14.61	3.64	.31	6.36	7.58	2.19	.48
.01	15.43	3.93	.38	6.07	8.00	2.32	.49
.01	16.12	4.11	.48	5.89	8.33	2.41	.49
.02	16.45	4.34	.55	5.66	8.49	2.50	.51
.02	16.61	4.48	.59	5.52	8.57	2.55	.52
.03	17.10	5.11	.85	4.89	8.77	2.79	.58
.03	17.25	5.32	.97	4.68	8.82	2.88	.60
.03	17.34	5.09	1.09	4.91	8.84	2.80	.58
.04	17.50	5.52	1.26	4.48	8.89	2.98	.62
.05	17.64	5.60	1.51	4.40	8.90	3.02	.63
.05	17.69	5.69	1.69	4.31	8.89	3.06	.64
.06	17.87	5.81	2.03	4.19	8.91	3.13	.65
.07	17.96	6.01	2.32	3.99	8.93	3.24	.67
.08	17.86	6.17	2.75	3.83	8.83	3.31	.70
.10	18.23	6.16	3.29	3.84	8.96	3.33	.69
.14	18.51	6.10	4.69	3.90	8.94	3.29	.68
.18	18.94	6.06	5.93	3.94	9.01	3.29	.67
.20	19.12	6.00	6.55	4.00	9.03	3.26	.66
.22	19.15	5.90	7.17	4.10	8.97	3.19	.66
.24	19.35	5.73	7.95	4.27	8.98	3.10	.64
.26	19.54	5.55	8.57	4.45	8.99	3.02	.62
.29	19.48	5.51	9.38	4.49	8.87	2.98	.62
.31	18.96	5.60	10.20	4.41	8.53	2.94	.66
.34	18.46	5.60	11.01	4.41	8.20	2.86	.68
.38	17.49	5.64	12.31	4.37	7.61	2.74	.74
.40	16.72	5.51	13.13	4.49	7.17	2.60	.77
.44	17.58	5.37	14.30	4.64	7.43	2.60	.72
.47	18.16	5.42	15.21	4.59	7.59	2.65	.71
.49	18.28	5.44	15.93	4.57	7.56	2.66	.72
.52	18.23	5.28	16.84	4.74	7.44	2.57	.71
.54	18.36	5.08	17.56	4.94	7.42	2.50	.68
.56	18.26	5.00	18.24	5.02	7.30	2.45	.69
.59	18.09	5.24	19.19	4.78	7.12	2.49	.74

TEST NAME: C14.05
CONSOLIDATED-UNDRAINED TEST, COMPACTED PARIS BORROW CLAY

HEIGHT PRIOR TO SHEAR   3.11 in
DIAMETER PRIOR TO SHEAR   1.56 in

AREA CORRECTION FACTOR   1.00
EFFECTIVE CONSOLIDATION PRESSURE   5.00 psi

DEF. (in)	FORCE (lb)	P.PRES. (psi)	AXIAL STRAIN %	MINOR PRIN STRESS psi	DEVIATORIC STRESS psi	STRESS RATIO	A COEF
.00	.00	.00	.00	5.00	.00	1.00	.00
.00	2.91	.42	.03	4.58	1.52	1.33	.27
.00	5.61	.83	.06	4.17	2.92	1.70	.28
.00	7.88	1.25	.09	3.75	4.11	2.10	.31
.00	9.64	1.57	.12	3.43	5.02	2.47	.31
.01	12.07	2.05	.18	2.95	6.28	3.13	.33
.01	13.53	2.30	.24	2.70	7.03	3.61	.33
.01	14.53	2.43	.30	2.57	7.54	3.94	.32
.01	15.22	2.47	.37	2.53	7.89	4.12	.31
.02	15.83	2.34	.53	2.66	8.17	4.07	.29
.02	15.68	2.27	.67	2.73	8.07	3.95	.28
.03	15.61	2.21	.92	2.79	7.98	3.86	.28
.03	15.65	2.20	1.09	2.80	7.96	3.84	.28
.04	15.85	2.12	1.36	2.88	8.01	3.78	.26
.05	15.00	2.24	1.63	2.76	7.52	3.72	.30
.06	16.08	2.04	1.85	2.96	8.03	3.71	.25
.07	16.02	2.12	2.34	2.88	7.94	3.75	.27
.09	15.81	1.99	2.82	3.01	7.78	3.59	.26
.10	15.69	1.92	3.12	3.08	7.69	3.50	.25
.11	15.39	1.93	3.57	3.07	7.49	3.44	.26
.13	15.28	1.74	4.02	3.26	7.39	3.27	.23
.14	14.52	1.60	4.50	3.40	6.97	3.05	.23
.18	15.07	1.43	5.72	3.57	7.13	2.99	.20
.20	14.87	1.58	6.53	3.42	6.95	3.03	.23
.23	15.21	1.55	7.30	3.45	7.04	3.04	.22
.25	15.34	1.53	7.88	3.47	7.05	3.03	.22
.27	15.52	1.50	8.65	3.50	7.06	3.02	.21
.29	15.73	1.41	9.26	3.59	7.10	2.98	.20
.31	15.00	1.35	9.87	3.66	6.70	2.83	.20
.35	15.77	1.30	11.13	3.70	6.94	2.87	.19
.37	15.79	1.31	11.96	3.70	6.86	2.86	.19
.40	16.11	1.20	12.80	3.81	6.93	2.82	.17
.42	15.92	1.19	13.63	3.81	6.76	2.77	.18
.47	16.18	1.17	15.05	3.84	6.73	2.75	.17
.49	16.38	1.14	15.88	3.87	6.73	2.74	.17
.51	16.45	1.10	16.50	3.91	6.70	2.71	.16
.55	16.69	.88	17.75	4.14	6.68	2.61	.13
.57	16.87	.83	18.39	4.19	6.69	2.59	.12
.59	16.92	.80	19.00	4.22	6.64	2.57	.12
.61	16.63	.83	19.61	4.19	6.46	2.54	.13

TEST NAME: C15.21
CONSOLIDATED-UNDRAINED TEST, COMPACTED PARIS BORROW CLAY

HEIGHT PRIOR TO SHEAR   3.05 in
DIAMETER PRIOR TO SHEAR   1.52 in

AREA CORRECTION FACTOR   1.00
EFFECTIVE CONSOLIDATION PRESSURE   21.00 psi

DEF. (in)	FORCE (lb)	P.PRES. (psi)	AXIAL STRAIN %	MINOR PRIN STRESS psi	DEVIATORIC STRESS psi	STRESS RATIO	A COEF
.00	.00	.00	.00	21.00	.00	1.00	.00
.00	3.13	.80	.03	20.20	1.72	1.09	.47
.00	6.07	1.36	.06	19.64	3.33	1.17	.41
.00	8.14	1.86	.09	19.14	4.47	1.23	.42
.00	10.97	2.70	.14	18.30	6.02	1.33	.45
.01	13.19	3.43	.20	17.57	7.23	1.41	.47
.01	14.65	3.94	.26	17.06	8.02	1.47	.49
.03	24.15	6.31	1.06	14.69	13.03	1.89	.48
.04	25.10	6.86	1.19	14.14	13.52	1.96	.51
.04	26.14	7.77	1.45	13.23	14.01	2.06	.55
.05	26.66	8.30	1.71	12.70	14.23	2.12	.58
.06	28.35	8.83	1.96	12.17	15.07	2.24	.59
.07	29.14	9.03	2.30	11.97	15.43	2.29	.59
.08	29.95	9.52	2.61	11.48	15.81	2.38	.60
.09	30.67	9.85	2.96	11.15	16.13	2.45	.61
.11	31.45	10.23	3.48	10.77	16.45	2.53	.62
.13	32.29	10.56	4.10	10.44	16.78	2.61	.63
.14	32.93	10.31	4.72	10.69	16.99	2.59	.61
.17	33.09	10.75	5.51	10.25	16.92	2.65	.64
.18	33.73	10.36	5.93	10.64	17.17	2.61	.60
.19	34.46	10.52	6.36	10.48	17.46	2.67	.60
.22	34.78	10.13	7.18	10.87	17.45	2.61	.58
.24	34.99	10.21	8.00	10.79	17.39	2.61	.59
.26	35.53	10.16	8.43	10.84	17.57	2.62	.58
.27	35.80	9.86	8.82	11.14	17.62	2.58	.56
.29	37.26	9.54	9.64	11.47	18.17	2.58	.52
.32	36.04	9.26	10.46	11.74	17.39	2.48	.53
.34	37.24	8.69	11.05	12.32	17.85	2.45	.49
.35	36.43	8.41	11.48	12.59	17.36	2.38	.48
.36	36.36	8.36	11.90	12.64	17.23	2.36	.49
.39	36.54	8.28	12.75	12.73	17.13	2.35	.48
.42	35.86	8.55	13.64	12.46	16.62	2.33	.51
.44	35.76	8.57	14.46	12.44	16.39	2.32	.52
.47	35.90	8.30	15.54	12.72	16.23	2.28	.51
.50	35.23	7.89	16.39	13.12	15.74	2.20	.50
.53	36.05	7.57	17.25	13.44	15.93	2.18	.48
.54	36.24	7.46	17.67	13.56	15.92	2.17	.47
.55	36.34	7.47	18.10	13.55	15.88	2.17	.47
.57	36.62	7.35	18.72	13.67	15.87	2.16	.46
.60	36.57	7.16	19.61	13.87	15.65	2.13	.46

TEST NAME: C20.35
CONSOLIDATED-UNDRAINED TEST, COMPACTED PARIS EMBANKMENT CLAY

HEIGHT PRIOR TO SHEAR   2.95 in
DIAMETER PRIOR TO SHEAR   1.53 in

AREA CORRECTION FACTOR   1.00
EFFECTIVE CONSOLIDATION PRESSURE   35.00 psi

DEF. (in)	FORCE (lb)	P.PRES. (psi)	AXIAL STRAIN %	MINOR PRIN STRESS psi	DEVIATORIC STRESS psi	STRESS RATIO	A COEF
.00	.00	.00	.00	35.00	.00	1.00	.00
.00	8.01	3.79	.06	31.21	4.34	1.14	.87
.00	11.00	4.94	.12	30.06	5.96	1.20	.83
.01	14.19	6.14	.18	28.86	7.68	1.27	.80
.01	16.61	7.42	.26	27.58	8.98	1.33	.83
.01	17.92	8.11	.33	26.89	9.67	1.36	.84
.01	19.06	8.68	.39	26.32	10.28	1.39	.84
.01	20.19	9.12	.47	25.88	10.87	1.42	.84
.02	21.64	10.11	.57	24.89	11.63	1.47	.87
.02	22.72	11.00	.66	24.00	12.19	1.51	.90
.02	23.29	11.37	.73	23.63	12.48	1.53	.91
.03	24.33	12.01	.86	22.99	13.01	1.57	.92
.03	25.51	12.79	.99	22.21	13.61	1.61	.94
.03	26.48	13.58	1.14	21.42	14.10	1.66	.96
.04	27.58	14.06	1.32	20.94	14.64	1.70	.96
.05	28.85	14.75	1.56	20.25	15.25	1.75	.97
.06	30.35	15.33	1.90	19.67	15.96	1.81	.96
.07	31.78	16.08	2.24	18.92	16.65	1.88	.97
.08	32.87	17.88	2.59	17.12	17.16	2.00	1.04
.09	34.34	18.15	3.03	16.85	17.84	2.06	1.02
.10	34.93	18.08	3.32	16.92	18.10	2.07	1.00
.11	35.96	18.92	3.83	16.08	18.53	2.15	1.02
.13	36.82	19.10	4.31	15.90	18.88	2.19	1.01
.15	38.18	19.86	5.02	15.14	19.42	2.28	1.02
.17	39.24	20.06	5.66	14.94	19.82	2.33	1.01
.18	39.74	19.54	6.00	15.46	20.00	2.29	.98
.20	40.67	19.99	6.85	15.01	20.27	2.35	.99
.23	41.43	19.48	7.69	15.52	20.45	2.32	.95
.25	42.06	19.82	8.58	15.18	20.55	2.35	.96
.30	44.00	20.60	10.07	14.41	21.14	2.47	.97
.32	44.37	20.02	10.92	14.99	21.10	2.41	.95
.36	42.01	18.48	12.27	16.53	19.62	2.19	.94
.38	38.30	18.27	12.92	16.74	17.71	2.06	1.03
.41	36.85	18.65	13.93	16.36	16.80	2.03	1.11
.44	36.47	18.30	14.85	16.71	16.42	1.98	1.11
.46	36.21	18.10	15.73	16.91	16.12	1.95	1.12
.49	35.50	18.12	16.64	16.90	15.60	1.92	1.16
.52	35.54	17.00	17.53	18.02	15.43	1.86	1.10
.55	35.00	17.44	18.61	17.58	14.96	1.85	1.17
.57	34.55	17.80	19.49	17.22	14.58	1.85	1.22

TEST NAME: C22.12
CONSOLIDATED-UNDRAINED TEST, COMPACTED PARIS EMBANKMENT CLAY

HEIGHT PRIOR TO SHEAR   3.08 in
DIAMETER PRIOR TO SHEAR   1.53 in

AREA CORRECTION FACTOR   1.00
EFFECTIVE CONSOLIDATION PRESSURE   12.00 psi

DEF. (in)	FORCE (lb)	P.PRES. (psi)	AXIAL STRAIN %	MINOR PRIN STRESS psi	DEVIATORIC STRESS psi	STRESS RATIO	A COEF
.00	.00	.00	.00	12.00	.00	1.00	.00
.00	3.78	.54	.01	11.46	2.06	1.18	.26
.00	7.86	1.08	.06	10.92	4.27	1.39	.25
.00	10.27	1.57	.11	10.43	5.57	1.53	.28
.01	11.99	2.19	.17	9.81	6.49	1.66	.34
.01	13.33	2.78	.23	9.22	7.20	1.78	.39
.01	14.32	3.18	.31	8.82	7.73	1.88	.41
.01	15.30	3.54	.42	8.46	8.23	1.97	.43
.02	16.05	3.87	.52	8.13	8.62	2.06	.45
.02	16.46	3.93	.62	8.07	8.82	2.09	.45
.02	17.14	4.13	.78	7.87	9.15	2.16	.45
.03	17.48	4.33	.88	7.67	9.31	2.21	.46
.03	17.85	4.64	1.00	7.36	9.49	2.29	.49
.03	18.03	4.59	1.10	7.41	9.56	2.29	.48
.04	18.61	4.76	1.43	7.24	9.80	2.35	.49
.05	18.97	4.96	1.64	7.04	9.94	2.41	.50
.06	19.54	5.03	1.96	6.97	10.18	2.46	.49
.07	20.10	5.14	2.25	6.86	10.43	2.52	.49
.07	20.26	5.32	2.38	6.68	10.50	2.57	.51
.09	20.82	5.50	2.85	6.50	10.74	2.65	.51
.10	21.18	5.43	3.31	6.57	10.87	2.65	.50
.12	21.74	5.40	3.93	6.60	11.08	2.68	.49
.13	21.90	5.78	4.38	6.22	11.10	2.78	.52
.16	22.52	5.63	5.23	6.37	11.30	2.77	.50
.18	22.83	5.70	5.78	6.30	11.39	2.81	.50
.18	23.04	5.93	5.97	6.07	11.47	2.89	.52
.20	23.27	5.67	6.43	6.33	11.52	2.82	.49
.22	23.90	5.85	7.14	6.15	11.73	2.91	.50
.27	24.62	5.33	8.73	6.67	11.86	2.78	.45
.29	24.81	5.19	9.35	6.81	11.86	2.74	.44
.31	24.86	5.16	9.94	6.85	11.79	2.72	.44
.33	24.15	5.19	10.75	6.82	11.33	2.66	.46
.38	23.09	4.63	12.18	7.38	10.61	2.44	.44
.39	22.19	4.71	12.79	7.30	10.09	2.38	.47
.41	22.08	4.50	13.38	7.51	9.96	2.33	.45
.44	21.97	4.69	14.19	7.32	9.80	2.34	.48
.48	22.80	4.54	15.58	7.47	9.99	2.34	.45
.53	22.40	4.55	17.27	7.47	9.57	2.28	.48
.58	22.20	4.30	18.77	7.72	9.28	2.20	.46
.61	22.17	4.00	19.84	8.02	9.12	2.14	.44

TEST NAME: C23.23
CONSOLIDATED-UNDRAINED TEST, COMPACTED PARIS EMBANKMENT CLAY

HEIGHT PRIOR TO SHEAR   2.88 in
DIAMETER PRIOR TO SHEAR   1.51 in

AREA CORRECTION FACTOR   1.00
EFFECTIVE CONSOLIDATION PRESSURE   23.00 psi

DEF. (in)	FORCE (lb)	P.PRES. (psi)	AXIAL STRAIN %	MINOR PRIN STRESS psi	DEVIATORIC STRESS psi	STRESS RATIO	A COEF
.00	.00	.00	.00	23.00	.00	1.00	.00
.00	.99	.25	.04	22.75	.55	1.02	.46
.00	1.87	.56	.07	22.44	1.04	1.05	.54
.00	3.40	1.16	.11	21.84	1.89	1.09	.62
.00	6.57	2.36	.12	20.64	3.66	1.18	.65
.00	9.54	3.46	.13	19.54	5.32	1.27	.65
.01	12.20	4.60	.24	18.40	6.78	1.37	.68
.02	16.81	6.80	.69	16.20	9.26	1.57	.73
.03	18.00	7.97	1.04	15.03	9.84	1.65	.81
.04	18.85	8.41	1.29	14.59	10.25	1.70	.82
.05	19.58	9.20	1.56	13.80	10.59	1.77	.87
.06	21.37	10.37	1.93	12.63	11.49	1.91	.90
.07	22.82	11.32	2.39	11.68	12.21	2.05	.93
.08	23.43	11.47	2.82	11.53	12.48	2.08	.92
.10	24.95	12.78	3.37	10.22	13.22	2.29	.97
.11	25.90	12.97	3.92	10.03	13.65	2.36	.95
.13	26.33	13.30	4.55	9.70	13.77	2.42	.97
.14	26.80	13.45	5.00	9.55	13.95	2.46	.96
.16	27.46	13.48	5.45	9.52	14.22	2.49	.95
.16	27.66	13.83	5.73	9.17	14.28	2.56	.97
.17	28.03	13.69	6.01	9.31	14.43	2.55	.95
.18	28.55	13.86	6.39	9.14	14.64	2.60	.95
.20	28.99	14.21	6.91	8.79	14.77	2.68	.96
.22	29.42	14.42	7.47	8.58	14.90	2.74	.97
.23	29.56	14.51	8.09	8.49	14.85	2.75	.98
.25	31.15	14.15	8.78	8.85	15.54	2.76	.91
.29	31.78	14.21	9.97	8.80	15.63	2.78	.91
.31	31.37	14.32	10.80	8.69	15.26	2.76	.94
.33	30.16	14.08	11.46	8.93	14.54	2.63	.97
.37	29.90	13.94	12.81	9.07	14.16	2.56	.98
.39	29.50	13.59	13.47	9.42	13.84	2.47	.98
.41	28.81	13.49	14.38	9.52	13.35	2.40	1.01
.43	28.56	13.45	14.83	9.56	13.15	2.37	1.02
.45	28.03	13.46	15.52	9.55	12.77	2.34	1.05
.48	28.34	13.18	16.67	9.84	12.72	2.29	1.04
.50	28.30	12.97	17.53	10.05	12.55	2.25	1.03
.52	28.28	12.89	18.23	10.13	12.42	2.23	1.04
.54	28.27	12.79	18.89	10.23	12.30	2.20	1.04
.56	28.46	12.64	19.58	10.38	12.26	2.18	1.03
.57	28.38	12.76	19.86	10.26	12.17	2.19	1.05

TEST NAME: C25.015
CONSOLIDATED-UNDRAINED TEST, COMPACTED PARIS EMBANKMENT CLAY

HEIGHT PRIOR TO SHEAR   3.07 in
DIAMETER PRIOR TO SHEAR   1.59 in

AREA CORRECTION FACTOR   1.00
EFFECTIVE CONSOLIDATION PRESSURE   1.50 psi

DEF. (in)	FORCE (lb)	P.PRES. (psi)	AXIAL STRAIN %	MINOR PRIN STRESS psi	DEVIATORIC STRESS psi	STRESS RATIO	A COEF
.00	.00	.00	.00	1.50	.00	1.00	.00
.00	1.90	.20	.02	1.30	.95	1.73	.22
.00	3.79	.43	.05	1.07	1.90	2.77	.23
.00	4.91	.62	.08	.88	2.45	3.80	.25
.00	5.86	.78	.10	.72	2.93	5.06	.27
.00	7.38	1.01	.16	.49	3.68	8.50	.27
.01	8.59	1.16	.22	.34	4.28	13.52	.27
.01	9.51	1.23	.28	.27	4.73	18.59	.26
.01	10.31	1.31	.34	.19	5.12	28.09	.26
.01	10.99	1.32	.43	.18	5.45	31.76	.24
.02	11.79	1.27	.52	.23	5.83	26.45	.22
.02	12.30	1.27	.62	.23	6.07	27.15	.21
.02	12.63	1.23	.71	.27	6.21	24.27	.20
.03	11.21	.87	.84	.63	5.48	9.72	.16
.03	10.34	.56	1.00	.94	5.02	6.32	.11
.03	10.23	.44	1.13	1.06	4.94	5.66	.09
.04	10.20	.42	1.26	1.08	4.91	5.56	.09
.04	10.22	.40	1.39	1.10	4.89	5.44	.08
.05	10.28	.36	1.55	1.14	4.90	5.31	.07
.05	10.40	.34	1.65	1.16	4.94	5.27	.07
.06	10.60	.26	1.90	1.24	5.00	5.02	.05
.07	10.82	.18	2.16	1.32	5.08	4.84	.04
.08	11.07	.07	2.47	1.43	5.18	4.63	.01
.08	11.24	-.02	2.73	1.52	5.24	4.45	0.00
.09	11.35	-.07	3.05	1.57	5.27	4.36	-.01
.11	11.35	-.21	3.55	1.71	5.23	4.06	-.04
.12	11.63	-.25	4.04	1.75	5.33	4.04	-.05
.14	11.57	-.19	4.69	1.69	5.26	4.10	-.04
.17	12.15	-.38	5.67	1.89	5.46	3.89	-.07
.22	12.06	-.70	7.10	2.20	5.31	3.41	-.13
.25	11.84	-.69	8.18	2.19	5.12	3.34	-.13
.29	12.55	-1.20	9.61	2.71	5.34	2.97	-.23
.34	12.39	-1.17	11.04	2.68	5.15	2.92	-.23
.39	12.19	-1.11	12.64	2.62	4.94	2.89	-.22
.42	12.32	-1.07	13.62	2.58	4.92	2.90	-.22
.45	12.77	-1.28	14.63	2.79	5.03	2.80	-.25
.50	13.61	-1.48	16.19	2.99	5.26	2.76	-.28
.51	13.59	-1.38	16.71	2.89	5.21	2.80	-.26
.56	14.14	-1.31	18.31	2.83	5.30	2.87	-.25
.61	14.71	-1.36	19.71	2.88	5.41	2.87	-.25

TEST NAME: C26.01
CONSOLIDATED-DRAINED TEST, COMPACTED PARIS EMBANKMENT CLAY

HEIGHT PRIOR TO SHEAR   3.15 in
DIAMETER PRIOR TO SHEAR   1.58 in

AREA CORRECTION FACTOR   1.00
EFFECTIVE CONSOLIDATION PRESSURE   1.00 psi

DEF. (in)	FORCE (lb)	VOLUME CHANGE (cc)	AXIAL STRAIN %	VOLUMETRIC STRAIN %	DEVIATORIC STRESS psi
.00	.00	.00	.00	.00	.00
.00	2.36	.01	.02	.01	1.20
.00	4.02	.02	.05	.02	2.05
.00	5.99	.03	.11	.03	3.04
.01	7.22	.05	.18	.05	3.66
.01	8.72	.08	.27	.08	4.42
.01	9.50	.10	.33	.10	4.81
.01	10.24	.12	.39	.12	5.17
.02	11.21	.15	.49	.15	5.65
.02	12.10	.18	.58	.18	6.09
.02	12.64	.20	.64	.20	6.36
.02	13.61	.24	.77	.24	6.83
.03	14.45	.27	.89	.27	7.23
.03	14.98	.30	.99	.30	7.49
.03	15.38	.33	1.08	.33	7.67
.04	15.81	.38	1.21	.38	7.87
.04	15.81	.40	1.27	.40	7.86
.04	15.62	.43	1.37	.43	7.74
.05	12.23	.47	1.47	.47	6.01
.05	10.37	.50	1.57	.50	5.05
.05	9.56	.44	1.73	.44	4.62
.06	9.30	.37	1.92	.37	4.45
.07	9.01	.24	2.25	.24	4.27
.08	9.49	.12	2.57	.12	4.48
.09	9.92	.00	2.96	.00	4.67
.11	10.02	-.07	3.56	-.07	4.67
.13	9.98	-.21	4.19	-.21	4.60
.15	10.34	-.36	4.83	-.36	4.73
.18	10.52	-.69	5.78	-.68	4.73
.21	10.09	-1.02	6.79	-1.01	4.44
.24	9.30	-1.36	7.62	-1.35	4.01
.29	9.23	-1.97	9.27	-1.95	3.84
.32	9.31	-2.26	10.29	-2.24	3.81
.36	8.70	-2.74	11.33	-2.71	3.46
.43	8.76	-2.81	13.52	-2.78	3.35
.48	9.05	-2.96	15.17	-2.93	3.37
.52	9.09	-3.18	16.41	-3.15	3.31
.56	9.30	-3.40	17.71	-3.37	3.31
.60	9.69	-3.61	18.98	-3.58	3.38
.62	9.52	-3.90	19.59	-3.86	3.27

TEST NAME: C27.05
CONSOLIDATED-UNDRAINED TEST, COMPACTED PARIS EMBANKMENT CLAY

HEIGHT PRIOR TO SHEAR   3.05 in
DIAMETER PRIOR TO SHEAR   1.57 in

AREA CORRECTION FACTOR   1.00
EFFECTIVE CONSOLIDATION PRESSURE   5.00 psi

DEF. (in)	FORCE (lb)	P.PRES. (psi)	AXIAL STRAIN %	MINOR PRIN STRESS psi	DEVIATORIC STRESS psi	STRESS RATIO	A COEF
.00	.00	.00	.00	5.00	.00	1.00	.00
.00	1.75	.19	.02	4.81	.90	1.19	.21
.00	3.69	.37	.06	4.63	1.89	1.41	.20
.00	4.19	.51	.11	4.49	2.14	1.48	.24
.00	5.18	.73	.15	4.27	2.65	1.62	.28
.01	5.58	.83	.18	4.17	2.84	1.68	.29
.01	6.46	1.01	.22	3.99	3.29	1.82	.31
.01	9.78	1.63	.27	3.37	4.99	2.48	.33
.01	11.35	1.92	.31	3.08	5.78	2.88	.33
.01	13.19	2.21	.37	2.79	6.72	3.41	.33
.01	14.81	2.42	.45	2.58	7.53	3.92	.32
.02	15.93	2.49	.55	2.51	8.08	4.22	.31
.02	16.83	2.50	.72	2.50	8.51	4.40	.29
.03	17.30	2.50	.85	2.50	8.72	4.49	.29
.03	17.62	2.48	.97	2.52	8.86	4.52	.28
.03	17.75	2.40	1.14	2.60	8.89	4.42	.27
.04	17.78	2.25	1.35	2.75	8.86	4.22	.25
.05	17.93	1.98	1.67	3.02	8.87	3.94	.22
.06	18.06	1.91	1.89	3.09	8.89	3.88	.21
.06	18.15	1.86	2.07	3.14	8.90	3.84	.21
.07	18.28	1.81	2.34	3.19	8.94	3.80	.20
.08	18.37	1.78	2.56	3.22	8.96	3.78	.20
.08	18.43	1.76	2.75	3.24	8.97	3.77	.20
.09	18.47	1.72	2.97	3.28	8.96	3.73	.19
.11	18.67	1.52	3.51	3.48	9.00	3.59	.17
.12	18.63	1.11	4.03	3.89	8.92	3.29	.12
.15	18.77	.49	4.82	4.51	8.90	2.97	.06
.16	18.93	.36	5.18	4.64	8.94	2.93	.04
.18	19.16	.20	5.97	4.80	8.96	2.87	.02
.20	18.99	.58	6.66	4.42	8.80	2.99	.07
.25	18.89	.74	8.03	4.27	8.60	3.01	.09
.30	19.84	.14	9.84	4.86	8.83	2.82	.02
.35	20.41	-.41	11.34	5.42	8.91	2.64	-.05
.37	20.58	-.62	12.26	5.63	8.88	2.58	-.07
.42	19.97	.03	13.70	4.98	8.43	2.69	0.00
.46	19.85	-.17	15.11	5.18	8.21	2.58	-.02
.51	20.96	-.29	16.66	5.30	8.51	2.60	-.03
.55	21.74	-.35	17.90	5.37	8.68	2.62	-.04
.58	21.81	-.55	19.18	5.57	8.55	2.53	-.06
.62	22.00	-.73	20.33	5.75	8.48	2.47	-.09

TEST NAME: S31.35
CONSOLIDATED-UNDRAINED TEST, NORMALLY CONSOLIDATED PARIS CLAY

HEIGHT PRIOR TO SHEAR   2.72 in
DIAMETER PRIOR TO SHEAR   1.26 in

AREA CORRECTION FACTOR   1.00
EFFECTIVE CONSOLIDATION PRESSURE   35.00 psi

DEF. (in)	FORCE (lb)	P.PRES. (psi)	AXIAL STRAIN %	MINOR PRIN STRESS psi	DEVIATORIC STRESS psi	STRESS RATIO	A COEF
.00	.00	.00	.00	35.00	.00	1.00	.00
.00	5.89	2.21	.18	32.78	4.69	1.14	.47
.01	7.98	3.19	.28	31.81	6.34	1.20	.50
.01	11.35	4.77	.36	30.23	9.01	1.30	.53
.01	13.36	6.03	.46	28.97	10.60	1.37	.57
.01	14.86	7.10	.55	27.90	11.77	1.42	.60
.02	15.86	7.91	.64	27.09	12.54	1.46	.63
.02	16.81	8.55	.74	26.45	13.27	1.50	.64
.02	17.88	9.14	.88	25.86	14.08	1.54	.65
.03	18.70	9.89	.97	25.11	14.70	1.59	.67
.03	19.23	10.49	1.06	24.51	15.10	1.62	.69
.03	19.85	11.04	1.16	23.96	15.56	1.65	.71
.03	20.46	11.85	1.25	23.15	16.01	1.69	.74
.04	21.57	12.32	1.49	22.68	16.81	1.74	.73
.05	22.59	13.28	1.72	21.72	17.54	1.81	.76
.05	23.64	14.12	1.96	20.88	18.29	1.88	.77
.07	25.08	15.11	2.43	19.89	19.31	1.97	.78
.08	26.44	16.25	2.94	18.75	20.26	2.08	.80
.10	27.91	17.07	3.53	17.93	21.26	2.19	.80
.12	29.18	18.05	4.30	16.95	22.05	2.30	.82
.13	29.84	18.55	4.89	16.45	22.40	2.36	.83
.15	30.52	19.31	5.44	15.69	22.77	2.45	.85
.17	31.28	18.99	6.14	16.01	23.16	2.45	.82
.19	31.54	19.59	6.84	15.41	23.16	2.50	.85
.20	31.71	20.23	7.54	14.77	23.10	2.56	.88
.22	30.85	19.71	8.24	15.29	22.27	2.46	.88
.24	28.92	20.06	8.93	14.94	20.68	2.38	.97
.27	28.42	19.61	9.78	15.40	20.10	2.31	.98
.29	27.11	19.33	10.51	15.68	18.98	2.21	1.02
.31	25.98	18.99	11.25	16.02	18.00	2.12	1.06
.33	24.73	18.79	11.99	16.22	16.95	2.04	1.11
.35	24.19	18.79	12.72	16.22	16.41	2.01	1.15
.37	24.56	18.74	13.46	16.27	16.51	2.01	1.14
.39	25.00	18.78	14.19	16.23	16.65	2.03	1.13
.41	25.46	18.60	15.15	16.42	16.75	2.02	1.11
.43	25.97	18.47	15.88	16.55	16.93	2.02	1.09
.45	26.24	18.63	16.62	16.39	16.94	2.03	1.10
.48	26.48	18.86	17.57	16.16	16.88	2.04	1.12
.50	26.69	19.09	18.31	15.93	16.85	2.06	1.13
.51	26.83	18.88	18.79	16.14	16.83	2.04	1.12

TEST NAME: S32.10
CONSOLIDATED-UNDRAINED TEST, NORMALLY CONSOLIDATED PARIS CLAY

HEIGHT PRIOR TO SHEAR   2.98 in
DIAMETER PRIOR TO SHEAR   1.29 in

AREA CORRECTION FACTOR   1.40
EFFECTIVE CONSOLIDATION PRESSURE   10.00 psi

DEF. (in)	FORCE (lb)	P.PRES. (psi)	AXIAL STRAIN %	MINOR PRIN STRESS psi	DEVIATORIC STRESS psi	STRESS RATIO	A COEF
.00	.00	.00	.00	10.00	.00	1.00	.00
.00	4.00	.80	.07	9.20	3.04	1.33	.26
.00	5.47	1.60	.15	8.40	4.16	1.49	.38
.01	6.01	2.29	.24	7.71	4.55	1.59	.50
.01	6.49	2.71	.33	7.29	4.89	1.67	.55
.01	6.85	3.05	.42	6.95	5.14	1.74	.59
.01	7.14	3.02	.50	6.98	5.35	1.77	.57
.02	7.42	3.28	.58	6.73	5.55	1.82	.59
.02	7.69	3.50	.67	6.50	5.73	1.88	.61
.02	8.02	3.81	.81	6.19	5.95	1.96	.64
.03	8.24	4.08	.90	5.92	6.09	2.03	.67
.03	8.57	4.21	1.07	5.79	6.30	2.09	.67
.04	8.93	4.00	1.25	6.00	6.52	2.09	.61
.04	9.22	4.76	1.43	5.24	6.70	2.28	.71
.05	9.57	5.16	1.70	4.84	6.90	2.43	.75
.06	9.96	5.36	2.01	4.64	7.11	2.53	.75
.07	10.44	5.71	2.48	4.29	7.41	2.73	.77
.09	10.82	6.04	2.96	3.96	7.62	2.93	.79
.11	11.27	6.50	3.66	3.50	7.86	3.24	.83
.12	11.49	6.57	4.16	3.43	7.94	3.32	.83
.14	11.68	6.66	4.63	3.34	8.01	3.40	.83
.16	11.83	6.68	5.20	3.33	8.04	3.42	.83
.18	11.86	6.88	6.01	3.12	7.94	3.54	.87
.20	11.69	7.17	6.61	2.83	7.73	3.73	.93
.22	11.77	7.09	7.21	2.91	7.70	3.65	.92
.24	11.27	7.41	8.05	2.59	7.24	3.79	1.02
.26	11.07	7.23	8.89	2.78	6.99	3.52	1.03
.28	10.85	7.23	9.56	⁻2.78	6.75	3.43	1.07
.31	10.78	7.07	10.23	2.94	6.62	3.25	1.07
.32	10.80	7.05	10.91	2.96	6.54	3.21	1.08
.34	10.76	7.09	11.58	2.92	6.42	3.20	1.10
.36	10.75	7.01	12.21	3.00	6.33	3.11	1.11
.38	10.73	6.96	12.85	3.05	6.23	3.04	1.12
.40	10.74	6.97	13.52	3.05	6.15	3.02	1.13
.44	10.82	7.01	14.87	3.01	6.02	3.00	1.16
.48	10.65	7.03	16.17	2.99	5.74	2.92	1.22
.50	10.76	7.06	16.85	2.96	5.71	2.93	1.23
.52	10.88	7.09	17.52	2.93	5.69	2.94	1.24
.54	10.93	7.10	18.19	2.93	5.63	2.92	1.26
.58	11.08	6.97	19.46	3.05	5.54	2.81	1.26

TEST NAME: S33.04
CONSOLIDATED-UNDRAINED TEST, NORMALLY CONSOLIDATED PARIS CLAY

HEIGHT PRIOR TO SHEAR   3.08 in
DIAMETER PRIOR TO SHEAR   1.35 in

AREA CORRECTION FACTOR   1.40
EFFECTIVE CONSOLIDATION PRESSURE   4.00 psi

DEF. (in)	FORCE (lb)	P.PRES. (psi)	AXIAL STRAIN %	MINOR PRIN STRESS psi	DEVIATORIC STRESS psi	STRESS RATIO	A COEF
.00	.00	.00	.00	4.00	.00	1.00	.00
.00	1.88	.32	.06	3.68	1.31	1.36	.25
.00	2.41	.65	.14	3.35	1.66	1.50	.39
.01	2.79	.89	.22	3.11	1.92	1.62	.47
.01	3.08	1.06	.31	2.94	2.10	1.72	.50
.01	3.21	1.18	.39	2.82	2.18	1.78	.54
.01	3.51	1.39	.47	2.61	2.38	1.91	.59
.02	3.66	1.59	.56	2.41	2.46	2.02	.64
.02	3.78	1.70	.64	2.30	2.54	2.10	.67
.03	4.03	1.89	.81	2.11	2.67	2.26	.71
.03	4.25	2.06	.98	1.94	2.80	2.44	.73
.04	4.45	2.20	1.16	1.80	2.90	2.61	.76
.04	4.64	2.39	1.33	1.61	3.00	2.86	.80
.04	4.74	2.39	1.44	1.61	3.05	2.89	.78
.05	4.93	2.46	1.65	1.54	3.14	3.04	.78
.06	5.07	2.65	1.88	1.35	3.20	3.36	.83
.06	5.17	2.64	2.09	1.36	3.23	3.37	.82
.07	5.27	2.77	2.30	1.23	3.28	3.66	.84
.08	5.36	2.85	2.53	1.15	3.33	3.89	.85
.09	5.45	2.86	2.90	1.14	3.37	3.95	.85
.10	5.46	2.92	3.28	1.08	3.35	4.08	.87
.12	5.61	3.00	3.80	1.00	3.41	4.41	.88
.13	5.72	2.97	4.06	1.03	3.46	4.34	.86
.13	5.82	3.05	4.32	.96	3.51	4.67	.87
.14	5.88	2.97	4.55	1.04	3.53	4.41	.84
.16	5.89	2.98	5.26	1.03	3.48	4.40	.85
.18	5.77	3.04	5.94	.97	3.35	4.47	.91
.19	5.85	3.19	6.23	.81	3.38	5.16	.94
.22	5.99	3.10	7.31	.91	3.39	4.74	.91
.25	6.07	3.14	8.15	.86	3.37	4.91	.93
.28	5.92	3.09	9.22	.92	3.20	4.48	.96
.30	5.79	3.02	9.87	.98	3.07	4.12	.98
.33	5.90	3.06	10.71	.95	3.07	4.25	1.00
.38	5.91	3.06	12.21	.95	2.96	4.11	1.03
.40	5.78	3.07	13.05	.94	2.83	4.01	1.08
.45	5.97	3.18	14.55	.83	2.82	4.39	1.13
.48	5.95	3.10	15.62	.92	2.73	3.97	1.13
.53	6.07	3.15	17.08	.87	2.68	4.09	1.18
.56	5.94	3.11	18.34	.91	2.51	3.76	1.24
.60	5.74	3.12	19.61	.91	2.32	3.55	1.34

TEST NAME: S34.25
CONSOLIDATED-UNDRAINED TEST, NORMALLY CONSOLIDATED PARIS CLAY

HEIGHT PRIOR TO SHEAR   2.77 in
DIAMETER PRIOR TO SHEAR   1.28 in

AREA CORRECTION FACTOR   1.00
EFFECTIVE CONSOLIDATION PRESSURE   25.00 psi

DEF. (in)	FORCE (lb)	P.PRES. (psi)	AXIAL STRAIN %	MINOR PRIN STRESS psi	DEVIATORIC STRESS psi	STRESS RATIO	A COEF
.00	.00	.00	.00	25.00	.00	1.00	.00
.00	3.61	1.17	.04	23.83	2.80	1.12	.42
.00	4.82	1.84	.10	23.16	3.73	1.16	.49
.00	5.57	2.34	.16	22.66	4.30	1.19	.54
.01	6.99	3.29	.27	21.71	5.38	1.25	.61
.01	8.38	4.19	.37	20.81	6.44	1.31	.65
.01	9.38	4.98	.46	20.02	7.20	1.36	.69
.02	10.51	5.61	.56	19.39	8.05	1.42	.70
.02	11.41	6.11	.65	18.89	8.73	1.46	.70
.02	11.98	6.70	.74	18.30	9.14	1.50	.73
.02	12.62	7.12	.83	17.88	9.62	1.54	.74
.03	13.23	7.51	.93	17.49	10.06	1.58	.75
.03	13.72	7.98	1.01	17.02	10.42	1.61	.77
.03	14.18	8.31	1.11	16.69	10.75	1.64	.77
.03	14.81	8.56	1.25	16.44	11.20	1.68	.76
.04	15.45	9.24	1.38	15.76	11.65	1.74	.79
.04	16.01	9.76	1.53	15.24	12.04	1.79	.81
.05	16.77	10.39	1.72	14.61	12.57	1.86	.83
.05	17.22	10.33	1.86	14.67	12.88	1.88	.80
.06	18.20	11.03	2.19	13.97	13.55	1.97	.81
.08	19.64	12.13	2.77	12.87	14.55	2.13	.83
.08	20.20	12.45	3.06	12.55	14.92	2.19	.83
.09	20.48	12.57	3.25	12.43	15.10	2.21	.83
.10	21.13	12.86	3.75	12.14	15.49	2.28	.83
.11	21.65	12.84	4.01	12.16	15.84	2.30	.81
.13	22.11	13.31	4.51	11.69	16.08	2.38	.83
.15	23.05	14.17	5.34	10.83	16.62	2.53	.85
.16	23.44	14.09	5.78	10.91	16.82	2.54	.84
.18	23.77	13.92	6.35	11.08	16.94	2.53	.82
.19	23.90	14.21	6.93	10.79	16.91	2.57	.84
.20	23.97	14.45	7.36	10.55	16.88	2.60	.86
.22	24.23	14.69	7.94	10.31	16.94	2.64	.87
.24	24.46	14.54	8.66	10.46	16.96	2.62	.86
.28	23.71	14.46	10.04	10.55	16.14	2.53	.90
.31	22.05	14.15	11.01	10.86	14.79	2.36	.96
.35	20.91	14.01	12.71	11.00	13.69	2.24	1.02
.40	20.14	13.97	14.58	11.04	12.84	2.16	1.09
.46	20.11	13.74	16.50	11.28	12.48	2.11	1.10
.48	20.84	13.54	17.47	11.48	12.78	2.11	1.06
.52	21.01	14.13	18.88	10.89	12.63	2.16	1.12

TEST NAME: S35.17
CONSOLIDATED-UNDRAINED TEST, NORMALLY CONSOLIDATED PARIS CLAY

HEIGHT PRIOR TO SHEAR   2.84 in
DIAMETER PRIOR TO SHEAR   1.30 in

AREA CORRECTION FACTOR   1.00
EFFECTIVE CONSOLIDATION PRESSURE   17.00 psi

DEF. (in)	FORCE (lb)	P.PRES. (psi)	AXIAL STRAIN %	MINOR PRIN STRESS psi	DEVIATORIC STRESS psi	STRESS RATIO	A COEF
.00	.00	.00	.00	17.00	.00	1.00	.00
.00	3.15	1.04	.04	15.96	2.36	1.15	.44
.00	5.37	1.83	.09	15.18	4.01	1.26	.45
.00	6.98	2.17	.12	14.83	5.22	1.35	.42
.01	8.46	2.69	.21	14.31	6.31	1.44	.43
.01	9.24	3.38	.31	13.62	6.87	1.50	.49
.01	9.76	3.66	.40	13.34	7.24	1.54	.51
.01	10.30	4.09	.50	12.91	7.62	1.59	.54
.02	10.80	4.70	.60	12.30	7.97	1.65	.59
.02	11.00	5.01	.69	11.99	8.10	1.68	.62
.02	11.60	5.31	.78	11.69	8.53	1.73	.62
.03	11.93	5.63	.88	11.37	8.75	1.77	.64
.03	12.22	6.00	.98	11.00	8.94	1.81	.67
.03	12.60	6.04	1.07	10.96	9.21	1.84	.66
.03	12.87	6.16	1.15	10.84	9.38	1.87	.66
.04	13.23	6.43	1.23	10.57	9.63	1.91	.67
.04	13.58	6.62	1.33	10.38	9.87	1.95	.67
.04	13.88	6.90	1.44	10.10	10.06	2.00	.69
.05	14.37	7.13	1.62	9.87	10.38	2.05	.69
.05	14.57	7.64	1.77	9.36	10.49	2.12	.73
.07	15.75	8.06	2.31	8.94	11.26	2.26	.72
.08	16.17	9.02	2.74	7.98	11.50	2.44	.78
.09	16.90	8.95	2.99	8.05	12.00	2.49	.75
.11	17.69	9.45	3.83	7.55	12.45	2.65	.76
.12	18.13	9.75	4.26	7.26	12.70	2.75	.77
.14	18.25	10.15	5.10	6.85	12.65	2.85	.80
.16	18.35	10.58	5.63	6.42	12.64	2.97	.84
.19	18.43	10.59	6.54	6.41	12.55	2.96	.84
.20	18.42	10.51	7.14	6.49	12.45	2.92	.84
.23	18.41	10.50	7.98	6.50	12.31	2.89	.85
.25	18.34	10.36	8.65	6.64	12.16	2.83	.85
.28	17.56	10.51	9.95	6.50	11.42	2.76	.92
.32	17.08	10.54	11.12	6.47	10.93	2.69	.96
.35	17.71	10.20	12.49	6.81	11.14	2.64	.92
.39	17.44	10.42	13.86	6.59	10.75	2.63	.97
.43	17.45	10.22	15.23	6.79	10.55	2.55	.97
.47	17.42	10.16	16.39	6.86	10.36	2.51	.98
.49	17.18	10.37	17.06	6.65	10.11	2.52	1.03
.52	17.25	10.30	18.47	6.72	9.94	2.48	1.04
.56	17.49	10.19	19.59	6.84	9.92	2.45	1.03

TEST NAME: S36.02
CONSOLIDATED-UNDRAINED TEST, NORMALLY CONSOLIDATED PARIS CLAY

HEIGHT PRIOR TO SHEAR   2.81 in
DIAMETER PRIOR TO SHEAR   1.41 in

AREA CORRECTION FACTOR   1.40
EFFECTIVE CONSOLIDATION PRESSURE   2.00 psi

DEF. (in)	FORCE (lb)	P.PRES. (psi)	AXIAL STRAIN %	MINOR PRIN STRESS psi	DEVIATORIC STRESS psi	STRESS RATIO	A COEF
.00	.00	.00	.00	2.00	.00	1.00	.00
.00	1.63	.25	.04	1.75	1.05	1.60	.24
.00	1.99	.54	.08	1.46	1.27	1.87	.42
.00	2.12	.75	.12	1.25	1.35	2.08	.56
.02	3.02	1.28	.66	.72	1.84	3.55	.70
.02	3.13	1.50	.75	.50	1.89	4.81	.80
.03	3.22	1.65	.90	.35	1.93	6.51	.86
.03	3.29	1.69	1.19	.31	1.92	7.19	.88
.04	3.29	1.65	1.33	.35	1.90	6.39	.87
.04	3.31	1.65	1.42	.35	1.89	6.48	.87
.05	3.28	1.59	1.70	.41	1.84	5.52	.87
.05	3.31	1.56	1.84	.44	1.83	5.17	.85
.06	3.33	1.63	1.98	.37	1.82	5.87	.89
.06	3.32	1.63	2.16	.37	1.80	5.90	.91
.07	3.34	1.61	2.35	.39	1.81	5.66	.89
.07	3.35	1.56	2.53	.44	1.80	5.07	.86
.08	3.37	1.61	2.72	.39	1.81	5.66	.89
.09	3.48	1.52	3.09	.48	1.85	4.88	.82
.10	3.60	1.67	3.46	.33	1.91	6.85	.87
.11	3.66	1.64	3.84	.36	1.93	6.32	.85
.12	3.72	1.69	4.23	.32	1.94	7.16	.87
.13	3.79	1.61	4.70	.39	1.96	5.98	.82
.14	3.72	1.61	5.09	.39	1.90	5.85	.85
.16	3.66	1.65	5.55	.35	1.84	6.30	.90
.17	3.63	1.63	6.01	.37	1.80	5.84	.91
.19	3.71	1.60	6.58	.40	1.82	5.52	.88
.20	3.86	1.66	7.05	.34	1.88	6.48	.88
.21	3.98	1.62	7.62	.38	1.92	6.05	.84
.23	3.91	1.66	8.29	.34	1.85	6.45	.90
.28	3.81	1.51	9.89	.49	1.71	4.46	.88
.31	4.04	1.61	10.85	.39	1.78	5.51	.91
.32	4.11	1.67	11.42	.34	1.79	6.26	.93
.34	4.01	1.63	12.14	.38	1.70	5.44	.96
.37	3.89	1.65	13.17	.36	1.58	5.34	1.04
.42	4.20	1.62	14.91	.39	1.64	5.22	.99
.47	4.03	1.70	16.65	.32	1.47	5.56	1.16
.49	4.16	1.67	17.37	.34	1.49	5.34	1.13
.51	4.29	1.64	18.08	.38	1.51	5.00	1.09
.53	4.31	1.64	18.90	.38	1.48	4.90	1.11
.56	4.11	1.63	19.93	.39	1.33	4.40	1.23

TEST NAME: W40.08
CONSOLIDATED-UNDRAINED TEST, WETTED & DRIED PARIS CLAY

HEIGHT PRIOR TO SHEAR   2.66 in
DIAMETER PRIOR TO SHEAR   1.31 in

AREA CORRECTION FACTOR   1.40
EFFECTIVE CONSOLIDATION PRESSURE   8.00 psi

DEF. (in)	FORCE (lb)	P.PRES. (psi)	AXIAL STRAIN %	MINOR PRIN STRESS psi	DEVIATORIC STRESS psi	STRESS RATIO	A COEF
.00	.00	.00	.00	8.00	.00	1.00	.00
.00	2.49	.57	.04	7.43	1.83	1.25	.31
.00	4.50	.98	.12	7.02	3.31	1.47	.30
.01	5.21	1.36	.22	6.64	3.81	1.57	.36
.01	5.64	1.66	.32	6.34	4.11	1.65	.40
.01	6.02	1.95	.42	6.05	4.37	1.72	.45
.02	6.63	2.51	.62	5.49	4.78	1.87	.53
.02	6.87	2.67	.72	5.33	4.93	1.93	.54
.02	7.42	2.73	.90	5.27	5.29	2.00	.52
.03	7.85	3.18	1.10	4.82	5.56	2.15	.57
.03	8.15	3.60	1.31	4.40	5.74	2.30	.63
.04	8.42	3.83	1.51	4.17	5.89	2.41	.65
.05	8.84	4.10	1.91	3.90	6.09	2.56	.67
.06	8.93	4.40	2.13	3.60	6:13	2.70	.72
.06	9.06	4.35	2.37	3.65	6.19	2.70	.70
.08	9.26	4.81	2.86	3.19	6.28	2.97	.77
.08	9.35	4.85	3.11	3.15	6.31	3.00	.77
.09	9.36	5.08	3.35	2.92	6.29	3.15	.81
.10	9.46	5.14	3.61	2.86	6.33	3.21	.81
.10	9.51	5.16	3.87	2.84	6.34	3.23	.81
.11	9.68	5.28	4.25	2.72	6.41	3.36	.82
.13	9.91	5.39	4.85	2.61	6.50	3.49	.83
.14	10.01	5.43	5.19	2.57	6.53	3.54	.83
.15	10.07	5.51	5.71	2.49	6.50	3.61	.85
.17	10.01	5.59	6.32	2.41	6.39	3.65	.87
.18	10.04	5.72	6.77	2.28	6.35	3.79	.90
.20	10.10	5.51	7.44	2.49	6.31	3.53	.87
.22	10.12	5.70	8.20	2.30	6.23	3.71	.91
.24	10.24	5.58	8.87	2.42	6.23	3.57	.90
.25	9.89	5.65	9.59	2.36	5.91	3.51	.95
.27	9.58	5.73	10.26	2.28	5.64	3.47	1.02
.29	9.55	5.67	11.09	2.34	5.52	3.36	1.03
.32	9.61	5.46	12.07	2.55	5.44	3.13	1.00
.36	9.33	5.50	13.50	2.52	5.10	3.03	1.08
.39	9.14	5.51	14.51	2.51	4.87	2.94	1.13
.41	9.22	5.35	15.23	2.66	4.84	2.82	1.11
.43	9.48	5.31	15.98	2.71	4.90	2.81	1.08
.45	9.38	5.34	16.95	2.68	4.73	2.77	1.13
.47	9.24	5.34	17.71	2.68	4.56	2.70	1.17
.49	9.40	5.29	18.35	2.73	4.58	2.68	1.16

TEST NAME: W41.12
CONSOLIDATED-UNDRAINED TEST, WETTED & DRIED PARIS CLAY

HEIGHT PRIOR TO SHEAR   2.52 in
DIAMETER PRIOR TO SHEAR   1.35 in

AREA CORRECTION FACTOR   1.40
EFFECTIVE CONSOLIDATION PRESSURE   12.00 psi

DEF. (in)	FORCE (lb)	P.PRES. (psi)	AXIAL STRAIN %	MINOR PRIN STRESS psi	DEVIATORIC STRESS psi	STRESS RATIO	A COEF
.00	.00	.00	.00	12.00	.00	1.00	.00
.00	3.05	.92	.08	11.08	2.11	1.19	.44
.00	4.21	1.36	.20	10.64	2.90	1.27	.47
.01	5.36	2.07	.31	9.93	3.67	1.37	.56
.01	5.95	2.60	.42	9.40	4.06	1.43	.64
.02	7.01	3.43	.63	8.57	4.75	1.55	.72
.02	7.42	3.64	.73	8.36	5.01	1.60	.73
.02	7.83	3.69	.84	8.31	5.27	1.63	.70
.03	8.90	4.49	1.16	7.51	5.93	1.79	.76
.03	9.44	4.93	1.32	7.07	6.27	1.89	.79
.04	10.02	5.26	1.48	6.74	6.63	1.98	.79
.04	10.37	5.58	1.63	6.42	6.83	2.06	.82
.05	10.98	5.93	1.94	6.08	7.17	2.18	.83
.05	11.01	6.11	2.10	5.90	7.16	2.21	.85
.06	11.32	6.30	2.24	5.70	7.35	2.29	.86
.06	11.61	6.34	2.50	5.66	7.51	2.33	.84
.07	11.77	6.76	2.78	5.24	7.58	2.45	.89
.08	11.94	6.95	3.06	5.05	7.66	2.52	.91
.08	12.07	7.11	3.33	4.89	7.71	2.58	.92
.10	12.57	7.48	3.88	4.52	7.96	2.76	.94
.10	12.73	7.54	4.17	4.46	8.03	2.80	.94
.13	13.40	7.75	4.96	4.25	8.35	2.97	.93
.13	13.76	7.93	5.36	4.07	8.52	3.10	.93
.14	13.72	7.85	5.75	4.15	8.44	3.03	.93
.16	13.49	7.94	6.51	4.06	8.18	3.02	.97
.17	13.18	8.05	6.90	3.95	7.92	3.01	1.02
.19	13.18	8.39	7.42	3.61	7.85	3.17	1.07
.20	14.12	8.04	7.86	3.96	8.37	3.11	.96
.21	14.39	8.20	8.33	3.80	8.46	3.23	.97
.23	14.92	8.19	9.05	3.81	8.67	3.27	.95
.24	14.89	8.20	9.48	3.80	8.58	3.26	.96
.26	14.50	8.17	10.16	3.83	8.24	3.15	.99
.27	13.91	8.31	10.63	3.69	7.81	3.11	1.06
.29	14.65	8.14	11.43	3.86	8.12	3.10	1.00
.32	14.85	7.87	12.74	4.14	8.02	2.94	.98
.34	14.47	7.87	13.49	4.14	7.69	2.86	1.02
.36	14.31	7.97	14.25	4.04	7.48	2.85	1.07
.39	14.53	7.87	15.32	4.14	7.43	2.79	1.06
.42	14.70	7.81	16.67	4.21	7.30	2.74	1.07
.45	14.43	7.71	17.90	4.31	6.96	2.61	1.11

TEST NAME: W42.20
CONSOLIDATED-UNDRAINED TEST, WETTED & DRIED PARIS CLAY

HEIGHT PRIOR TO SHEAR   2.76 in
DIAMETER PRIOR TO SHEAR   1.36 in

AREA CORRECTION FACTOR   1.00
EFFECTIVE CONSOLIDATION PRESSURE   20.00 psi

DEF. (in)	FORCE (1b)	P.PRES. (psi)	AXIAL STRAIN %	MINOR PRIN STRESS psi	DEVIATORIC STRESS psi	STRESS RATIO	A COEF
.00	.00	.00	.00	20.00	.00	1.00	.00
.00	4.07	1.50	.04	18.50	2.80	1.15	.54
.00	6.28	2.00	.09	18.00	4.31	1.24	.46
.00	7.03	2.33	.14	17.67	4.81	1.27	.48
.01	7.96	2.90	.25	17.10	5.43	1.32	.53
.01	8.69	3.59	.34	16.41	5.91	1.36	.61
.01	9.50	4.36	.44	15.64	6.45	1.41	.68
.02	10.63	5.35	.59	14.65	7.19	1.49	.74
.02	11.20	6.00	.69	14.00	7.56	1.54	.79
.02	11.93	6.51	.84	13.49	8.03	1.60	.81
.03	12.44	7.00	.99	13.00	8.34	1.64	.84
.03	12.86	7.20	1.08	12.80	8.60	1.67	.84
.03	13.25	7.57	1.18	12.44	8.85	1.71	.86
.04	13.72	7.89	1.31	12.11	9.14	1.75	.86
.04	14.13	8.10	1.45	11.90	9.38	1.79	.86
.05	14.60	8.35	1.64	11.65	9.65	1.83	.87
.05	15.01	8.90	1.83	11.10	9.89	1.89	.90
.06	15.70	9.44	2.12	10.56	10.30	1.97	.92
.07	16.33	9.74	2.39	10.26	10.68	2.04	.91
.07	16.85	10.33	2.67	9.67	11.00	2.14	.94
.08	17.79	10.85	3.07	9.15	11.57	2.26	.94
.10	18.08	11.39	3.51	8.61	11.70	2.36	.97
.10	18.53	11.59	3.80	8.41	11.96	2.42	.97
.12	19.26	11.75	4.24	8.25	12.37	2.50	.95
.13	19.49	12.12	4.67	7.88	12.46	2.58	.97
.14	20.01	12.22	5.14	7.78	12.73	2.64	.96
.15	20.21	12.48	5.58	7.52	12.79	2.70	.98
.17	20.42	12.34	6.01	7.66	12.85	2.68	.96
.19	20.79	12.47	6.85	7.53	12.96	2.72	.96
.21	20.95	12.68	7.46	7.32	12.96	2.77	.98
.22	21.02	12.36	7.83	7.64	12.95	2.69	.95
.25	19.15	12.21	8.99	7.79	11.58	2.49	1.05
.27	18.56	11.88	9.78	8.13	11.10	2.37	1.07
.31	18.89	11.80	11.20	8.21	11.09	2.35	1.06
.34	18.86	11.69	12.39	8.32	10.90	2.31	1.07
.38	18.77	11.76	13.80	8.25	10.63	2.29	1.11
.42	18.92	11.83	15.25	8.18	10.50	2.28	1.13
.46	19.36	12.07	16.70	7.95	10.54	2.33	1.15
.48	19.69	11.81	17.43	8.21	10.62	2.29	1.11
.51	20.13	11.80	18.33	8.22	10.73	2.30	1.10

TEST NAME: W43.04
CONSOLIDATED-UNDRAINED TEST, WETTED & DRIED PARIS CLAY

HEIGHT PRIOR TO SHEAR   2.72 in
DIAMETER PRIOR TO SHEAR   1.36 in

AREA CORRECTION FACTOR   1.40
EFFECTIVE CONSOLIDATION PRESSURE   4.00 psi

DEF. (in)	FORCE (lb)	P.PRES. (psi)	AXIAL STRAIN %	MINOR PRIN STRESS psi	DEVIATORIC STRESS psi	STRESS RATIO	A COEF
.00	.00	.00	.00	4.00	.00	1.00	.00
.00	1.80	.18	.06	3.82	1.24	1.32	.15
.00	3.10	.31	.09	3.69	2.13	1.58	.15
.00	3.46	.31	.12	3.69	2.38	1.64	.13
.00	4.59	.61	.17	3.39	3.15	1.93	.19
.01	5.28	.86	.26	3.14	3.61	2.15	.24
.01	5.09	1.00	.36	3.00	3.46	2.15	.29
.02	5.37	1.38	.56	2.62	3.62	2.38	.38
.02	5.57	1.69	.76	2.31	3.71	2.61	.46
.03	5.89	1.83	1.04	2.17	3.88	2.79	.47
.03	5.97	1.88	1.23	2.12	3.90	2.83	.48
.04	6.07	2.06	1.43	1.94	3.93	3.03	.53
.05	6.25	2.24	1.82	1.76	3.97	3.25	.56
.06	6.39	2.38	2.11	1.62	4.02	3.48	.59
.06	6.46	2.47	2.31	1.53	4.05	3.65	.61
.07	6.56	2.49	2.64	1.51	4.09	3.70	.61
.08	6.53	2.66	2.94	1.34	4.05	4.02	.66
.09	6.54	2.63	3.22	1.37	4.03	3.94	.65
.10	6.53	2.66	3.50	1.34	4.00	3.98	.66
.11	6.61	2.73	4.19	1.27	4.00	4.14	.68
.13	6.68	2.71	4.78	1.29	3.99	4.10	.68
.15	6.72	2.73	5.37	1.27	3.97	4.13	.69
.16	6.82	2.78	5.96	1.23	3.99	4.25	.70
.18	6.96	2.90	6.51	1.11	4.03	4.64	.72
.19	6.93	2.99	7.10	1.01	3.96	4.90	.75
.21	6.90	2.97	7.68	1.04	3.89	4.75	.76
.22	6.93	2.97	8.27	1.03	3.85	4.74	.77
.25	7.01	2.99	9.08	1.01	3.83	4.78	.78
.27	7.11	2.88	9.78	1.12	3.83	4.41	.75
.29	7.22	2.85	10.74	1.15	3.82	4.31	.75
.31	7.21	2.92	11.47	1.09	3.75	4.44	.78
.33	7.24	2.95	12.21	1.06	3.70	4.48	.80
.35	7.41	2.84	12.94	1.17	3.73	4.19	.76
.37	7.50	2.81	13.64	1.20	3.72	4.09	.75
.39	7.53	2.74	14.34	1.27	3.67	3.88	.75
.43	7.66	2.84	15.81	1.18	3.61	4.06	.79
.45	7.78	2.79	16.54	1.23	3.60	3.92	.77
.47	7.82	2.76	17.24	1.26	3.56	3.82	.78
.51	7.87	2.84	18.68	1.18	3.45	3.92	.82
.53	7.88	2.81	19.38	1.21	3.39	3.79	.83

TEST NAME: W44.30
CONSOLIDATED-UNDRAINED TEST, WETTED & DRIED PARIS CLAY

HEIGHT PRIOR TO SHEAR   2.72 in
DIAMETER PRIOR TO SHEAR   1.23 in

AREA CORRECTION FACTOR   1.00
EFFECTIVE CONSOLIDATION PRESSURE   30.00 psi

DEF. (in)	FORCE (lb)	P.PRES. (psi)	AXIAL STRAIN %	MINOR PRIN STRESS psi	DEVIATORIC STRESS psi	STRESS RATIO	A COEF
.00	.00	.00	.00	30.00	.00	1.00	.00
.00	3.80	1.61	.05	28.39	3.21	1.11	.50
.00	6.30	2.78	.09	27.22	5.31	1.19	.52
.00	7.64	3.58	.15	26.42	6.43	1.24	.56
.01	8.74	4.33	.20	25.67	7.34	1.29	.59
.01	9.47	4.81	.24	25.19	7.95	1.32	.61
.01	10.74	5.82	.35	24.18	9.00	1.37	.65
.01	11.65	6.23	.43	23.77	9.74	1.41	.64
.01	12.48	6.84	.53	23.16	10.41	1.45	.66
.02	13.23	7.61	.64	22.39	11.02	1.49	.69
.02	13.95	7.85	.71	22.15	11.60	1.52	.68
.02	14.58	8.59	.82	21.41	12.10	1.57	.71
.02	15.05	9.01	.92	21.00	12.47	1.59	.72
.03	16.17	9.94	1.11	20.06	13.35	1.67	.74
.03	16.64	10.30	1.21	19.70	13.71	1.70	.75
.04	17.41	11.02	1.35	18.98	14.31	1.75	.77
.04	18.01	11.89	1.52	18.11	14.76	1.82	.81
.05	19.24	12.36	1.80	17.64	15.70	1.89	.79
.06	20.47	13.70	2.20	16.30	16.62	2.02	.82
.07	21.83	14.02	2.58	15.98	17.66	2.11	.79
.08	22.83	14.64	2.98	15.36	18.40	2.20	.80
.09	23.32	14.78	3.17	15.22	18.76	2.23	.79
.10	23.61	15.54	3.61	14.46	18.90	2.31	.82
.11	23.85	16.11	3.93	13.89	19.02	2.37	.85
.12	24.44	16.26	4.52	13.74	19.37	2.41	.84
.13	24.93	16.50	4.82	13.50	19.70	2.46	.84
.14	25.38	16.63	5.22	13.37	19.96	2.49	.83
.17	22.32	16.90	6.21	13.10	17.30	2.32	.98
.19	21.73	16.62	6.91	13.38	16.69	2.25	1.00
.20	21.31	17.03	7.46	12.97	16.25	2.25	1.05
.23	20.65	17.53	8.31	12.47	15.57	2.25	1.13
.24	21.20	17.45	8.93	12.56	15.87	2.26	1.10
.26	20.44	17.30	9.63	12.71	15.15	2.19	1.14
.30	21.00	17.76	11.07	12.25	15.29	2.25	1.16
.32	21.44	17.60	11.80	12.41	15.47	2.25	1.14
.36	21.65	17.66	13.20	12.35	15.35	2.24	1.15
.38	22.29	18.01	14.15	12.00	15.62	2.30	1.15
.42	22.22	17.99	15.59	12.03	15.26	2.27	1.18
.44	21.93	18.14	16.32	11.88	14.91	2.25	1.22
.48	21.99	18.00	17.54	12.02	14.70	2.22	1.22

TEST NAME: W45.02
CONSOLIDATED-UNDRAINED TEST, WETTED & DRIED PARIS CLAY

HEIGHT PRIOR TO SHEAR   2.97 in
DIAMETER PRIOR TO SHEAR   1.37 in

AREA CORRECTION FACTOR   1.40
EFFECTIVE CONSOLIDATION PRESSURE   2.00 psi

DEF. (in)	FORCE (lb)	P.PRES. (psi)	AXIAL STRAIN %	MINOR PRIN STRESS psi	DEVIATORIC STRESS psi	STRESS RATIO	A COEF
.00	.00	– .00	.00	2.00	.00	1.00	.00
.00	.99	.10	.03	1.90	.66	1.35	.16
.00	1.67	.21	.07	1.79	1.12	1.63	.19
.00	1.71	.24	.08	1.76	1.14	1.65	.21
.00	1.87	.37	.14	1.63	1.25	1.76	.30
.01	2.05	.53	.21	1.47	1.36	1.92	.39
.01	2.18	.66	.30	1.34	1.43	2.07	.46
.01	2.33	.79	.42	1.21	1.51	2.25	.52
.02	2.46	.87	.56	1.13	1.58	2.40	.55
.02	2.55	.97	.68	1.03	1.62	2.57	.60
.03	2.70	1.06	.89	.94	1.69	2.79	.63
.03	2.82	1.14	1.11	.86	1.72	3.01	.66
.04	2.89	1.18	1.29	.82	1.75	3.13	.68
.04	2.96	1.22	1.46	.78	1.77	3.27	.69
.05	3.01	1.26	1.68	.74	1.76	3.39	.72
.05	3.07	1.30	1.85	.70	1.77	3.54	.74
.06	3.09	1.38	2.07	.62	1.76	3.81	.78
.07	3.15	1.47	2.49	.53	1.78	4.35	.83
.09	3.19	1.54	3.04	.46	1.77	4.88	.87
.11	3.23	1.55	3.60	.45	1.78	4.94	.87
.12	3.25	1.52	4.04	.48	1.76	4.71	.86
.14	3.37	1.55	4.71	.45	1.81	5.00	.85
.16	3.39	1.67	5.45	.33	1.78	6.34	.94
.19	3.40	1.73	6.23	.28	1.76	7.34	.98
.21	3.41	1.69	7.00	.31	1.72	6.50	.98
.23	3.47	1.64	7.61	.36	1.72	5.75	.95
.25	3.55	1.62	8.42	.39	1.73	5.46	.93
.27	3.57	1.75	9.19	.26	1.71	7.57	1.02
.30	3.63	1.71	10.17	.30	1.69	6.70	1.01
.33	3.71	1.65	11.18	.36	1.68	5.71	.98
.35	3.81	1.77	11.95	.24	1.70	8.07	1.04
.38	3.58	1.76	12.73	.25	1.53	7.12	1.15
.40	3.74	1.71	13.54	.30	1.57	6.19	1.09
.43	3.82	1.64	14.34	.37	1.57	5.28	1.04
.45	3.71	1.75	15.12	.27	1.47	6.47	1.19
.48	4.01	1.73	16.30	.28	1.57	6.53	1.11
.51	4.08	1.67	17.27	.34	1.55	5.51	1.08
.55	4.24	1.76	18.59	.26	1.55	7.05	1.14
.59	4.47	1.74	19.87	.29	1.59	6.48	1.09
.64	4.59	1.78	21.45	.25	1.55	7.21	1.15

TEST NAME: S51.04
CONSOLIDATED-UNDRAINED TEST, NORMALLY CONSOLIDATED BEAUMONT CLAY
CONSLIDATED IN 3-INCH DIAMETER TUBE AND SAMPLED PRIOR TO TESTING

HEIGHT PRIOR TO SHEAR   2.72 in
DIAMETER PRIOR TO SHEAR   1.38 in

AREA CORRECTION FACTOR   1.00
EFFECTIVE CONSOLIDATION PRESSURE   4.00 psi

DEF. (in)	FORCE (lb)	P.PRES. (psi)	AXIAL STRAIN %	MINOR PRIN STRESS psi	DEVIATORIC STRESS psi	STRESS RATIO	A COEF
.00	.00	.00	.00	4.00	.00	1.00	.00
.00	1.07	.07	.01	3.93	.72	1.18	.09
.00	1.58	.15	.04	3.85	1.06	1.28	.14
.00	1.69	.24	.08	3.76	1.13	1.30	.21
.00	1.95	.37	.15	3.63	1.29	1.36	.29
.01	2.50	.58	.22	3.42	1.64	1.48	.36
.01	2.95	.86	.33	3.14	1.93	1.62	.45
.01	3.14	1.06	.46	2.94	2.04	1.69	.52
.02	3.70	1.38	.65	2.62	2.38	1.91	.58
.02	4.07	1.69	.84	2.31	2.59	2.12	.65
.03	4.39	1.89	1.03	2.11	2.78	2.32	.68
.03	4.55	2.05	1.22	1.95	2.86	2.46	.72
.04	4.71	2.24	1.52	1.76	2.91	2.65	.77
.05	4.90	2.44	1.92	1.56	2.96	2.90	.82
.06	5.07	2.55	2.22	1.45	3.05	3.11	.84
.07	5.20	2.65	2.51	1.35	3.12	3.32	.85
.08	5.35	2.71	2.79	1.29	3.21	3.48	.84
.09	5.48	2.77	3.32	1.23	3.26	3.66	.85
.11	5.64	2.84	4.04	1.16	3.32	3.85	.85
.13	5.77	2.90	4.63	1.10	3.37	4.07	.86
.14	5.92	2.95	5.33	1.06	3.43	4.25	.86
.16	5.99	2.97	5.92	1.04	3.44	4.32	.86
.17	5.99	2.97	6.36	1.03	3.41	4.31	.87
.19	5.97	2.96	6.80	1.04	3.38	4.25	.88
.19	6.12	2.96	7.10	1.05	3.45	4.30	.86
.20	6.12	3.01	7.50	1.00	3.43	4.44	.88
.22	6.03	3.02	8.24	.98	3.33	4.39	.91
.24	5.90	3.03	8.82	.98	3.21	4.28	.94
.26	5.82	3.03	9.56	.98	3.12	4.19	.97
.29	5.61	2.89	10.85	1.12	2.92	3.61	.99
.31	5.62	2.88	11.29	1.13	2.90	3.57	.99
.32	5.66	2.92	11.88	1.09	2.89	3.66	1.01
.35	5.77	2.77	12.90	1.24	2.90	3.33	.96
.39	5.81	2.91	14.30	1.10	2.84	3.58	1.03
.42	5.86	2.97	15.44	1.04	2.80	3.68	1.06
.45	5.87	3.04	16.62	.98	2.74	3.80	1.11
.49	5.88	2.81	17.90	1.21	2.67	3.20	1.05
.53	6.02	2.87	19.34	1.16	2.66	3.30	1.08
.56	5.98	2.97	20.74	1.06	2.56	3.42	1.16

TEST NAME: S52.25
CONSOLIDATED-UNDRAINED TEST, NORMALLY CONSOLIDATED BEAUMONT CLAY

HEIGHT PRIOR TO SHEAR   2.71 in
DIAMETER PRIOR TO SHEAR   1.32 in

AREA CORRECTION FACTOR   1.00
EFFECTIVE CONSOLIDATION PRESSURE   25.00 psi

DEF. (in)	FORCE (lb)	P.PRES. (psi)	AXIAL STRAIN %	MINOR PRIN STRESS psi	DEVIATORIC STRESS psi	STRESS RATIO	A COEF
.00	.00	.00	.00	25.00	.00	1.00	.00
.00	3.90	2.23	.05	22.77	2.86	1.13	.78
.00	6.91	3.73	.12	21.27	5.06	1.24	.74
.00	9.40	5.09	.18	19.91	6.87	1.35	.74
.01	11.17	6.16	.23	18.84	8.16	1.43	.76
.01	12.70	7.36	.33	17.64	9.26	1.52	.80
.01	14.10	8.54	.42	16.46	10.26	1.62	.83
.01	15.06	9.52	.51	15.48	10.94	1.71	.87
.02	16.37	10.12	.59	14.88	11.88	1.80	.85
.02	17.10	10.98	.69	14.02	12.38	1.88	.89
.02	17.94	11.73	.79	13.27	12.97	1.98	.90
.02	18.57	12.17	.88	12.83	13.40	2.04	.91
.03	20.22	12.85	1.08	12.15	14.55	2.20	.88
.03	21.14	13.50	1.27	11.50	15.16	2.32	.89
.06	24.29	15.54	2.13	9.46	17.18	2.82	.90
.06	24.58	15.63	2.33	9.37	17.35	2.85	.90
.07	25.18	15.93	2.62	9.07	17.72	2.95	.90
.08	25.21	16.29	2.96	8.71	17.68	3.03	.92
.09	25.77	16.57	3.37	8.43	17.99	3.13	.92
.10	26.16	16.50	3.76	8.50	18.18	3.14	.91
.11	25.76	16.82	4.24	8.18	17.80	3.18	.94
.12	25.86	16.97	4.58	8.03	17.80	3.22	.95
.13	26.18	17.00	4.91	8.00	17.96	3.24	.95
.16	26.66	16.97	5.76	8.03	18.11	3.25	.94
.17	26.82	17.02	6.13	7.98	18.14	3.27	.94
.18	27.03	17.00	6.64	8.00	18.17	3.27	.94
.19	26.91	16.61	7.12	8.39	17.98	3.14	.92
.21	26.30	16.68	7.64	8.32	17.46	3.10	.96
.22	25.72	16.97	8.23	8.03	16.94	3.11	1.00
.24	25.99	17.21	8.89	7.79	16.98	3.18	1.01
.27	26.08	16.80	9.85	8.21	16.84	3.05	1.00
.28	26.05	16.94	10.37	8.07	16.71	3.07	1.01
.30	25.95	16.87	11.14	8.14	16.48	3.03	1.02
.32	26.64	16.83	11.99	8.18	16.75	3.05	1.00
.36	26.97	16.78	13.17	8.23	16.71	3.03	1.00
.38	27.90	17.00	14.13	8.01	17.08	3.13	1.00
.41	28.15	16.93	15.09	8.08	17.02	3.11	.99
.45	26.80	16.61	16.79	8.41	15.81	2.88	1.05
.50	26.19	17.04	18.27	7.98	15.13	2.90	1.13
.52	26.55	16.81	19.08	8.21	15.17	2.85	1.11

TEST NAME: S53.04
CONSOLIDATED-UNDRAINED TEST, NORMALLY CONSOLIDATED BEAUMONT CLAY

HEIGHT PRIOR TO SHEAR   3.12 in
DIAMETER PRIOR TO SHEAR   1.39 in

AREA CORRECTION FACTOR   1.40
EFFECTIVE CONSOLIDATION PRESSURE   4.00 psi

DEF. (in)	FORCE (lb)	P.PRES. (psi)	AXIAL STRAIN %	MINOR PRIN STRESS psi	DEVIATORIC STRESS psi	STRESS RATIO	A COEF
.00	.00	.00	.00	4.00	.00	1.00	.00
.00	2.08	.26	.04	3.74	1.37	1.37	.19
.00	3.40	.47	.07	3.53	2.23	1.63	.21
.01	4.03	.84	.16	3.16	2.64	1.84	.32
.01	4.37	1.07	.25	2.93	2.84	1.97	.38
.01	4.61	1.32	.33	2.68	2.99	2.11	.44
.01	4.82	1.54	.42	2.46	3.11	2.26	.50
.02	4.78	1.74	.51	2.27	3.07	2.36	.56
.02	4.94	1.82	.60	2.18	3.16	2.45	.58
.02	5.12	1.87	.75	2.13	3.25	2.53	.58
.03	5.21	2.11	.92	1.89	3.28	2.73	.64
.03	5.39	2.21	1.08	1.79	3.36	2.88	.66
.04	5.44	2.22	1.25	1.78	3.36	2.89	.66
.04	5.56	2.31	1.42	1.69	3.41	3.02	.68
.05	5.63	2.37	1.59	1.63	3.43	3.10	.69
.05	5.75	2.42	1.76	1.58	3.47	3.20	.70
.07	5.96	2.55	2.19	1.45	3.55	3.45	.72
.08	6.06	2.57	2.45	1.43	3.59	3.52	.72
.08	6.09	2.55	2.62	1.45	3.60	3.49	.71
.10	6.23	2.63	3.12	1.37	3.65	3.66	.72
.11	5.81	2.71	3.46	1.29	3.36	3.61	.81
.12	5.79	2.76	3.81	1.24	3.32	3.67	.83
.13	5.76	2.78	4.29	1.23	3.27	3.67	.85
.16	6.12	2.83	5.00	1.17	3.44	3.93	.82
.17	6.56	2.84	5.57	1.16	3.67	4.17	.78
.19	6.55	2.89	5.99	1.11	3.63	4.27	.80
.20	6.67	2.76	6.28	1.25	3.68	3.95	.75
.22	6.42	2.84	7.01	1.16	3.47	3.99	.82
.25	6.57	2.81	7.91	1.19	3.49	3.93	.81
.27	6.58	2.74	8.74	1.26	3.43	3.72	.80
.32	6.67	2.80	10.25	1.20	3.36	3.80	.83
.36	6.77	2.76	11.50	1.25	3.32	3.66	.83
.38	6.76	2.68	12.11	1.32	3.26	3.46	.82
.41	6.78	2.76	12.97	1.25	3.20	3.57	.86
.43	6.74	2.79	13.61	1.22	3.13	3.57	.89
.44	7.24	2.74	14.25	1.27	3.35	3.64	.82
.47	7.26	2.69	15.09	1.32	3.29	3.48	.82
.51	7.28	2.79	16.34	1.23	3.19	3.59	.87
.55	7.48	2.72	17.58	1.30	3.18	3.46	.86
.58	7.55	2.80	18.64	1.22	3.13	3.56	.90

TEST NAME: S55.08
CONSOLIDATED-UNDRAINED TEST, NORMALLY CONSOLIDATED BEAUMONT CLAY

HEIGHT PRIOR TO SHEAR   2.87 in
DIAMETER PRIOR TO SHEAR   1.30 in

AREA CORRECTION FACTOR   1.40
EFFECTIVE CONSOLIDATION PRESSURE   8.00 psi

DEF. (in)	FORCE (lb)	P.PRES. (psi)	AXIAL STRAIN %	MINOR PRIN STRESS psi	DEVIATORIC STRESS psi	STRESS RATIO	A COEF
.00	.00	.00	.00	8.00	.00	1.00	.00
.00	2.46	.62	.03	7.38	1.84	1.25	.34
.00	4.36	1.07	.08	6.93	3.26	1.47	.33
.01	6.61	2.13	.25	5.87	4.90	1.84	.43
.01	7.06	2.64	.38	5.36	5.21	1.97	.51
.02	7.79	3.57	.75	4.43	5.67	2.28	.63
.04	8.52	4.46	1.30	3.54	6.09	2.72	.73
.07	9.55	5.25	2.39	2.75	6.62	3.40	.79
.08	9.49	5.28	2.66	2.72	6.55	3.41	.81
.09	9.23	5.34	3.21	2.66	6.29	3.37	.85
.10	10.61	5.42	3.58	2.58	7.24	3.80	.75
.12	10.51	5.53	4.04	2.47	7.11	3.88	.78
.13	10.83	5.53	4.42	2.47	7.28	3.95	.76
.13	10.80	5.65	4.70	2.35	7.22	4.07	.78
.15	11.09	5.57	5.08	2.44	7.38	4.03	.75
.15	11.12	5.64	5.36	2.37	7.36	4.11	.77
.16	11.33	5.60	5.71	2.40	7.46	4.10	.75
.18	11.42	5.67	6.19	2.33	7.45	4.19	.76
.19	11.59	5.57	6.65	2.43	7.50	4.08	.74
.20	11.58	5.48	7.10	2.52	7.43	3.95	.74
.22	11.69	5.45	7.55	2.55	7.44	3.92	.73
.23	11.70	5.61	8.00	2.39	7.39	4.09	.76
.24	11.64	5.62	8.46	2.39	7.28	4.05	.77
.27	11.32	5.49	9.53	2.51	6.92	3.75	.79
.29	11.83	5.41	10.23	2.60	7.16	3.75	.76
.31	12.00	5.39	10.89	2.61	7.17	3.74	.75
.33	12.09	5.42	11.59	2.59	7.12	3.76	.76
.35	12.12	5.43	12.28	2.58	7.04	3.73	.77
.36	12.39	5.46	12.63	2.55	7.16	3.81	.76
.38	12.54	5.41	13.29	2.60	7.15	3.75	.76
.41	12.65	5.41	14.30	2.60	7.06	3.71	.77
.43	12.56	5.45	14.96	2.57	6.91	3.69	.79
.45	12.65	5.45	15.69	2.57	6.85	3.67	.80
.49	13.10	5.32	17.01	2.70	6.91	3.56	.77
.52	12.98	5.40	18.02	2.62	6.69	3.55	.81
.55	13.60	5.48	19.07	2.55	6.86	3.70	.80
.53	13.05	5.46	18.37	2.56	6.67	3.61	.82
.58	14.02	5.36	20.08	2.67	6.93	3.60	.77
.61	13.95	5.39	21.05	2.64	6.73	3.55	.80
.62	13.83	5.43	21.40	2.60	6.61	3.54	.82

TEST NAME: S56.02
CONSOLIDATED-UNDRAINED TEST, NORMALLY CONSOLIDATED BEAUMONT CLAY

HEIGHT PRIOR TO SHEAR   2.97 in
DIAMETER PRIOR TO SHEAR   1.40 in

AREA CORRECTION FACTOR   1.40
EFFECTIVE CONSOLIDATION PRESSURE   2.00 psi

DEF. (in)	FORCE (lb)	P.PRES. (psi)	AXIAL STRAIN %	MINOR PRIN STRESS psi	DEVIATORIC STRESS psi	STRESS RATIO	A COEF
.00	.00	.00	.00	2.00	.00	1.00	.00
.00	2.16	.16	.04	1.84	1.40	1.76	.12
.00	2.63	.39	.13	1.61	1.69	2.05	.23
.01	2.83	.55	.22	1.45	1.80	2.24	.30
.01	2.96	.67	.31	1.33	1.87	2.41	.36
.01	3.10	.76	.40	1.24	1.95	2.58	.39
.02	3.20	.86	.53	1.14	1.99	2.75	.43
.02	3.38	.96	.71	1.04	2.08	3.00	.46
.03	3.43	1.00	.87	1.00	2.08	3.08	.48
.03	3.46	1.10	1.09	.90	2.06	3.28	.53
.04	3.58	1.14	1.31	.86	2.11	3.44	.54
.04	3.64	1.14	1.48	.86	2.11	3.46	.54
.05	3.73	1.21	1.70	.79	2.13	3.70	.57
.06	3.78	1.23	1.92	.77	2.13	3.75	.58
.06	3.75	1.22	2.13	.78	2.09	3.67	.58
.07	3.83	1.26	2.36	.74	2.13	3.89	.59
.08	3.80	1.32	2.63	.68	2.09	4.07	.63
.08	3.82	1.34	2.85	.66	2.09	4.15	.64
.10	3.89	1.37	3.28	.63	2.12	4.37	.65
.11	3.94	1.39	3.84	.61	2.12	4.46	.65
.13	3.95	1.35	4.37	.65	2.10	4.24	.64
.14	4.03	1.36	4.85	.65	2.12	4.29	.64
.16	4.06	1.35	5.25	.66	2.11	4.22	.64
.17	4.08	1.40	5.82	.60	2.10	4.49	.67
.20	4.16	1.42	6.70	.58	2.10	4.61	.68
.22	4.21	1.37	7.57	.63	2.08	4.29	.66
.25	4.30	1.41	8.31	.60	2.09	4.49	.67
.27	4.30	1.43	9.19	.57	2.03	4.57	.71
.30	4.36	1.40	10.06	.60	2.02	4.36	.69
.32	4.39	1.37	10.94	.64	1.99	4.11	.69
.35	4.41	1.36	11.64	.64	1.96	4.04	.70
.37	4.46	1.41	12.52	.60	1.93	4.24	.73
.43	4.60	1.37	14.47	.65	1.90	3.93	.72
.49	4.60	1.38	16.45	.63	1.78	3.81	.78
.52	4.74	1.35	17.43	.67	1.79	3.66	.75
.56	4.74	1.40	18.71	.62	1.71	3.74	.82
.58	4.70	1.37	19.68	.66	1.63	3.48	.84
.62	4.69	1.35	21.00	.68	1.55	3.28	.87
.65	4.62	1.38	21.97	.65	1.46	3.23	.94
.67	4.63	1.38	22.61	.66	1.42	3.17	.97

TEST NAME: S57.15
CONSOLIDATED-UNDRAINED TEST, NORMALLY CONSOLIDATED BEAUMONT CLAY

HEIGHT PRIOR TO SHEAR   2.75 in
DIAMETER PRIOR TO SHEAR   1.31 in

AREA CORRECTION FACTOR   1.40
EFFECTIVE CONSOLIDATION PRESSURE   15.00 psi

DEF. (in)	FORCE (lb)	P.PRES. (psi)	AXIAL STRAIN %	MINOR PRIN STRESS psi	DEVIATORIC STRESS psi	STRESS RATIO	A COEF
.00	.00	.00	.00	15.00	.00	1.00	.00
.00	3.16	.91	.02	14.09	2.34	1.17	.39
.00	5.92	1.60	.06	13.40	4.38	1.33	.37
.00	8.14	2.28	.09	12.72	6.02	1.47	.38
.00	10.85	3.16	.17	11.84	8.01	1.68	.39
.01	12.59	4.23	.27	10.77	9.26	1.86	.46
.01	13.30	5.00	.39	10.00	9.76	1.98	.51
.01	13.98	5.72	.54	9.28	10.22	2.10	.56
.02	14.22	6.07	.61	8.93	10.37	2.16	.59
.02	14.58	6.53	.72	8.48	10.60	2.25	.62
.03	15.09	7.24	.93	7.76	10.91	2.41	.66
.03	15.56	7.78	1.14	7.22	11.19	2.55	.70
.04	15.88	8.19	1.33	6.81	11.37	2.67	.72
.04	16.13	8.40	1.44	6.60	11.52	2.75	.73
.04	16.29	8.57	1.55	6.43	11.60	2.80	.74
.05	16.49	8.83	1.73	6.17	11.69	2.89	.76
.07	17.06	9.62	2.42	5.38	11.93	3.22	.81
.09	17.60	10.00	3.30	5.00	12.14	3.43	.82
.12	18.15	10.08	4.32	4.92	12.32	3.50	.82
.14	18.56	10.40	5.16	4.60	12.43	3.70	.84
.16	18.79	10.53	5.89	4.47	12.43	3.78	.85
.18	19.04	10.43	6.61	4.57	12.44	3.72	.84
.20	19.20	10.24	7.19	4.76	12.42	3.61	.82
.22	19.46	10.29	7.92	4.71	12.44	3.64	.83
.24	19.67	10.46	8.76	4.54	12.39	3.73	.84
.26	20.51	10.25	9.48	4.76	12.77	3.68	.80
.28	20.61	10.20	10.17	4.81	12.67	3.64	.81
.30	20.78	10.04	11.01	4.97	12.58	3.53	.80
.32	20.97	10.23	11.74	4.78	12.53	3.62	.82
.35	21.09	10.37	12.61	4.64	12.40	3.67	.84
.37	21.18	10.18	13.30	4.83	12.29	3.54	.83
.39	20.50	10.07	14.28	4.94	11.65	3.36	.86
.42	20.78	10.25	15.15	4.76	11.61	3.44	.88
.44	19.82	10.29	16.10	4.73	10.84	3.29	.95
.47	18.93	10.11	17.08	4.91	10.11	3.06	1.00
.50	20.26	10.23	18.24	4.79	10.60	3.21	.97
.53	20.62	10.36	19.40	4.67	10.53	3.26	.98
.57	20.87	10.16	20.60	4.87	10.38	3.13	.98
.60	21.16	10.23	21.80	4.80	10.25	3.13	1.00
.63	22.99	10.24	22.93	4.80	10.90	3.27	.94

TEST NAME: S58.34
CONSOLIDATED-UNDRAINED TEST, NORMALLY CONSOLIDATED BEAUMONT CLAY

HEIGHT PRIOR TO SHEAR   2.67 in
DIAMETER PRIOR TO SHEAR   1.28 in

AREA CORRECTION FACTOR   1.00
EFFECTIVE CONSOLIDATION PRESSURE   34.00 psi

DEF. (in)	FORCE (lb)	P.PRES. (psi)	AXIAL STRAIN %	MINOR PRIN STRESS psi	DEVIATORIC STRESS psi	STRESS RATIO	A COEF
.00	.00	.00	.00	34.00	.00	1.00	.00
.00	3.74	.90	.02	33.10	2.91	1.09	.31
.00	7.25	2.01	.04	31.99	5.65	1.18	.36
.00	10.07	3.03	.06	30.97	7.84	1.25	.39
.00	13.45	4.76	.10	29.24	10.46	1.36	.46
.00	15.41	5.96	.15	28.04	11.97	1.43	.50
.01	18.38	8.39	.26	25.61	14.25	1.56	.59
.01	20.38	10.42	.40	23.58	15.76	1.67	.66
.02	22.34	12.31	.60	21.69	17.22	1.79	.71
.02	23.82	13.71	.80	20.29	18.30	1.90	.75
.03	25.11	15.03	1.05	18.97	19.21	2.01	.78
.03	26.21	16.12	1.30	17.88	19.97	2.12	.81
.04	27.04	16.80	1.51	17.20	20.53	2.19	.82
.05	27.85	17.41	1.71	16.59	21.08	2.27	.83
.05	28.38	17.90	1.91	16.10	21.42	2.33	.84
.06	29.15	18.42	2.16	15.58	21.93	2.41	.84
.06	29.56	18.79	2.36	15.21	22.19	2.46	.85
.07	29.92	19.17	2.55	14.83	22.42	2.51	.86
.07	30.37	19.49	2.76	14.51	22.71	2.56	.86
.08	30.73	19.84	3.00	14.16	22.92	2.62	.87
.09	31.54	20.48	3.48	13.52	23.40	2.73	.88
.11	32.22	20.87	3.97	13.13	23.78	2.81	.88
.12	32.85	21.07	4.49	12.93	24.11	2.86	.87
.14	33.22	21.14	5.09	12.86	24.22	2.88	.87
.15	33.83	21.14	5.73	12.86	24.49	2.90	.86
.17	34.23	21.15	6.22	12.85	24.64	2.92	.86
.18	34.62	21.25	6.85	12.75	24.74	2.94	.86
.20	34.84	21.34	7.34	12.66	24.76	2.96	.86
.21	35.14	21.35	7.83	12.65	24.83	2.96	.86
.22	35.31	21.18	8.35	12.82	24.80	2.93	.85
.24	35.53	20.98	8.84	13.02	24.81	2.91	.85
.26	35.95	20.82	9.74	13.19	24.84	2.88	.84
.28	35.85	21.01	10.34	13.00	24.59	2.89	.85
.31	36.34	21.01	11.46	13.00	24.59	2.89	.85
.34	36.67	20.80	12.70	13.21	24.44	2.85	.85
.37	36.61	20.94	13.93	13.07	24.02	2.84	.87
.41	37.03	20.72	15.17	13.30	23.92	2.80	.87
.44	37.60	20.28	16.40	13.74	23.91	2.74	.85
.47	37.59	20.48	17.64	13.54	23.52	2.74	.87
.50	37.99	20.61	18.80	13.41	23.41	2.75	.88

TEST NAME: S59.05
CONSOLIDATED-UNDRAINED TEST, NORMALLY CONSOLIDATED BEAUMONT CLAY

HEIGHT PRIOR TO SHEAR   2.99 in
DIAMETER PRIOR TO SHEAR   1.33 in

AREA CORRECTION FACTOR   1.40
EFFECTIVE CONSOLIDATION PRESSURE   5.00 psi

DEF. (in)	FORCE (lb)	P.PRES. (psi)	AXIAL STRAIN %	MINOR PRIN STRESS psi	DEVIATORIC STRESS psi	STRESS RATIO	A COEF
.00	.00	.00	.00	5.00	.00	1.00	.00
.00	1.82	.32	.02	4.68	1.30	1.28	.24
.00	3.29	.57	.06	4.43	2.36	1.53	.24
.00	3.95	.78	.12	4.22	2.82	1.67	.28
.01	4.52	1.13	.21	3.87	3.21	1.83	.35
.01	5.13	1.61	.39	3.39	3.62	2.07	.45
.02	5.54	1.93	.57	3.07	3.87	2.26	.50
.02	5.96	2.26	.80	2.74	4.13	2.50	.55
.03	6.29	2.45	1.02	2.55	4.31	2.69	.57
.04	6.59	2.62	1.25	2.38	4.48	2.89	.59
.04	6.78	2.77	1.47	2.23	4.57	3.05	.61
.05	6.83	2.83	1.65	2.17	4.57	3.10	.62
.06	7.03	2.95	2.00	2.05	4.63	3.26	.64
.07	7.25	3.10	2.42	1.90	4.75	3.50	.65
.08	7.25	3.18	2.75	1.82	4.72	3.59	.67
.10	7.30	3.23	3.29	1.77	4.70	3.66	.69
.13	7.43	3.35	4.18	1.65	4.71	3.85	.71
.14	7.55	3.35	4.58	1.65	4.75	3.87	.70
.15	7.74	3.30	4.98	1.70	4.84	3.85	.68
.17	7.83	3.40	5.65	1.60	4.84	4.03	.70
.18	7.92	3.44	6.09	1.56	4.85	4.10	.71
.19	7.93	3.43	6.35	1.57	4.84	4.08	.71
.20	8.01	3.39	6.69	1.61	4.86	4.01	.70
.21	8.07	3.35	7.02	1.65	4.86	3.95	.69
.22	8.04	3.33	7.36	1.68	4.81	3.87	.69
.23	8.15	3.29	7.83	1.71	4.83	3.82	.68
.25	8.27	3.27	8.33	1.73	4.86	3.80	.67
.26	8.30	3.30	8.80	1.71	4.83	3.83	.68
.29	8.36	3.27	9.83	1.74	4.76	3.74	.69
.33	8.51	3.24	11.14	1.77	4.72	3.66	.69
.36	8.58	3.26	12.17	1.75	4.65	3.66	.70
.40	8.66	3.28	13.34	1.73	4.58	3.64	.72
.43	8.80	3.21	14.28	1.80	4.55	3.52	.70
.46	8.91	3.26	15.45	1.76	4.49	3.56	.73
.51	8.98	3.25	16.99	1.77	4.37	3.46	.74
.52	9.13	3.21	17.56	1.81	4.38	3.43	.73
.55	9.25	3.29	18.39	1.73	4.35	3.52	.76
.59	9.26	3.23	19.80	1.79	4.20	3.35	.77
.63	9.34	3.19	20.97	1.84	4.11	3.23	.78
.65	9.46	3.20	21.81	1.83	4.08	3.23	.78

TEST NAME: W60.07
CONSOLIDATED-UNDRAINED TEST, WETTED & DRIED BEAUMONT CLAY

HEIGHT PRIOR TO SHEAR   2.94 in
DIAMETER PRIOR TO SHEAR   1.40 in

AREA CORRECTION FACTOR   1.40
EFFECTIVE CONSOLIDATION PRESSURE   7.00 psi

DEF. (in)	FORCE (lb)	P.PRES. (psi)	AXIAL STRAIN %	MINOR PRIN STRESS psi	DEVIATORIC STRESS psi	STRESS RATIO	A COEF
.00	.00	.00	.00	7.00	.00	1.00	.00
.00	2.74	.55	.04	6.45	1.77	1.27	.31
.00	4.26	1.00	.08	6.00	2.74	1.46	.37
.00	4.91	1.38	.13	5.62	3.15	1.56	.44
.01	5.43	1.66	.18	5.34	3.48	1.65	.48
.01	6.07	2.04	.26	4.96	3.87	1.78	.53
.01	6.31	2.19	.31	4.81	4.02	1.84	.55
.01	6.99	2.85	.49	4.15	4.42	2.07	.64
.02	7.32	3.09	.59	3.91	4.62	2.18	.67
.02	7.54	3.33	.68	3.67	4.74	2.29	.70
.03	8.11	3.85	.96	3.15	5.05	2.60	.76
.03	8.23	3.92	1.05	3.08	5.10	2.66	.77
.04	8.45	4.20	1.24	2.80	5.20	2.86	.81
.04	8.61	4.54	1.38	2.46	5.28	3.14	.86
.05	8.80	4.82	1.68	2.18	5.33	3.44	.90
.06	8.92	5.11	1.94	1.89	5.35	3.83	.96
.06	8.93	5.13	2.08	1.87	5.34	3.85	.96
.06	8.96	5.17	2.21	1.83	5.34	3.92	.97
.08	9.20	5.22	2.68	1.78	5.45	4.06	.96
.08	9.32	5.28	2.88	1.72	5.50	4.20	.96
.09	9.40	5.21	3.11	1.79	5.53	4.08	.94
.11	9.40	5.17	3.64	1.83	5.47	3.98	.94
.12	9.53	5.27	4.05	1.73	5.51	4.19	.96
.13	9.67	5.15	4.42	1.85	5.55	4.00	.93
.16	10.60	5.51	5.27	1.50	6.02	5.03	.91
.17	10.70	5.40	5.64	1.60	6.04	4.77	.89
.17	10.91	5.40	5.92	1.60	6.13	4.83	.88
.19	10.53	5.39	6.29	1.62	5.87	4.63	.92
.21	10.71	5.18	7.00	1.83	5.89	4.22	.88
.23	10.86	5.32	7.96	1.68	5.87	4.49	.91
.25	11.07	5.38	8.50	1.62	5.92	4.65	.91
.28	11.49	5.17	9.45	1.84	6.05	4.29	.85
.29	11.56	5.10	9.86	1.90	6.04	4.17	.84
.33	11.94	5.29	11.08	1.72	6.10	4.54	.87
.34	12.20	5.19	11.63	1.82	6.17	4.40	.84
.37	12.51	5.22	12.58	1.79	6.21	4.47	.84
.41	12.84	5.21	13.91	1.80	6.21	4.45	.84
.44	13.26	5.14	14.99	1.88	6.28	4.34	.82
.47	13.66	5.11	16.12	1.91	6.32	4.31	.81
.56	14.59	5.10	18.97	1.92	6.36	4.31	.80

TEST NAME: W61.20
CONSOLIDATED-UNDRAINED TEST, WETTED & DRIED BEAUMONT CLAY

HEIGHT PRIOR TO SHEAR   2.84 in
DIAMETER PRIOR TO SHEAR   1.38 in

AREA CORRECTION FACTOR   1.00
EFFECTIVE CONSOLIDATION PRESSURE   20.00 psi

DEF. (in)	FORCE (lb)	P.PRES. (psi)	AXIAL STRAIN %	MINOR PRIN STRESS psi	DEVIATORIC STRESS psi	STRESS RATIO	A COEF
.00	.00	.00	.00	20.00	.00	1.00	.00
.00	3.92	1.02	.02	18.98	2.61	1.14	.39
.00	8.08	2.16	.06	17.84	5.38	1.30	.40
.00	10.29	3.02	.10	16.98	6.85	1.40	.44
.01	12.73	4.30	.20	15.70	8.45	1.54	.51
.01	14.10	5.26	.29	14.74	9.34	1.63	.56
.01	15.13	6.05	.39	13.95	10.01	1.72	.60
.01	15.97	6.68	.47	13.32	10.55	1.79	.63
.02	16.68	7.23	.56	12.77	10.99	1.86	.66
.02	17.33	7.68	.66	12.32	11.40	1.93	.67
.02	17.90	8.09	.75	11.91	11.76	1.99	.69
.03	18.87	8.81	.94	11.19	12.35	2.10	.71
.03	19.28	9.13	1.03	10.88	12.60	2.16	.72
.03	19.86	9.53	1.17	10.47	12.94	2.24	.74
.04	20.66	10.13	1.40	9.87	13.40	2.36	.76
.04	20.95	10.36	1.50	9.64	13.57	2.41	.76
.05	21.59	10.85	1.74	9.15	13.92	2.52	.78
.05	21.99	11.07	1.88	8.93	14.14	2.58	.78
.06	22.26	11.25	2.03	8.75	14.28	2.63	.79
.06	22.72	11.49	2.24	8.51	14.55	2.71	.79
.08	23.54	11.88	2.73	8.12	15.00	2.85	.79
.08	23.86	11.99	2.94	8.01	15.17	2.89	.79
.09	24.00	12.15	3.30	7.85	15.19	2.94	.80
.10	24.62	12.31	3.66	7.69	15.53	3.02	.79
.12	25.35	12.34	4.19	7.66	15.90	3.08	.78
.14	25.96	12.46	4.89	7.54	16.15	3.14	.77
.15	26.39	12.51	5.32	7.49	16.34	3.18	.77
.17	27.10	12.28	6.02	7.72	16.65	3.16	.74
.19	27.87	12.20	6.69	7.80	17.00	3.18	.72
.21	28.56	12.12	7.54	7.88	17.25	3.19	.70
.24	29.17	12.04	8.35	7.96	17.45	3.19	.69
.26	29.91	11.94	9.19	8.06	17.72	3.20	.67
.30	30.54	11.80	10.63	8.21	17.78	3.17	.66
.33	31.28	11.71	11.76	8.30	17.97	3.17	.65
.35	32.08	11.24	12.46	8.77	18.27	3.08	.62
.39	32.48	10.94	13.73	9.07	18.21	3.01	.60
.41	33.09	10.74	14.47	9.27	18.38	2.98	.58
.44	33.51	10.69	15.56	9.32	18.36	2.97	.58
.48	33.89	10.64	17.01	9.38	18.22	2.94	.58
.53	34.34	10.70	18.80	9.32	18.02	2.93	.59

TEST NAME: W62.03
CONSOLIDATED-UNDRAINED TEST, WETTED & DRIED BEAUMONT CLAY

HEIGHT PRIOR TO SHEAR   2.85 in
DIAMETER PRIOR TO SHEAR   1.43 in

AREA CORRECTION FACTOR   1.40
EFFECTIVE CONSOLIDATION PRESSURE   3.00 psi

DEF. (in)	FORCE (lb)	P.PRES. (psi)	AXIAL STRAIN %	MINOR PRIN STRESS psi	DEVIATORIC STRESS psi	STRESS RATIO	A COEF
.00	.00	.00	.00	3.00	.00	1.00	.00
.02	3.26	.53	.59	2.47	1.93	1.78	.27
.02	3.74	.84	.69	2.16	2.21	2.02	.38
.02	4.09	1.06	.78	1.94	2.41	2.24	.44
.03	4.43	1.34	.93	1.66	2.59	2.56	.52
.03	4.69	1.59	1.11	1.41	2.72	2.93	.58
.04	4.84	1.73	1.25	1.27	2.79	3.19	.62
.04	4.99	1.90	1.45	1.10	2.85	3.59	.67
.05	5.16	2.05	1.68	.95	2.91	4.05	.70
.05	5.17	2.09	1.87	.91	2.88	4.16	.72
.06	5.26	2.20	2.10	.80	2.91	4.64	.76
.07	5.34	2.26	2.34	.74	2.94	4.96	.77
.07	5.38	2.33	2.53	.67	2.95	5.39	.79
.08	5.41	2.38	2.76	.62	2.95	5.79	.81
.09	5.53	2.49	3.02	.51	3.01	6.88	.83
.09	5.53	2.51	3.24	.49	2.99	7.08	.84
.10	5.57	2.52	3.38	.48	3.01	7.25	.84
.10	5.60	2.57	3.47	.43	3.02	7.99	.85
.10	5.62	2.56	3.58	.44	3.03	7.84	.84
.10	5.68	2.53	3.65	.47	3.06	7.47	.83
.11	5.84	2.45	3.82	.55	3.14	6.68	.78
.12	5.93	2.34	4.18	.66	3.17	5.78	.74
.13	5.99	2.24	4.49	.76	3.18	5.17	.70
.14	6.10	2.20	4.84	.80	3.22	5.01	.68
.15	6.24	2.23	5.26	.77	3.27	5.23	.68
.16	6.27	2.22	5.61	.78	3.26	5.17	.68
.18	6.37	2.22	6.42	.78	3.26	5.19	.68
.20	6.60	2.16	7.02	.84	3.35	4.96	.64
.22	6.83	2.14	7.82	.87	3.42	4.95	.63
.25	7.03	2.11	8.84	.90	3.45	4.85	.61
.28	7.12	2.20	9.65	.81	3.43	5.25	.64
.31	7.41	2.05	10.70	.96	3.51	4.66	.58
.33	7.86	1.94	11.72	1.07	3.65	4.41	.53
.38	7.86	1.99	13.26	1.02	3.52	4.45	.56
.42	8.40	1.87	14.63	1.14	3.67	4.21	.51
.44	8.57	1.86	15.33	1.15	3.69	4.20	.50
.46	8.63	1.89	16.04	1.13	3.66	4.25	.52
.51	8.89	1.78	17.75	1.24	3.62	3.92	.49
.55	9.37	1.82	19.16	1.20	3.71	4.08	.49
.57	9.62	1.83	20.00	1.20	3.73	4.12	.49

TEST NAME: W63.12
CONSOLIDATED-UNDRAINED TEST, WETTED & DRIED BEAUMONT CLAY

HEIGHT PRIOR TO SHEAR   2.78 in
DIAMETER PRIOR TO SHEAR   1.40 in

AREA CORRECTION FACTOR   1.40
EFFECTIVE CONSOLIDATION PRESSURE   12.00 psi

DEF. (in)	FORCE (1b)	P.PRES. (psi)	AXIAL STRAIN %	MINOR PRIN STRESS psi	DEVIATORIC STRESS psi	STRESS RATIO	A COEF
.00	.00	.00	.00	12.00	.00	1.00	.00
.00	2.88	.41	.01	11.59	1.87	1.16	.22
.00	4.88	.83	.03	11.17	3.16	1.28	.26
.00	6.53	1.21	.05	10.79	4.23	1.39	.29
.00	7.32	1.50	.07	10.50	4.74	1.45	.32
.00	8.39	2.07	.13	9.93	5.42	1.55	.38
.01	9.33	2.66	.20	9.34	6.02	1.64	.44
.01	10.52	3.65	.34	8.35	6.76	1.81	.54
.01	11.39	4.27	.47	7.73	7.28	1.94	.59
.02	12.10	4.79	.63	7.21	7.71	2.07	.62
.02	12.71	5.26	.76	6.74	8.06	2.20	.65
.03	13.18	5.65	.91	6.35	8.33	2.31	.68
.03	13.52	6.03	1.09	5.97	8.50	2.42	.71
.04	13.96	6.49	1.33	5.51	8.72	2.58	.74
.05	14.35	6.87	1.62	5.13	8.89	2.73	.77
.06	14.70	7.27	2.01	4.73	9.01	2.90	.81
.07	15.01	7.59	2.38	4.41	9.15	3.07	.83
.08	15.29	7.63	2.74	4.37	9.27	3.12	.82
.09	15.39	7.70	3.09	4.30	9.28	3.16	.83
.09	15.69	7.80	3.39	4.20	9.41	3.24	.83
.11	16.06	7.81	3.88	4.19	9.56	3.28	.82
.12	16.39	7.82	4.35	4.18	9.69	3.32	.81
.14	16.71	7.94	4.96	4.06	9.78	3.41	.81
.15	16.97	8.05	5.54	3.95	9.84	3.49	.82
.17	17.44	8.00	6.26	4.00	9.99	3.50	.80
.20	18.23	7.93	7.12	4.07	10.30	3.53	.77
.21	18.50	7.87	7.59	4.13	10.37	3.51	.76
.24	19.00	7.80	8.78	4.21	10.44	3.48	.75
.27	19.45	7.77	9.64	4.23	10.52	3.49	.74
.29	19.88	7.60	10.32	4.40	10.63	3.42	.72
.31	20.30	7.39	11.19	4.61	10.69	3.32	.69
.35	21.06	7.35	12.59	4.66	10.81	3.32	.68
.40	22.05	7.18	14.39	4.83	10.95	3.27	.66
.43	22.83	7.35	15.32	4.67	11.14	3.39	.66
.46	22.59	7.16	16.47	4.86	10.77	3.22	.66
.50	23.15	6.88	17.81	5.14	10.74	3.09	.64
.53	23.73	6.81	18.92	5.21	10.76	3.07	.63
.55	24.18	6.85	19.68	5.18	10.80	3.09	.63
.58	24.81	6.61	21.01	5.42	10.77	2.99	.61
.61	25.33	6.55	22.29	5.48	10.74	2.96	.61

TEST NAME: W64.30
CONSOLIDATED-UNDRAINED TEST, WETTED & DRIED BEAUMONT CLAY

HEIGHT PRIOR TO SHEAR   2.65 in
DIAMETER PRIOR TO SHEAR   1.39 in

AREA CORRECTION FACTOR   1.00
EFFECTIVE CONSOLIDATION PRESSURE   30.00 psi

DEF. (in)	FORCE (lb)	P.PRES. (psi)	AXIAL STRAIN %	MINOR PRIN STRESS psi	DEVIATORIC STRESS psi	STRESS RATIO	A COEF
.00	.00	.00	.00	30.00	.00	1.00	.00
.00	1.17	.18	.01	29.82	.78	1.03	.23
.00	4.00	.88	.03	29.12	2.65	1.09	.33
.00	6.05	1.38	.04	28.62	4.01	1.14	.35
.00	8.89	2.18	.06	27.82	5.88	1.21	.37
.00	12.97	3.51	.10	26.49	8.57	1.32	.41
.00	14.20	4.05	.13	25.95	9.38	1.36	.43
.00	15.98	4.93	.17	25.07	10.55	1.42	.47
.01	17.42	6.22	.24	23.78	11.48	1.48	.54
.01	20.33	8.80	.44	21.20	13.35	1.63	.66
.02	22.09	10.27	.59	19.73	14.47	1.73	.71
.02	23.99	11.77	.79	18.23	15.66	1.86	.75
.03	25.55	12.99	1.00	17.01	16.63	1.98	.78
.03	26.85	13.92	1.20	16.08	17.42	2.08	.80
.04	28.30	14.95	1.46	15.05	18.28	2.21	.82
.05	29.43	15.78	1.71	14.22	18.94	2.33	.83
.05	30.45	16.41	1.95	13.59	19.52	2.44	.84
.06	31.32	16.88	2.20	13.12	20.02	2.53	.84
.07	32.63	17.74	2.65	12.26	20.77	2.69	.85
.09	34.38	18.98	3.45	11.02	21.70	2.97	.87
.11	35.65	19.32	4.08	10.68	22.35	3.09	.86
.13	36.94	19.48	4.79	10.52	22.98	3.18	.85
.14	38.00	19.49	5.47	10.51	23.47	3.23	.83
.16	38.84	19.46	6.19	10.54	23.80	3.26	.82
.18	39.48	19.50	6.79	10.50	24.03	3.29	.81
.20	40.42	19.23	7.58	10.77	24.38	3.26	.79
.22	41.44	18.71	8.34	11.29	24.78	3.19	.75
.24	42.21	18.43	9.06	11.57	25.04	3.16	.74
.26	42.81	18.26	9.85	11.75	25.16	3.14	.73
.28	43.35	18.28	10.64	11.73	25.24	3.15	.72
.32	44.75	17.58	12.11	12.43	25.60	3.06	.69
.35	45.72	17.25	13.25	12.76	25.80	3.02	.67
.38	46.51	17.18	14.49	12.83	25.85	3.01	.66
.41	47.50	16.73	15.58	13.28	26.05	2.96	.64
.44	48.36	16.38	16.49	13.64	26.22	2.92	.62
.46	48.73	16.48	17.36	13.54	26.13	2.93	.63
.49	49.96	16.03	18.60	13.99	26.37	2.88	.61
.53	51.39	15.52	20.11	14.51	26.60	2.83	.58
.56	51.94	15.97	21.32	14.06	26.45	2.88	.60
.61	54.47	14.91	23.13	15.12	27.08	2.79	.55

TEST NAME: W65.02
CONSOLIDATED-UNDRAINED TEST, WETTED & DRIED BEAUMONT CLAY

HEIGHT PRIOR TO SHEAR   3.20 in
DIAMETER PRIOR TO SHEAR   1.42 in

AREA CORRECTION FACTOR   1.40
EFFECTIVE CONSOLIDATION PRESSURE   2.00 psi

DEF. (in)	FORCE (lb)	P.PRES. (psi)	AXIAL STRAIN %	MINOR PRIN STRESS psi	DEVIATORIC STRESS psi	STRESS RATIO	A COEF
.00	.00	.00	.00	2.00	.00	1.00	.00
.00	.81	.05	.01	1.95	.51	1.26	.09
.00	1.00	.16	.04	1.84	.62	1.34	.25
.00	2.00	.27	.10	1.73	1.24	1.72	.22
.00	2.21	.45	.15	1.55	1.37	1.88	.33
.01	2.39	.56	.24	1.44	1.47	2.02	.38
.01	2.48	.62	.30	1.38	1.52	2.10	.41
.01	2.56	.67	.36	1.33	1.55	2.17	.43
.01	2.72	.78	.44	1.22	1.64	2.35	.48
.02	2.82	.83	.53	1.17	1.69	2.45	.49
.02	2.91	.95	.65	1.05	1.73	2.64	.55
.03	3.00	.98	.81	1.02	1.76	2.73	.56
.03	3.03	1.08	.93	.92	1.75	2.90	.61
.03	3.07	1.13	1.03	.87	1.77	3.04	.64
.04	3.11	1.19	1.16	.81	1.77	3.18	.67
.04	3.19	1.22	1.28	.78	1.80	3.32	.68
.05	3.25	1.32	1.54	.68	1.80	3.63	.73
.06	3.36	1.41	1.86	.59	1.81	4.08	.78
.07	3.50	1.40	2.16	.60	1.87	4.13	.75
.08	3.53	1.36	2.63	.64	1.86	3.89	.73
.10	3.57	1.33	3.22	.67	1.86	3.78	.72
.12	3.71	1.31	3.84	.69	1.91	3.76	.68
.14	3.91	1.49	4.47	.51	2.00	4.90	.74
.16	4.01	1.45	5.09	.55	2.02	4.70	.72
.19	4.09	1.46	5.81	.54	2.03	4.75	.72
.21	4.21	1.33	6.53	.67	2.06	4.07	.65
.23	4.42	1.38	7.13	.63	2.15	4.43	.64
.25	4.44	1.32	7.75	.68	2.13	4.13	.62
.27	4.56	1.35	8.34	.65	2.16	4.32	.63
.29	4.56	1.31	8.94	.70	2.13	4.04	.61
.31	4.64	1.30	9.69	.70	2.13	4.02	.61
.34	4.79	1.45	10.56	.56	2.16	4.87	.67
.37	4.94	1.35	11.41	.65	2.19	4.34	.62
.39	5.00	1.25	12.22	.76	2.17	3.85	.58
.42	5.22	1.43	13.22	.58	2.22	4.80	.64
.48	5.51	1.23	15.12	.79	2.24	3.85	.55
.53	5.84	1.31	16.59	.71	2.31	4.27	.57
.57	5.95	1.18	17.81	.84	2.27	3.70	.52
.62	6.10	1.31	19.22	.72	2.25	4.13	.58
.71	6.74	1.23	22.28	.80	2.31	3.89	.53

TEST NAME: WL63.02
CONSOLIDATED-UNDRAINED TEST ON WETTED & DRIED BEAUMONT SPECIMEN
WHICH WAS SUBJECTED TO WETTING AND DRYING WHILE UNDER A VERTICAL
PRESSURE OF 2 PSI (RESULTS OF TEST NOT DISCUSSED IN MAIN CHAPTERS)

HEIGHT PRIOR TO SHEAR   2.62 in
DIAMETER PRIOR TO SHEAR   1.52 in

AREA CORRECTION FACTOR   1.40
EFFECTIVE CONSOLIDATION PRESSURE   2.00 psi

DEF. (in)	FORCE (lb)	P.PRES. (psi)	AXIAL STRAIN %	MINOR PRIN STRESS psi	DEVIATORIC STRESS psi	STRESS RATIO	A COEF
.00	.00	.00	.00	2.00	.00	1.00	.00
.00	1.78	.20	.04	1.80	.98	1.55	.20
.00	5.10	.48	.09	1.52	2.81	2.85	.17
.00	6.71	.72	.19	1.28	3.68	3.88	.20
.01	7.51	.92	.33	1.08	4.10	4.80	.23
.01	7.97	.93	.49	1.07	4.32	5.05	.22
.02	8.59	1.00	.90	1.00	4.59	5.60	.22
.03	8.69	.98	1.11	1.02	4.60	5.52	.21
.03	8.76	1.03	1.32	.97	4.60	5.75	.22
.04	8.85	1.01	1.53	.99	4.61	5.66	.22
.05	8.90	1.03	1.73	.97	4.59	5.74	.22
.05	8.97	1.00	1.94	1.00	4.59	5.60	.22
.06	8.99	.97	2.15	1.03	4.58	5.46	.21
.06	9.05	1.00	2.41	1.00	4.59	5.60	.22
.07	9.21	.99	2.61	1.01	4.66	5.62	.21
.08	9.31	1.00	2.91	1.00	4.68	5.69	.21
.09	9.53	.82	3.61	1.18	4.74	5.02	.17
.10	9.64	.84	4.01	1.16	4.76	5.10	.18
.12	9.74	.82	4.43	1.18	4.77	5.05	.17
.13	9.99	.77	4.85	1.23	4.86	4.96	.16
.14	10.15	.81	5.23	1.19	4.91	5.12	.16
.15	10.36	.80	5.65	1.20	4.98	5.15	.16
.16	10.52	.79	6.04	1.22	5.02	5.13	.16
.17	8.36	.82	6.61	1.18	3.88	4.29	.21
.20	8.92	.63	7.83	1.37	4.06	3.96	.16
.23	9.19	.67	8.82	1.33	4.10	4.08	.16
.26	9.46	.65	9.82	1.35	4.14	4.06	.16
.29	8.94	.49	11.04	1.52	3.79	3.50	.13
.31	9.37	.48	12.03	1.53	3.90	3.56	.12
.34	9.23	.48	13.03	1.53	3.75	3.46	.13
.37	10.60	.43	14.25	1.58	4.25	3.69	.10
.41	10.90	.27	15.47	1.74	4.26	3.45	.06
.43	11.05	.34	16.50	1.67	4.22	3.52	.08
.46	11.29	.30	17.49	1.72	4.22	3.46	.07
.49	11.60	.14	18.72	1.88	4.22	3.25	.03
.54	11.73	.24	20.47	1.78	4.09	3.29	.06
.57	12.34	.18	21.70	1.85	4.19	3.26	.04
.62	12.50	.12	23.68	1.91	4.03	3.11	.03

APPENDIX D.   CORRECTIONS FOR TRIAXIAL TESTS DATA

INTRODUCTION

Stresses in the triaxial specimens were corrected for the effects of filter paper and rubber membrane as well as for the effect of changing area due to axial and lateral deformation of the specimen during shear. Careful measurements were made to obtain appropriate area corrections that account for the effect of specimen deformation at large strains. These corrections are presented and discussed in this Appendix.

FILTER AND MEMBRANE CORRECTIONS

Filter and membrane corrections were computed using the recommendations of Duncan and Seed (1965). Filter paper and membrane corrections were applied to all of the triaxial tests.

Filter Correction

The filter paper correction consists of a correction to the axial stress calculated according to the following equation:

$$\Delta\sigma_{afp} = k_{fp} \frac{P}{A_s}$$

where $\Delta\sigma_{afp}$ = Correction to the axial stress for load carried by filter paper drains.

k_{fp} = Load carried by filter paper drain per unit length of perimeter covered by filter paper (0.165 lb/in; Gourlay and Wright, 1984).

P = Perimeter of specimen covered by the filter paper.

A_s = Area of specimen.

The value of k_{fp} was taken to be 0.165 lb/inch after Gourlay and Wright (1984). No corrections were made to the lateral stresses for the filter paper.

Membrane Correction

Rubber membrane corrections were applied to the axial and the lateral stresses based on the following equations:

$$\Delta\sigma_{am} = -C_{am}(\frac{2}{3})E_m \frac{4t_{om}}{D_{os}}$$

$$\Delta\sigma_{lm} = -C_{lm}(\frac{2}{3})E_m \frac{2t_{om}}{D_{os}}$$

where $\Delta\sigma_{am}$ = Correction to axial stress for membrane strength.

$\Delta\sigma_{lm}$ = Correction to lateral stress for membrane strength.

E_m = Young's Modulus of the membrane.

D_{os} = Initial diameter of the specimen (at end of consolidation).

t_{om} = Initial thickness of the membrane.

$$C_{am} = \frac{1+2\varepsilon_{at} - \sqrt{\dfrac{1-\varepsilon_v}{1-\varepsilon_{at}}}}{1-\varepsilon_v}$$

$$C_{lm} = \frac{2+\varepsilon_{at} - 2\sqrt{\dfrac{1-\varepsilon_v}{1-\varepsilon_{at}}}}{1-\varepsilon_v}$$

ε_{at} = Axial strain due to consolidation and/or undrained deformation.

ε_v = volumetric strain during consolidation.

Young's modulus for the membrane was taken to be 135 psi based on Gourlay and Wright (1984). A membrane thickness (t_{om}) of 0.0054 inches was

used for *two* membranes based on values also reported by Gourlay and Wright (1984).

Because the measured cohesion intercept has a significant influence on the computed factors of safety for shallow slides, it was decided to investigate the effect of the membrane and filter paper corrections on the effective principal stresses at failure, as well as on the measured failure envelopes for specimens subjected to wetting and drying. The corrected and uncorrected minor principal stress and peak principal stress difference are plotted versus the effective nominal consolidation pressures in Figure D.1 for the Paris clay and in Figure D.2 for the Beaumont clay. Similar plots for the data at large strains are shown in Figure D.3 for the Paris clay and in Figure D.4 for the Beaumont clay. It can be seen that filter paper and membrane corrections have almost no effect on the computed minor principal stresses and

that they result in only a small reduction in the principal stress difference for both the peak strength and at large strains. The corrections do not vary with the applied effective consolidation pressure.

The corrected and uncorrected effective stress failure envelopes (for stress path tangency) are shown for comparison, in Figure D.5 for the Paris clay and in Figure D.6 for the Beaumont clay. The corrected and uncorrected effective stress failure envelopes for large strains are shown in Figure D.7 for the Paris clay and in Figure D.8 for the Beaumont clay. The filter paper and membrane corrections can be seen to have little influence on the measured failure envelopes. The filter paper and membrane corrections result in a reduction in shear strength of approximately 1.5 percent at effective stress path tangency and 2.5 percent at large strains.
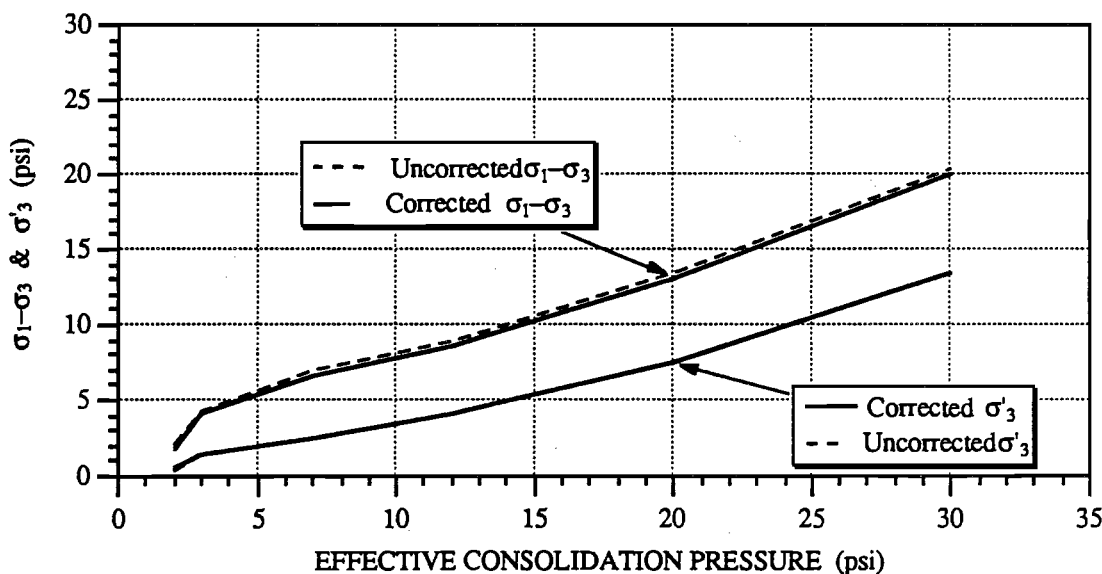
Figure D.1   Uncorrected and corrected minor principal stress and peak stress difference versus the effective consolidation pressure for Paris clay specimens
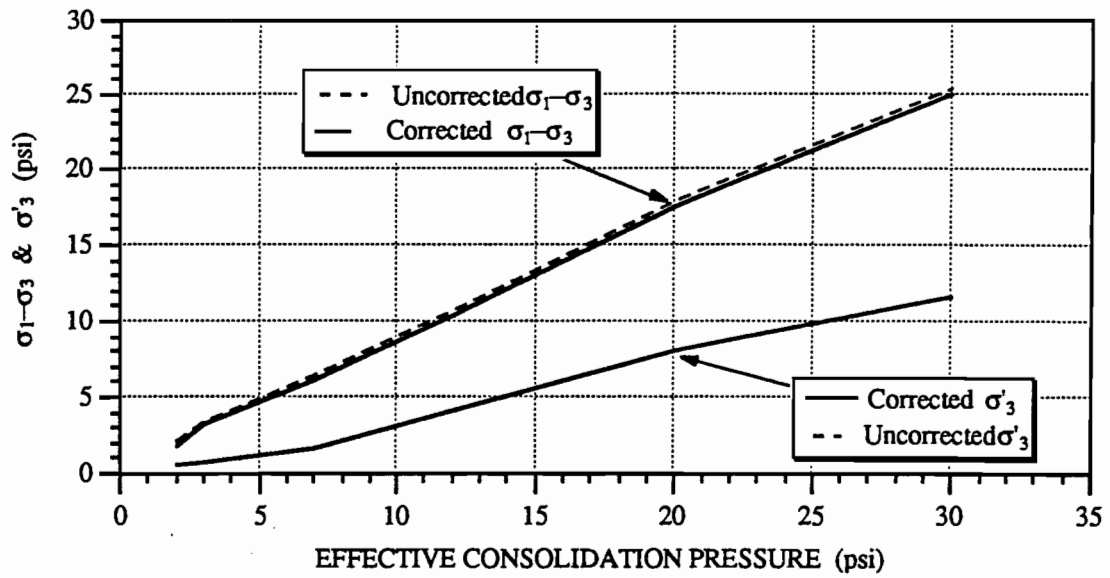
Figure D.2   Uncorrected and corrected minor principal stress and peak stress difference versus the effective consolidation pressure for Beaumont clay specimens
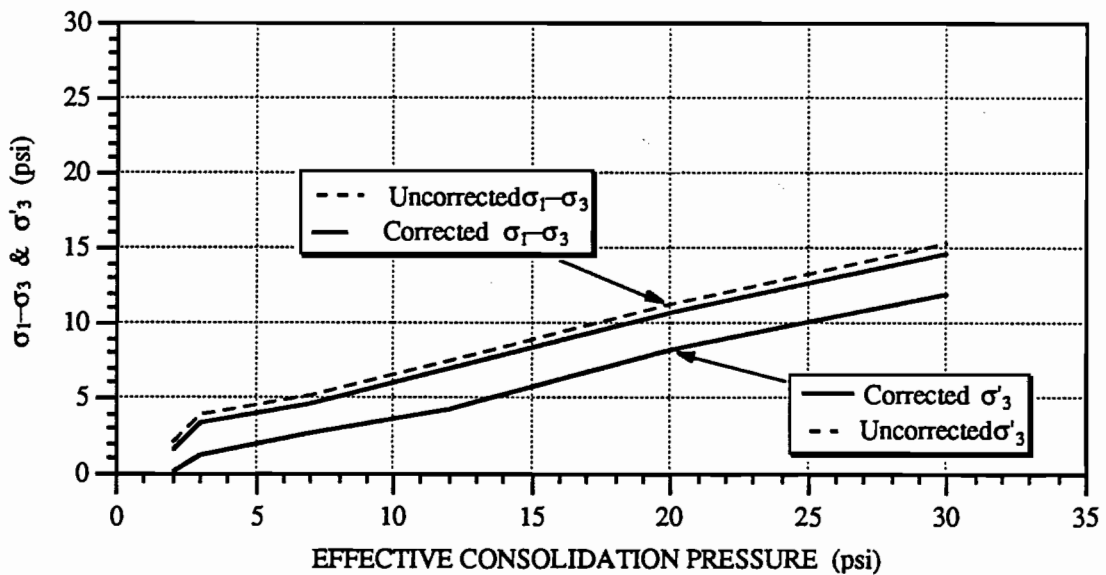
Figure D.3   Uncorrected and corrected minor principal stress and stress difference at large strains versus the effective consolidation pressure for Paris clay specimens
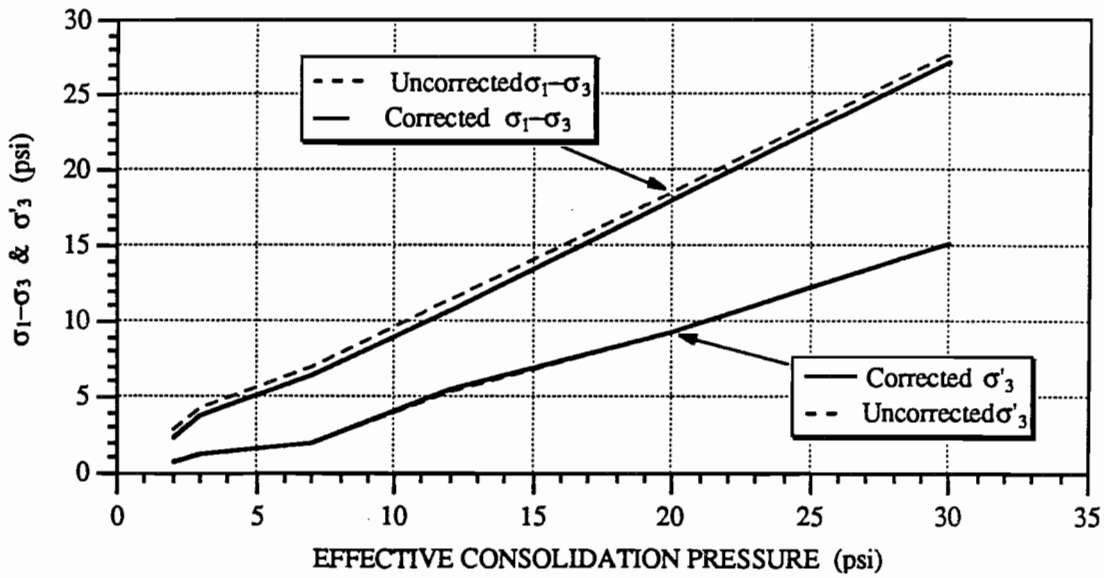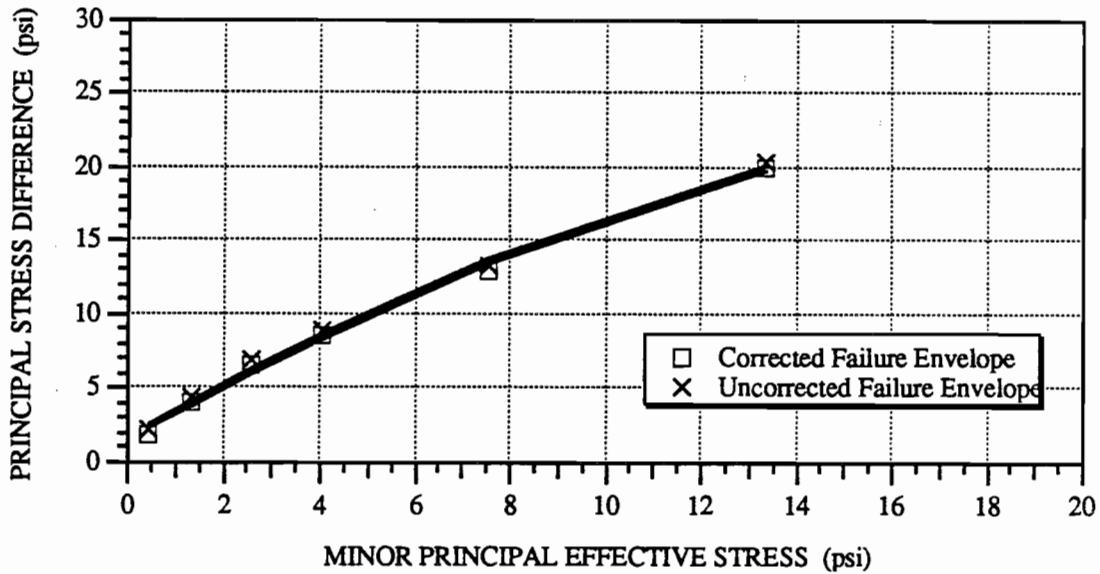
Figure D.4 Uncorrected and corrected minor principal stress and stress difference at large strains versus the effective consolidation pressure for Beaumont clay specimens

Figure D.5 Uncorrected and corrected effective stress path tangency failure envelopes for Paris clay specimens which were subjected to wetting and drying
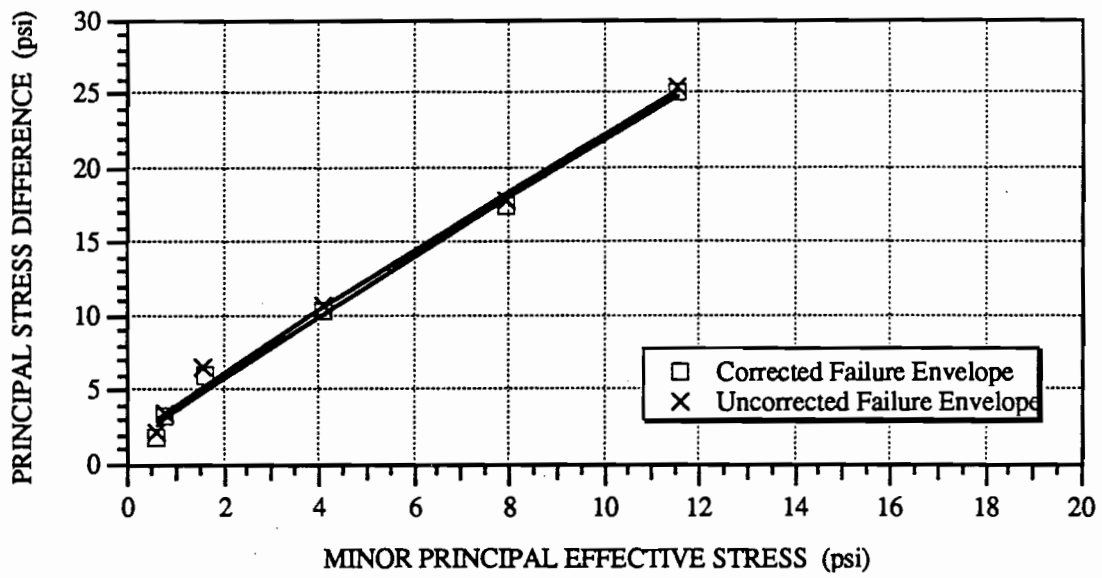
Figure D.6 Uncorrected and corrected effective stress path tangency failure envelopes for Beaumont clay specimens which were subjected to wetting and drying
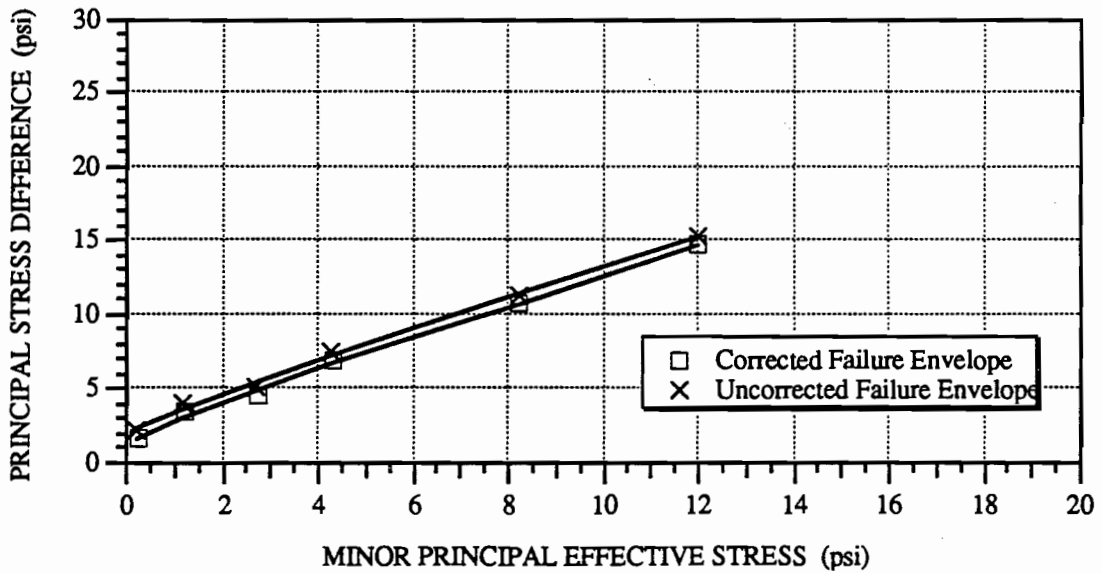
Figure D.7 Uncorrected and corrected large strains failure envelopes for Paris clay specimens which were subjected to wetting and drying
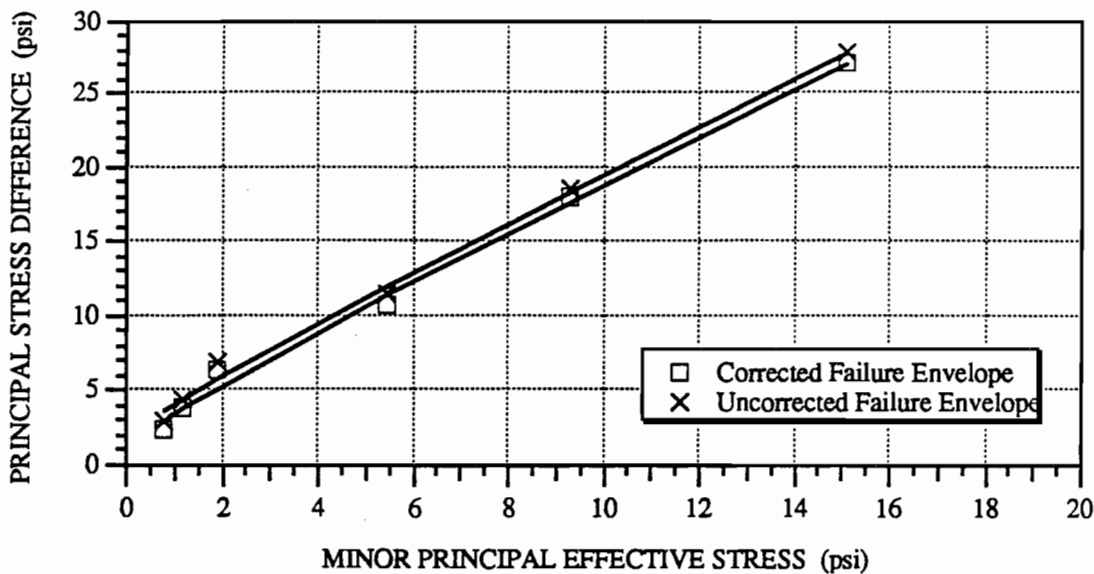
Figure D.8 Uncorrected and corrected large strains failure envelopes for Beaumont clay specimens which were subjected to wetting and drying

AREA CORRECTIONS

Two modes of failure were typically observed in triaxial specimens: bulging failure and failure with a distinct shear plane. These two failure modes are illustrated in Figure D.9. Bulging failure was observed to occur in normally consolidated and wetted and dried specimens which were consolidated to effective consolidation pressures of no more than 15 psi. Failure with a distinct shear plane was observed in all specimens which were consolidated to effective consolidation pressures greater than 15 psi. All specimens tested in their as-compacted state failed with a distinct shear plane regardless of the value of the effective consolidation pressure.

The area correction during shear was evaluated according to the following equation:

$$A = \frac{A_o}{1 - a\varepsilon} \qquad (1)$$

where
- A = Corrected area at axial strain ε.
- ε = Measured axial strain during shear.
- A_o = Initial area at end of consolidation.
- a = Area correction factor.

BULGING FAILURE   SHEAR PLANE FAILURE
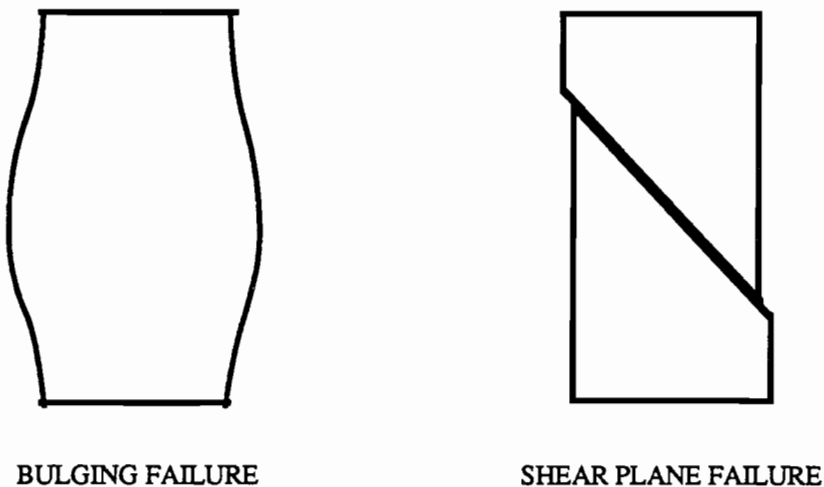
Figure D.9 Bulging failure and failure along a distinct shear plane observed in specimens tested in triaxial shear

The corrected area at the end of consolidation (A_o) was calculated by measuring the moisture content and specimen weight at the end of shear, and by measuring the height of the specimen at the end of consolidation. Based on these measurements, and assuming a 100 percent degree of saturation, the total unit weight of the soil was computed, and the volume of the specimen at the end of shear (or at the end of consolidation for an undrained test) was calculated. The corrected area at the end of consolidation was obtained by dividing the volume of the specimen over its measured height at the end of consolidation.

The area correction factor "a" depends on the pattern of deformation of the specimen. If a specimen deforms as a cylinder over its entire length, "a" is unity. If a specimen deforms as a cylinder over its middle half, "a" is two. Germaine and Ladd (1988) define the "a" factor as the length of the zone of bulging divided by the length of the specimen. In order to determine the appropriate area corrections for the tests in the current study, the factor "a" was back-calculated from actual measurements of specimen dimensions at the end of shear.

Bulging Failure

The "a" factor was back-calculated at the end of shear using the following equation:

$$a = \frac{1}{\varepsilon}(1 - \frac{A_o}{A}) \qquad (2)$$

where   A = Corrected area at the end of shear.

ε = Final axial strain.

A_o = Initial area at end of consolidation.

The area, A, was estimated by measuring the deformed shapes of specimens after shear. The deformed shapes were determined by measuring the diameters of specimens at 0.1-inch increments over the height of the specimens. The deformed shapes are plotted in terms of the radius of the specimen for ten specimens in Figures D.10, D.11, and D.12. It can be seen that the upper and lower ends of each specimen experienced negligible lateral deformation.

Cross-sectional areas were computed based on the deformation in the zone where significant deformation had taken place The zone of significant deformation, referred to herein as the "bulging zone," is shown for the ten specimens (between pairs of straight lines) in Figures D.10, D.11, and D.12.

Cross-sectional areas were computed within the bulging zone at 0.1-inch increments. The mean of the areas in the bulging zone were then calculated to determine a corrected area (A) at the end of shear. The corrected area was then used to back-calculate the area correction factor (a) in equation (2). The computed area correction factors are tabulated for each test in Table D.1. An average area correction factor of 1.4 was found by this procedure.

To evaluate the significance of averaging the areas over the bulging zone only, the areas were also averaged over the entire height of the specimen. The computed area correction factors for the entire height of the specimen are also tabulated in Table D.1. The computed area correction factors based on areas averaged over the entire length of the specimens were 1.2 compared with 1.4 when averaged over the bulging zone only. Accordingly, an area correction factor of 1.4, based on the average area over the bulging zone, was adopted for subsequent use in data reduction for the specimens that failed by bulging. The difference between the corrected areas at the peak principal stress difference, using area correction factors of 1.0 and 1.4, did not exceed 3 percent.

### Failure With a Distinct Shear Plane

To determine the areas for specimens that failed with distinct failure planes, the major and minor diameters of the elliptical failure surface and the inclination of the surface were measured at the end of shear. The elliptical surface was subsequently projected onto a horizontal plane to calculate the corrected area at large strains (La Rochelle et al, 1977). Because the cylindrical area correction is typically used for specimens that fail along a shear plane, the computed areas were compared with areas corrected according to the cylindrical area correction equation (a = 1 in equation 1). The measured data and the calculated areas are tabulated for nine specimens in Table D.2. It can be seen that the percentage difference between areas corrected using the cylindrical area correction and the actual measured areas does not exceed 8 percent. Therefore, the cylindrical area correction (a = 1) was adopted for correcting areas for specimens that failed along a distinct shear plane.
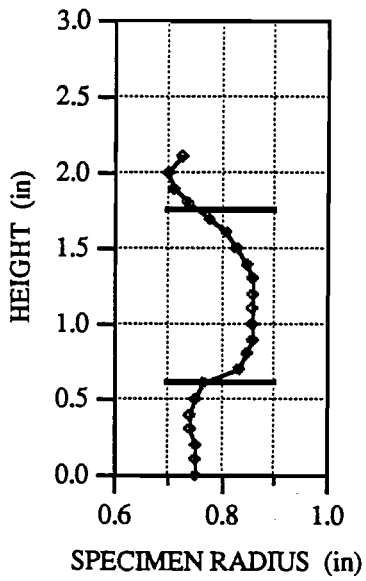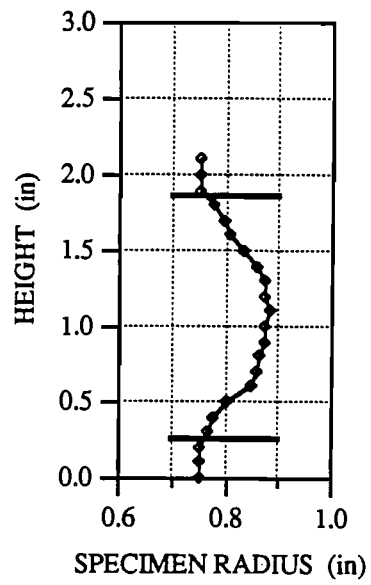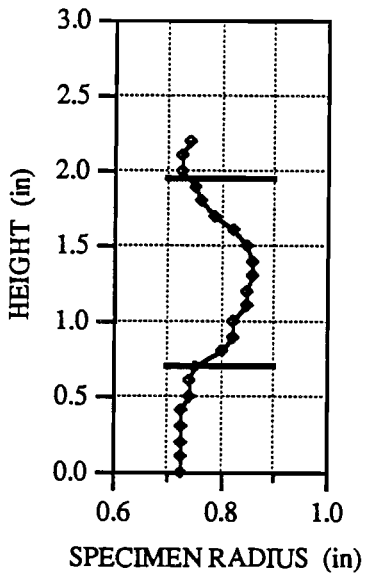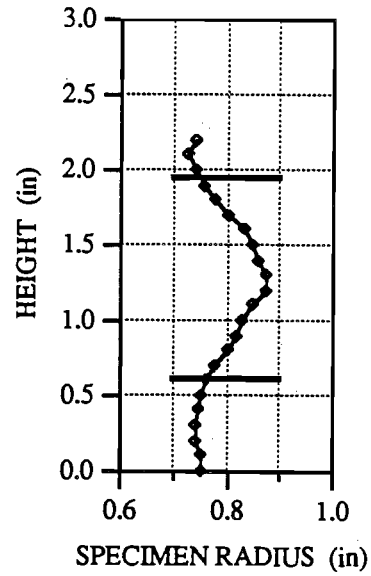
Figure D.10 Deformation patterns for triaxial specimens failing in bulging *(Bulging zones are shown between two marked horizontal lines for each specimen)*
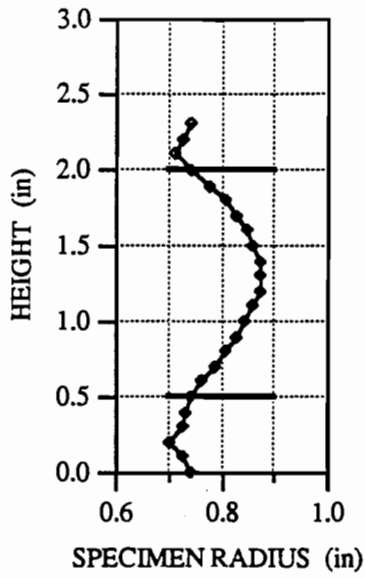
TEST S59.05
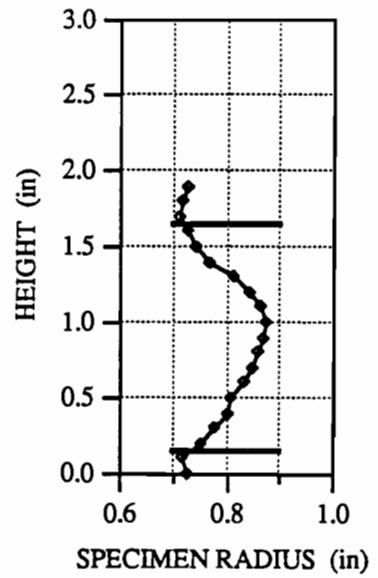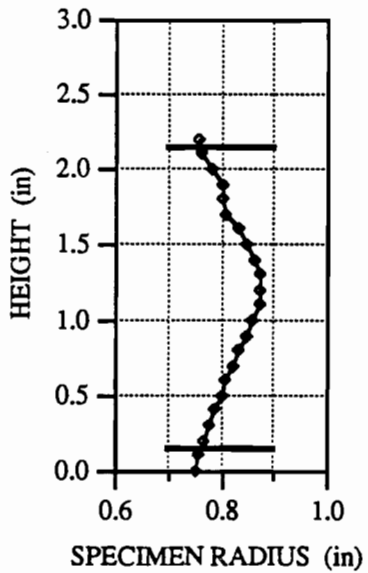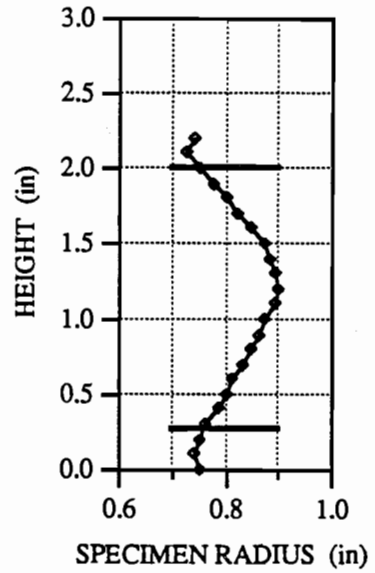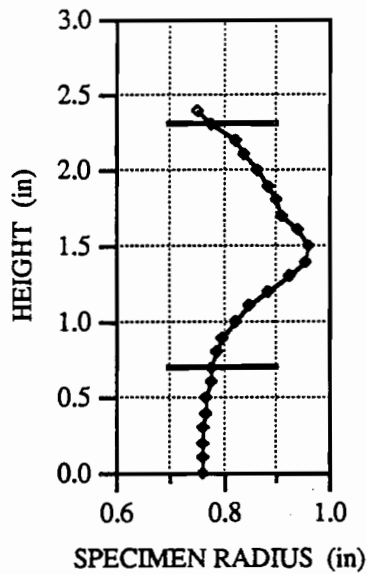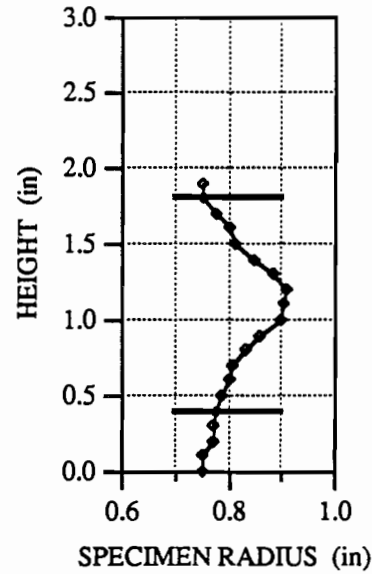
TEST S57.15

TEST S56.02

TEST W62.03

Figure D.11 Deformation patterns for triaxial specimens failing in bulging (Bulging zones are shown between two marked horizontal lines for each specimen)

TEST W65.02   TEST W63.12

Figure D.12 Deformation patterns for triaxial specimens failing in bulging *(Bulging zones are shown between two marked horizontal lines for each specimen)*

Table D.1   Area corrections for specimens failing in bulging

Test Number	Final Strain (%)	Initial Area (in²)	$A_{bulging\ zone}$ (in²)	$a_{bulging\ zone}$	$A_{entire\ length}$ (in²)	$a_{entire\ length}$
S36.02	22	1.55	2.10	1.19	1.97	0.97
W62.03	20	1.61	2.22	1.37	2.10	1.16
S59.05	22	1.39	2.13	1.58	1.96	1.34
W45.02	21	1.47	2.05	1.35	1.87	1.01
W63.12	22	1.54	2.23	1.41	2.07	1.16
S54.03	22	1.47	2.22	1.53	2.08	1.32
S55.08	21	1.34	2.15	1.79	1.97	1.48
S56.02	21	1.54	2.15	1.37	2.08	1.23
S57.15	23	1.35	2.08	1.52	1.96	1.36
S65.02	22	1.59	2.24	1.32	1.59	2.19

114

Table D.2 Area corrections for specimens failing along a shear plane

Test Number	Major x Minor Elliptical Diameters (inches)	Inclination of Shear Plane (degrees)	Projected Area (in^2)	Corrected Area (a-1) (in^2)	Percentage Difference (%)
S58.34	2.0 × 1.60	55	1.49	1.44	3.4
C73.05	2.7 × 1.65	50	2.24	2.21	1.3
W64.30	2.1 × 1.85	50	1.96	2.00	2.0
C72.02	2.6 × 1.70	50	2.23	2.22	0.5
C74.16	2.5 × 1.70	50	2.14	2.23	4.2
C75.03	2.5 × 1.70	51	2.10	2.19	4.3
C26.01	2.6 × 1.80	52	2.26	2.43	7.4
C27.05	2.5 × 1.70	45	2.36	2.44	3.4
C25.015	2.6 × 1.75	50	2.30	2.48	7.9

APPENDIX E. SUMMARY OF FAILURES OF EMBANKMENTS CONSTRUCTED OF PARIS AND BEAUMONT CLAYS

Thirty-four slope failures which occurred in embankments constructed of Paris and Beaumont clays are summarized in Tables E.1 and E.2, respectively. Sixteen of the embankments were constructed of Paris clay; eighteen were constructed of Beaumont clay. The failures either were previously described by Stauffer and Wright (1984) or were reported by personnel from the Texas State Department of Highways and Public Transportation (SDHPT). The summary includes the location of the embankments, age of the slope at failure, slope height, slope inclination, and the height and depth of slide. In addition, the back-calculated values of the pore water pressure coefficients (r_u) and heights of water tables (H_w), based on peak strength and large strains failure envelopes for specimens subjected to wetting and drying, are also listed for each slope. The back-calculated values for r_u and H_w are listed in pairs for each slope (separated by a comma), with the first value corresponding to the peak strength envelope and the second value corresponding to the envelope for large strains.

Table E.1   Summary of slope failures constructed of Paris clay

Embankment Slope Location	Slope Age (years)	Slope Height (feet)	Slope Ratio (cotβ)	Height of Slide (feet)	Depth of Slide (feet)	Pore Pressure Coefficient	Height of Water Table (feet)
Loop 286 @ T&P railroad (Missouri Pacific) SE Quadrant, Lamar Co.	19	20.0	3.0	18	4.0	0.60, 0.46	20.0, 16.8
Loop 286 @ SH 271 Interchange NW Quadrant, Lamar Co.	14	14.1	2.5	14.1	4.0	0.55, 0.41	13.7, 11.1
Loop 286 @ Missouri Pacific) Railroad Overpass SW Quadrant, Lamar Co. *(two slope failures)*	18 18	27.0 29.6	2.9 2.8	15.0 26.2	8.0 6.0	0.54, 0.41 0.52, 0.38	26.0, 21.0 28.6, 22.0
Loop 286 @ Missouri Pacific Railroad Overpass NW Quadrant, Lamar Co.	18	27.4	2.7	27.4	10.0	0.51, 0.37	25.4, 20.0
Loop 286 @ FM 79 Pacific SW Quadrant, Lamar Co.	19	23.9	2.3	23.9	4.0	0.44, 0.28	20.6, 15.2

Table E.1 (continued)   Summary of slope failures constructed of Paris clay

Embankment Slope Location	Slope Age (years)	Slope Height (feet)	Slope Ratio (cotβ)	Height of Slide (feet)	Depth of Slide (feet)	Pore Pressure Coefficient	Height of Water Table (feet)
SH 271 North, SE of the Missouri Pacific Railroad South Embank., Lamar Co.	18	21	2.8	18	6	0.57, 0.43	20.7, 18.0
Loop 286 & Still House Railroad Overpass (North) East Abutment, Lamar Co.	18	19	2.3	15	6	0.50, 0.32	16.9, 13.2
Loop 286 & Still House Railroad Overpass (North) West Abutment, Lamar Co.	18	22	3.0	17	5	0.50, 0.32	19.9, 16.2
Loop 286 & SH 271 NW Quadrant Lamar Co.	18	16	2.7	12	4	0.59, 0.45	16.0, 12.5
Loop 286 & SH 271 Overpass (North) East of Railroad, Lamar Co.	18	14	3.2	10	2	0.57, 0.43	13.7, 11.0

Table E.1 (continued)   Summary of slope failures constructed of Paris clay

Embankment Slope Location	Slope Age (years)	Slope Height (feet)	Slope Ratio (cotβ)	Height of Slide (feet)	Depth of Slide (feet)	Pore Pressure Coefficient	Height of Water Table (feet)
SH 271 North, SE of the Missouri Pacific Railroad North Embank., Lamar Co.	19	16	2.7	12	4	0.55, 0.42	15.4, 11.7
SH 271 South, NW of the Missouri Pacific Railroad Lamar Co.	19	19	2.3	18	6	0.50, 0.32	16.9, 13.2
SH 271 South, SW of the Missouri Pacific Railroad Lamar Co.	19	19	2.3	16	6	0.58, 0.45	19.0, 15.4
SH 271 East, West of the Missouri Pacific Railroad Lamar Co.	19	21	3.0	18	4	0.57, 0.43	20.7, 18.0
SH 271 North, NW of the Missouri Pacific Railroad Lamar Co.	19	16	2.7	11	4	0.60, 0.54	16.0, 15.1

Table E.2   Summary of slope failures constructed of Beaumont clay

Embankment Slope Location	Slope Age (years)	Slope Height (feet)	Slope Ratio (cot β)	Height of Slide (feet)	Depth of Slide (feet)	Pore Pressure Coefficient	Height of Water Table (feet)
IH 610 @ Scott Str. NE Quadrant Harris Co.	17	19.0	2.5	17	3.5	0.51, 0.39	18.6, 17.5
SH 225 @ SH 146 SW Quadrant Harris Co.	31	15.0	3.0	13.0	4.3	0.58, 0.52	15.0, 14.7
SH 225 @ SH 146 NW Quadrant Harris Co.	31	17.6	3.1	14.0	2.4	0.60, 0.53	17.6, 17.5
SH 225 @ SH 146 SE Quadrant Harris Co.	31	13.5	3.4	13.5	3.5	0.60, 0.58	13.5, 13.5
SH 225 @ Southern Pacific Railroad Overpass SE Quadrant Harris Co. (*two slope failures*)	20 20	26.5 19.2	2.6 3.1	21.0 12.0	4.0 3.0	0.50, 0.41 0.60, 0.53	25.5, 24.2 19.2, 19.1

Table E.2 (continued)   Summary of slope failures constructed of Beaumont clay

Embankment Slope Location	Slope Age (years)	Slope Height (feet)	Slope Ratio (cotβ)	Height of Slide (feet)	Depth of Slide (feet)	Pore Pressure Coefficient	Height of Water Table (feet)
SH 225 @ Southern Pacific Railroad Overpass SE Quadrant, Harris Co.	20	23.5	2.4	23.5	5.0	0.50, 0.39	22.5, 21.0
SH 225 @ Southern Pacific Railroad Overpass NW Quadrant, Harris Co.	20	10.2	3.1	10.2	2.5	0.60, 0.55	10.2, 10.1
SH 225 @ Scarborough, SE Quadrant, Harris Co.	17	19.0	2.1	19.0	3.0	0.49, 0.32	17.6, 16.9
IH 610 @ SH 225 SE Quadrant, Harris Co.	19	17.4	2.7	12.0	2.0	0.54, 0.46	17.3, 16.3
IH 610 @ Richmond Str. SW Quadrant, Harris Co.	18	25.7	2.7	22.0	5.0	0.54, 0.45	25.6, 23.8
IH 10 @ Crosby-Lynchburg NW Quadrant, Harris Co.	25	25.1	2.6	19.0	5.0	0.52, 0.43	24.7, 23.1

Table E.2 (continued)   Summary of slope failures constructed of Beaumont clay

Embankment Slope Location	Slope Age (years)	Slope Height (feet)	Slope Ratio (cotβ)	Height of Slide (feet)	Depth of Slide (feet)	Pore Pressure Coefficient	Height of Water Table (feet)
IH 45 @ SH 146 SE Quadrant, Harris Co.	14	15.5	3.0	15.0	3.0	0.58, 0.50	15.5, 15.3
IH 45 @ SH 146 South Side, Harris Co.	14	14.8	3.1	13.0	3.5	0.60, 0.51	14.8, 14.7
IH 45 @ SH 146 NE Quadrant, Harris Co.	12	17.2	2.5	15.0	2.5	0.50, 0.40	16.7, 15.9
IH 610 @ College Str. NE Quadrant, Harris Co.	18	11.4	3.0	11.4	2.0	0.58, 0.49	11.4, 11.3
US 59 @ FM 525 NE Quadrant, Harris Co.	24	16.4	2.4	16.4	3.0	0.49, 0.37	15.6, 14.9
US 59 @ Shepard Str. SE Quadrant, Harris Co.	22	13.3	3.1	13.3	3.5	0.60, 0.51	13.3, 13.2

BIBLIOGRAPHY

AASHTO (1989). *Interim Specifications and Methods of Sampling and Testing Adopted by the AASHTO Sub-committee on Materials,* American Association of State Highway and Transportation Officials, Washington, D.C.

Al-Shaikh-Ali, M. M. H. (1979), "The Behavior of Cheshire Basin Lodgement Till in Motorway Construction," *Proceedings of the Conference of Clay Fills,* Institution of Civil Engineers, London, pp 15-23.

Anderson, M. G. and P. E. Kneale (1980), "Pore Water Pressure Changes in a Road Embankment," *The Journal of the Institution of Highway Engineers,* London, Volume 27, No. 5, pp 11-17.

Anderson, M. G., M. G. Hubbard and P. E. Kneale (1982), "The Influence of Shrinkage Cracks on Pore-Water Pressures Within a Clay Embankment," *Quarterly Journal of Engineering Geology,* Volume 15, pp 9-14.

ASTM (1989). *Annual Book of ASTM Standards: Section 4,* American Society for Testing and Materials, Philadelphia, PA.

Bishop, A. W. and D. J. Henkel (1957), *The Measurement of Soil Properties in the Triaxial Test,* Edward Arnold Ltd., London, 190 pp.

Bishop, A. W. and D. J. Henkel (1962), *The Measurement of Soil Properties in the Triaxial Test,* Second Edition, Edward Arnold Ltd., London, 228 pp.

Bishop, A. W. and N. Morgenstern (1960), "Stability Coefficients for Earth Slopes," *Geotechnique,* The Institution of Civil Engineers, London, Volume 10, No. 4, pp 129-151.

Blight, G. E. (1963), "The Effect of Non-uniform Pore Pressures on Laboratory Measurements of the Shear Strength of Soils," *ASTM Special Technical Publication* No. 361, pp 173-184.

Brindley, G. W. and G. Brown (1980). *Crystal Structures of Clay Minerals and Their X-Ray Identification,* Mineralogical Society, London, pp 426-427.

British Standards Institution (1975). *Methods of Testing Soils for Civil Engineering Purposes; British Standard No. 1377: 1975.* British Standards Institution, London.

Brown, G. W. (1961). *The X-ray Identification and Crystal Structures of Clay Minerals,* Mineralogical Society, London, p 492.

Byrd, T. (1982), "Motorway Slip Report Warns 'Go Easy' with Clay Embankments," *New Civil Engineer,* Institution of Civil Engineers, No. 516, pp 18-19.

Chandler, R. J. (1974), "Lias Clay: The Long-Term Stability of Cutting Slopes," *Geotechnique,* Volume 24, No. 1, pp 21-38.

Chandler, R. J. and M. Pachakis (1973), "Long-Term Failure of a Bank on a Solifluction Sheet," *Proceedings of the 8th International Conference of Soil Mechanics and Foundation Engineering*, Volume 2.2, pp 45-51.

Chandler, R. J., M. Pachakis, J. Mercer, and J. Wrightman (1973), "Four Long-term Failures of Embankments Founded on Areas of Landslip," *Quarterly Journal of Engineering Geology*, Volume 6, pp 405-422.

Day, R. W. and G. W. Axten (1989), "Surficial Stability of Compacted Clay Slopes," *ASCE Journal of Geotechnical Engineering*, Volume 115, No. 4, pp 577-580.

Dixon, J. B. and S. B. Weed (1989). *Minerals in Soil Environments*, Soil Science Society of America, Madison, Wisconsin, Second Edition, 677 pp.

Duncan, J. M. and H. B. Seed (1965), "Errors in Strength Tests and Recommended Corrections," *Report No. TE 65-4*, Department of Civil Engineering, University of California, Berkeley, California, p 54.

Germaine, J. T. and C. C. Ladd (1988), "Triaxial Testing of Saturated Cohesive Soils," *Advanced Triaxial Testing of Soil and Rock, ASTM STP 977*, American Society for Testing and Materials, Philadelphia, pp 421-459.

Gourlay, A. W. and S. G. Wright (1984), "Initial Laboratory Study of the Shear Strength Properties of Compacted Highly Plastic Clays Used for Highway Embankment Construction in the Area of Houston, Texas," *A Report on Laboratory Testing Performed Under Inter-agency Contract No.'s (82-83) 2187 and (84-85) 1026*, Center for Transportation Research, The University of Texas at Austin, p 202.

Green, Roger and S. G. Wright (1986), "Factors Affecting the Long Term Strength of Compacted Beaumont Clay," *Research Report No. 436-1*, Center for Transportation Research, The University of Texas at Austin, p 210.

Greenwood, J. R., D. A. Holt and G. W. Herrick (1985), "Shallow Slips in Highway Embankments Constructed of Overconsolidated Clay," *Proceedings of the Symposium on Failures in Earthworks*, Institution of Civil Engineers, London, pp 79-92.

Ingold, T. S. and C. R. I. Clayton (1978), "Some Observations on the Performance of a Composite Fill Embankment," *Proceedings of the Conference of Clay Fills*, Institution of Civil Engineers, London, pp 133-136.

JCPDS (1989), Joint Committee for Powder Diffraction Standards. International Centre for Diffraction Data, 16001 Park Lane, Swarthmore, PA, 19081, USA.

Kayyal, M. K. (1986), "Effects of Wetting and Drying on Long-Term Strength of Compacted Taylor Marl Clay," Master's Thesis, The University of Texas at Austin, p 110.

La Rochelle, P., S. Leroueil, B. Trak, L. Blais-Leroux, and F. Tavenas (1988), "Observational Approach to Membrane and Area Corrections in Triaxial Tests," *Advanced Triaxial Testing of Soil and Rock, ASTM STP 977*, American Society for Testing and Materials, Philadelphia, pp 715-731.

Liljestrand, H. M., J. D. Mohr, and M. A. Stafford (1986), "Methods for the Validation of Precipitation pH: Application to Texas Data," *Journal of Environmental Science and Health*, A21(2), pp 151-168.

Lumb, P. (1975), "Slope Failures in Hong Kong," *Quarterly Journal of Engineering Geology*, Volume 8, pp 31-65.

Methods of Soil Analysis (1982). *Chemical and Microbiological Properties, Second Edition*, American Society of Agronomy, Inc. and Soil Science of America, Inc., Madison, Wisconsin, pp 159-262.

Odom, G. (1990), Personal Communication.

Osipov, V. I., N. N. Bik, and N. A. Rumjantseva (1987), "Cyclic Swelling of Clays," *Applied Clay Science,* Volume 2, pp 363-374.

Parsons, A. W. and J. Perry (1985), "Slope Stability Problems in Ageing Highway Earthworks," *Proceedings of the Symposium on Failures in Earthworks,* Institution of Civil Engineers, London, pp 63-78.

Rogers, L. E. and S. G. Wright (1986), "The Effects of Wetting and Drying on the Long-Term Shear Strength Parameters for Compacted Beaumont Clay," *Research Report No. 436-2F,* Center for Transportation Research, The University of Texas at Austin, p 139.

Skempton, A. W. (1977), "Slope Stability of Cuttings in Brown London Clay," *Proceedings of the 9th International Conference of Soil Mechanics and Foundation Engineering,* Volume 3, pp 261-270.

Skempton, A. W. (1954), "The Pore Pressure Coefficients A and B," *Geotechnique,* Vol. 4, No. 4, pp 143-147.

Snedker, E. A. (1979), "Discussion: Engineering Properties and Performance of Clay Fills," Edited by D. W. Hight and D. M. Farrar. *Proceedings of the Conference of Clay Fills,* Institution of Civil Engineers, London, pp 229-232.

Stauffer, P. A. and S. G. Wright (1984), "An Examination of Earth Slope Failures in Texas," *Research Report No. 353-3F,* Center for Transportation Research, The University of Texas at Austin, p 241.

Symons, I. F. (1979), "General Report: Performance of Clay Fills," *Proceedings of the Conference of Clay Fills,* Institution of Civil Engineers, London, pp 297-302.

Texas SDHPT (1978). *Manual of Testing Procedures,* Texas State Department of Highways and Public Transportation, Austin, Texas.

Threadgold, L. (1979), "Discussion: Engineering Properties and Performance of Clay Fills," Edited by D. W. Hight and D. M. Farrar. *Proceedings of the Conference of Clay Fills,* Institution of Civil Engineers, London, pp 232-234.

Vail, A. J. and A. A. Beattie (1985), "Earthworks in Hong Kong—Their Failure and Stabilisation," *Proceedings of the Symposium on Failures in Earthworks,* Institution of Civil Engineers, London, pp 15-28.

Van Olphen, H. (1963). *An Introduction to Clay Colloid Chemistry,* Interscience Publishers, New York, pp 69-148.

Vaughan, P. R. and H. J. Walbancke (1973), "Pore Pressure Changes and the Delayed Failure of Cutting Slopes in Overconsolidated Clay," *Geotechnique,* Volume 23, pp 531-539.

Vaughan, P. R., D. W. Hight, V. G. Sodha, and H. J. Walbancke (1978), "Factors Controlling the Stability of Clay Fills in Britain," *Proceedings of the Conference of Clay Fills,* Institution of Civil Engineers, London, pp 205-217.

Widger, R. A. and D. G. Fredlund (1979), "Stability of Swelling Clay Embankments," *Canadian Geotechnical Journal,* Volume 16, pp 140-151.

Wilson, S. D., and P. E. Mikkelsen (1978), "Field Instrumentation," *Transportation Research Record Special Report No. 176 on Landslides; Analysis and Control,* Transportation Research Board, Washington, D.C., pp 112-138.

Wright, S. G. and J. D. Roecker (1984), "UTEXAS—A Computer Program for Slope Stability Calculations," *Research Report No. 353-1,* Center for Transportation Research, The University of Texas at Austin.